Project Report No. 100

MODEL STUDIES - LAWRENCE AVENUE SEWER SYSTEM, CITY OF CHICAGO

by
Alvin G. Anderson
and
Warren Q. Dahlin

Prepared for
HARZA ENGINEERING COMPANY
Chicago, Illinois

October 1968

CONTENTS

PREFACE

This report describes the model studies of the drop shaft to be incorporated into the Lawrence Avenue Sewer System and used to transport surface runoff down to deep tunnels which serve as temporary reservoirs. The purpose of the model studies was to assist in the development of an effective drop shaft and to study its operating characteristics for various flow conditions in the individual structure and in the system as a whole. Modifications were introduced to improve the operation based upon the results of these experiments. Through this process a drop shaft geometry was evolved that appeared to provide optimum flow conditions for the various variable discharges which the structure was to handle.

When an optimum design had evolved from the studies, additional experiments were carried out to examine the various operating characteristics of the structure. These included measurements of the air entrainment by the jet entering the drop shaft, the release of this air through the air vent, and the hydraulic gradients that might be expected when the structure is submerged. Other experiments were made on a partial model of the system in which a number of idealized drop shafts were connected in order to examine the nature of the surges that may be generated within the system when only one drop shaft is operating. These results were to serve as a check on a computer program developed to predict surging in the prototype system.

The model tests described in this report were sponsored by the Harza Engineering Company of Chicago, Illinois, represented by Dr. David Louie, and were carried out at the St. Anthony Falls Hydraulic Laboratory, Professor E. Silberman, Director. The study for the city of Chicago was under the immediate direction of Professor Alvin G. Anderson and was conducted by Warren Q. Dahlin, Research Engineer. The models were fabricated and maintained by the Laboratory shop personnel under the direction of Frank R. Dressel, Superintendent.

During the course of the experimental program many status reports were submitted to the sponsor. These covered in considerable detail the specific tests and areas of investigation, the data from which were needed for design purposes. These reports are on file in the offices of the sponsor and at the St. Anthony Falls Hydraulic Laboratory.

MODEL STUDIES - LAWRENCE AVENUE SEWER SYSTEM
CITY OF CHICAGO

I. INTRODUCTION

The Lawrence Avenue Sewer System will incorporate a large deep tunnel for temporary storage of the surface runoff that will be fed to it by a series of drop shafts placed at intervals along the axis of the tunnel. Each drop shaft will be designed to handle a variable discharge, the peak value of which will be different for each. As the volume of runoff increases, the tailwater elevation may change from zero to a maximum which is governed by overflow facilities. The objectives of the research described in this report are

(a) to investigate the nature of the flow in the drop shafts, suggest an optimum design, and describe the flow patterns in the final design; and

(b) to examine the surges in the overall system when it is subjected to discharges of various magnitudes and in various sequences.

The essential purpose of a drop shaft is to transport water from one elevation and energy level to a lower elevation and lower energy level. Its function is to dissipate the energy of the incoming flow in the course of its passage down the drop shaft to its new elevation and new flow pattern. Conceivably, this may be done in one of several ways or by combining ways. If the drop shaft runs full, the energy change may be accomplished by friction along the wall of the drop shaft so that its energy at the bottom of the shaft is equal to that of the outflowing water. When the drop shaft is partly full, the change in energy might be accomplished by the impact of the falling water on the bottom of the shaft. For variable discharges, this change of energy might be accomplished by a combination of boundary friction and impact. In a system involving drop shafts of the height prescribed by the Lawrence Avenue Sewer System, dissipation of energy by boundary friction alone requires that the diameter be relatively small and that the flow velocities be quite high. It also requires that the drop shaft run full for all discharges that will be handled.

For a larger diameter and possibly lesser velocity, the full flow condition could be attained in one of several ways. It is possible to maintain full flow in a drop shaft of a given size and variable discharge by the use of a valve at the bottom of the shaft. Full flow for a range of discharges might also be attained by the introduction of air into the flow in varying amounts so that the water bulk will be increased sufficiently to fill the drop shaft. From the hydraulic point of view, the use of a valve at the foot of the drop shaft is rather attractive, but it would have the disadvantage of being located far underground in the outlet tunnel and would require special instrumentation so that the valve opening could be governed by the inflow discharge. In addition, the valve would be subject to possible damage by sediment and other debris transported through the system. With the second alternative--that is, the introduction of air into the flow--all obstructions to the flow and the necessity of moving parts would be eliminated; but the problem involving the development of a homogeneous mixture of air and water in the drop shaft, particularly for small discharges, would probably be much more serious.

Because of the advantages that appear to be inherent in the air-entraining type of drop shaft and because of experiences gained in previous studies of such drop shafts, the investigations for the Lawrence Avenue Sewer System were directed toward further development of such structures. This report will describe the results of experiments on several alternate designs which involve the entrainment of air in the drop shaft and the removal of this air from the flow at the bottom.

A. Description of Models

The model of the drop shaft used in this study was fabricated of a transparent plastic so that the flow patterns within could be observed and photographed. For the surge model only one drop shaft was transparent, while the rest of the model was assembled using opaque plastic standard fittings.

The water supply was obtained from the Mississippi River through the Laboratory supply system. It was controlled by valves in the supply lines to each model and measured by means of calibrated Venturi meters. Before entering the drop shaft section, the flow was passed through a wire mesh in order to remove large fluctuations and to provide a reasonably uniform flow into the drop shaft

system. The tailwater elevation in the models was maintained at prescribed elevations by means of gate valves. From the models, the discharge was returned to the river through the Laboratory drainage system.

Since a free water surface exposed to atmospheric pressure exists within the drop shaft, it represents a hydraulic system operating under the force of gravity and the velocities, pressures, and water surface elevations are gravitational phenomena. For this kind of a system, dynamic similarity is obtained when the model-prototype relationships are established by the Froude law. The following expressions for velocity, discharge, pressure, etc., in terms of the length scale ratio, L_r, are then obtained:

$$V_P = V_m L_r^{1/2}$$
$$Q_P = Q_m L_r^{5/2}$$
$$P_P = P_m L_r$$
$$T_P = T_m L_r^{1/2}$$
$$f_p = f_m / L_r^{1/2}$$

where V is velocity in fps, Q is discharge in cfs, P is pressure in ft of water, T is time, and f is frequency. The subscripts p and m represent prototype and model magnitudes respectively. By utilizing the above equations, the model discharge can be determined and the pressures and velocities as measured in the model can be readily translated into prototype values. Complete similarity for the air entrainment and air removal process cannot in general be obtained because the mechanism of entrainment and the size of the air bubbles generated in the model are subject to forces other than the force of gravity. However, the processes involved are qualitatively similar, and it is believed that the observations made in the model regarding the flow characteristics of the aerated mixtures and the flow patterns generated in the drop shaft will be qualitatively correct.

The peak discharge of each drop shaft in the system will be determined in accordance with the local conditions at the site of the structure. The model, however, will be applicable to all of the proposed structures, since the study

is a generalized investigation of flow in a drop structure. Each drop shaft can be sized to correspond to the expected peak discharge by application of the Froude law.

1. Drop Shaft Model

The transparent plastic model used for this study was built to a scale of 1:27--that is, $L_r = 27$--so that a standard size plastic tube, 4 inches in diameter, could conveniently be used as the drop shaft to correspond to the 9 ft diameter of the preliminary prototype design. Photo 1 is a view of the model being assembled and erected for testing, while Photo 2 shows the assembled model during the course of an experiment. The model was fitted with piezometer taps at significant pressure points so that pressures could be transmitted to a bank of manometers from which they could be read during the course of the run. The model was designed so that the various components could be modified as indicated by results obtained from the experiments. The transparency of the plastic permitted observations and photographs to be made of the flow patterns at various points within the structure.

2. Surge Model

The surge model consisted of a series of five drop shafts connected at intervals to a portion of the main tunnel. This model was built on a scale of 1:54. The drop shafts consisted of 2 in. I.D. conduits, and the main tunnel was a 3 in. plastic pipe. The drop shafts were located at 20 ft intervals along the model tunnel. This represented a prototype spacing of 1080 ft. The first drop shaft was connected to the water supply through a Venturi meter and a quick-opening valve. The discharge could be measured so that any flow within the range of the prototype discharges could be introduced. The quick-opening valve permitted the generation of a sudden discharge surge which would be propagated down the sewer system. Within each model drop shaft the two wires of a capacitive stage recorder were connected so that the electrical effects of the changing water level could be transmitted to the recorder chart. A four-channel recorder was used so that simultaneous records of the four instrumented drop shafts could be made and ultimately compared. In each test, water at a prescribed discharge was introduced in one drop shaft (either drop shaft 1 or drop shaft 3) and the surges were measured in the other four. Photos 3 and 4

are overall views of the surge model. Photo 3 shows the Type A surge model in which the inflow is restricted to drop shaft number 1. The drop shafts have been numbered 1 through 5 with drop shaft 3 fabricated of clear plastic so that the water level movements can be observed. The photograph also shows the quick-opening valve and the inlet section of the drop shaft system. The successive drop shafts are attached to the tunnel at the end of which is located the tailwater control. Photo 4 shows the Type B surge model. This is similar except that the discharge is introduced in the center of the model at drop shaft 3 so that the surge will be propagated in both directions.

II. EXPERIMENTAL DESIGN OF DROP SHAFT

The drop shaft and its model consist essentially of three parts. The inlet section contains the upper tunnel and the inlet to the drop shaft. The inlet section is curved downward so that the incoming flow is directed more or less down the shaft. The drop shaft proper is a vertical conduit fitted with various devices for introducing air and constructed so that changes can be made in its geometry. At the bottom of the drop shaft is the so-called sump, which provides for the absorption of the impact forces generated by the downward-flowing water. Downstream of the sump is an air collector designed to facilitate the separation of the entrained air from the water and the release of this air to the atmosphere or to direct it up the shaft for recirculation into the downward-flowing water. These components were examined separately and in conjunction with each other in order to evolve an optimum design. The various studies are described below.

A. Type A Drop Shaft - Separate Air Vent

The first structure consisted of the vertical circular drop shaft fitted with a sump containing an impact cup. The air collector had a sloping upper boundary to facilitate the transport of air to the vent, which was separate from the drop shaft proper. A similar structure of this type had been previously investigated, and it served effectively as the initial model. This structure, designated as Type A, is described in Chart 1, which gives the dimensions and the geometrical arrangement of the various components.

The pressure distribution measured at various points along the flow path is shown for several discharges and tailwater elevations in Charts 2, 3, and 4. The results shown in these charts are typical of those obtained for the various arrangements of Type A described in Chart 1. In the chart showing the hydraulic gradelines, the distance along the drop shaft has been plotted horizontally so that the pressures as measured at various elevations along the drop shaft can be plotted vertically. Chart 2 shows the hydraulic gradelines for discharges varying from 100 to 1200 cfs when the tailwater is constant at 10 ft above the bottom of the sump. Chart 3 shows similar data with the tailwater maintained at 100 ft above the bottom of the sump, while in Chart 4 the tailwater is shown as 190 ft above the bottom of the sump. The charts show that for all discharges the pressures in the drop shaft are essentially atmospheric until the gradeline approaches the elevation of the tailwater. For the lowest tailwater (Chart 2), the pressures in the impact cup are considerably higher than the pressures along the drop shaft or in the downstream tunnel. As would be expected, these impact pressures are higher for the larger discharges. It is also interesting to note that the impact pressure is greater near the edge of the impact cup than near the center. Since the flow enters the drop shaft from the side, the jet is reflected from the opposite wall. It appears that the reflection is such that for this flow condition it enters the sump at the side of the impact cup. For the higher tailwater it appears that the oscillating flow is dissipated in the tailwater pool so that the pressures in the impact cup are constant. For the intermediate tailwater level, certain irregularities in the hydraulic gradeline developed as it approached the tailwater level. This might also be due to impact pressures in the piezometer tubes generated by the oscillating flow. Below the elevation of the tailwater, the hydraulic gradelines again become quite regular and approach the constant value of the tailwater level without further disturbance. When the tailwater is raised to the maximum height, the drop shaft is almost completely submerged and the jet from the inlet tunnel is immediately submerged in the tailwater pool. The relatively smooth hydraulic gradelines for the high tailwater level are shown in Chart 4 for the several discharges tested.

Typical flow patterns in the Type A drop shaft are shown in Photos 5 through 8 for two different discharges and two tailwater elevations. Photo 5

shows the inlet portion of the drop shaft for a discharge of 600 cfs and very low tailwater. For this discharge the jet follows the curve of the inlet section rather closely, but even so it is apparent that as the flow progresses down the shaft there are small transverse components of velocities. These are generated by the movement of air bubbles. Air is insufflated at the top by the falling jet and the turbulence generated as it flows down the shaft. The insufflated air is not uniformly mixed with the water, so that the air concentration varies widely both longitudinally and transversely in the shaft. Photo 6 shows the lower portion of the drop shaft for the same flow conditions and illustrates the mechanism by which the entrained air is released in the air collector and discharged into the atmosphere through the vent pipe. The impact cup for this design is very effective in breaking up the large masses of water so that as it leaves the cup, the air is very uniformly distributed.

For the larger discharge of 1200 cfs, particularly for the higher tailwater levels, the drop shaft is more nearly filled with water. This is apparent in Photos 7 and 8, which show the flow pattern for a discharge of 1200 cfs when the tailwater is maintained at 100 ft above the bottom of the sump. For this discharge the jet tends to separate from the inlet curve and to impinge on the opposite wall. It is then reflected to the other side of the drop shaft and generates a certain type of instability. The entrained air in the upper portion of the drop shaft is irregularly distributed, but when it reaches the level governed by the tailwater, the pool causes a more uniform distribution. It is apparent from Photo 8, as indicated by the large quantity of air in the sump, that more air is entrained at the high discharge. Further, the air in the vent forms large bubbles which rise through the foamy mixture that fills the air vent.

It would appear from these experiments that a modification which would tend to reduce the instabilities and provide a more uniform air-water mixture would be more conducive to dissipation of energy along the walls of the drop shaft. It also appears from the pressure gradelines shown in Charts 2, 3, and 4 that the water is falling freely down the shaft and that energy is being dissipated through the insufflation of air and by turbulent mixing rather than by friction on the drop shaft walls.

B. Type B-3 Drop Shaft - Solid Divider Wall

Drop shaft Type B-3 incorporates two changes in geometry from the Type A drop shaft. In order to eliminate the separate air vent, it was combined with the drop shaft proper by dividing the drop shaft into two parts using a longitudinal dividing wall. It was expected that this reduction in cross-sectional area for the water flow could be compensated for by an increase in overall diameter. On the other hand, the inclusion of the air vent within the drop shaft itself would tend to reduce the construction costs. The second modification was the replacement of the impact cup by a 12-ft weir at the exit of the sump to the air collector. In view of the results obtained with the Type A structure, it was thought that the impact energy of the falling jet could be dissipated in the pool established by the weir. Two small openings at the bottom of the weir would provide for drainage of the sump between periods of use. The geometry of the Type B-3 drop shaft is shown in Chart 1.

The results of pressure measurements made at several points along the inlet tunnel, drop shaft, and outlet tunnel have been plotted in Charts 5, 6, and 7. The results for Type B are very similar to those obtained for drop shaft Type A, except for several minor differences. For the maximum discharge of 1200 cfs, small negative pressures in the upper portion and positive pressures in the lower portions as the flow approached the tailwater elevation indicated that the drop shaft tended to run full. This was the case for both the low tailwater and the intermediate tailwater shown in Charts 5 and 6. For small discharges, it appears that the water was falling freely since the pressures were nearly atmospheric. The pressures at the bottom of the sump were not appreciably different from those measured in the impact cup for Type A.

Typical flow patterns for the Type B geometry (including impact cup) are shown in Photos 9 through 12. Photos 9 and 10 show the upper and lower portions of the drop shaft for a discharge of 300 cfs with the tailwater maintained at 10 ft. As might be expected, the inlet tunnel is only partly full and the flow follows the curve of the inlet section quite closely. Very little air is entrained, and this is poorly mixed with the water. For the Type B structure, the impact cup is in place, and Photo 10 shows the effect of the cup breaking up the jets as they fall to the bottom of the sump. Because of the low tailwater, the air vent is devoid of water and is simply a passage for the

air to the atmosphere. Photos 11 and 12 are similar views for a discharge of 1200 cfs with the tailwater maintained at 100 ft above the bottom of the sump. The jet from the inlet tunnel strikes the dividing wall in the area near the inlet causing a high degree of turbulence and air insufflation at this point. The drop shaft appears to be running nearly full, and any regions not occupied by water are filled with an agitated mixture of air and water. This is particularly apparent in Photo 12 of the lower part of the drop shaft. This condition is similar to that shown in Chart 6 for the maximum discharge of 1200 cfs. The air is separated from the flow within the air collector chamber and is released through the air vent. The release of the air and the high tailwater leave a frothy mixture in the air vent through which large bubbles of air rise to the top.

These results from the Type B structure suggest that with the solid divided wall, full flow occurs when the discharge is about 1200 cfs, and that for smaller discharges, the flow tends to drop freely. Conceivably, the insufflation of air might be adjusted so that for each discharge the drop shaft would flow full and more of the energy could be dissipated along the walls of the drop shaft. In Types A and B, all the air is insufflated at the top of the drop shaft and the volume of air entrained increases with an increase in discharge. It follows that if the amount of air entrained could be adjusted to that necessary to cause full flow for all discharges, a better flow pattern would be obtained.

C. Type C-3 Drop Shaft - Slotted Divider Wall

The design of the Type C-3 drop shaft is an attempt to provide a means by which air can be insufflated into the flow at various points along the drop shaft so that the mixture will be more uniform and the volume of air entrained will be sufficient for the drop shaft to flow full. Type C-3 is similar to Type B-3, except that sloping slots were cut in the dividing wall at a number of points to connect the portion carrying water with the air vent. The slots were so designed that the falling jet would suck air from the air vent into the flow and thus more uniformly aerate the falling water. In addition, for these tests the impact cup was removed and replaced by a 12-ft weir at the entrance to the air collecting chamber. The various Type C designs are shown in Chart 1.

The results of the pressure measurements for the Type C-3 design are given in Charts 8, 9, and 10. Chart 8 shows the pressures throughout the drop shaft for several discharges with the tailwater at 10 ft above the bottom of the sump. Here the pressures for the low discharges are essentially atmospheric, while that for the maximum discharge of 1200 cfs appears to be positive in the upper reaches and forms a smooth transition into the downstream tailwater level. It would be expected that since the air in the air vent is at atmospheric pressure, the pressures within the drop shaft itself would have to be less than atmospheric in order for air to be drawn into the flow. The purpose of the lips on the upper edge of the slots on the water side is to deflect the flow away from the opening of the slot and presumably reduce the pressure in the flow in this region so that air can be drawn through the slot. The charts show, however, that all the pressures are either atmospheric or slightly positive, and thus it would seem that the air-water mixture was falling freely. This is partly borne out by the fact that the impact pressures on the floor of the sump are considerably higher than the pressures in the tailwater or in the end of the drop shaft.

When the tailwater is at elevation 100 ft, as shown in Chart 9, the hydraulic gradient for the maximum flow is positive at all points along the drop shaft, and those for the smaller flows appear to be near atmospheric. This condition may indicate that the drop shaft is flowing full of the air-water mixture, since the pressures in all the taps along the drop shafts are positive and the hydraulic gradelines are quite regular throughout the system. The excess pressure in the sump for this condition exists only for the maximum discharge and is considerably less than in the previous case. For a tailwater of 190 ft (Chart 10), the hydraulic gradelines for discharges of 300 and 600 cfs only were observed. For both of these cases, the hydraulic gradelines are very regular, and since the tailwater was so very high, the drop shaft was flowing full of the air-water mixture.

The appearance of the flow for the conditions described in the above charts is shown in Photos 11 and 12. Photo 11 shows the upper portion of the drop shaft with a discharge of 600 cfs flowing through it. As before, the jet clings to the curve of the inlet section and enters the drop shaft smoothly. The deflection of the flow at the lips on the upstream side of the slots is

clearly apparent, as is the entrainment of air through the slots from the appearance of the falling water. In the lower portion shown in Photo 12, the mixture appears to be quite uniform as it reaches the sump. The air that is released in the downstream air collector is fed up the air shaft and presumably circulated back into the flow. At 1200 cfs, with a high tailwater (150 ft above the bottom of the sump), the drop shaft flows full of water, and no air is entrained in the upper portion. In the region near the sump, however, some air is entrained and carried into the sump. Although the tailwater is maintained at 150 ft, it appears from the photograph that there is a considerable amount of free air which is circulating within the sump and relatively little air is rising through the air vent.

The appearance of the flow pattern and the characteristics of the air entrainment in the lower portion of the Type C-3 drop shaft for various discharges and tailwaters are given in Photos 13 through 18. In the Type C-3 drop shaft, the impact cup has been removed and replaced by the 12 ft weir at the entrance to the air collector. In Photos 13 and 14, the discharge is 300 cfs and the tailwater elevations are 10 ft and 190 ft respectively. In Photo 13, the aerated water has penetrated to the bottom of the sump and is flowing over the weir. In Photo 14, because of the high tailwater, the down-flowing jet does not penetrate to the floor of the sump, but the relatively small amount of air is quickly separated in the air collector. It appears that the flow for the low tailwater is considerably more aerated than that for the high tailwater. This is undoubtedly due to the intake of air from the air vent. In Photos 15 and 16, the discharge has been increased to 600 cfs. In Photo 15, with the low tailwater, the downcoming jet penetrates to the bottom of the sump, and the high degree of turbulence thoroughly mixes the water and the air. When the tailwater has been raised to 190 ft, the flow in the drop shaft and in the air vent is nearly solid water, the air being easily separated. When the discharge is 1200 cfs, the flow is much rougher for the low tailwater. A large quantity of air is entrained, as shown in Photo 17, so that it cannot be separated in the air collector, and much of the air goes down the tunnel. The downward flow shows that the air-water mixture is uniformly distributed. In Photo 18, the tailwater has been raised to 150 ft, and it can be seen that the sump is effectively submerged and the entrainment of air has been greatly reduced.

It would appear, in comparison with the previous types, that some improvement in flow pattern had been attained by the introduction of the slotted dividing wall, and that further improvement might be attained by adjusting the spacing of the slots so that the entrainment of air would be more uniform. Thus, the spacing of the slots should be less in the lower portion of the drop shaft than in the upper portion. In addition, the shape of the slots might be modified to provide a more efficient intake of air.

Some additional experiments were made with the slotted divider wall in order to examine other aspects of this structure. The Type C-1 drop shaft contains the slotted divider wall and the impact cup in the sump. It was characterized, however, by the closure of the top of the drop shaft so that no air could be drawn through that opening. Chart 11 shows the results of this experiment for various discharges and with the tailwater at 10 ft above the bottom of the sump. The significant difference between this result and those for the Type C-3 drop shaft is that for the high discharge the pipe will run full and the pressure will be highly negative. Chart 11 also shows that the hydraulic gradeline at the top of the drop shaft is nearly 100 ft below the inlet in prototype values. In actuality, this condition would not occur in the prototype since the maximum negative pressure could not exceed the vapor pressure without causing cavities in the flow. For the smaller discharges, however, the pressure in the drop shaft appears to be atmospheric, suggesting that since the inlet tunnel was only partly full for these conditions, the pressure in this region was maintained at the atmospheric pressure.

Chart 15 shows the result of a similar experiment made with a Type C-4 drop shaft in which the lower six slots were closed. This chart indicated that the closing of these slots had little or no effect on the hydraulic gradelines (Compare with Chart 9).

In the course of the experiments, some observations were made to determine for a given discharge the maximum tailwater obtainable in the model at which the inlet is submerged. These results are tabulated in Table I. For example, in Types A and B drop structures, relatively large discharges can be passed through the structure with high tailwater elevation. The maximum discharge in the Type C drop structure is considerably reduced, however, presumably because of the entrainment of large quantities of air through the slotted dividing wall (Table I).

Since for each runoff event the discharge hydrograph consists of the v very low discharges as well as the peak discharges, an ideal structure would be one in which all discharges above a given magnitude would cause the pipe or the drop shaft to run full by the entrainment of air into the flow. In this way, the operation of the structure would be more uniform and systematic. The results obtained with the Type C-3 drop shaft are encouraging in that the flow has been improved and might be further improved with additional modifications of the system.

TABLE I

Maximum Tailwater Elevations for Specified Discharges

Type	Q cfs	Max. T.W.* ft
A	600	217
A	900	217
A	1200	208
A	1500	203
A	1800	91.2
B	900	217
B	1200	201
B	1500	181
B	1870	148
B-3	900	200
B-3	1200	201
B-3	1500	181
B-3	1800	159
C	600	215
C	900	207
C	1200	149
C-1	600	---
C-1	900	210
C-1	1200	162
C-2	900	208
C-2	1200	179
C-2	1300	7.2
C-3	900	207
C-3	1200	181
C-3	1300	7.8
C-4	900	208
C-4	1200	179
C-4	1280	7.8

*Tailwater at which the flow in the drop shaft submerges the inlet and begins to flow into the air vent.

D. Type D Drop Shaft - Horizontal Air Collector

Based upon the results of other experiments, the drop shaft model was modified to incorporate an air collector consisting of a vertical enlargement of the downstream tunnel so that the roof was horizontal and the exit to the tunnel was abrupt enough to trap the released air in the collector. An air vent could be connected to the roof of the collector to release the air to the atmosphere. A description of the various modifications of the Type D structure is given in Chart 13, which also identifies two aspects of the tests on the Type D drop shaft. One aspect deals with the influence of weir height on the flow pattern. The weir is designed to provide an impingement pool for the water and to direct the water into the air collector. The other phase describes the experiments dealing with the geometry of the slots in the dividing wall.

Pressure measurements made at various points along the drop shaft, in the sump, and in the downstream tunnel are shown in Charts 14 and 15. Specifically are shown pressure gradelines for a discharge of 600 cfs and tailwater elevation of 10 ft and 100 ft respectively. The pressure measurements for 4 alternate weir heights designated D, D-1, D-2, and D-3 are shown in Chart 14. The results indicate that except in the region of the sump where the effect of the weir can be felt, the pressures are essentially equal and independent of the weir height. This was expected, since the purpose of testing various weir heights was to modify the pattern of flow from the sump into the air collection chamber in an attempt to improve the air release process. The chart shows that in the drop shaft the pressures are essentially atmospheric. The pressures on the bottom of the sump show the effect of the impact of the falling jet and represent average pressures in this region. Although the tailwater is at elevation 10 ft, the maximum average pressure on the bottom of the sump is nearly 45 ft. It might be expected that momentary pressures would be considerably higher. Only in those portions of the drop shaft which flow full does the pressure gradient show the effect of friction along the walls. This is shown in Chart 15 where the tailwater is at 100 ft. It is apparent here that the pressures become positive, or greater than atmospheric, at a point in the pipe above the tailwater. Hence, the hydraulic gradeline departs from the line of the drop shaft and approaches that of tailwater, and the

effect of the weir height is essentially eliminated. These measurements show that the pattern of pressures is very similar to that measured in previous tests and is relatively independent of the minor geometrical changes in the system.

The nature of the flow in the drop shaft and particularly in the sump and air collector has been recorded by photographs. In Photo 19, the lower portion of the drop shaft is shown with a discharge of 600 cfs and a very high tailwater elevation of 190 ft. For such tailwater heights, a considerably lessened amount of air is mixed with the flow, and that which is introduced is easily separated in the sump; it can be seen rising through the air vents in the form of bubbles. The pattern is much different, however, when the discharge is increased to 1200 cfs and the tailwater elevation is reduced to 100 ft. This is shown in Photo 20, where the large quantities of entrained air which cannot be released from the air collector are carried on into the tunnel. It appears from the photograph that for this discharge a 12 ft weir is so high that the space available for flow to the air collector from the sump is completely filled with the air-water mixture, which means that air which is separated in the air collector cannot return into the sump to pass up the air vent. Although 1200 cfs is beyond the capacity of the drop shaft, this photograph shows clearly the effect of this design and suggests how modifications should be made.

1. Effect of Weir Height on Air Separation

The purpose of the weir separating the sump from the air collector is to create a pool at the bottom of the sump to absorb the impact of the water falling through the drop shaft. At the same time, the weir tends to constrict the space available for the air-water mixture to flow into the air collector. A high weir would provide a better pool, but would cause a greater constriction to the flow passage, while a low weir would reduce the cushion effect but would make the flow passage larger. It is apparent from the pressure grade-lines that the weirs had relatively little effect on the pressures in either the drop shaft of the sump. Consequently, it appears that a low weir or none at all would be most effective in eliminating the air. On the other hand, however, with the jet from the sump entering the air collector at a lower

level, it might not be possible for the entrained air to rise to the top of the collector before it was carried into the tunnel. This would require that the air collector be of considerable length.

Photos 21 and 22 compare the pattern generated by the 12 ft weir and the 8 ft weir when the tailwater elevation has been increased to 100 ft. In these two photos the value of reducing the weir from 12 ft to 8 ft is quite apparent. In Photo 21, the flow over the 12 ft weir essentially fills the space leading to the air collector so that the air collected cannot easily return to the air vent. Consequently, the increased pressure forces the water level in the air collector down toward the top of the downstream tunnel and permits much air to escape into the tunnel. In addition, the jet over the weir plunges to the bottom of the tunnel so that bubbles rising in the air collector reach the surface near the downstream end. On the other hand, Photo 22 shows a lower weir, where the space leading to the air vent is not so confined; air can be more easily released and the level of the water in the air collector is close to the top. Such an arrangement is effective in preventing the air from entering the tunnel. It is apparent, however, in both Photos 21 and 22 that the air must escape from the air collector to the air vent in large gulps which also rise through the air vent, creating an uneven flow pattern. These tests suggest that the space available for the return flow of air should be appreciably enlarged, perhaps by sloping the top of the air collector. For larger discharges and low tailwaters, as shown in Photos 23 and 24, the air collector is completely ineffective in preventing air from entering the tunnel or providing means for the release of air through the vent. In these photographs, the discharge has been increased to 1200 cfs and the tailwater reduced to 10 ft. In Photo 23, a 4 ft weir has been introduced while in Photo 24, the weir has been removed entirely. Although a discharge of 1200 cfs is far beyond the capacity of the structure, the photographs do who the pattern that may be expected for extreme conditions.

Photos 25 and 26 show that when an additional air vent from the air collector is introduced the operation of the sump and air collector is much improved. This demonstrates the importance of providing an unrestricted access back into the sump. It appears by comparison of the two photographs that the air vent located near the upstream end of the air collector is

slightly more effective in removing air than that located at the downstream end. At least, it provides more space at the downstream end for unaerated water, and hence it is somewhat less likely that air will be carried into the tunnel. For these tests, with the air vent and with the tailwater reduced to 75 ft, the flow pattern was considerably better than that without the air vent shown in Photos 21 and 22.

E. Type E-14 Drop Shaft - Sloping Air Collector

The Type E-14 drop shaft evolved from the experiments on the earlier types and incorporated the improvements suggested by these experiments. The most significant change was an increase in the height of the sump and the addition of a sloping section which was expected to aid in the air movement to the vent. The increase in height was introduced in order to provide a larger opening into the air vent. In addition, the diameter of the sump proper was reduced to approximately 19 ft as compared with approximately 26 ft for the Type D structure. It was felt that the diameter could be reduced without seriously disrupting the flow from the drop shaft and into the downstream exit tunnel. The later versions of the Type E drop shaft that were examined are given in Chart 16.

The Type E drop shaft structure and the various modifications of it leading up to the Type E-14 drop shaft structure were tested by observing the flow patterns in the sump and the air collector and the mechanism of air release through the air vent. These flow patterns were photographed so that the results of various modifications could be compared. Although many photographs for various flow conditions were made, flows which show typical flow patterns are included in this report.

Photo 27 shows a discharge of 600 cfs with 100 ft tailwater elevation through the Type E structure. This structure incorporates an 8 ft weir between the sump and the air collector for the purpose of providing a pool to absorb the impact in the sump. The aerated mixture flows over the weir into the air collector where the air is separated so that the flow leaving the air collector is free of air. The Type E structure appears to be quite effective in removing the entrained air and permitting a reasonably air-free flow to take place in the exit tunnel. The structure with a horizontal portion of the

air collector and the added sloping portion appeared to be unnecessarily long. It was expected that it could be shortened somewhat without seriously reducing its effectiveness in separating the air from the water.

The suggestion that the structure could be shortened was tested by removing the sloping portion of the Type E drop shaft to form the Type E-1 drop shaft as shown in Photo 28. Here a discharge of 600 cfs with a tailwater at 100 ft is introduced into the structure with the result that an appreciable portion of the air-water mixture entered the exit tunnel and a large separation zone formed at the tunnel inlet. It appears that for these conditions, the air which collects at the top of the air collector cannot escape freely into the air vent so that some of it is carried into the downstream conduit. This photograph indicates that the sloping portion of the air collector is necessary for effective operation. The design was again modified by replacing the sloping section of the air collector and shortening the section which incorporated the horizontal roof. The consequence of this change is shown in Photo 29 for the same flow conditions, that is 600 cfs and a tailwater elevation of 100 ft as before. The effectiveness of the sloping portion of the air collector is clearly shown in this photograph. The air is essentially separated from the water so that only a little air escapes into the exit tunnel.

The next change in the sump and air collector structure was designated as Type E-7. In this design the sloping section was incorporated above that portion of the air collector with the horizontal roof as shown in Photo 30. It appeared from the previous test that if more space were provided above the sump to provide easier access to the air vent, the air collector could be shortened. However, this is evidently not an effective solution because in Photo 30 with a discharge of 600 cfs and tailwater at 100 ft, a very appreciable separation occurs as the flow enters the exit tunnel and relatively large quantities of air are permitted to escape into the tunnel. In Type E-8, the height of the weir was increased to 12 ft with the thought that separation of the air from the water would take place at a higher elevation and no air would enter the exit tunnel, but this change was not sufficient to improve the flow pattern. In Type E-9, the height of the weir was increased again to 16 ft with similar results. It was quite clear that modifications involving weir height were not effective in preventing air from escaping to

the exit tunnel. Rounding the entrance to the exit tunnel to prevent such extreme separation did not improve the situation. An attempt was made to introduce greater curvature to see if the separation would be prevented. These changes are shown in Photo 31 which shows the 4 1/2 ft radius curved projection at the exit tunnel and the weir height reduced to 8 ft. With a discharge of 600 cfs and tailwater at 100 ft, the flow pattern was not appreciably improved and it was apparent that an appreciable quantity of air was being discharged into the downstream tunnel. Type E-13 was similar to Type E-11 except that the projection was extended to the top of the sump as shown in Photo 32. It is apparent that some air is still being released into the downstream tunnel. These tests showed that a short air collector would not be effective, that changing the height of the weir did not appreciably improve the situation, but that the sloping roof was quite effective in facilitating the release of air into the air vent. It became apparent that improvement would probably be achieved if the downstream section of the air collector with a sloping top were replaced in the structure.

The revised design designated as Type E-14 is shown in Photo 33. Here we see that the entire air collector contains the sloping roof and that it has been extended to essentially the original length of the Type E design. The 12 ft weir has been included in order to provide a pool for the plunging water from the drop shaft. This design is relatively simple in that the air collector consists of a single structure with a sloping roof and sufficient space to facilitate the separation of the air from the water. Photos 33 through 36 show the flow patterns generated by a discharge of 600 cfs with tailwater elevations ranging from 10 ft to 190 ft. In Photo 33 with the tailwater at 10 ft, the air collector appears to be barely adequate, however, very little air can enter the downstream tunnel. It should be noted that a tailwater elevation of 10 ft is the minimum for which the air collector can be effective. Since the downstream exit tunnel is 9 ft high, a tailwater elevation of less than 10 ft would cause the tunnel to run only partly full, and of course air would fill the remainder of the tunnel. Photo 33 does show, however, that even for a tailwater elevation of 10 ft the sump and air collector are quite effective. Photo 34 shows the same conditions when the tailwater has been increased to an elevation of 50 ft. For this tailwater, the structure is quite effective in releasing the air from the water and

permitting its escape up the air vent. The conditions are still further improved when the tailwater is raised to 100 ft and 190 ft as shown in Photos 35 and 36. For these tailwaters, the air is released in the upper portions of the structure and passes relatively freely up the air vent. It should be noted that when the tailwater is less than about a 100 ft elevation, the incoming jets plunge to the bottom of the sump before the tailwater flows out over the weir. Above this tailwater elevation, particularly at 190 ft, much of the energy of the falling jet has been absorbed, and it appears that the air is no longer carried to the bottom of the sump.

Although this structure was designed for a discharge of 600 cfs, some tests were made when the discharge was doubled to 1200 cfs. Photos 37 and 38 show the resulting flow pattern when the tailwater is controlled at elevation 50 ft and 100 ft respectively. These photographs show that this discharge exceeds the capacity of the structure and even though the tailwater has been increased to 100 ft (Photo 38), the air collector is ineffective in removing the air and much of it escapes into the downstream tunnel. It is therefore quite apparent that the capacity of this size of drop structure is in the neighborhood of 600 cfs.

Having observed the characteristics of the flow in the Type E-14 drop structure, particularly with reference to the function of the weir at the exit of the sump to the air collector, it was suggested that the flow pattern might not be appreciably changed if the weir were removed. The function of the weir initially was to provide a pool on which the jet would impinge in order to reduce the impact pressures at the bottom of the sump. It had the disadvantage, however, of interfering with the movement of machinery from the sump into the downstream tunnel. This movement would be greatly improved if the weir were removed. Thus, tests were carried out without the weir to examine the effect upon the flow pattern and upon the release of the entrained air to the air vent. The Type E-14 structure with the weir removed was designated Type E-15. In Photos 39 and 40, the discharge was maintained at 600 cfs with the tailwater at elevation 10 ft and 50 ft. These photos are to be compared with Photos 33 and 34. The greatest difference in the flow patterns occurs when the tailwater is at elevation 10 ft as seen in Photos 33 and 34. The removal of the weir permits the air-water mixture to penetrate into the air

collector at a considerably lower level. In spite of this, however, the air is effectively released in the air collector and the flow patterns are very similar as the flow enters the downstream tunnel. These differences are still further reduced as the tailwater elevation is raised. This can be observed by comparison of Photos 34 and 40.

It appears that if the impact pressures at the base of the drop shaft are not excessive, the weir at the entrance to the air collector really serves no useful purpose and can be eliminated without introducing any deleterious effects.

1. Development of Flow Deflectors Above Dividing Wall Slots

In this drop shaft, the air vent was incorporated by inserting a dividing wall in the shaft so that the water would flow downward on one side, and the air could escape on the other. In the course of these experiments, an attempt was made to utilize the escaping air with consequent modifications in the dividing wall.

The nature of the flow when the shaft is fitted with a solid dividing wall is shown in Photos 41 and 42. In Photo 41, a discharge of 600 cfs is flowing through the structure with the tailwater at elevation 100 ft, while in Photo 42, the discharge is 1200 cfs, again with a tailwater elevation of 100 ft. In both cases, all of the air that is entrained by the flow is entrained by the jet as it enters at the top of the structure. The entrainment of the air is not uniform and the water flows more or less heterogeneously with large volumes of solid water interspersed with regions of high air content. In Photo 42, the intensity of the air entrainment for large discharges is clearly shown.

It was suggested that the whole flow pattern might be improved if air could be introduced at various points along the flow pattern, rather than depending upon that which is entrained at the inlet. For this purpose, it was proposed that a series of slots be cut into the dividing wall so that air could be drawn into the flowing water from the air vent. The character of the flow past the dividing wall with the slots is shown in Photos 43 and 44. This design is characterized by the fact that the slots did not work as expected. Because of the somewhat higher pressure in the water passage, water

was ejected through the slots into the air vent rather than air being drawn into the water. The reverse flow through the slots is quite apparent for discharges of 600 cfs (Photo 43) and 1200 cfs (Photo 44).

It appeared from these tests that some sort of a deflector just upstream of the slots would be desirable and necessary to create a pressure difference sufficiently large so that air might be entrained. The initial design provided for a deflector whose cross-section was triangular with equal sides. The pattern of flow in the structure fitted with this deflector was vastly improved, as is shown in Photos 45 and 46. It is apparent from these photographs that no water is being ejected into the air vent; rather, the flow in the water passage appears to be much more homogeneous with a more uniform air concentraion. This is particularly apparent in Photo 46, where the large deflectors are very effective in mixing the air and water. One possible drawback to this deflector is that its abrupt projection into the flow makes it more subject to damage by solid bodies carried by the flow. It was felt that by decreasing the angle on the upstream side it would be easier to deflect any such solid body with less damage to the deflector. At the same time, a test was made to determine if a smaller deflector might be equally effective. For this purpose, a design that projected out only half as far as the original deflector but which was of equal longitudinal length so that it had a considerably smaller upstream angle was proposed. The flow pattern past this deflector is shown in Photos 47 and 48. In Photo 47, which is a close-up of the vertical portion of the drop shaft, the flow in the water passage is relatively smooth, but it appears that there is insufficient air entrainment to thoroughly mix with the flow. The deflection of the streamlines near the wall is not enough to draw in sufficient air through the slot. A somewhat similar condition is shown in Photo 48, where the discharge is 1200 cfs. Although the deflector is effective, it was felt that it should be somewhat larger to make the entrainment of air more positive.

The deflector was modified simply by increasing the size so that its projection into the flow was equal to the original design. It is shown on Chart 16. This is the deflector which was incorporated into the Type E-14 drop structure. The character of the flow past this deflector is shown in

Photos 49 and 50. These photographs also show discharges of 600 cfs with tailwater elevation at 10 ft and 100 ft, respectively. In both of these photographs it is apparent that the revised deflector is very effective in providing a uniform distribution of air in the form of relatively small bubbles that lend themselves to more homogeneous flow. Because of the general appearance of the flow as observed in the experiments, it was proposed that the deflectors used in the Type E-14 drop structure be utilized.

III. OPERATING CHARACTERISTICS OF THE TYPES E-14 AND E-15 DROP SHAFTS

The Type E-14 drop shaft appeared to possess essentially the optimum characteristics for performing the function for which it was designed. It evolved from the previous designs through successive improvements. Following the adoption of the basic design, additional tests were made to establish its operating characteristics.

A. Hydraulic Gradients - Type E-14 and E-15 Drop Shafts

The pressures generated by the flow through the Type E-14 drop structure are shown in Charts 17, 18, and 19 on which the hydraulic gradelines through the structure for different discharges and tailwater elevations have been plotted. The pressures distributions shown in the Charts are typical of those obtained in the previous drop shaft designs in that the pressures are nearly atmospheric, and that deviations from the tailwater level occur only in the sump. The pressures at the bottom of the sump, particularly for the low tailwaters, will be increased appreciably above the tailwater level reaching a maximum of approximately 75 ft when the discharge is 1200 cfs. It should be remembered, however, that the pressures shown in Charts 17, 18, and 19 are average pressures as measured by means of piezometer taps. Superimposed on these average pressures will be the momentary impact pressures that may reach much larger values. It is of interest that the pressures in Taps 16, 17, and 18 which are just outside of the zone of jet impact are greatly reduced, and the effect of the jet is hardly noticeable for a normal discharge of 600 cfs.

The hydraulic gradelines and pressure characteristics for the Type E-15 drop shaft are given in Charts 20, 21, and 22 which are similar to and may be compared with corresponding measurements for the Type E-14 structure given in Charts 17, 18, and 19. As may be expected, the results are almost identical

with the pressures observed in the E-14 drop shaft. The only noticeable difference is at Tap 28 which is located just upstream of the weir for the low tailwater elevation. When the discharge is 1200 cfs and tailwater elevation is 10 ft, the average static pressure at Tap 28 is about 87 ft as compared with 74.5 ft when the weir is in place. This difference is also negligibly small compared to the pressures that will be encountered when the tailwater is very high. In addition, it must be remembered that the pressure fluctuations must be superimposed upon the plotted values.

The experiments indicate that as far as the pressures are concerned the weir at the exit of the sump into the air collector is relatively ineffective and could be eliminated. Further tests are necessary, however, in order to determine whether there are appreciable changes in the impact forces as a result of the removal of this downstream weir.

B. Air Entrainment

The Type E-14 drop shaft is characterized by the use of air slots in the dividing wall. The function of these slots is to feed air into the downflowing stream of water in order to mix with the flow and provide a more homogeneous mixture of air and water to fill the flow section. Photographs show that the air and water are rather uniformly mixed (see Photos 49 and 50). Measurements of the air concentration for various flows in both the Type E-14 and Type E-15 structures were made to determine both the magnitude and the distribution of the air insufflated from the air vent through the air slots.

The air concentration meter used in these measurements consisted of two small parallel plates and associated circuitry attached to a probe that could be inserted into the flow at various elevations through the side of the drop shaft. This device,[1] which has been used in other research, utilizes the fact that the conductivity of air is less than that of water, and consequently the conductivity of the air-water mixture between the two plates depends upon the air concentration. Three measurements were made at each elevation and were

---

[1] Owen P. Lamb and John M. Killen, "An Electrical Method for Measuring Air Concentration in Flowing Air-Water Mixtures." Technical Paper No. 2, Series B, St. Anthony Falls Hydraulic Laboratory, University of Minnesota, March 1950.

averaged to determine the mean air concentration. These data are given in Charts 23 and 24.

In Chart 23, the air concentration distribution throughout the drop shaft for both Type E-14 and Type E-15 are compared for a normal discharge of 600 cfs. It is obvious from the similarity of the distribution graphs for these two structures that the presence or absence of the weir has no effect on the insufflation of air nor on its distribution. The air concentration for a discharge of 600 cfs is about 75 percent in the region above the tailwater level and then drops to a lesser amount (approximately 25 per cent) below the tailwater elevation. The reduced concentration below the tailwater appears to depend upon the tailwater height within the structure. For the low tailwater elevation of 10 ft, the air concentraion tends to increase slightly with depth in the region above the tailwater. This is also apparent when the tailwater is raised to elevation 50 ft, but at higher tailwater elevations this effect is masked by the abrupt drop in air concentration in the region below the tailwater level.

In Chart 24, the air concentrations as measured in Type E-15 for various discharges and tailwater elevations are compared. As might be expected, the air concentrations in the region above the tailwater level are smaller for the larger discharges and larger for the small discharges. However, they are remarkably constant and independent of the discharge in the region below the tailwater level. As in Type E-14, the concentration below the tailwater level is approximately 25 per cent.

C. Hydraulic Gradient through Submerged Drop Shafts

One of the conditions that must be considered in the operation of these structures is the effect of the backwater created by a high tailwater in the event that the tunnel and drop shaft systems are filled with water. In the model the centerline of the incoming tunnel was located at elevation 225 ft, and the bottom of the sump was at elevation zero ft. It was assumed that the tailwater could be increased to elevation 225 ft and thus raise the water surface elevation in the open shaft and in the inlet tunnel.

Photo 51 shows the inlet to the drop shaft when the tailwater elevation has been increased to 190 ft approximately 35 ft below the inlet centerline for

a discharge of 600 cfs. For this situation, the incoming water flows around the inlet section and drops into the pool created by the tailwater. For such a tailwater elevation the pressure within the inlet tunnel is atmospheric so that the shaft is not quite submerged. When the tailwater is raised to 225 ft as shown in Photo 52, however, the water level in the drop shaft rises above the top of the tunnel so that the pressure in the tunnel is greater than atmospheric. The large air cavity shown in the incoming tunnel in Photo 52 is air that has been trapped as the tailwater was raised.

For these tailwater conditions and for various discharges, the piezometric pressures were observed at various points along the vertical and horizontal portions of the drop shaft. These have been plotted in Charts 25 through 27. The charts show the hydraulic gradeline for the various discharges when the tailwater is maintained at elevation 225 ft. The gradeline systematically steepened as the discharge increased, reaching the maximum when the discharge was 1200 cfs. These larger discharges were included only to see how the upstream elevation could change for a larger range of discharges. It is apparent that the hydraulic gradelines for each modification are very similar and are relatively independent of the minor changes that were introduced to improve the flow pattern. For a discharge of 600 cfs, which represents the design flow for this structure, the maximum piezometric pressure was approximately elevation 234 ft; this corresponds to an elevation approximately 4 1/2 ft above the crown or 9 ft above the centerline of the incoming tunnel. For smaller discharges, the effect of submergence is correspondingly reduced. The results show that the head loss through the structure is about 10 ft of water when it flows full at the design discharge of 600 cfs and about 39 ft for a discharge of 1200 cfs.

D. Measurement of Impact Forces in Sump

The drop shaft is over 200 ft deep, and it might be expected that in spite of the resistance offered by the walls there would be an impact on the floor of the sump that must be considered in the design. The magnitude of these impact forces will depend upon, in addition to the resistance of the walls, the tailwater elevation as well as the discharge. If a tailwater exists in the system, it is expected that some of the impact will be absorbed in the pool of water and so be reduced. This impact absorption should increase as the tailwater is increased. In addition, it might be expected that the impact forces would

increase with the discharge through the structure. The effect of the tailwater and discharge upon the impact forces could be readily determined in the model of the drop shaft itself. In order to determine if sidewalls had any effect upon the magnitude of the impact force, supplementary studies were made in an open tank providing for the free fall of the water in the absence of sidewalls for comparison with the measurements in the drop shaft.

1. Impact Model

It was intended that the impact would be measured by means of an electronic pressure transducer mounted in the floor of the sump. These pressure transducers are normally mounted flush with the surface in the area where the measurements are to be made. The size of the transducer, however, was such that flush mounting in the drop shaft sump would be rather difficult and would cover a relatively large area. Adavantage was taken of the supplementary model to compare the measurement of the impact forces using both the flush mounted arrangement and a mounting arrangement in which the transducer was fitted in a block and connected to the impact surface through a small pressure tap. These two mounting arrangements can be seen in Chart 30, which shows both the flush mounted and the block mounted pressure transducer. By using the block mounted cell, the area of impact could be greatly reduced and installation would be simplified. It was necessary, however, to compare measurements made in this manner with those made when the transducer was mounted in the normal manner, flush with the bottom.

The comparison of flush mounted transducers and block mounted transducers was carried out in the tank model, which was sufficiently large for both types of fitting to be used. The tank model was similar to the drop shaft except that the walls of the drop shaft were not present, and the water entering through the inlet dropped freely into the tank, which represented the sump. By adjusting the valve in the drain, the tailwater could be easily varied to correspond to any prescribed value. The inlet system was similar to the inlet of the drop shaft. The transducer was mounted directly below the inlet section so that the water falling freely from the inlet would impact in the tailwater pool directly above the pressure transducer. The arrangements for the tank model and its appurtenances are shown in Chart 30.

Typical measurements of the pressure fluctuation on the bottom of the tank model with a flush mounted transducer are shown in Charts 28 and 29. In Chart 28, the tailwater is at zero elevation and measurements were made for discharges of 300, 600, 1200, and 1800 cfs. The nature of these pressure fluctuations and their magnitudes can be seen from the typical records. The The separate peaks in the record for the small discharges are caused by the normal irregularity of the jet as it falls into the tank, occasionally impacting on the transducer or at the side of the transducer. The peak value of the impact force is approximately 200 ft. As the discharge increases, the jet becomes more solid, and there are more frequent impacts upon the pressure transducer. Peak values for these discharges are in some cases appreciably greater than 200 ft. In Chart 29, the tailwater elevation has been increased to 50 ft. The results show that for this tailwater, most of the impact forces are absorbed by the water in the pool and are greatly reduced on the bottom of the sump.

In order to make a quantitative comparison of the pressure fluctuations and impacts as measured by the flush mounted transducer and the block mounted transducer, the peak pressures as recorded on a representative section of recorder charts were counted and compared. Over a given section of tape, the number of peaks that were equal to or exceeded various magnitudes were counted for each discharge and various tailwater elevations. These results are shown in Chart 30, which shows the number of peaks for both the flush mounted and block mounted pressure cells in comparison. The ratio of the peak pressures for the flush mounted transducer to the peak pressures of the block mounted arrangement are plotted for each tailwater elevation on the Chart. Although this ratio varies approximately 10 per cent, it is rather uniformly distributed about the ratio of 1 for all tailwater elevations, and shows that on the average, these peaks are very similar for both the flush mounted and the block mounted arrangement. It may be concluded from these initial studies that the transducer mounted in a block as shown in Chart 30 will give results that are fully equivalent to those obtained with the flush mounted transducer.

2. Measurement of Impact Forces in Type E-14 and Type E-15 Drop Shafts

Records of the measurements of impact forces on the bottom of the sump in the drop shaft model are shown in Charts 31 and 32 for the Type E-14 drop shaft, and Chart 33 for the Type E-15 drop shaft. The portions of the pressure

records are typical of those obtained, although longer records are necessary and were used to obtain more quantitative data.

Several pressure taps had previously been installed in the bottom of the sump to measure the static pressures. These were used to attach the pressure transducer so that the impact at different points on the bottom of the sump could be measured and compared. In this way, a better estimate of the maximum forces could be made. The records shown in the charts indicate that the pressure fluctuation is similar at each tap, so presumably they represent the maximum impact forces. Measurements were made for three different discharges, including a discharge of 1200 cfs. This is considerably greater than the design discharge as determined from other experiments, but these measurements were made in order to see whether excessive impacts would result for discharges beyond the capacity of the drop shaft. The maximum values of the impact forces occur when the tailwater elevation is a minimum, as shown in Chart 31. The peak values decrease again as the tailwater elevation is increased, until they are practically negligible when the tailwater reaches an elevation of 50 ft. This is shown in Chart 32. These results may be compared with those shown in Chart 33 which were observed in the Type E-15 drop shaft.

The result of an analysis of the pressure record for the Type E-15 drop shaft is shown in Chart 34. The number of peaks per minute equal to or greater than the indicated elevation for a discharge of 600 cfs and for various tailwaters is for comparison. The results, as would be expected, indicate that the frequency of peaks of certain magnitude is greater at Tap 27, which is in the center of the sump, than at either Taps 26 or 28. The graphs show that although the frequency of these impacts was very low, there were some whose magnitude approached the height of the drop shaft.

In Chart 35, a direct comparison has been made between the results at Tap 27, for Types E-14 and E-15 drop shaft and the impact model. In all cases the pressure transducer was mounted in a block and connected by means of a small tube to the bottom of the sump. The comparison is reasonably good. The results show that without the weir at the exit of the sump, as in Type E-15, the frequency of the peak values of 75, 100, and 125 ft are considerably greater than in Type E-14, in which a weir is installed. The maximum values, however, are very similar in frequency, and it appears that the weir has

relatively little influence upon impacts of this magnitude. The comparison between the pressure measurement in Types E-14 and E-15 with the impact model shows that both the magnitude and the frequency of the impacts are very similar, and that the sidewalls in the drop shaft have relatively little effect in reducing the magnitude of the impact on the floor of the sump.

The results show that the maximum impact pressures occur for the lowest tailwaters and the highest discharges. For a given discharge, these impact forces decreased as the tailwater elevation was increased. For a given tailwater, the impact pressures increased as the discharge increased. The results also show that impact pressures having the same magnitude as the total drop through the drop shaft occurred particularly for the low tailwaters. The impact pressures were very similar in Type E-14 and in Type E-15 drop shafts. It appeared that the variations that did occur were the result more of the random nature of the flow down the drop shaft than of a difference in the drop shaft arrangement. This was particularly so for the higher tailwaters, since there were significant differences in frequency of impact of small magnitudes. This indicated that the pool was effective in absorbing these small impacts as compared to the case without the weir. On the other hand, the frequency of the maximum impact pressure was very similar for both types.

IV EFFECT OF DOUBLE INLET ON DROP SHAFT OPERATIONS

This section gives the results of experiments with the drop shaft fitted with two inlet conduits. It had been proposed that in certain instances several inlet conduits might feed a single drop shaft in the prototype. These inlets might enter the shaft from different directions and introduce the flow unsymmetrically into the drop shaft. The inlets might also operate simultaneously or separately, depending upon the local runoff condition. The multiple inlets were restricted to drop shats designed for the smaller discharges. In order to examine the effect of such inlets upon the flow pattern within the drop shaft, some additional experiments with specified relative discharges were made with the apparatus modified to accommodate two inlets.

The second inlet was fitted to the drop shaft at a point 35 ft above the original inlet. The angles of the inlets with respect to the dividing wall could be varied to simulate various prototype conditions. The model drop shaft

corresponded to the prototype drop shaft whose diameter was 6 ft 8 in. This required a scale ratio of 1:20. Using the basic Type E-14 drop shaft, the lower inlet was at elevation 166.7 ft at the new scale ratio relative to the bottom of the sump as elevation zero ft. The upper inlet was at elevation 201.7 ft.

Three entrance arrangements were tested. In the Type F structure, shown in Chart 36, the inlet conduits were 60 degrees apart and entered the drop shaft at angles of 30 degrees to the dividing wall. In Type F-1 (Chart 37), these angles were 45 degrees with a total separation of 90 degrees for the inlet. In Type F-2 (Chart 38), the lower or larger inlet conduit was normal to the dividing wall and the smaller or upper conduit entered the drop shaft 90 degrees from the lower conduit and parallel to the dividing wall. In all cases, the lower conduit was the same size as the drop shaft, that is 6 ft 8 in., while the upper conduit was only half as large, or 3 ft 4 in. The discharges varied up to a maximum of 150 cfs in the lower conduit and 100 cfs in the upper conduit. Tests were made of various combinations of discharge in the two inlets to observe the influence, if any, of these discharges upon the flow pattern.

The incoming flow in the Type F structure was diverted by the dividing wall to the side of the drop shaft and tended to form a vortex in the drop shaft. The diagonal flow created by the upper inlet can be seen in Photo 53. Since the lower inlet conduit approaches the drop shaft from the opposite direction, these transverse components tend to counteract those from the upper inlet, so that below the lower inlet the flow is much more regular and the secondary components are considerably smaller. When the tailwater is raised to elevation 180 ft, as shown in Photo 54, the flow pattern is essentially submerged and the secondary currents are greatly reduced. The flow below the lower inlet is therefore relatively straight and understood. The pressure profiles as measured for this geometry are shown in Chart 36. They show that there is essentially no effect on the flow pattern below the inlets as a result of this combination.

When the inlet conduits are spread further apart the secondary currents become more intense and, as shown in Photo 55, extend below the lower inlet. There is, however, no evidence that the secondary current reached the sump or

influenced the flow as it entered the sump from the drop shaft. Again, when these secondary effects are largely submerged, a typical flow pattern results which is similar to the previous observations of low discharges on a structure with a single inlet. The geometry of the Type F-1 and the pressure measurements as measured for various discharges in this arrangement are shown in Chart 37. As before, this combination of inlets has practically no influence upon the pressure distribution along the drop shaft and the exit tunnel.

For the Type F-2, the upper inlet enters the drop shaft in a direction parallel to the dividing wall. The jet from the inlet pipe then strikes the opposite wall and generates a still more intense secondary current. This can be seen in Photo 57, where the diagonal flow in the region above the lower inlet is shown. The lower inlet, however, is perpendicular to the dividing wall, and the jet from this conduit is more or less equally divided by the dividing wall. When the discharge is equal or greater than that from above, this flow rather effectively counteracts the secondary currents from the upper inlet and reduces the rotational intensity. In Photo 57 the diagonal currents below the lower inlet can also be seen in the photograph. Photo 58 shows the effect of submerging the structure on these diagonal currents. The submergence quite effectively damps out the nonsymmetrical flow and provides a smooth inlet into the sump. Chart 38 shows that the pressure distribution below the lower inlet is not changed by adding an inlet above the original.

The results of these tests in which relatively small discharges were applied to a drop structure having two inlets at various angles from each other indicate that such an arrangement has very little influence upon the flow pattern below the region of the inlet conduits. The downward flow through the drop shaft rather quickly absorbs these secondary effects, so that as it approaches the sump the flow pattern is quite uniform. No evidence of the divided flows at the inlet was apparent within the sump itself nor in the outlet conduit as the water flowed through the pipe to the main tunnel.

V. WATER LEVEL SURGING IN DROP SHAFT SYSTEM

This section describes the results of experiments on surging in the drop shafts when the flow to the system is restricted to only one inlet. When the tailwater in a series of drop shafts is appreciable, an inflow of sufficient magnitude in one of the drop shafts will cause the water to surge up and down

in the others. It was the purpose of these experiments to measure these surges in terms of the magnitude and duration of the inflow discharge. For this purpose the surge model was constructed and instrumented so that the surging of the water level in each of the drop shafts could be recorded simultaneously on a recorder chart. These experiments were arranged in a relatively simple pattern so that the results could be used to verify a computer program designed to predict the surging in the much more complicated prototype structure. If the computer results applied to the simple model agree with the measurements made on this model, it can then be used to predict the surging characteristics of the prototype.

Portions of the recorder charts that record the surging are presented from which measurements concerning frequency of surges and frictional resistance can be made in the drop shafts and the main tunnel. The instantaneous elevations of the water surface were measured by recording the signal from a two-wire capacitance type wave probe which is shown fitted to drop shaft 1 in Photo 59. The two parallel wires extend throughout the depth of the drop shaft with the connections to the recorder at the top. A close-up of the lower portion of drop shaft 1 showing the water surface and the parallel wires in more detail is given in Photo 60. In this experiment the discharge was 600 cfs and the tailwater elevation was maintained at 50 ft. Photo 61 shows the discharge being introduced in the Type B surge model at drop shaft 3. The flow, as it drops down the shaft, becomes highly aerated, and the surge created by this flow is transmitted to the remaining drop shafts. Photo 62 is a close-up of the aerated water in this drop shaft. The fluctuations in the water surface as measured in these experiments and recorded on the tape are presented in charts below.

The surging in the Type A surge model for a discharge of 600 cfs and various tailwater elevations is given in Charts 39 through 41. Three discharges--300, 600, and 1200 cfs--and two tailwater elevations, 10 ft and 100 ft, were tested. In one run the inflow discharge duration was limited to 10 sec to observe the effect of the rising discharge in association with the decreasing discharge. The chart for each drop shaft gives the sequence of water surface elevations as the discharge is suddenly turned on and equally suddenly stopped. A comparison of the four records for each chart shows how

the surge was propagated down the tunnel and shows the attenuation of this surge with distance down the tunnel. In Chart 39, the results for a discharge of 600 cfs with a tailwater at elevation 10 ft are shown, and Chart 40 gives the results for the same discharge but with the tailwater increased to 100 ft. The charts show the sudden increase in the water surface elevation shortly after the valve was opened and the gradual damping of the surge until it approaches an equilibrium. When the discharge is suddenly shut off, there is a momentary drop in the water surface elevation in each of the drop shafts with a gradual damping of the wave as it settles down to approach the controlled tailwater. A comparison of Charts 39 and 40 shows that the initial surges are very similar, but that the surges in the drop shafts when the water is suddenly turned off are considerably more drastic for the high tailwater. For the low tailwater the maximum surge occured at the initial inflow in drop shaft 3 where the water surface rose approximately 26 ft in approximately 30 seconds at the prototype scale. Chart 40 also shows the greatly increased surging that occurs for the high tailwater when the water is suddenly cut off. Here a drop in the water surface of approximately 22 ft occurred very rapidly. In Chart 41, the surging record is shown considerably compressed with respect to time, since the duration of flow was shortened to 10 sec in the model. The surging pattern appears to be very similar except that the sudden drop in elevation occurs close to the initial rise.

In the Type B surge model, the measurements of the surging for corresponding discharges and tailwaters are shown in Charts 42 through 44. In this case, since the inflow occurred in drop shaft 3, the surges were propagated in both directions in the tunnel. At the upstream end the tunnel was closed so that the surge would be reflected from the upstream bulkhead. This is reflected in the traces generated at drop shafts 1 and 2. At the downstream end of the tunnel the flow entered and passed the tailwater control box so that there was relatively little reflection of the surge. This is shown by the records obtained from drop shafts 4 and 5, which in general are considerably less in amplitude than those on the upstream side. The results are similar to those obtained in the Type A model for equivalent distances from the drop shaft into which the water is flowing. In Chart 43, the effect of tailwater elevation on the terminal surge when the discharge is stopped is clearly shown. The effect of shortening the duration of use as shown in Chart 44 is similar to

that observed in superposition of the two events in the very sudden change in direction of motion of the water surface elevation when the valve is closed.

Measurements of water surface elevations at various points along the tunnel could not be made accurately with the recorder. In order to determine the frictional characteristics of the system and water surface elevations for steady flow, piezometer taps and connections were attached to each drop shaft and carried to a common manometer board. For the same discharges and tailwater elevations and for steady flow the water surface elevations were measured at these points. From these data friction coefficients and hydraulic gradelines could be determined. These results are given to the model scale in Chart 45. These data are necessary in order to introduce the frictional coefficients into the computer program. It appears from the results that the friction factor in the Darcy formula is rather high for a smooth surface and possibly represents the effect of the drop shaft connections with the main tunnel.

VI. CONCLUSIONS

The experimental studies of the drop shafts to be used for the Lawrence Avenue Sewer System were concerned with the experimental design so that the tests were made in an attempt to develop an optimum system within the restrictions prescribed by its application. The results of these studies and experiments lead to the following conclusions:

(1) The experiments showed that the air vent could be effectively incorporated into the drop shaft proper and thus would eliminate the necessity of constructing a separate air vent.

(2) The presence of the air vent within the drop shaft provided a means by which air could be more uniformly insufflated into the flowing water with a resulting greater homogeneity of the flow.

(3) The impact pressures on the bottom of the sump were of the same magnitude as the height of fall when the tailwater was very low and were significantly reduced as the tailwater was increased to approximately 50 ft. The weir at the exit of the sump reduced the impact for very low discharges when the tailwater was a minimum. For the design discharge the weir had little effect in reducing the impact pressures and was somewhat detrimental for the

removal of the air from the air collector. The experiments showed that the system would operate approximately equally well with or without the weir at the exit of the sump.

(4) An air collector with a steeply sloping roof was necessary to provide for the separation of the air from the water and permit its release to the atmosphere. The final design, Type E-14, resulted in an effective air collector which prevented air from being carried into the downstream tunnel.

(5) The pressure gradients through the system were quite normal and showed that the pressures in the drop shaft were essentially atmospheric except in the region of the sump, where impacts of considerable magnitude were experienced on the floor of the sump.

(6) When the drop shaft is submerged by high tailwater, a pressure drop of approximately 9 ft through the structure occurred for the design discharge of 600 cfs. This increased to 39 ft when the discharge was 1200 cfs.

(7) The experiments showed that multiple inlets could be used without introducing detrimental flow patterns within the drop shaft. The inlet arrangements were such that in general the jets from each inlet counteracted the secondary currents generated by the other inlets, so that the flow was reasonably uniform as it approached the sump.

(8) Experiments in the surge model showed that if the inflow to the system is restricted to only one drop shaft, as may occur, it may rise to surge waves which are propagated through the system. This is more pronounced for the higher tailwaters, for which the main tunnel and a portion of the several drop shafts are filled with water.

LIST OF PHOTOS

PHOTO 1 (Serial No. 177-3) The drop shaft model was fabricated of a transparent plastic so that the flow patterns could be observed. The photograph shows the relative size of the model and its characteristic features.

PHOTO 2 (Serial No. 177-6) The piezometric pressures at various points along the drop shaft were measured by means of piezometric taps connected by tubing to a manometer board on which the pressures could be observed. The scale of the model is 1:27 and represents a drop shaft structure approximately 225 ft high.

PHOTO 3 (Serial No. 177-416) An overall view of the Type A surge model shows the length of the tunnel and the location of the drop shafts which were spaced at 20 ft intervals in the model. The inlet is at drop shaft 1 so that any surges generated could be propagated the entire length of the model tunnel.

PHOTO 4 (Serial No. 177-420) This is an overall view of the Type B surge model, which is similar to that shown in Photo 3 except that the flow is introduced in the center of the model at drop shaft 3. In this event any surges that are generated can be propagated in both directions in the tunnel.

PHOTO 5 (Serial No. 177-18) A discharge of 600 cfs entering the drop shaft follows the inlet curve quite smoothly to the point where the accelerations are such that the water begins to leave the jet and impinge upon the opposite wall. The air is insufflated at the top and the flow in general is quite irregular and highly turbulent.

PHOTO 6 (Serial No. 177-19) At the bottom of the drop shaft for a discharge of 600 cfs and a tailwater of only 10 ft, the masses of water plunge into the sump and, in this test, into the impact cup which is effective in breaking up the jet and creating a highly turbulent mixture of air and water. The air is separated from the flow in the air collector and is discharged into the atmosphere through the adjacent air vent. The air and water are not well mixed in the drop shaft itself.

PHOTO 7 (Serial No. 177-26) When the discharge is increased to 1200 cfs in the Type A drop shaft, the jet separates from the inlet curve and impinges on the far wall with the development of secondary currents in the drop shaft. A relatively large amount of air is entrained, but the character of the flow is such that the air is not thoroughly mixed with the water. The tailwater of 100 ft causes the air rising in the air vent to be mixed with the water to create a frothy mass through which large bubbles of air are carried.

PHOTO 8 (Serial No. 177-27) This is a view of the lower portion of the drop shaft for the discharge of 1200 cfs in the Type A structure. The flow was highly aerated and turbulent in the sump. This type of air collector, in combination with the impact cup, is effective in separating the air from the outgoing flow.

PHOTO 9 (Serial No. 177-30) The Type B drop shaft is characterized by a longitudinal divider wall which eliminates the external air vent. For a discharge of 300 cfs through this structure, there is relatively little entrainment of air and the water falls freely through the shaft into the sump. Since the tailwater is very low, the air vent is clear and air can pass freely out of the structure.

PHOTO 10 (Serial No. 177-31) This photograph shows the lower portion of the Type B drop shaft for a discharge of 300 cfs. It is quite effective in dissipating the drop shaft energy and separating the air from the water in the sump and air collector.

PHOTO 11 (Serial No. 177-44) In this photograph the discharge has been increased to 1200 cfs in the Type B drop shaft and the tailwater raised to 100 ft. This discharge effectively seals the upper portion of the drop shaft so that the drop shaft is closed. Relatively large quantities of air are insufflated into the turbulent flow created by the jet striking the far wall. Although the air is more uniformly distributed there are still relatively large volumes of air-free water dropping down the shaft.

PHOTO 12 (Serial No. 177-45) The lower portion of the Type B drop shaft is shown in this photograph, which clearly shows relatively large regions of clear water and the intervening spaces filled with highly agitated air-water mixture. The sump and impact cup are relatively effective in removing the air from the flow, so that only a small quantity of air enters the downstream tunnel. The air vent is also highly turbulent, and large bubbles of air rise intermittently through the foamy mixture.

PHOTO 13 (Serial No. 177-70) The Type C-3 drop shaft is characterized by the removal of the impact cup and the installation of a 12-ft weir at the inlet to the air collector. This photo shows the character of the flow for 300 cfs in the sump and over the weir. Because of the low tailwater, the jet penetrates to the bottom of the sump, where the turbulence effectively mixes the air and the water.

PHOTO 14 (Serial No. 177-72) When the tailwater is increased to 190 ft, the insufflated air is easily removed in the sump and both the downward flowing water-air mixture and the air vent are uniformly mixed.

PHOTO 15 (Serial No. 177-73) This photograph shows the character of the flow down the drop shaft and the functioning of the sump and air collector for a discharge of 600 cfs and a low tailwater.

PHOTO 16 (Serial No. 177-75) When the tailwater is increased to 190 ft for the same discharge in the Type C-3 drop shaft, the flow down the shaft and in the sump is relatively calm and the small amount of insufflated air is easily separated.

PHOTO 17 (Serial No. 177-76) A discharge of 1200 cfs in the Type C-3 drop shaft is extremely rugged and highly aerated when the tailwater is maintained at only 10 ft. A large quantity of air is transported into the downstream tunnel, and the flow in this area is generally unsatisfactory.

PHOTO 18 (Serial No. 177-78) When the tailwater is increased to 150 ft, the flow characteristics in the lower part of the Type C-3 drop shaft are considerably improved and the air reaching the downstream tunnel is very appreciably reduced.

PHOTO 19 (Serial No. 177-93) When the tailwater is raised to 190 ft, which is nearly to the top of the drop shaft, little air is entrained and it is easily removed in the sump and air collector.

PHOTO 20 (Serial No. 177-108) As the discharge is increased, however, the large volume of water seals off the air collector so that air separated from the flow cannot escape into the air vent. This forces the water level in the air collector down, and much air escapes into the downstream tunnel.

PHOTO 21 (Serial No. 177-80) In this photograph the tailwater has been raised to 100 ft. In spite of this, the high weir and discharge of 600 cfs tend to restrict the escape of air up the air vent, causing the water level in the air collector to be forced downward nearly to the crown of the tunnel, with the result that a considerable amount of air enters the tunnel.

PHOTO 22 (Serial No. 177-88) This condition, as described above, is greatly improved when the height of the weir is reduced to 8 ft. In this case, more air can escape back to the air vent. The lower pressure permits the water level in the air collector to rise toward the top of the collector, and no air can escape into the tunnel.

PHOTO 23 (Serial No. 177-114) For a discharge of 1200 cfs and a tailwater of 10 ft, the air collector is quite ineffective. This discharge appears to be beyond the capacity of the structure, and all the air can freely enter the downstream tunnel.

PHOTO 24 (Serial No. 177-116) In this photograph, the weir between the sump and the air collector has been completely removed. The large discharge of 1200 cfs sweeps through the air collector and carries all the air into the downstream tunnel.

PHOTO 25 (Serial No. 177-119) By providing an air vent from the air collector itself, the pattern of the air removal is greatly improved. For this condition, the height of the weir is 8 ft so that air can be released through both the air vent and the special vent on the air collector.

PHOTO 26 (Serial No. 177-120) In this test, the air vent was placed at the downstream end of the air collector and appears to be equally effective in the removal of air.

PHOTO 27 (Serial No. 177-178) When the tailwater is raised to elevation 100 ft, the air collector is effective in removing air from the flow and venting it up the air vent. It appears that the Type E structure is relatively effective in its initial design.

PHOTO 28 (Serial No. 177-189) In an attempt to shorten the air collector of the drop shaft the sloping portion was removed and a discharge of 600 cfs with a tailwater elevation of 100 ft was passed through the structure. The photographs show that a large separation zone occurs at the inlet to the downstream tunnel and that large quantities of air escape through it.

PHOTO 29 (Serial No. 177-198) In Type E-2 the horizontal portion of the air collector was shortened and the sloping section was replaced. This improved the flow pattern, and relatively little air escaped into the downstream tunnel. Here the discharge was again 600 cfs with a tailwater at elevation 100 ft.

PHOTO 30 (Serial No. 177-205) In Type E-7 drop structure the sloping portion was placed on top of the horizontal section with the thought that by providing a larger cross-section in this area, the air might more freely escape to the atmosphere through the air vent. The photograph shows, however, that this type is not effective in preventing the air from entering the downstream tunnel.

PHOTO 31 (Serial No. 177-219) In Type E-11 a faired entrance into the downstream tunnel was provided in order to prevent the separation at the inlet to the tunnel. The photograph shows that for a discharge of 600 cfs and tailwater at elevation 100 ft this device was also ineffective in preventing air from escaping into the tunnel.

PHOTO 32 (Serial No. 177-221) In Type E-13 the inward projection was extended to the roof of the air collector without any apparent improvement in the functioning of the air collector. The photograph shows the air escaping around the projection into the downstream tunnel.

PHOTO 33 (Serial No. 177-233) When the discharge is 600 cfs, the design capacity of the drop structure, considerably more air is entrained. But even when the tailwater is lowered to elevation 10 ft air is separated from the water and prevented from entering into the downstream tunnel.

PHOTO 34 (Serial No. 177-235) For a discharge of 600 cfs with tailwater at 50 ft the Type E-14 air collector effectively removes the air from the water and provides easy access to the air vent.

PHOTO 35 (Serial No. 177-237) When the tailwater is increased to 100 ft for a discharge of 600 cfs, the structure operates efficiently. With this high tailwater the jet still penetrates to the bottom of the sump.

PHOTO 36 (Serial No. 177-239) When the tailwater is raised to 190 ft the air concentration is greatly reduced and the jet no longer penetrates to the bottom of the sump. For these tailwaters air is easily removed from the mixture and released through the air vent.

PHOTO 37 (Serial No. 177-245) When the discharge is increased to 1200 cfs, much air escapes into the downstream tunnel even though the tailwater is at elevation 50 ft. This shows that a discharge of 1200 cfs is beyond the capacity of this drop structure design.

PHOTO 38 (Serial No. 177-247) Even when the tailwater is raised to elevation 100 ft the air collector cannot separate the air from the flow for a discharge of 1200 cfs. Here again an appreciable portion of the air can escape into the downstream tunnel.

PHOTO 39 (Serial No. 177-263) For a discharge of 600 cfs and the tailwater maintained at elevation 10 ft the Type E-15 successfully removes the air from the flow. A comparison with Photo 33 shows that the essential difference in flow pattern is that the highly insufflated air penetrates further into the air collector at a lower elevation.

PHOTO 40 (Serial No. 177-265) When the tailwater has been raised to elevation 50 ft the effect of the weir is less noticeable and the entrained air quickly rises to the top of the air collector so that none can escape into the downstream tunnel.

PHOTO 41 (Serial No. 177-38) With a solid wall deflector all the air must be entrained at the inlet to the drop shaft with a consequent irregular non-uniform flow. The regions of solid water and entrained air are clearly defined in this photograph.

PHOTO 42 (Serial No. 177-45) This photograph shows the character of the flow past the solid dividing wall at the lower portions of the drop structure. The tailwater elevation has been increased, so that large gulps of air are being released up the air vent.

PHOTO 43 (Serial No. 177-124) In this photograph, the flow past the slotted dividing wall without the deflector is shown. It shows the jets of water being forced through the slot to strike the opposite wall of the air vent. Also to be observed in this photograph is a relative non-uniformity of the flow in the water passage.

PHOTO 44 (Serial No. 177-138) When the discharge is increased to 1200 cfs through the structure with a divider wall with slots only, the jets through the slots are more intense and the flow is rather non-uniform.

PHOTO 45 (Serial No. 177-197) In this photograph is a discharge of 600 cfs through the structure with the original deflectors over the air slots. The flow pattern is considerably improved, and no water escapes through the slots into the air vent.

PHOTO 46 (Serial No. 177-201) For a discharge of 1200 cfs with the original deflectors in place, the flow is very uniform and the air is uniformly distributed.

PHOTO 47 (Serial No. 177-151) In this photograph is shown the flow past the smaller modified deflector. Although the flow appears to be rather uniform with a uniform air distribution, it appears that the deflection past the slots is relatively small and apparently ineffective.

PHOTO 48 (Serial No. 177-162) This shows the flow past the small deflectors in the lower region of the drop shaft. Again the air concentration appears to be well distributed, but the deflection of the streamlines at the deflector is negligibly small.

PHOTO 49 (Serial No. 177-232) This is a view of a larger asymmetrical deflector designated E-4. It shows the flow pattern when the discharge is 600 cfs.

PHOTO 50 (Serial No. 177-236) In this photograph the discharge is 600 cfs with a tailwater at elevation 100 ft. The flow past the wedges serving as deflectors is quite smooth and uniform.

PHOTO 51 (Serial No. 177-269) When the tailwater elevation is raised to 190 ft, which is somewhat below the elevation of the incoming tunnel, the discharge of 600 cfs flows smoothly around the inlet and into the drop shaft proper. As it flows into the drop shaft, air is entrained and mixed with the water. The pressures in the incoming tunnel are atmospheric and the water surface represents the hydraulic gradeline.

PHOTO 52 (Serial No. 177-272) When the tailwater is raised to 225 ft, however, the piezometric pressures in the upstream tunnel are increased and except for the entrapment of air in this tunnel, it would run full, since the piezometric pressures are above the top of the tunnel.

PHOTO 53 (Serial No. 177-474) In the Type F structure the upper and lower inlet conduits are 60 degrees from each other and symmetrical with the perpendicular from the dividing wall. This asymmetric flow at the two inlets generates secondary currents in opposite directions that tend to counteract each other in the region below the lower

inlet conduit. They can be seen, however, in the region between the inlet conduits where the entrained air delineates the diagonal currents. It appears that these secondary currents are largely eliminated as the water enters the sump below.

PHOTO 54 (Serial No. 177-477) When the tailwater is raised to elevation 180 ft, the lower inlet and most of the drop structure up to the upper inlet are submerged with a consequent significant reduction in the secondary currents. The photograph shows that for this tailwater elevation the flow pattern is quite straight and parallel to the drop shaft walls.

PHOTO 55 (Serial No. 177-493) In the Type F-1 structure the inlet conduits are separated by 90 degrees. This larger separation tends to increase the intensity of the secondary currents which are apparent in the region between the inlet conduits. Even these, however, are effectively dissipated as the flow proceeds down the drop shaft.

PHOTO 56 (Serial No. 177-494) The increased tailwater raised to elevation 180 ft is sufficient to reduce the secondary current, with the result that the flow below the lower inlet is relatively undisturbed.

PHOTO 57 (Serial No. 177-511) The effect of the secondary current from the upper inlet is further strengthened when the inlet conduit enters the drop shaft parallel to the dividing wall. The jet strikes the opposite corner and is strongly deflected around the curved wall of the drop shaft proper. These secondary currents between the inlets are clearly shown in the photograph.

PHOTO 58 (Serial No. 177-512) When the tailwater is raised to elevation 180 ft, the secondary currents generated by the upper inlets are absorbed by the tailwater and the symmetrical flow from the lower inlet.

PHOTO 59 (Serial No. 177-424) This photo shows the drop shaft and the attachment of the two-wire capacitance type wave recorder by means of which the water surface fluctuation could be measured. In this experiment the discharge is 600 cfs and the tailwater is 50 ft.

PHOTO 60 (Serial No. 177-425) This is a close-up of the drop shaft shown in Photo 59. The two wires of the wave recorder can be clearly seen.

PHOTO 61 (Serial No. 177-428) This shows a discharge of 600 cfs into drop shaft 3 when the tailwater is at elevation 50 ft. The incoming flow causes the water in the system to become highly aerated and turbulent.

PHOTO 62 (Serial No. 177-429) This is a close-up at the lower end of the drop shaft for the conditions shown in Photo 61.

PHOTO 1 (Serial No. 177-3) The drop shaft model was fabricated of a transparent plastic so that the flow patterns could be observed. The photograph shows the relative size of the model and its characteristic features.

PHOTO 2 (Serial No. 177-6) The piezometric pressures at various points along the drop shaft were measured by means of piezometric taps connected by tubing to a manometer board on which the pressures could be observed. The scale of the model is 1:27 and represents a drop shaft structure approximately 225 ft high.

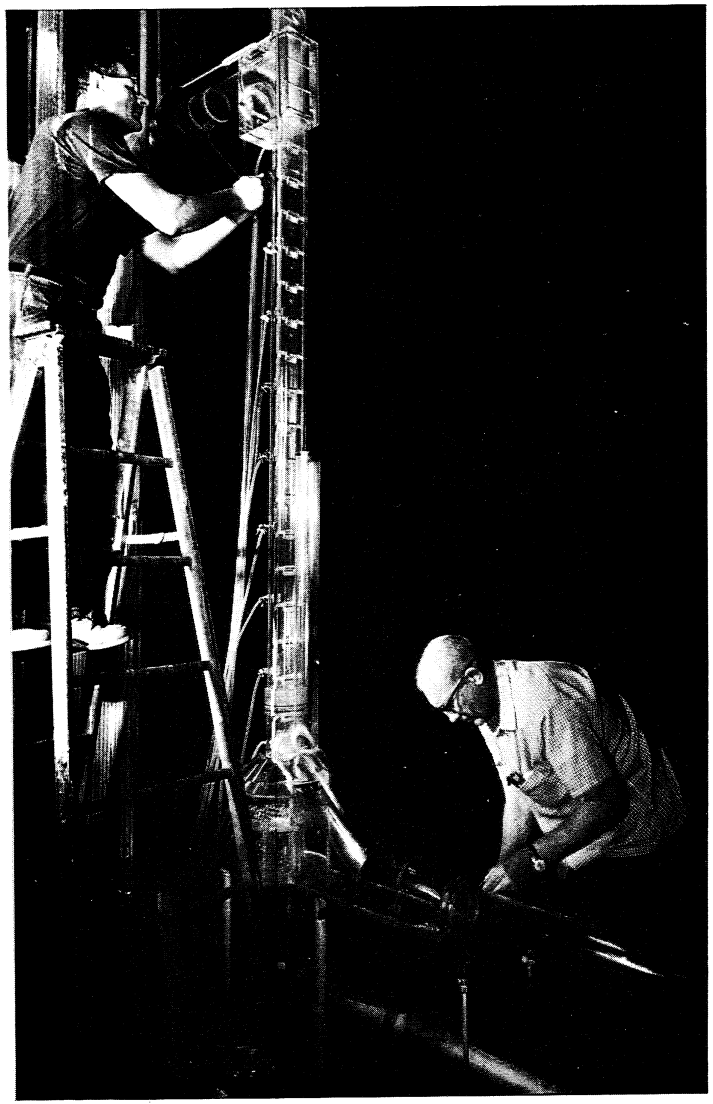

Photo 1

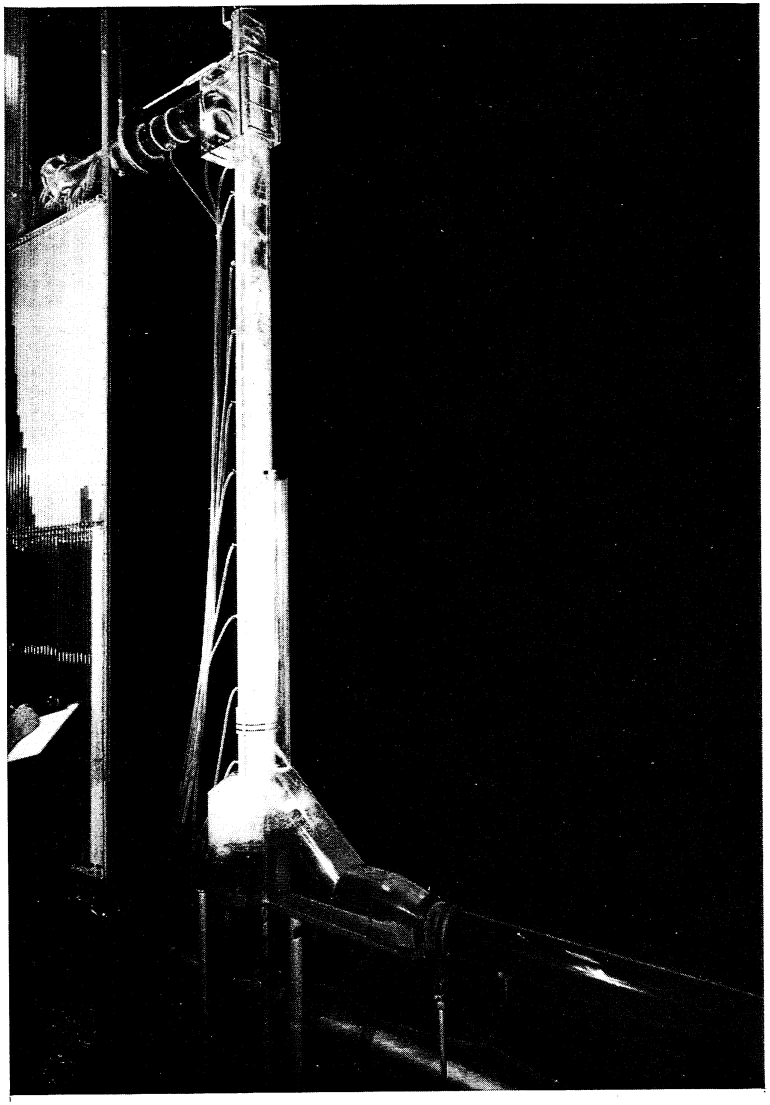

Photo 2

PHOTO 3 (Serial No. 177-416) An overall view of the Type A surge model shows the length of the tunnel and the location of the drop shafts which were spaced at 20 ft intervals in the model. The inlet is at drop shaft 1 so that any surges generated can be propagated the entire length of the model tunnel.

PHOTO 4 (Serial No. 177-420) This is an overall view of the Type B surge model, which is similar to that shown in Photo 3 except that the flow is introduced in the center of the model at drop shaft 3. In this event any surges that are generated can be propagated in both directions in the tunnel.

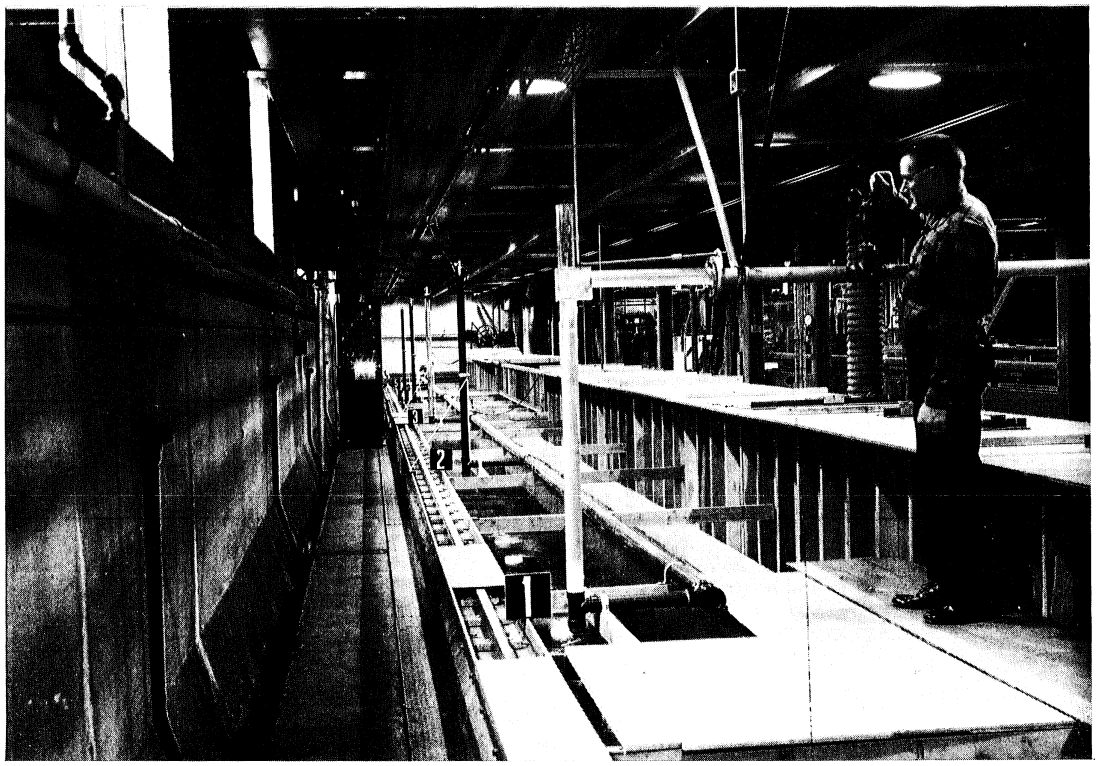

Photo 3

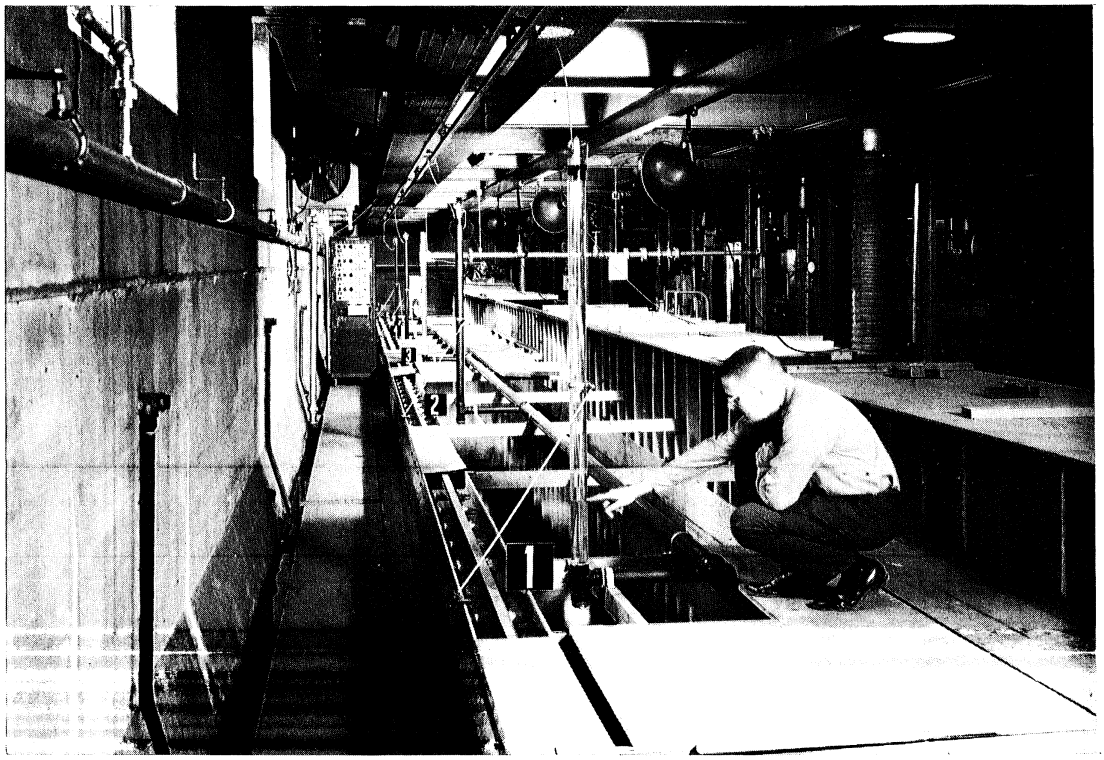

Photo 4

PHOTO 5 (Serial No. 177-18) A discharge of 600 cfs entering the drop shaft follows the inlet curve quite smoothly to the point where the accelerations are such that the water begins to leave the jet and impinge upon the opposite wall. The air is insufflated at the top and the flow in general is quite irregular and highly turbulent.

PHOTO 6 (Serial No. 177-19) At the bottom of the drop shaft for a discharge of 600 cfs and a tailwater of only 10 ft, the masses of water plunge into the sump and, in this test, into the impact cup which is effective in breaking up the jet and creating a highly turbulent mixture of air and water. The air is separated from the flow in the air collector and is discharged into the atmosphere through the adjacent air vent. The air and water are not well mixed in the drop shaft itself.

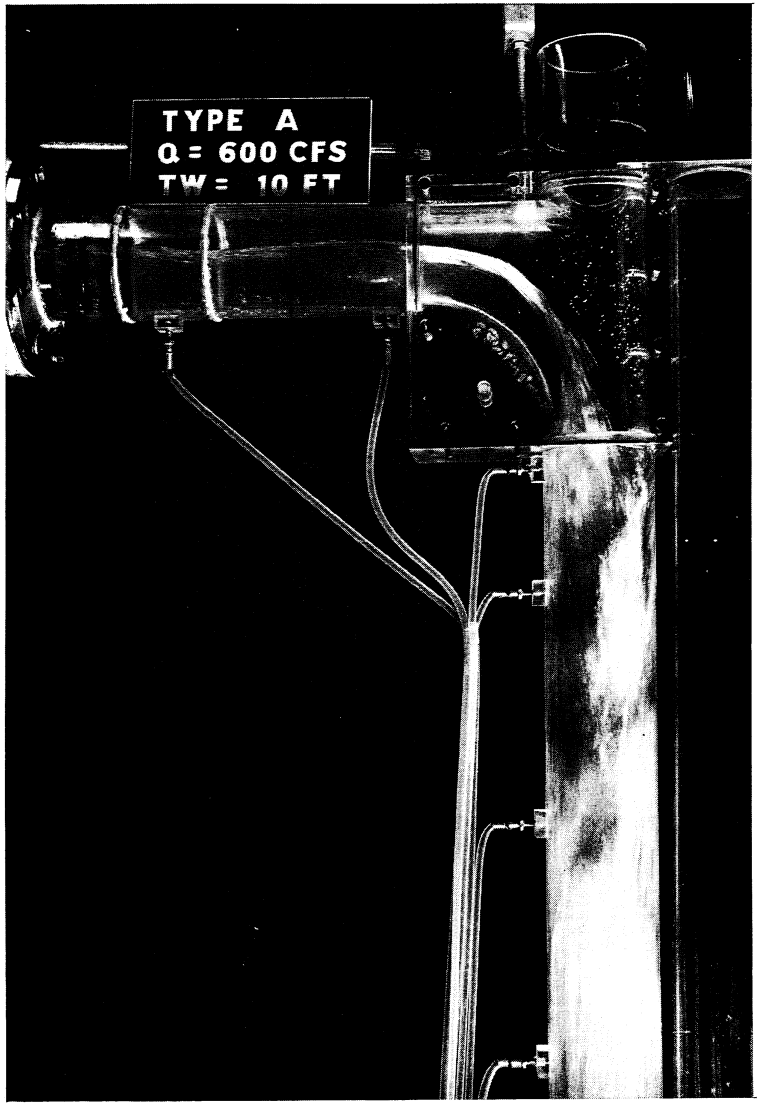

Photo 5

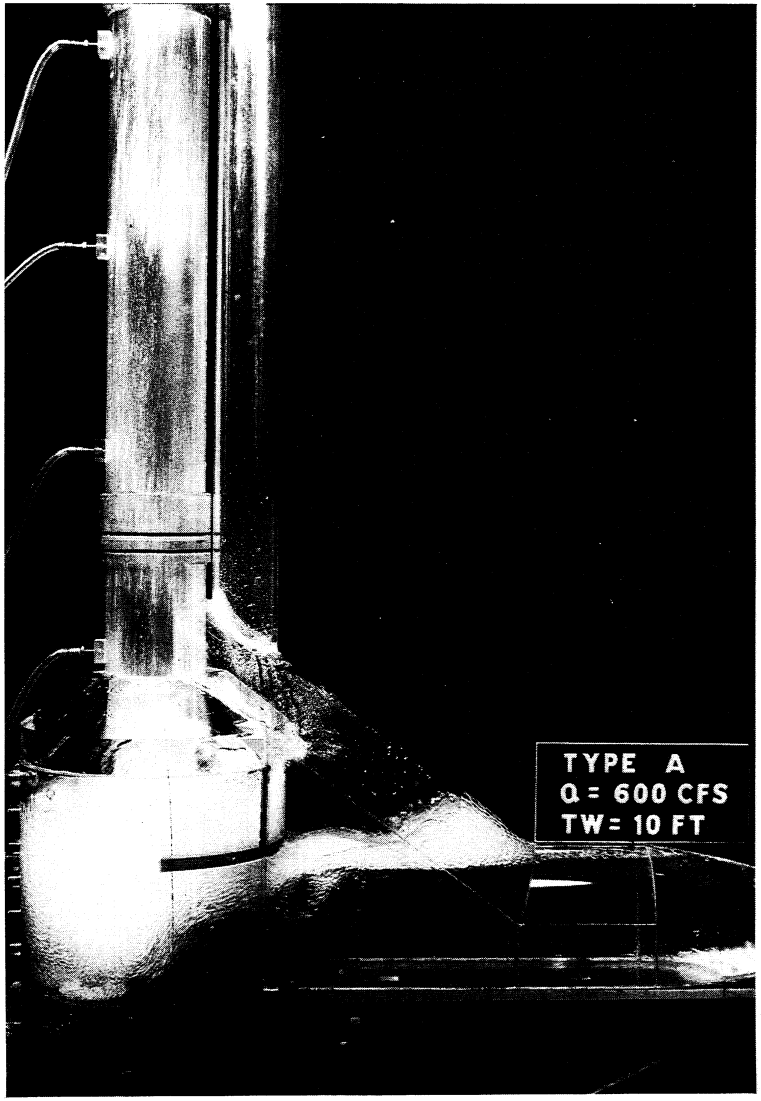

Photo 6

PHOTO 7 (Serial No. 177-26) When the discharge is increased to 1200 cfs in the Type A drop shaft, the jet separates from the inlet curve and impinges on the far wall with the development of secondary currents in the drop shaft. A relatively large amount of air is entrained, but the character of the flow is such that the air is not thoroughly mixed with the water. The tailwater of 100 ft causes the air rising in the air vent to be mixed with the water to create a frothy mass through which large bubbles of air are carried.

PHOTO 8 (Serial No. 177-27) This is a view of the lower portion of the drop shaft for the discharge of 1200 cfs in the Type A structure. The flow was highly aerated and turbulent in the sump. This type of air collector, in combination with the impact cup, is effective in separating the air from the outgoing flow.

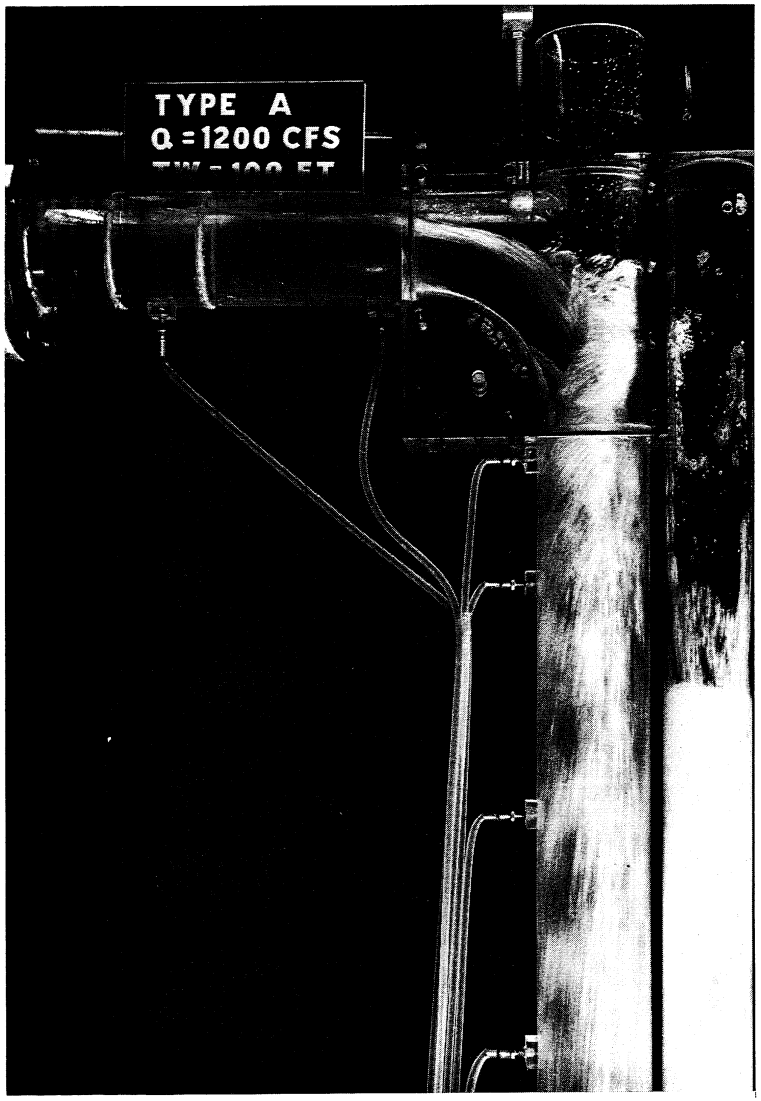

Photo 7

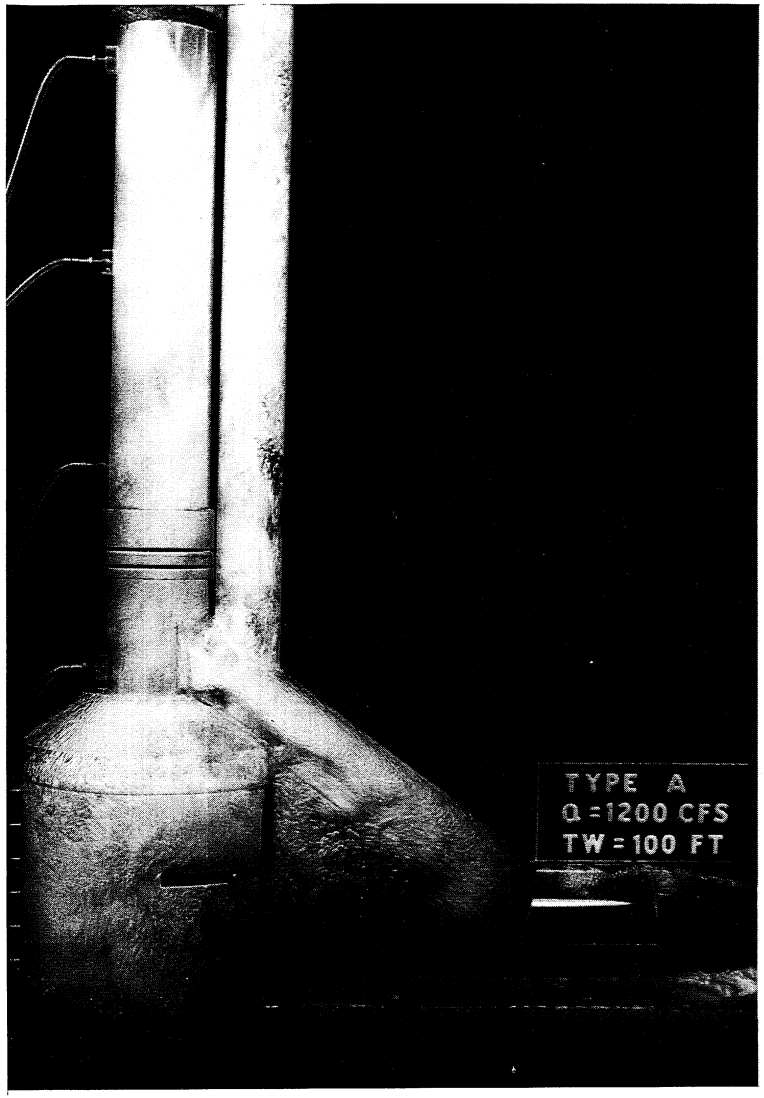

Photo 8

PHOTO 9 (Serial No. 177-30) The Type B drop shaft is characterized by a longitudinal divider wall which eliminates the external air vent. For a discharge of 300 cfs through this structure there is relatively little entrainment of air and the water falls freely through the shaft into the sump. Since the tailwater is very low, the air vent is clear and air can pass freely out of the structure.

PHOTO 10 (Serial No. 177-31) This photograph shows the lower portion of the Type B drop shaft for a discharge of 300 cfs. It is quite effective in dissipating the drop shaft energy and separating the air from the water in the sump and air collector.

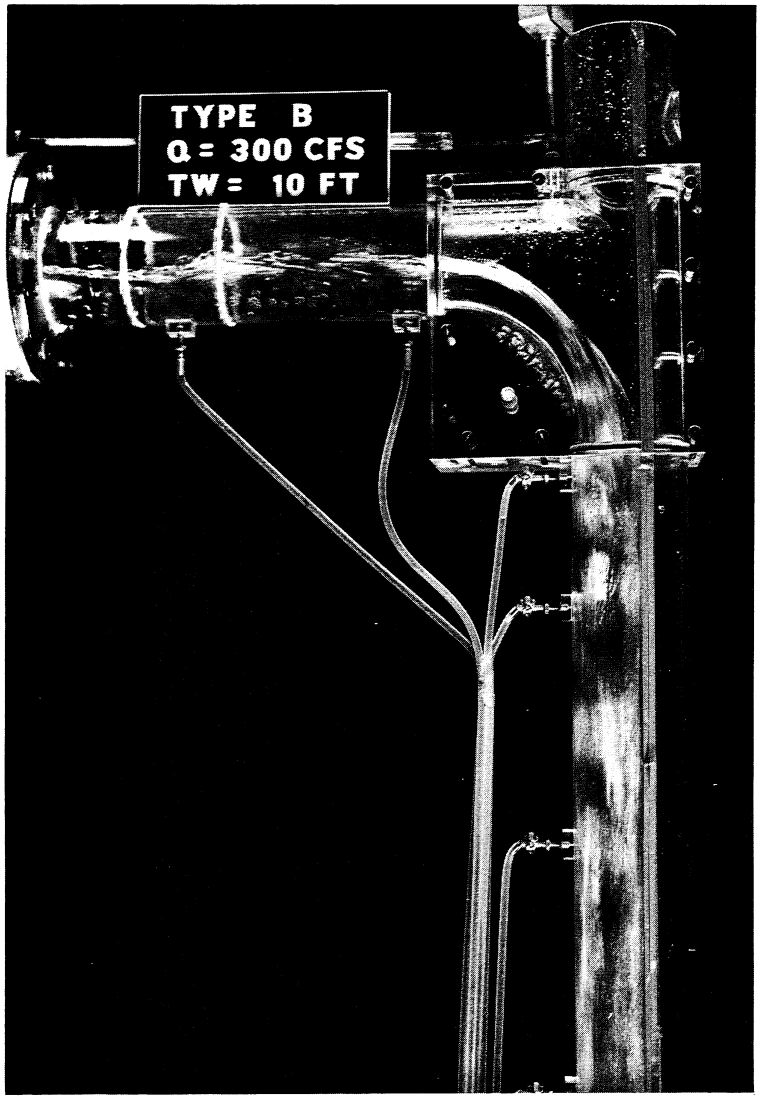

Photo 9

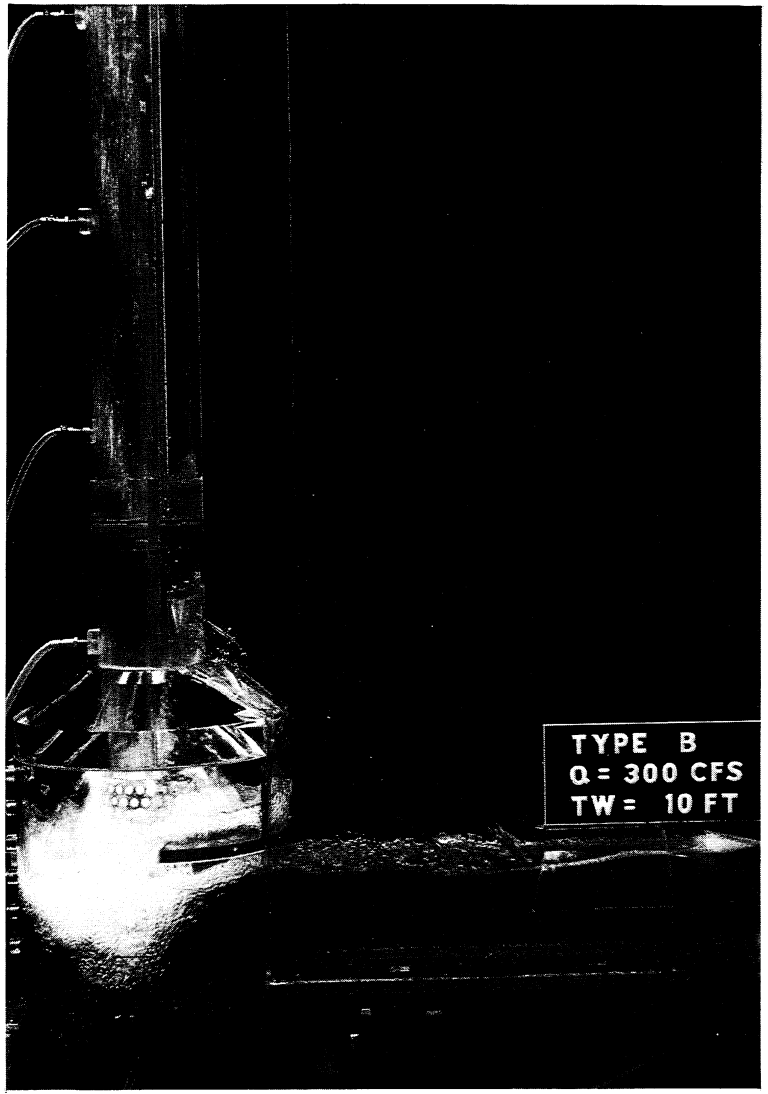

Photo 10

PHOTO 11 (Serial No. 177-44) In this photograph the discharge has been increased to 1200 cfs in the Type B drop shaft and the tailwater raised to 100 ft. This discharge effectively seals the upper portion of the drop shaft so that the drop shaft is closed. Relatively large quantities of air are insufflated into the turbulent flow created by the jet striking the far wall. Although the air is more uniformly distributed, there are still relatively large volumes of air-free water dropping down the shaft.

PHOTO 12 (Serial No. 177-45) The lower portion of the Type B drop shaft is shown in this photograph, which clearly shows relatively large regions of clear water and the intervening spaces filled with highly agitated air-water mixture. The sump and impact cup are relatively effective in removing the air from the flow, so that only a small quantity of air enters the downstream tunnel. The air vent is also highly turbulent, and large bubbles of air rise intermittently through the foamy mixture.

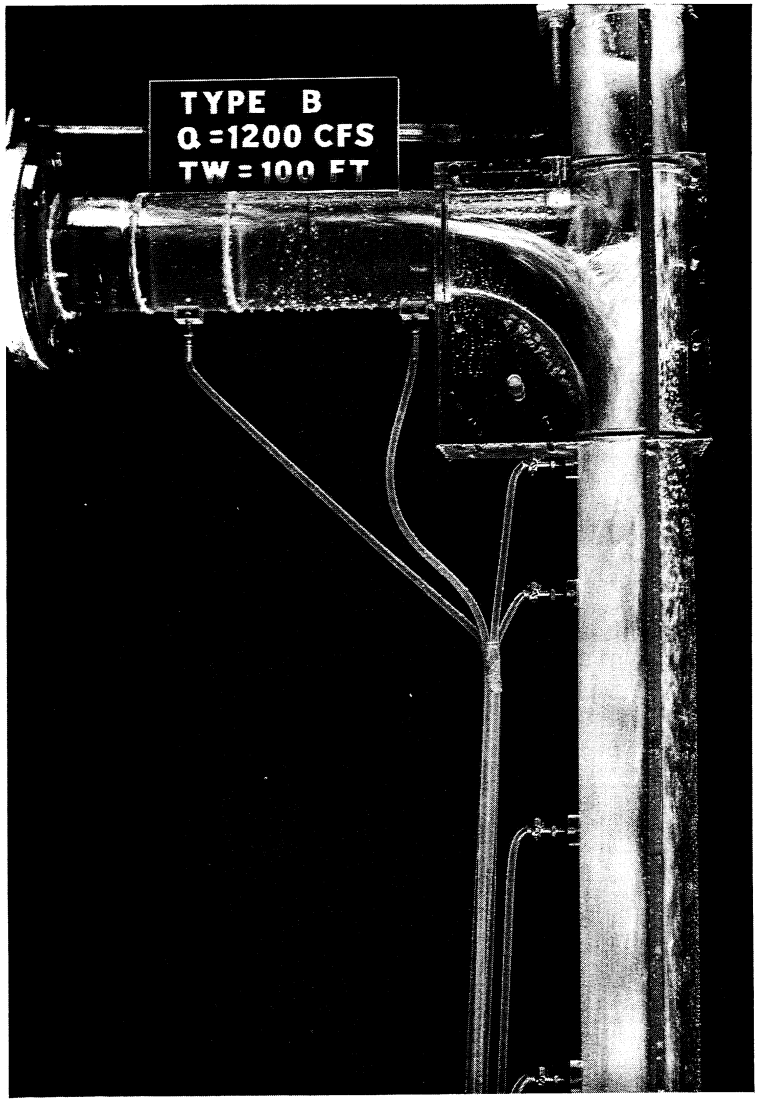

Photo 11

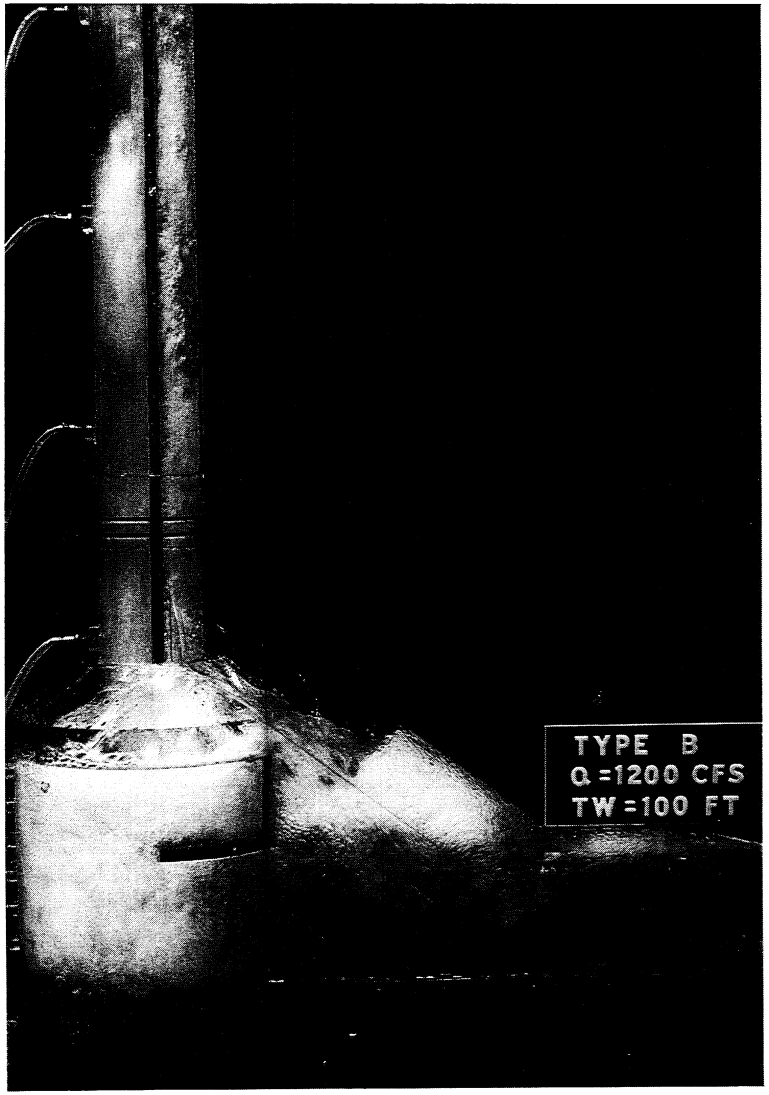

Photo 12

PHOTO 13 (Serial No. 177-70) The Type C-3 drop shaft is characterized by the removal of the impact cup and the installation of a 12-ft weir at the inlet to the air collector. This photo shows the character of the flow for 300 cfs in the sump and over the weir. Because of the low tailwater, the jet penetrates to the bottom of the sump, where the turbulence effectively mixes the air and the water.

PHOTO 14 (Serial No. 177-72) When the tailwater is increased to 190 ft, the insufflated air is easily removed in the sump and both the downward-flowing water-air mixture and the air vent are uniformly mixed.

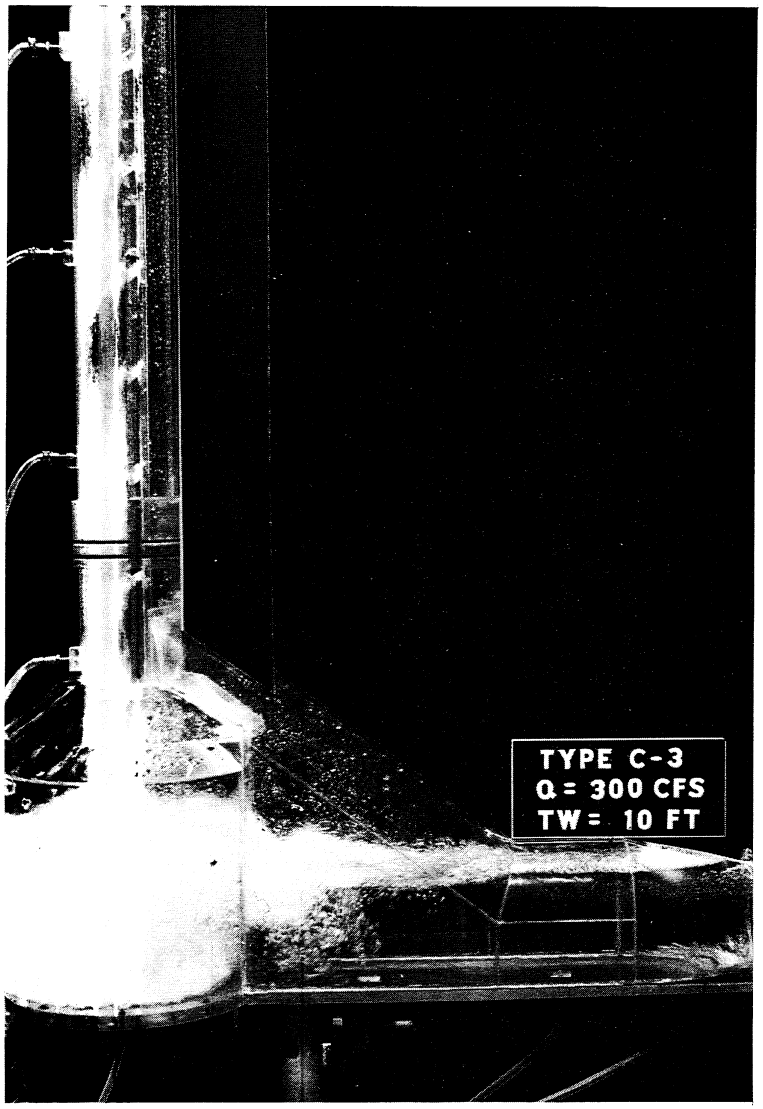

Photo 13

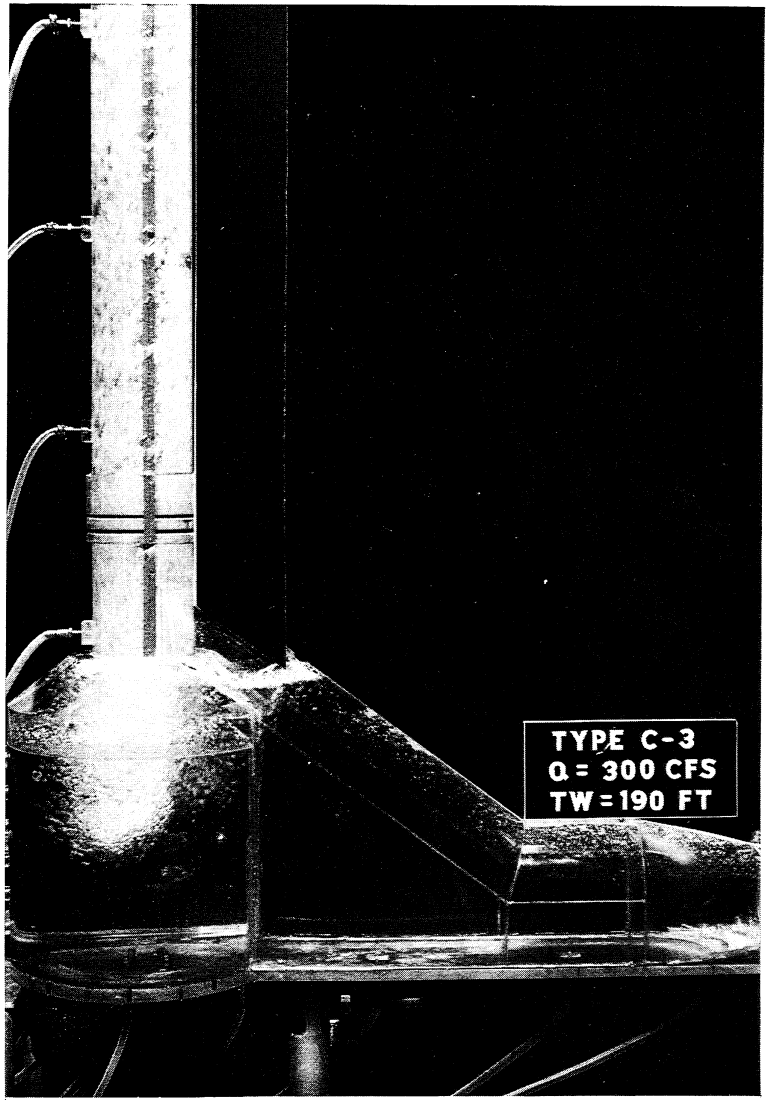

Photo 14

PHOTO 15 (Serial No. 177-73) This photograph shows the character of the flow down the drop shaft and the functioning of the sump and air collector for a discharge of 600 cfs and a low tailwater.

PHOTO 16 (Serial No. 177-75) When the tailwater is increased to 190 ft for the same discharge in the Type C-3 drop shaft, the flow down the shaft and in the sump is relatively calm and the small amount of insufflated air is easily separated.

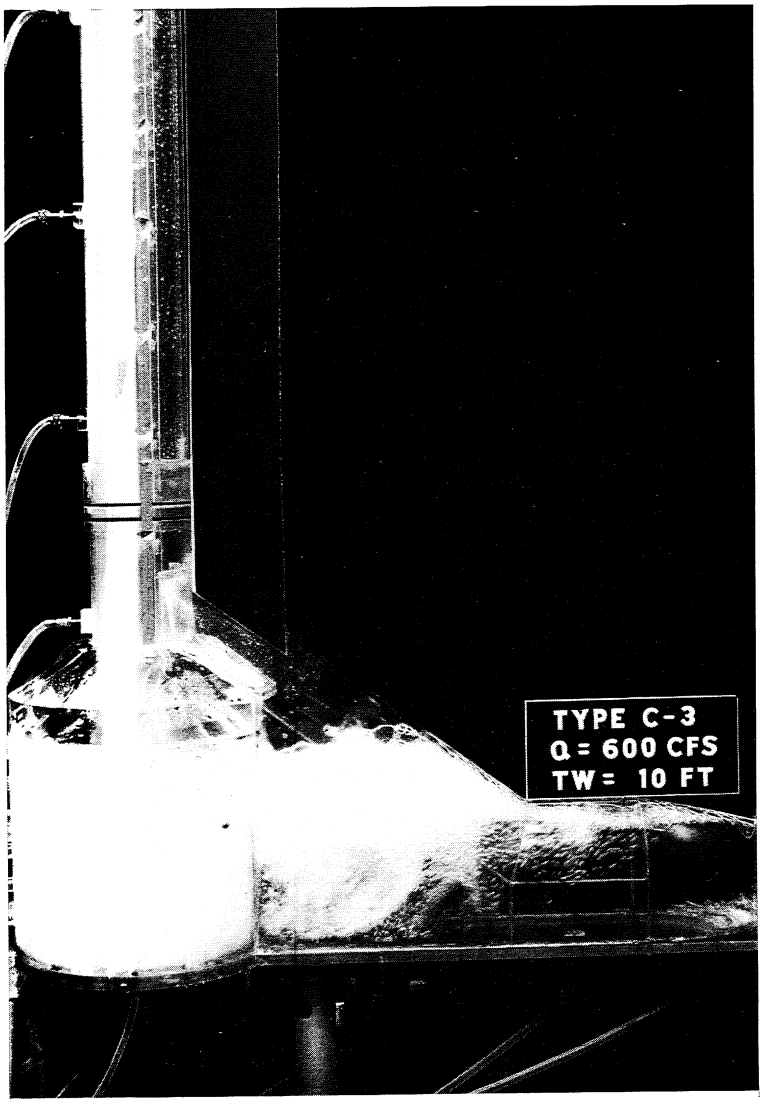

Photo 15

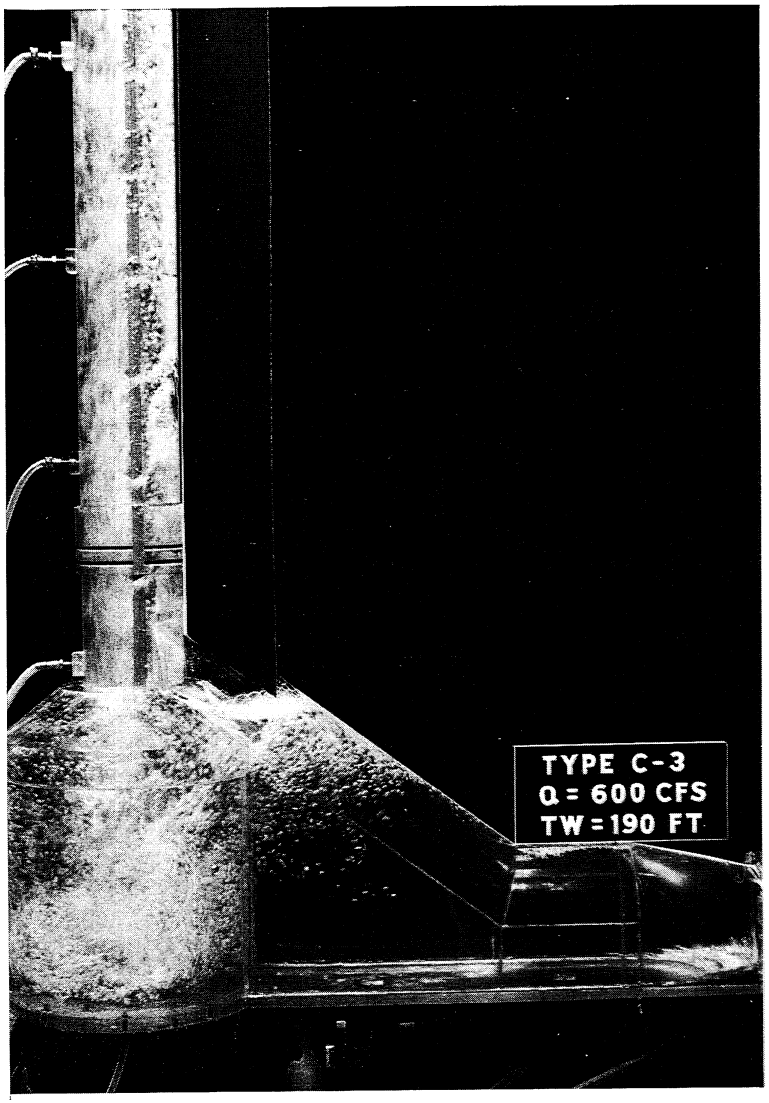

Photo 16

PHOTO 17 (Serial No. 177-76) A discharge of 1200 cfs in the Type C-3 drop shaft is extremely rugged and highly aerated when the tailwater is maintained at only 10 ft. A large quantity of air is transported into the downstream tunnel, and the flow in this area is generally unsatisfactory.

PHOTO 18 (Serial No. 177-78) When the tailwater is increased to 150 ft, the flow characteristics in the lower part of the Type C-3 drop shaft are considerably improved and the air reaching the downstream tunnel is very appreciably reduced.

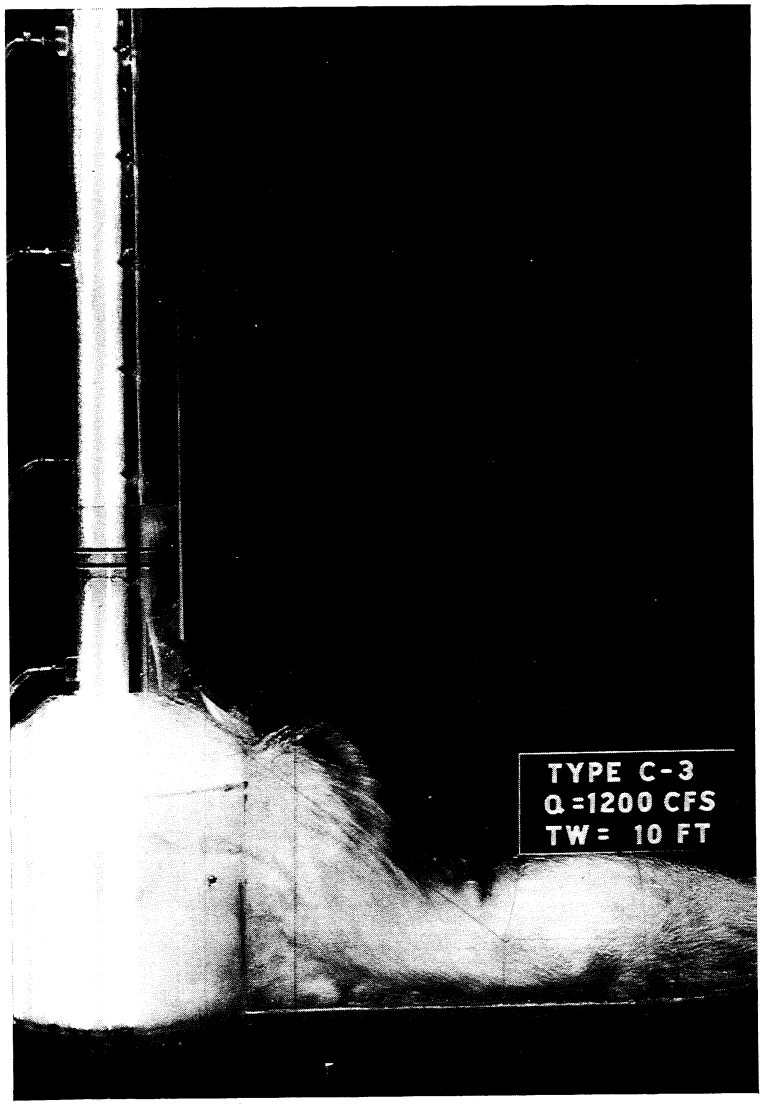

Photo 17

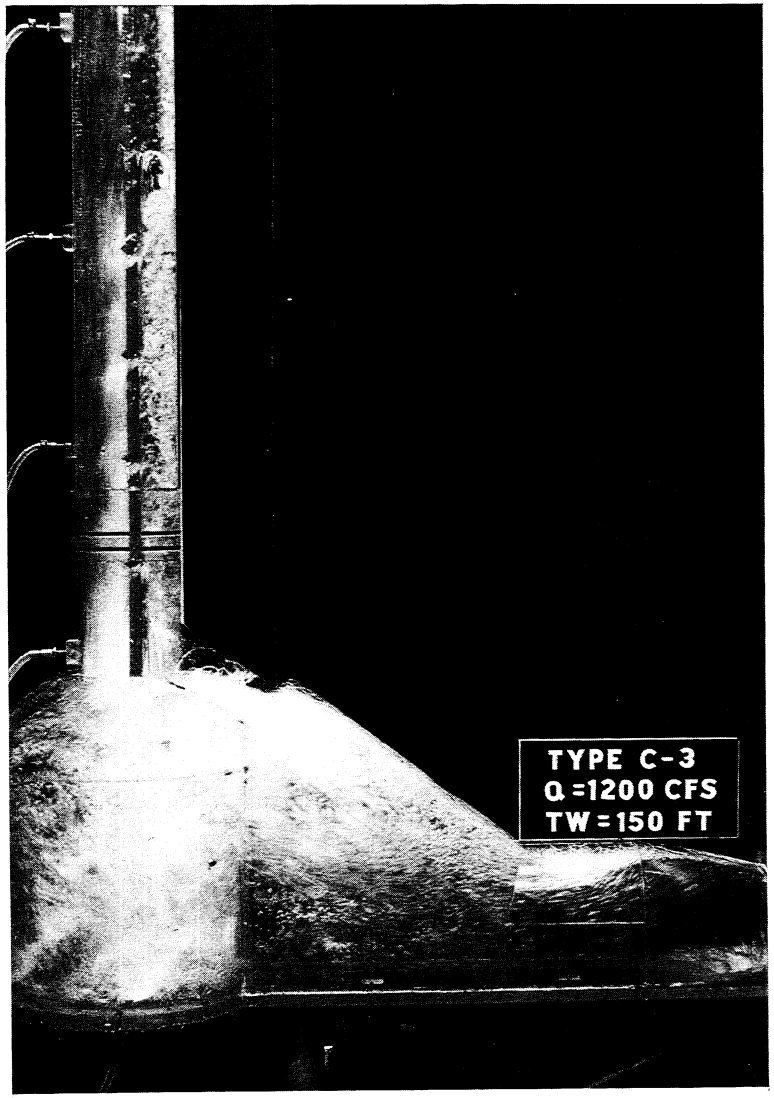

Photo 18

PHOTO 19 (Serial No. 177-93) When the tailwater is raised to 190 ft, which is nearly to the top of the drop shaft, little air is entrained and is easily removed in the sump and air collector.

PHOTO 20 (Serial No. 177-108) As the discharge is increased, however, the large volume of water seals off the air collector so that air separated from the flow cannot escape into the air vent. This forces the water level in the air collector down, and much air escapes into the downstream tunnel.

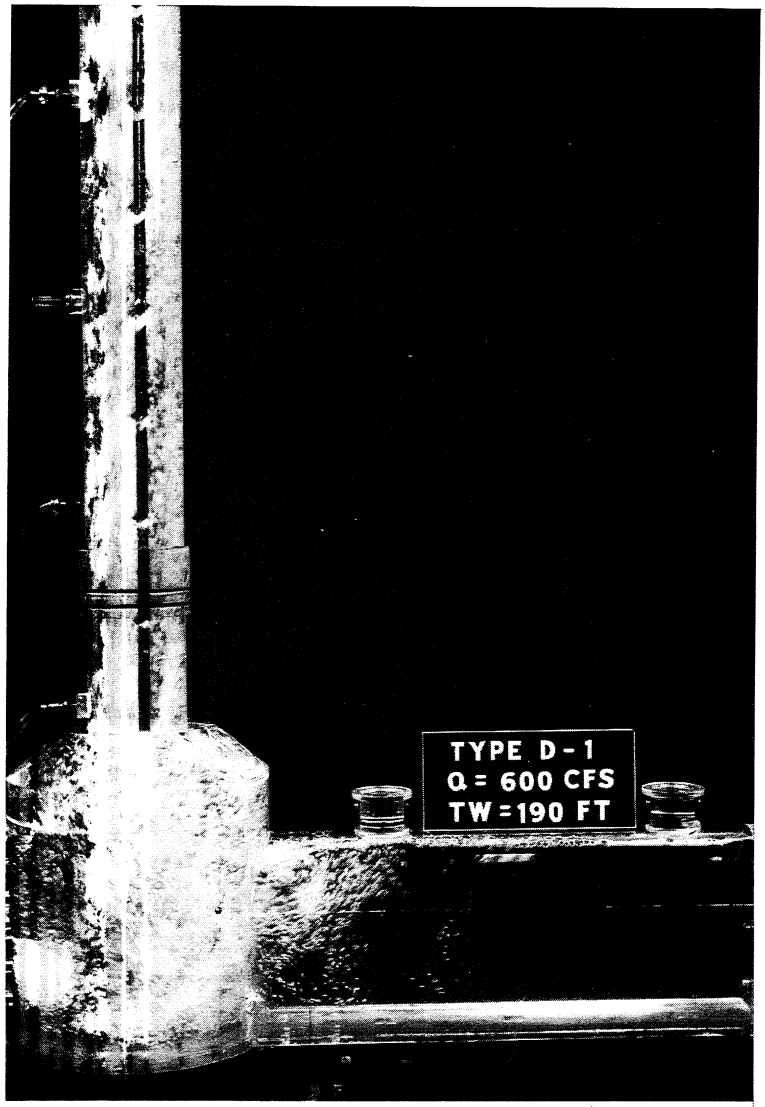

Photo 19

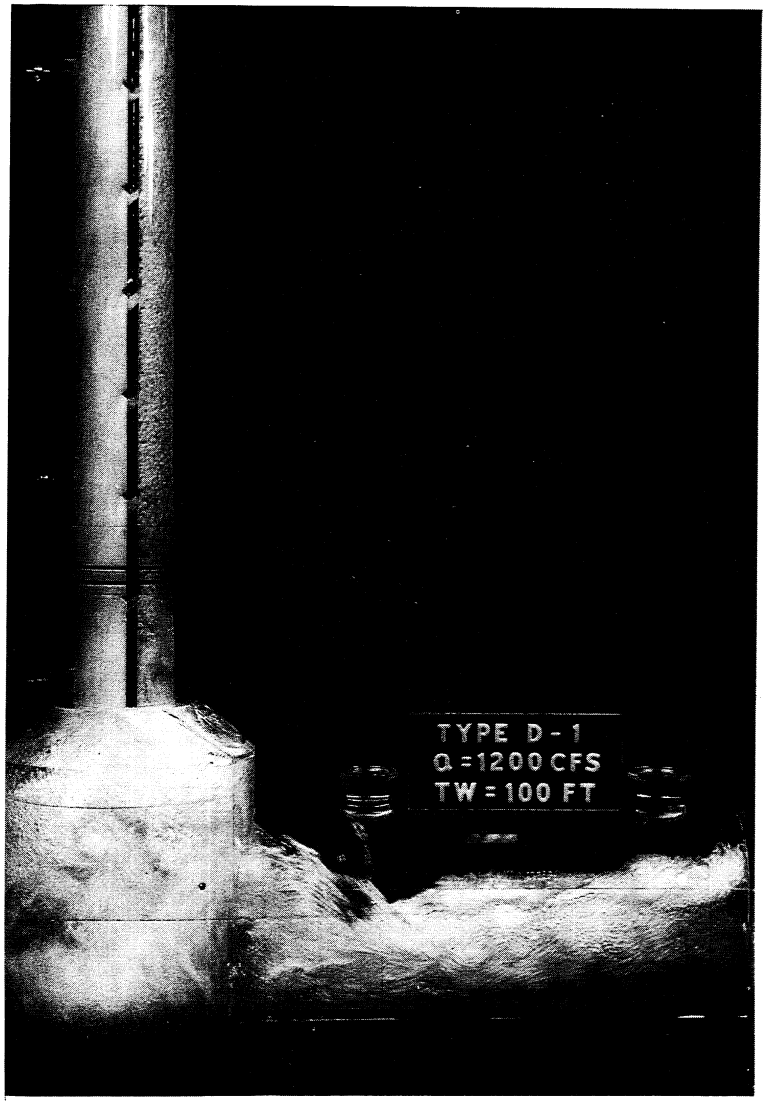

Photo 20

PHOTO 21 (Serial No. 177-80) In this photograph the tailwater has been raised to 100 ft. In spite of this, the high weir and discharge of 600 cfs tend to restrict the escape of air up the air vent, causing the water level in the air collector to be forced downward nearly to the crown of the tunnel, with the result that a considerable amount of air enters the tunnel.

PHOTO 22 (Serial No. 177-88) This condition, as described at the left, is greatly improved when the height of the weir is reduced to 8 ft. In this case, more air can escape back to the air vent. The lower pressure permits the water level in the air collector to rise toward the top of the collector, and no air can escape into the tunnel.

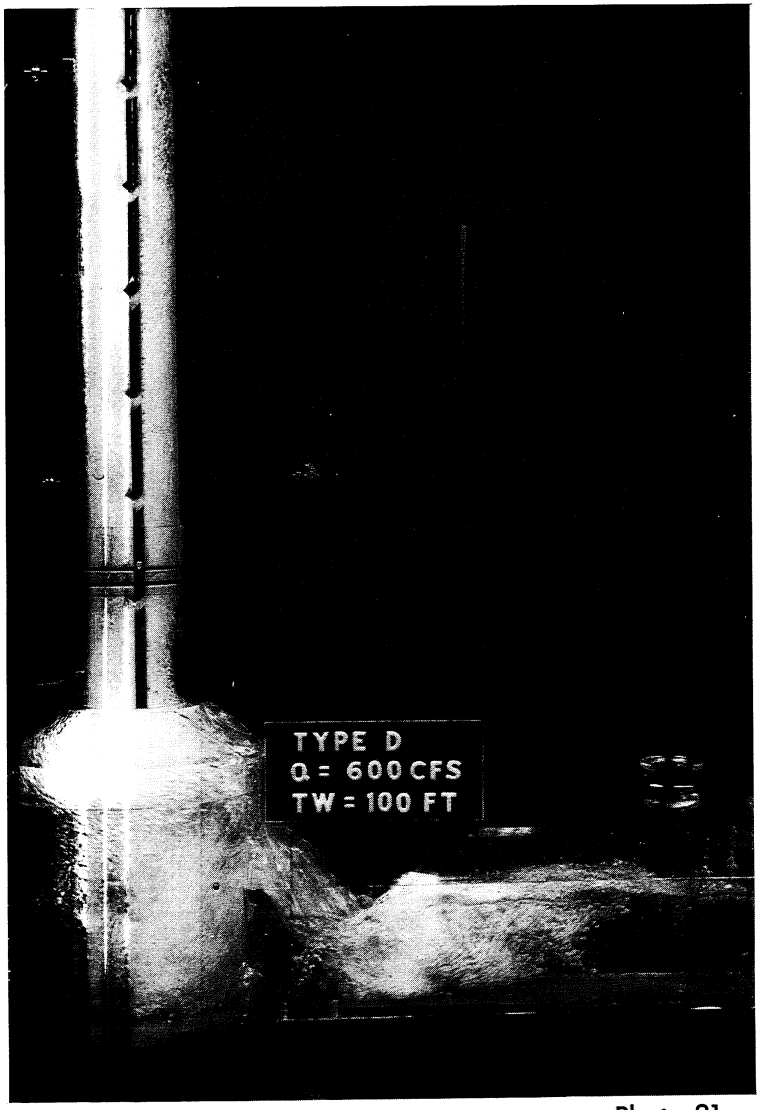

Photo 21

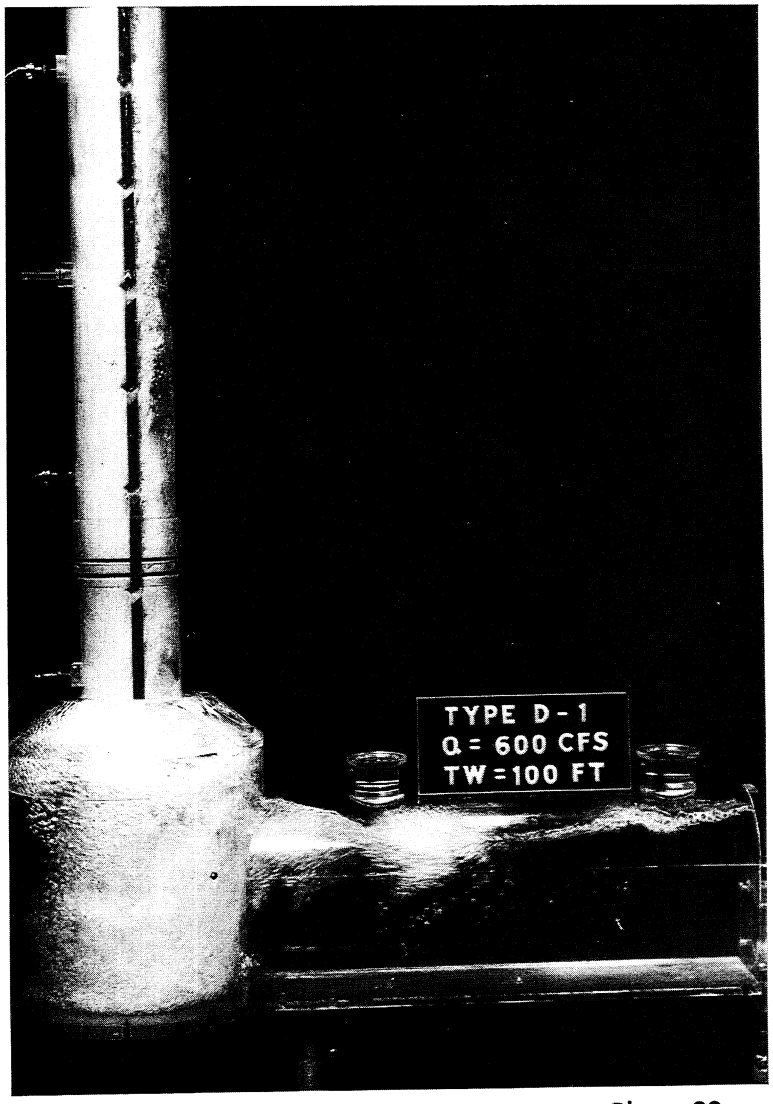

Photo 22

PHOTO 23 (Serial No. 177-114) For a discharge of 1200 cfs and a tailwater of 10 ft, the air collector is quite ineffective. This discharge appears to be beyond the capacity of the structure, and all the air can freely enter the downstream tunnel.

PHOTO 24 (Serial No. 177-116) In this photograph the weir between the sump and the air collector has been completely removed. The large discharge of 1200 cfs sweeps through the air collector and carries all the air into the downstream tunnel.

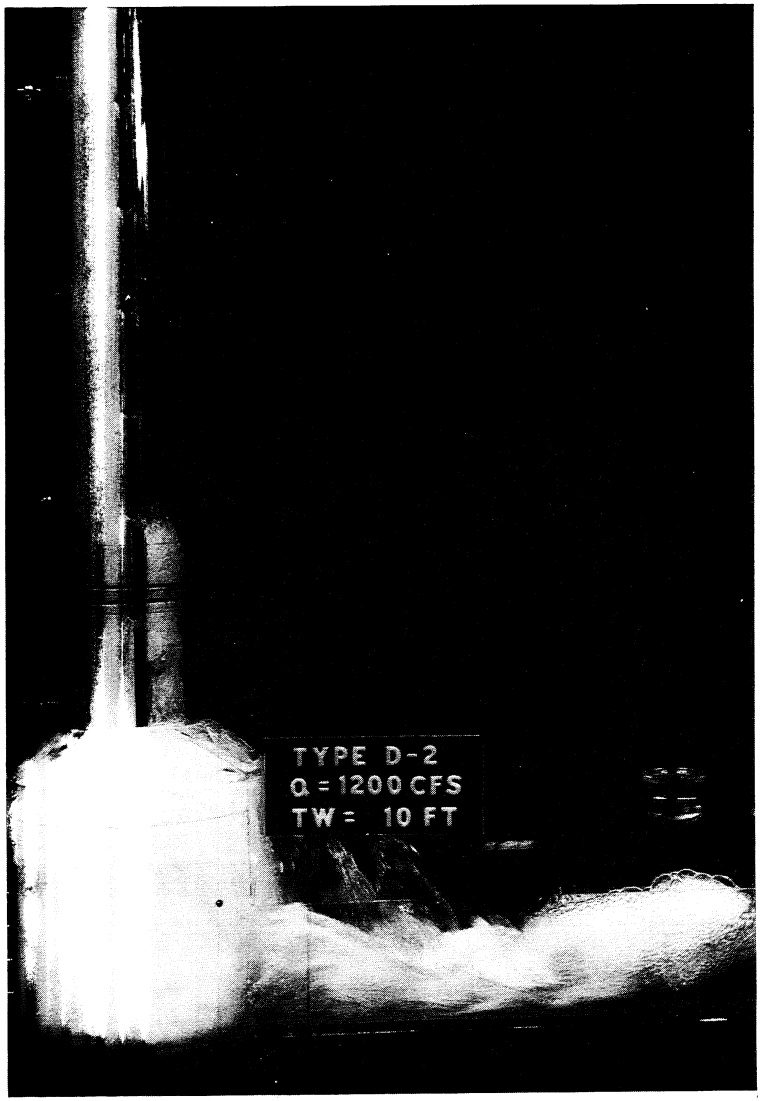

Photo 23

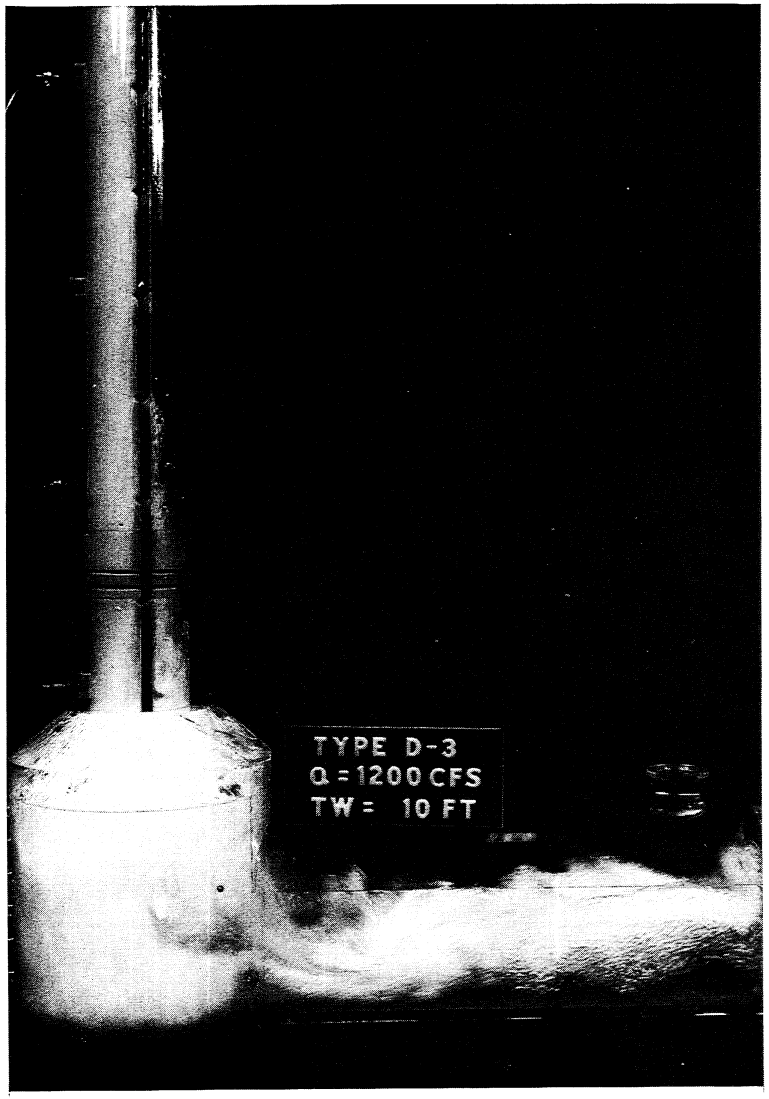

Photo 24

PHOTO 25 (Serial No. 177-119) By providing an air vent from the air collector itself, the pattern of air removal is greatly improved. For this condition the height of the weir is 8 ft so that air can be released through both the air vent and the special vent on the air collector.

PHOTO 26 (Serial No. 177-120) In this test, the air vent was placed at the downstream end of the air collector and appears to be equally effective in the removal of air.

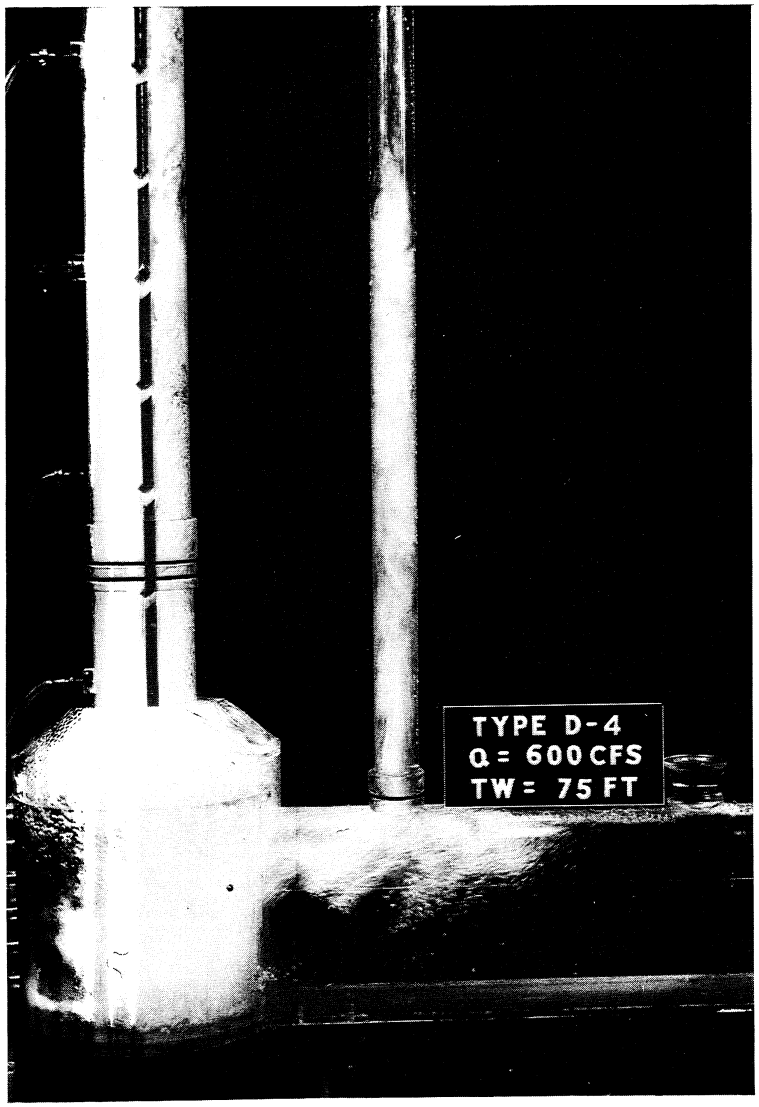

Photo 25

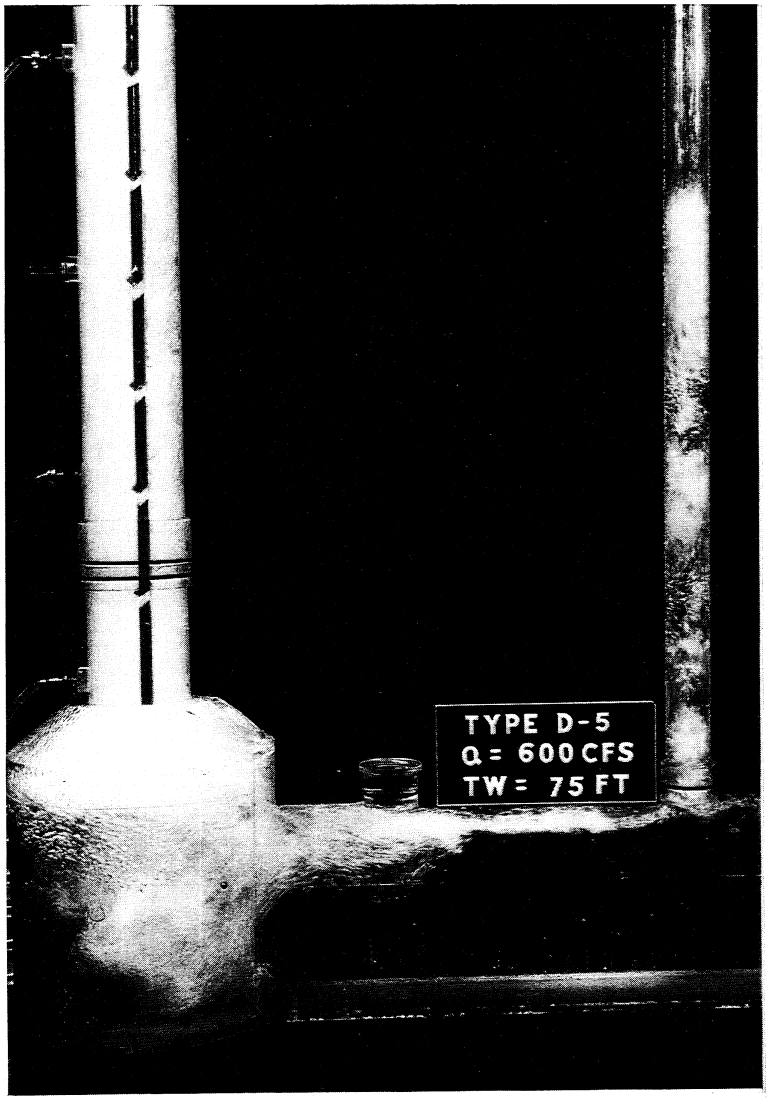

Photo 26

PHOTO 27 (Serial No. 177-178) When the tailwater is raised to elevation 100 ft, the air collector is effective in removing air from the flow and venting it up the air vent. It appears that the Type E structure is relatively effective in its initial design.

PHOTO 28 (Serial No. 177-189) In an attempt to shorten the air collector of the drop shaft the sloping portion was removed and a discharge of 600 cfs with a tailwater elevation of 100 ft was passed through the structure. The photographs show that a large separation zone occurs at the inlet to the downstream tunnel and that large quantities of air escape through it.

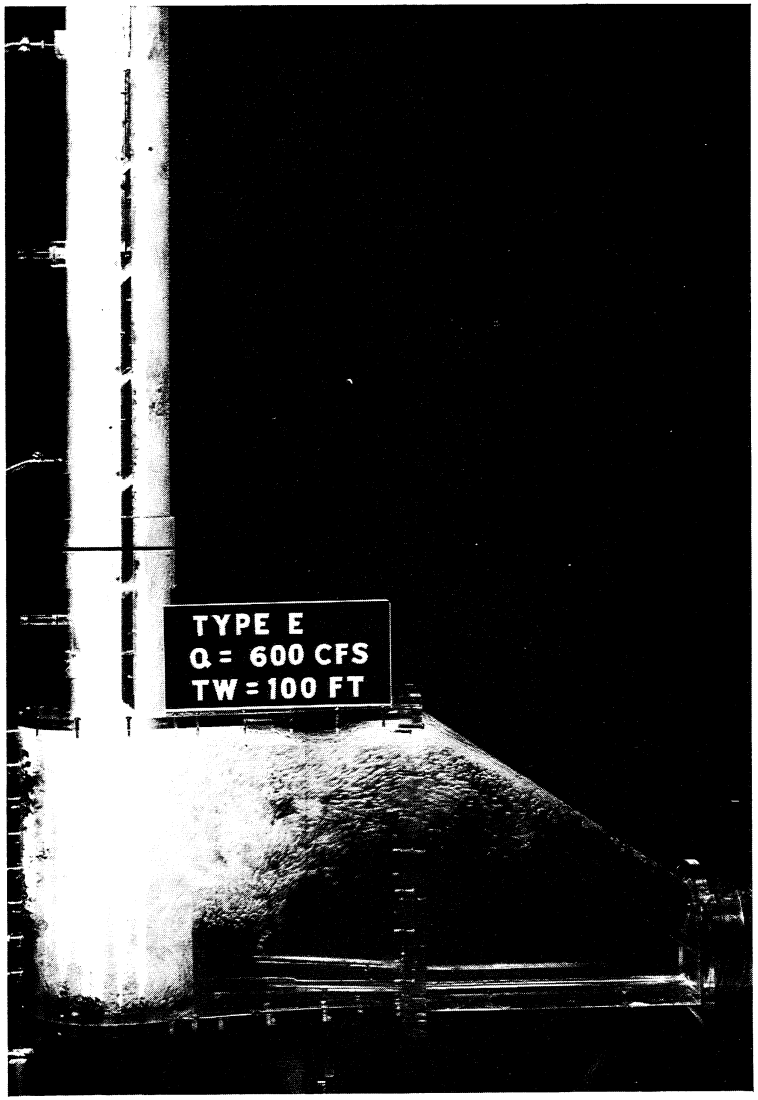

Photo 27

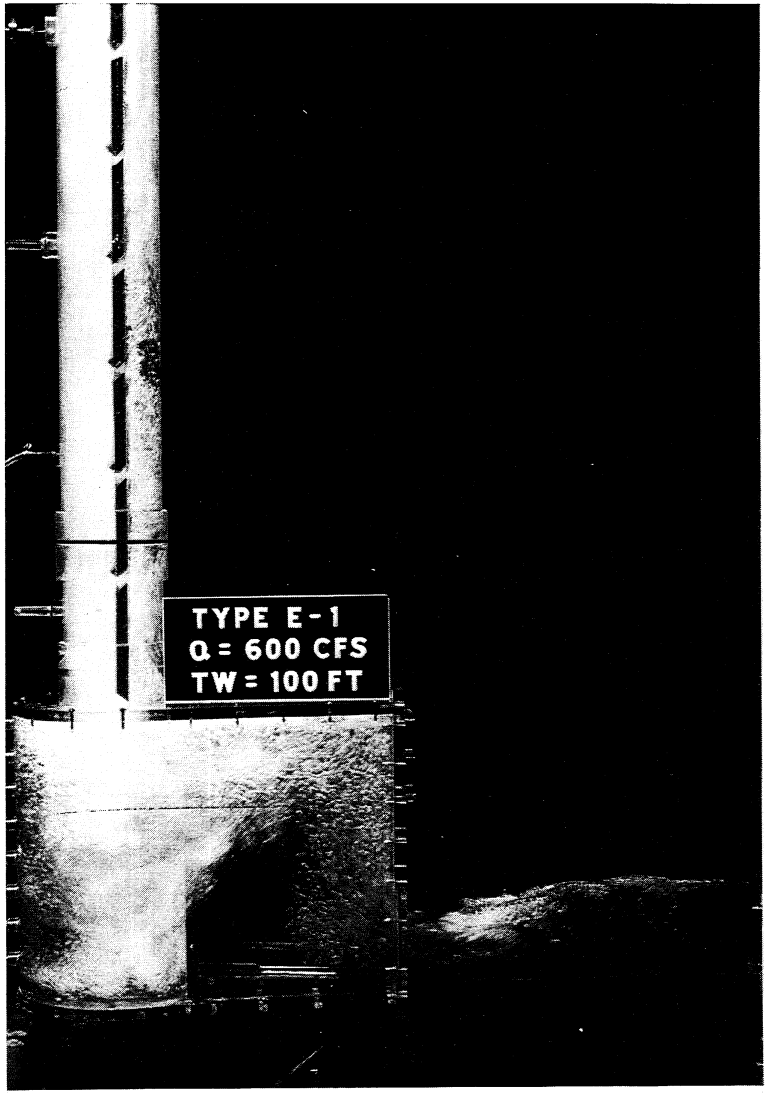

Photo 28

PHOTO 29 (Serial No. 177-198) In Type E-2 the horizontal portion of the air collector was shortened and the sloping section was replaced. This improved the flow pattern, and relatively little air escaped into the downstream tunnel. Here the discharge was again 600 cfs with a tailwater at elevation 100 ft.

PHOTO 30 (Serial No. 177-205) In Type E-7 drop structure the sloping portion was placed on top of the horizontal section with the thought that by providing a larger cross-section in this area, the air might more freely escape to the atmosphere through the air vent. The photograph shows, however, that this type is not effective in preventthe air from entering the downstream tunnel.

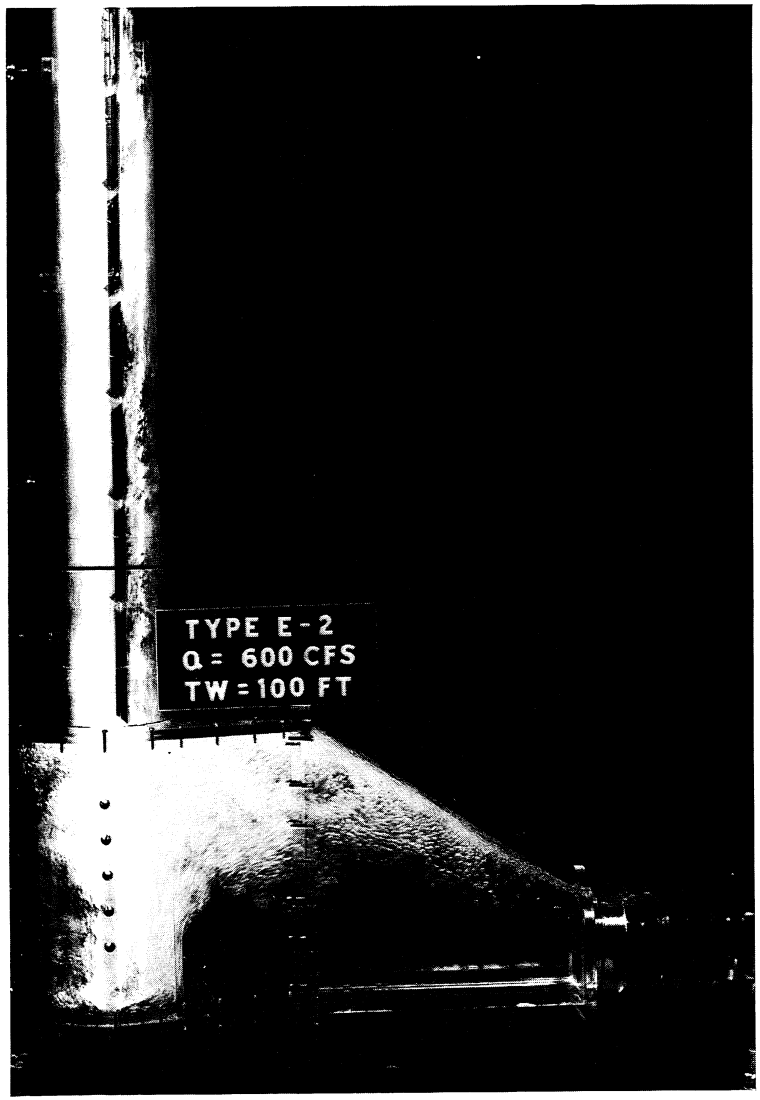

Photo 29

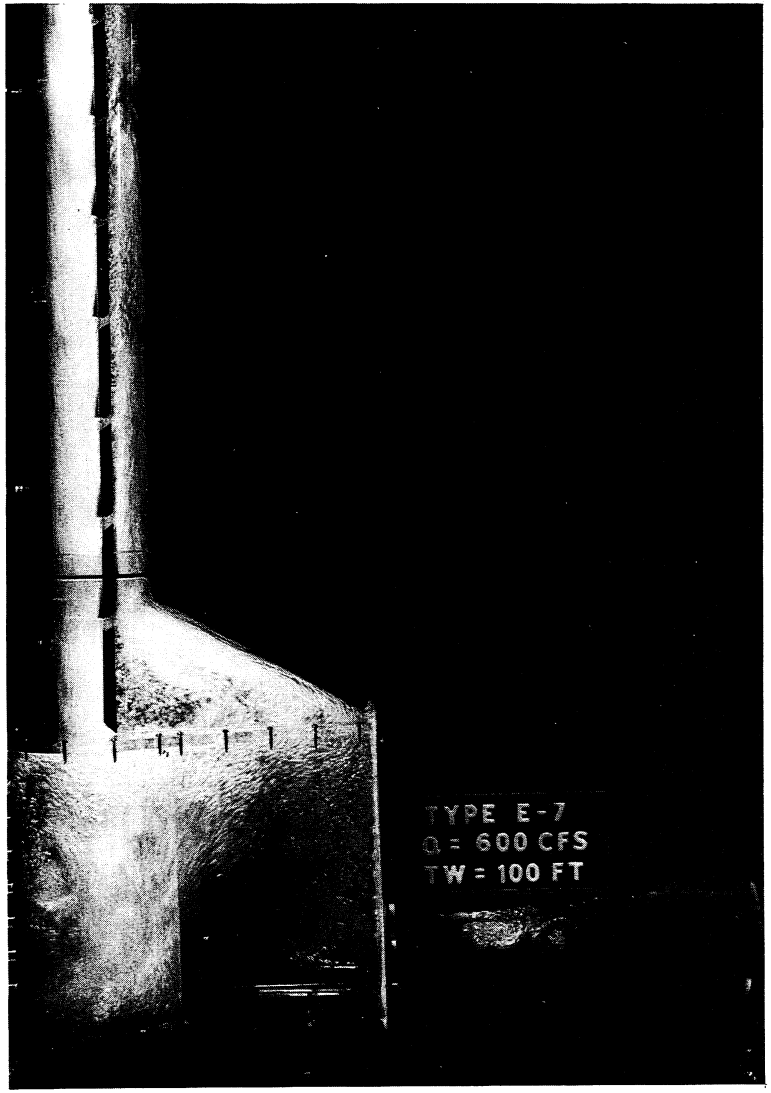

Photo 30

PHOTO 31 (Serial No. 177-219) In Type E-11 a faired entrance into the downstream tunnel was provided in order to prevent the separation at the inlet to the tunnel. The photograph shows that for a discharge of 600 cfs and tailwater at elevation 100 ft this device was also ineffective in preventing air from escaping into the tunnel.

PHOTO 32 (Serial No. 177-221) In Type E-13 the inward projection was extended to the roof of the air collector without any apparent improvement in the functioning of the air collector. The photograph shows the air escaping around the projection into the downstream tunnel.

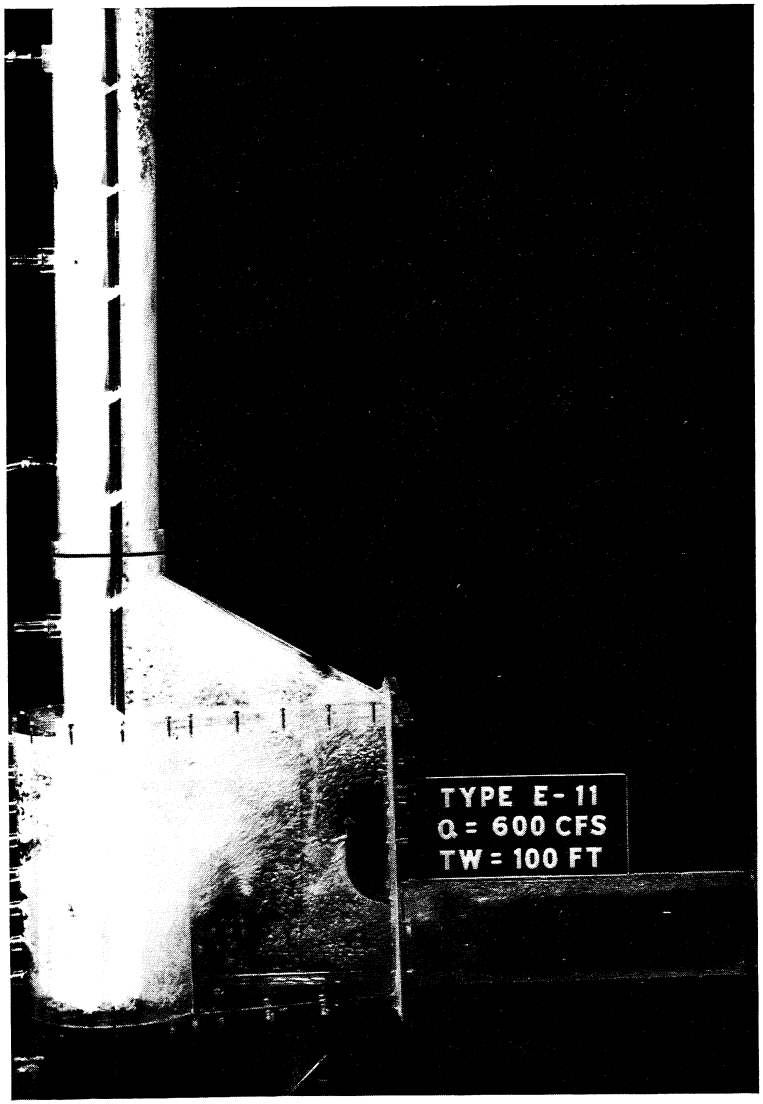

Photo 31

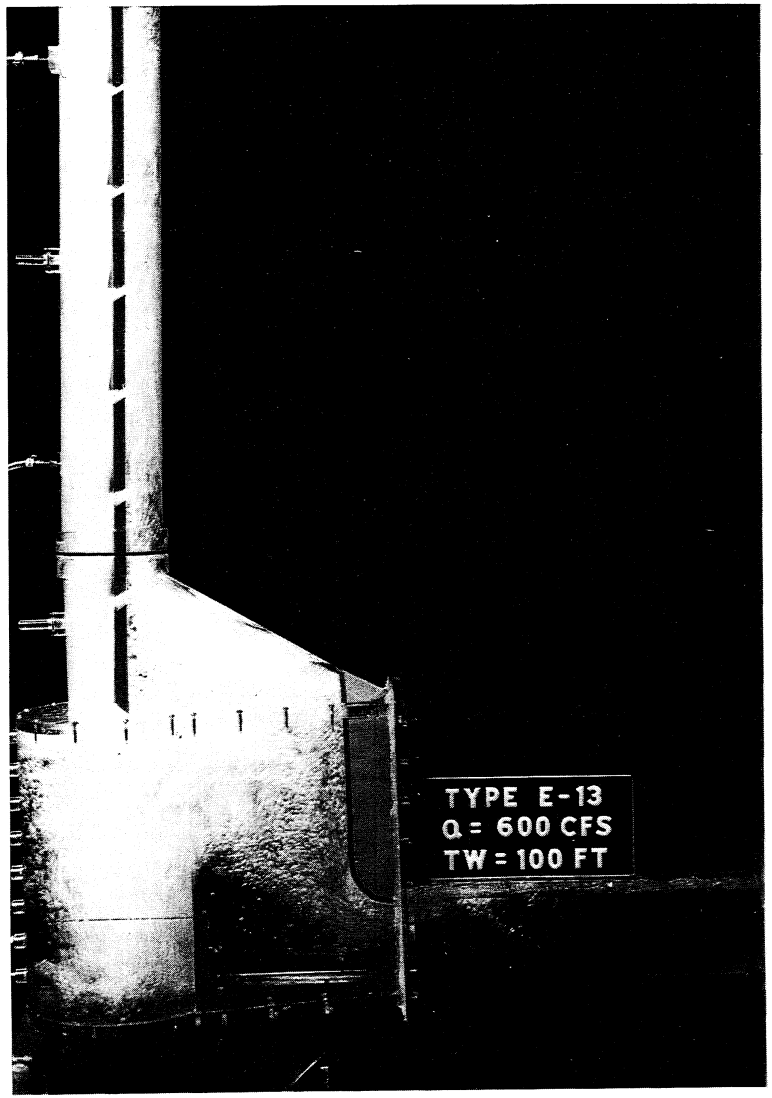

Photo 32

PHOTO 33 (Serial No. 177-233) When the discharge is 600 cfs, the design capacity of the drop structure, considerably more air is entrained. But even when the tailwater is lowered to elevation 10 ft air is separated from the water and prevented from entering into the downstream tunnel.

PHOTO 34 (Serial No. 177-235) For a discharge of 600 cfs with tailwater at 50 ft, the Type E-14 air collector effectively removes the air from the water and provides easy access to the air vent.

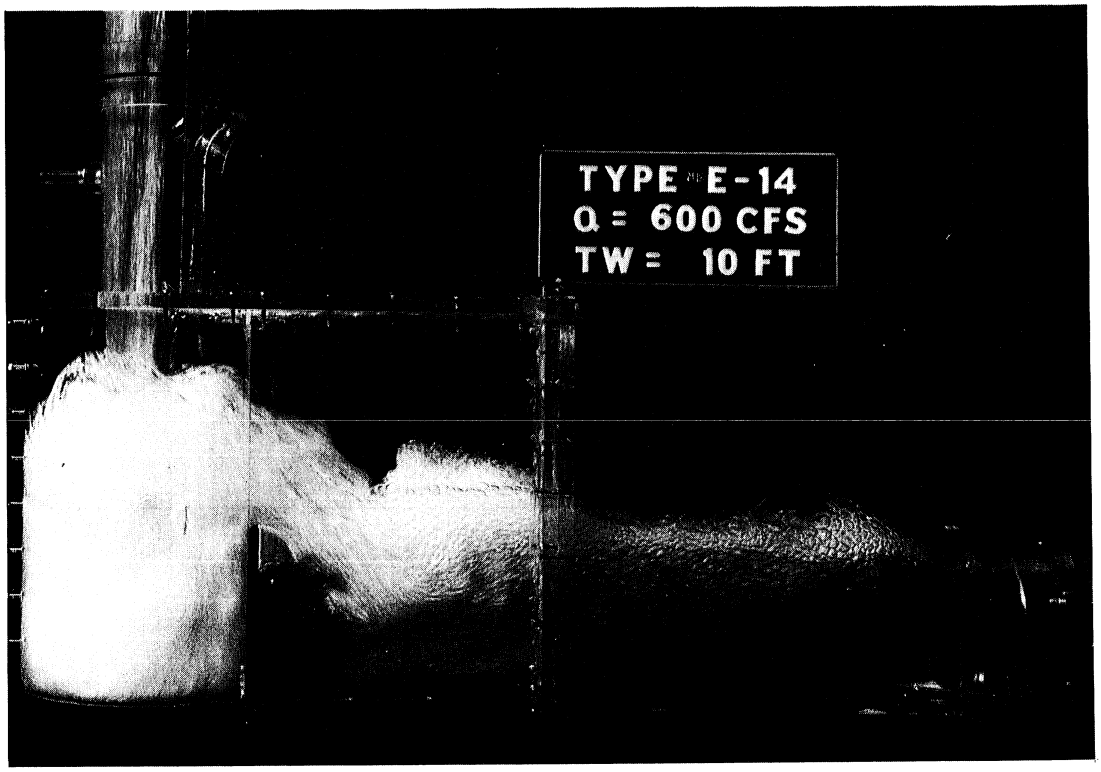

Photo 33

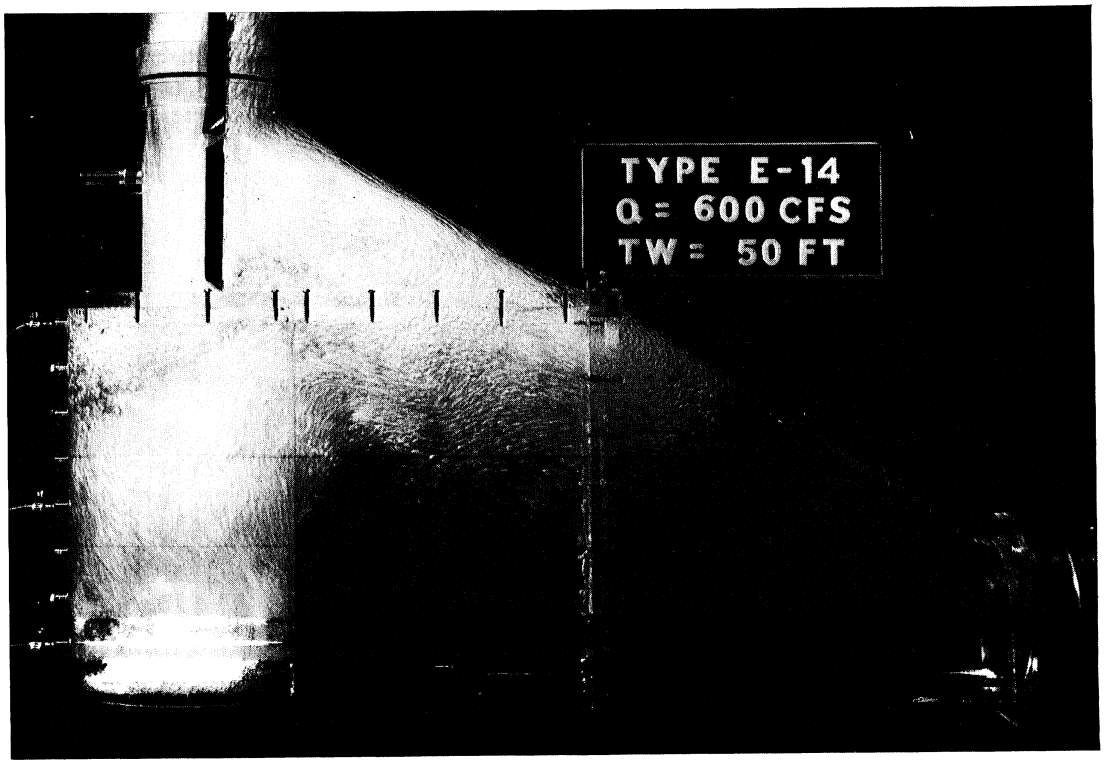

Photo 34

PHOTO 35 (Serial No. 177-237) When the tailwater is increased to 100 ft for a discharge of 600 cfs, the structure operates efficiently. With this high tailwater the jet still penetrates to the bottom of the sump.

PHOTO 36 (Serial No. 177-239) When the tailwater is raised to 190 ft the air concentration is greatly reduced and the jet no longer penetrates to the bottom of the sump. For these tailwaters air is easily removed from the mixture and released through the air vent.

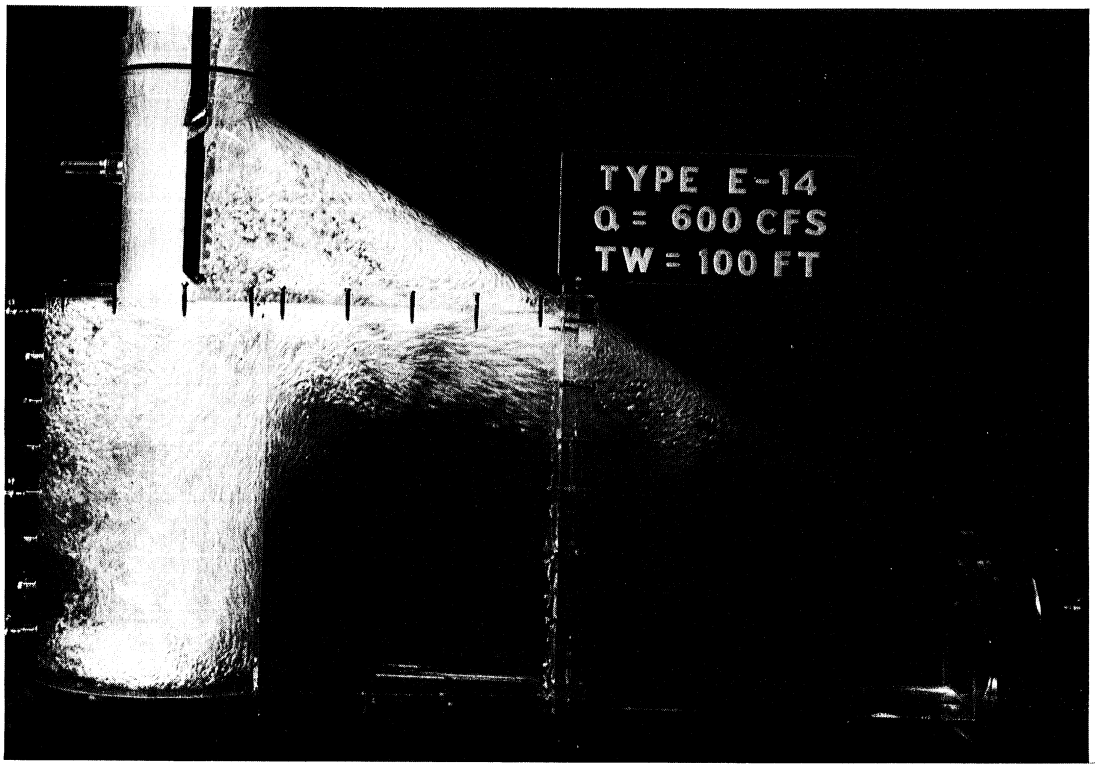

Photo 35

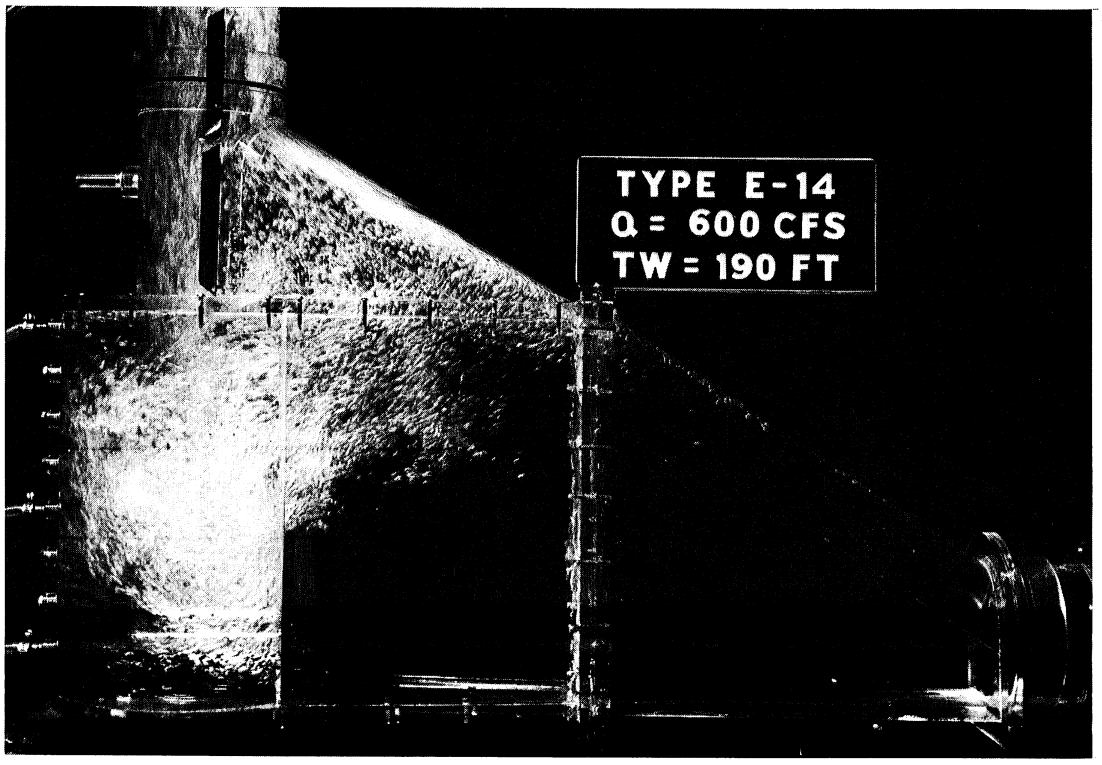

Photo 36

PHOTO 37 (Serial No. 177-245) When the discharge is increased to 1200 cfs, much air escapes into the downstream tunnel even though the tailwater is at elevation 50 ft. This shows that a discharge of 1200 cfs is beyond the capacity of this drop structure design.

PHOTO 38 (Serial No. 177-247) Even when the tailwater is raised to elevation 100 ft the air collector cannot separate the air from the flow for a discharge of 1200 cfs. Here again an appreciable portion of air can escape into the downstream tunnel.

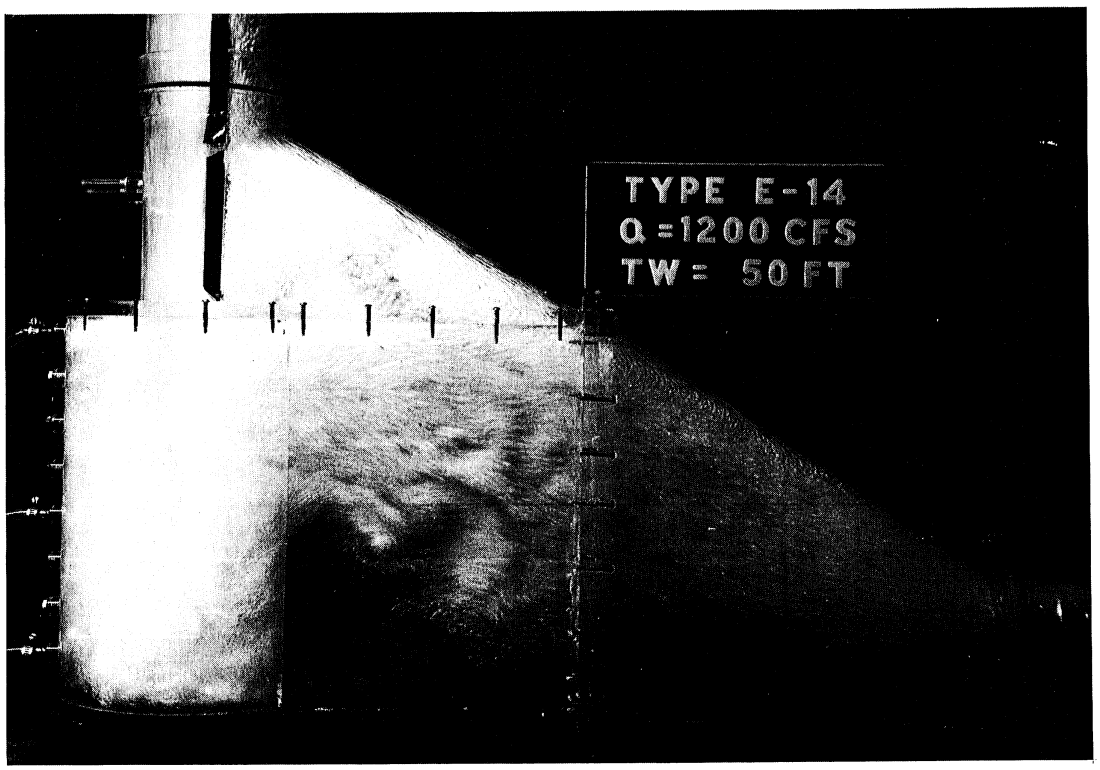

Photo 37

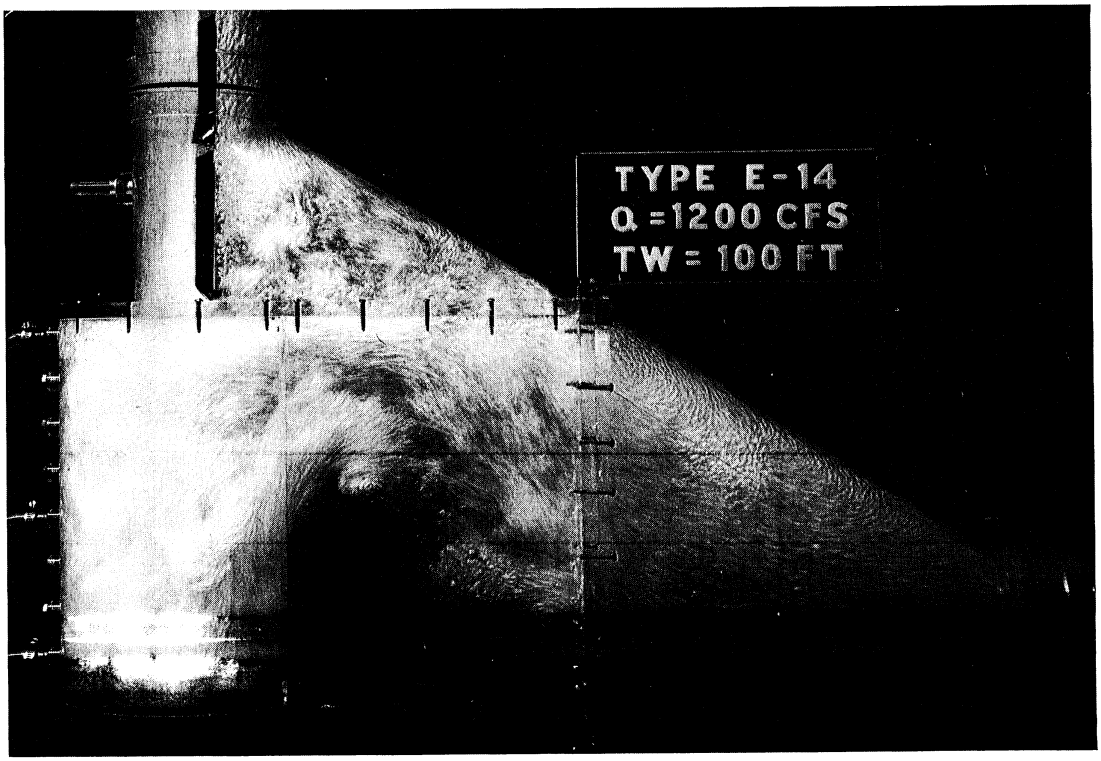

Photo 38

PHOTO 39 (Serial No. 177-263) For a discharge of 600 cfs and the tailwater maintained at elevation 10 ft, the Type E-15 successfully removes the air from the flow. A comparison with Photo 33 shows that the essential difference in flow pattern is that the highly insufflated air penetrates further into the air collector at a lower elevation.

PHOTO 40 (Serial No. 177-265) When the tailwater has been raised to elevation 50 ft the effect of the weir is less noticeable and the entrained air quickly rises to the top of the air collector so that none can escape into the downstream tunnel.

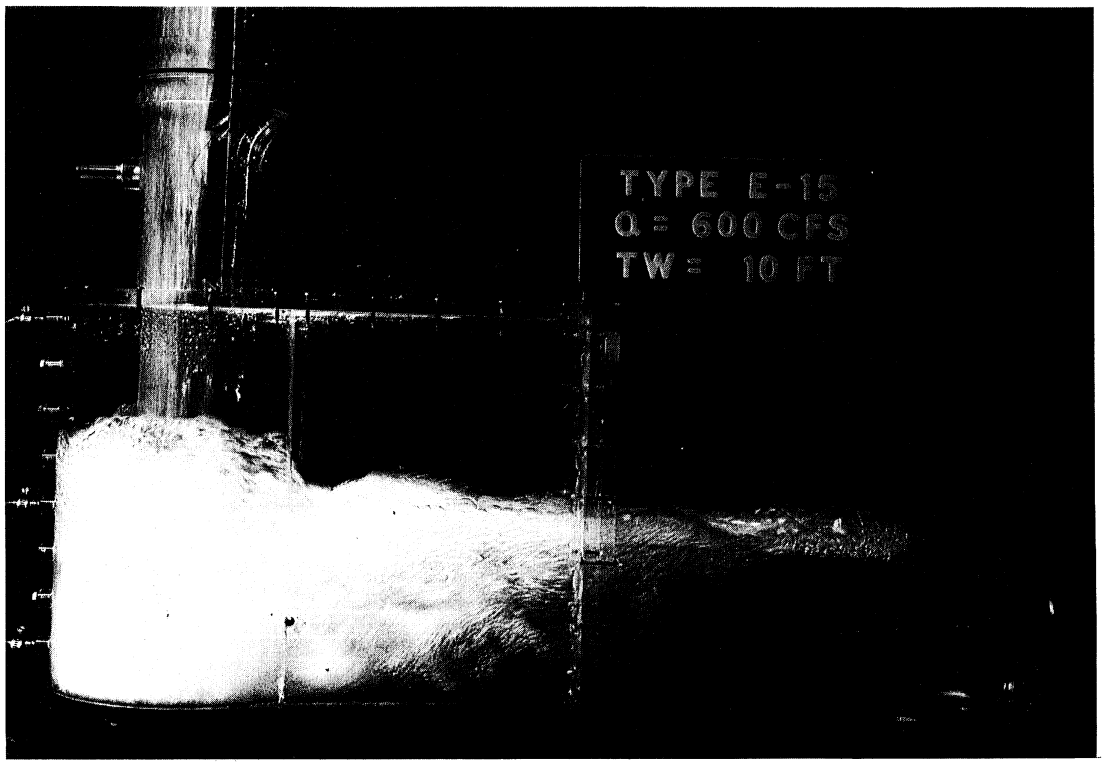

Photo 39

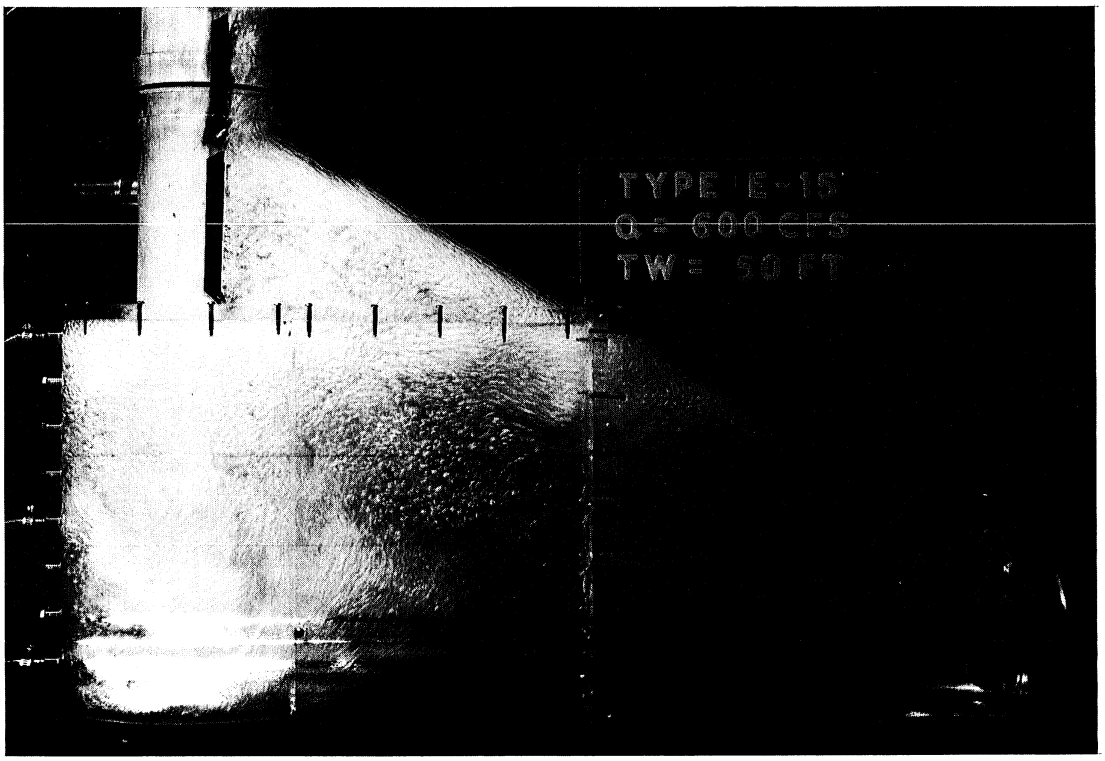

Photo 40

PHOTO 41 (Serial No. 177-38) With a solid wall deflector all the air must be entrained at the inlet to the drop shaft with a consequent irregular non-uniform flow. The regions of solid water and entrained air are clearly defined in this photograph.

PHOTO 42 (Serial No. 177-45) This photograph shows the character of the flow past the solid dividing wall at the lower portions of the drop structure. The tailwater elevation has been increased so that large gulps of air are being released up the air vent.

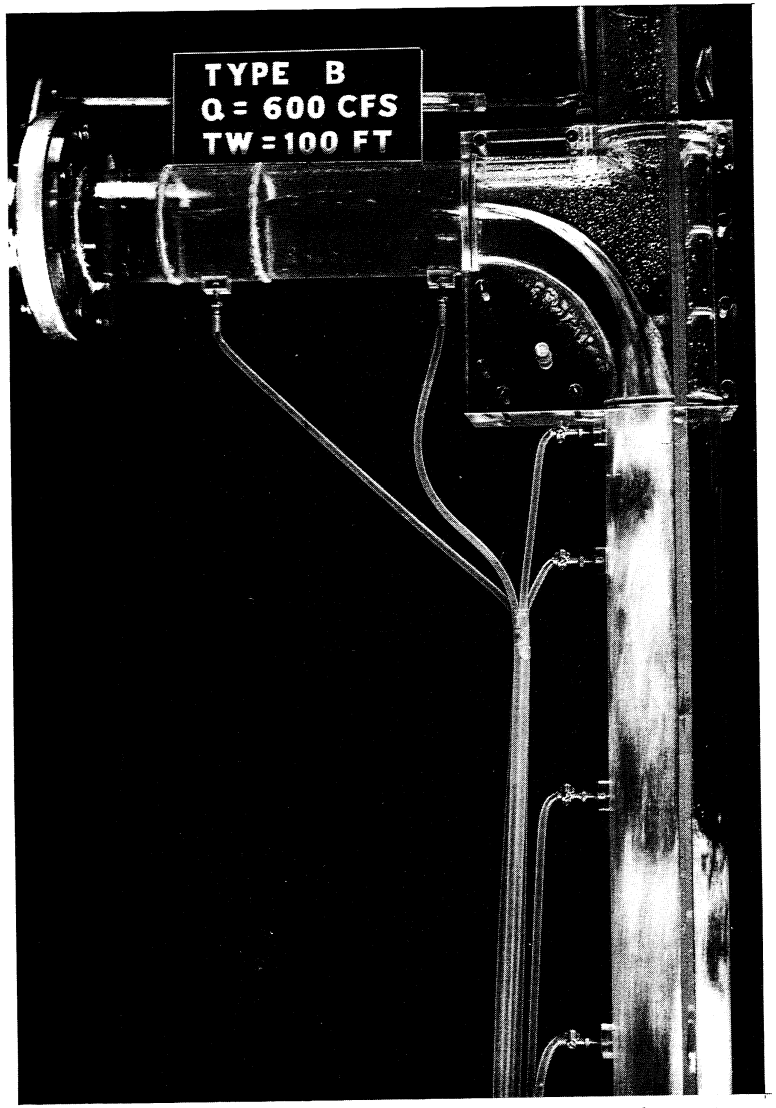

Photo 41

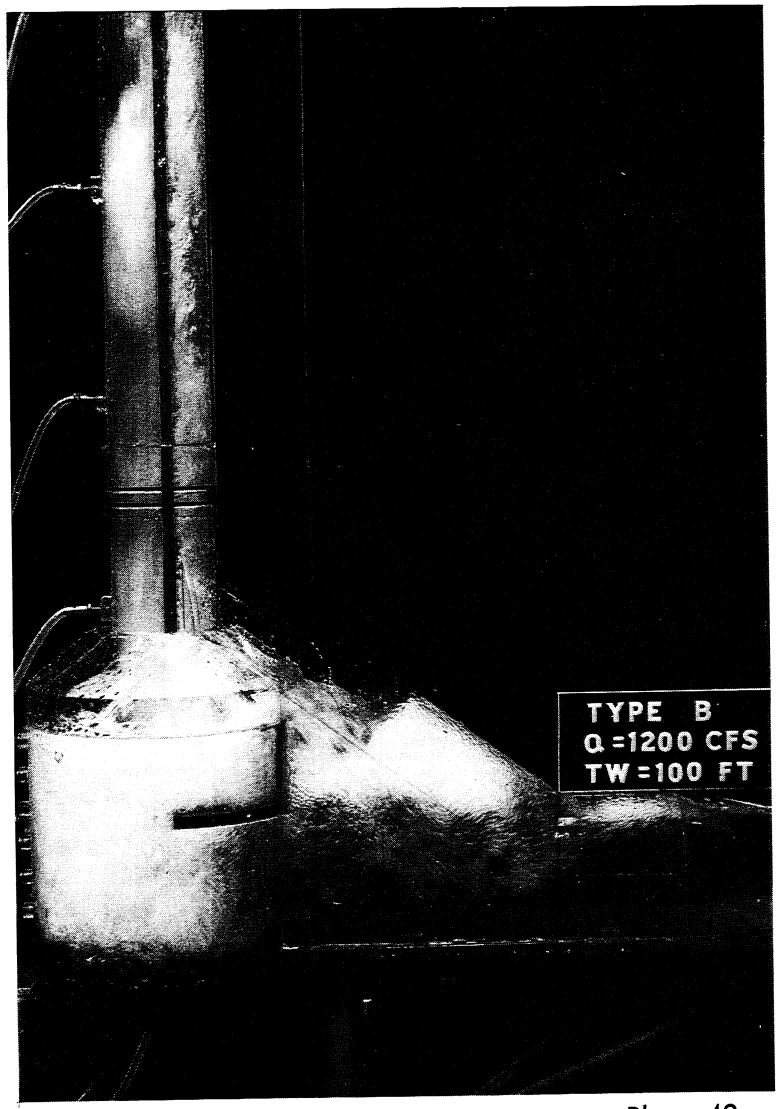

Photo 42

PHOTO 43 (Serial No. 177-124) In this photograph the flow past the slotted dividing wall without the deflector is shown. It shows the jets of water being forced through the slot to strike the opposite wall of the air vent. Also to be observed in this photograph is a relative non-uniformity of the flow in the water passage.

PHOTO 44 (Serial No. 177-138) When the discharge is increased to 1200 cfs through the structure with a divider wall with slots only, the jets through the slots are more intense and the flow is rather non-uniform.

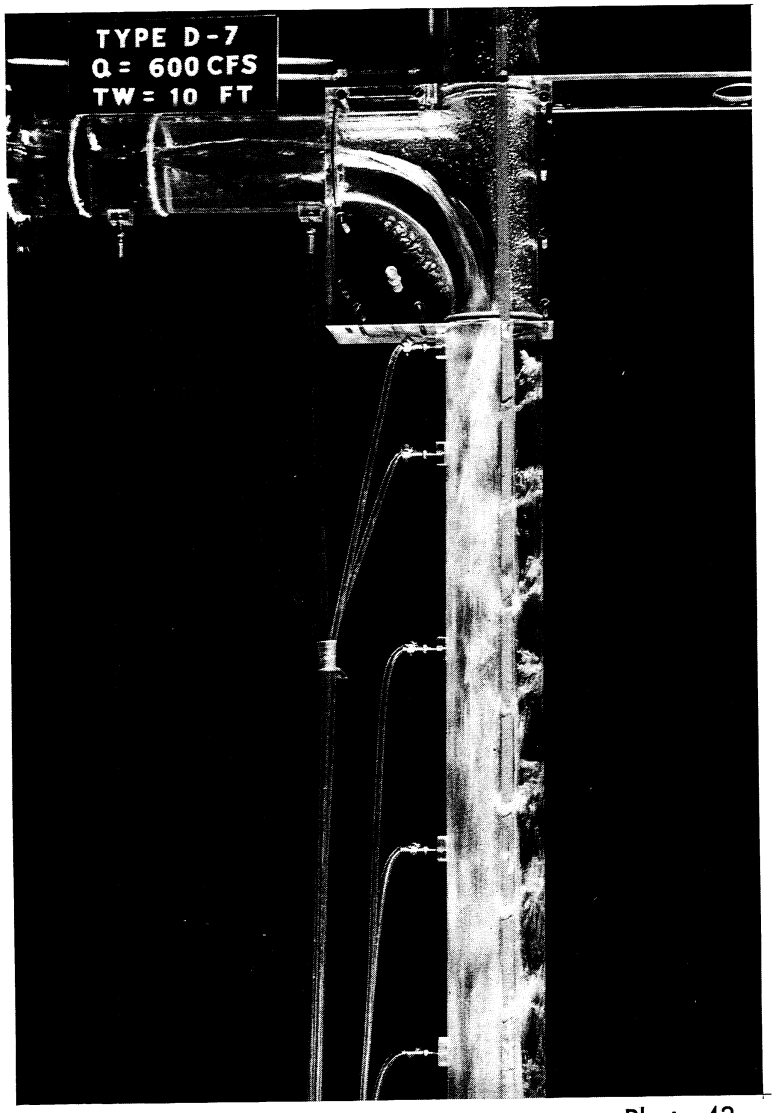

Photo 43

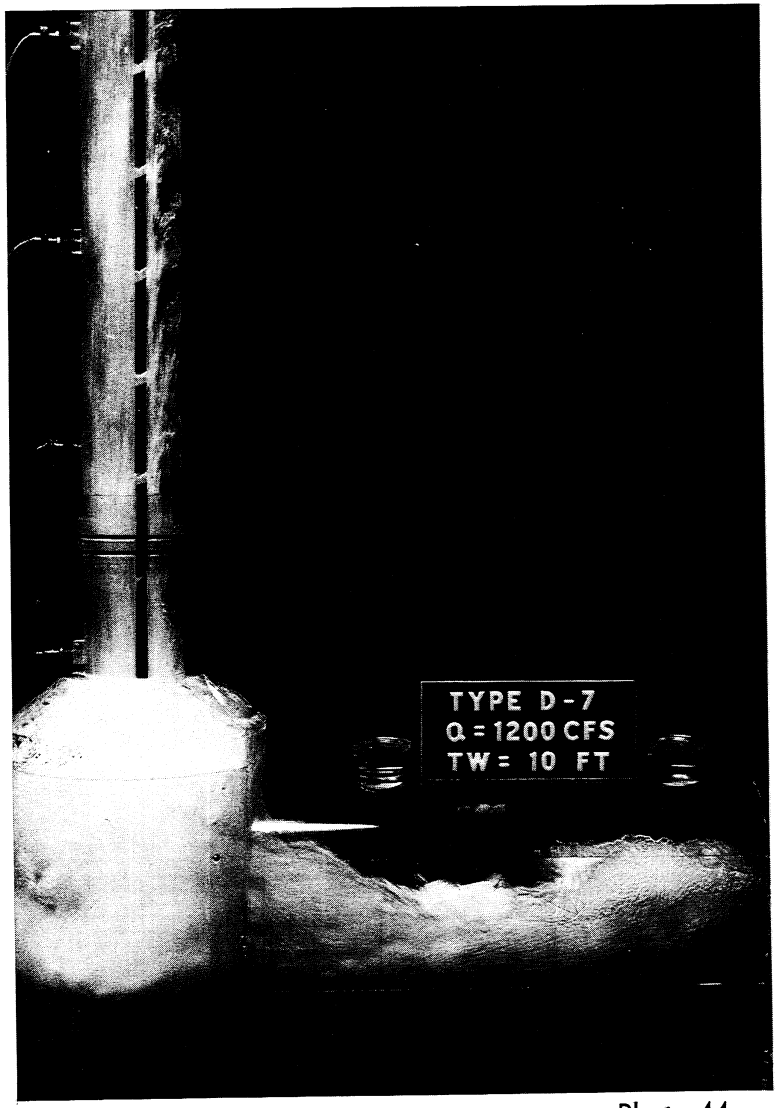

Photo 44

PHOTO 45 (Serial No. 177-197) In this photograph is a discharge of 600 cfs through the structure with the original deflector over the air slots. The flow pattern is considerably improved and no water escapes through the slots into the air vent.

PHOTO 46 (Serial No. 177-201) For a discharge of 1200 cfs with the original deflectors in place the flow is very uniform and the air is uniformly distributed.

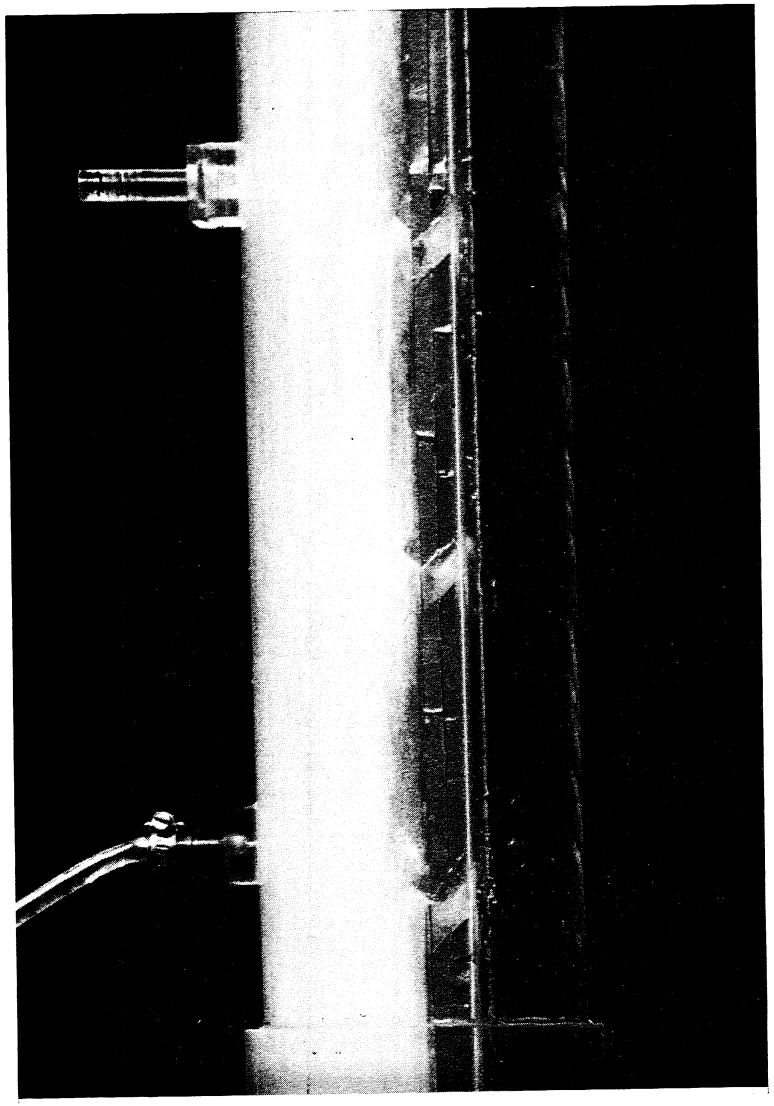

Photo 45

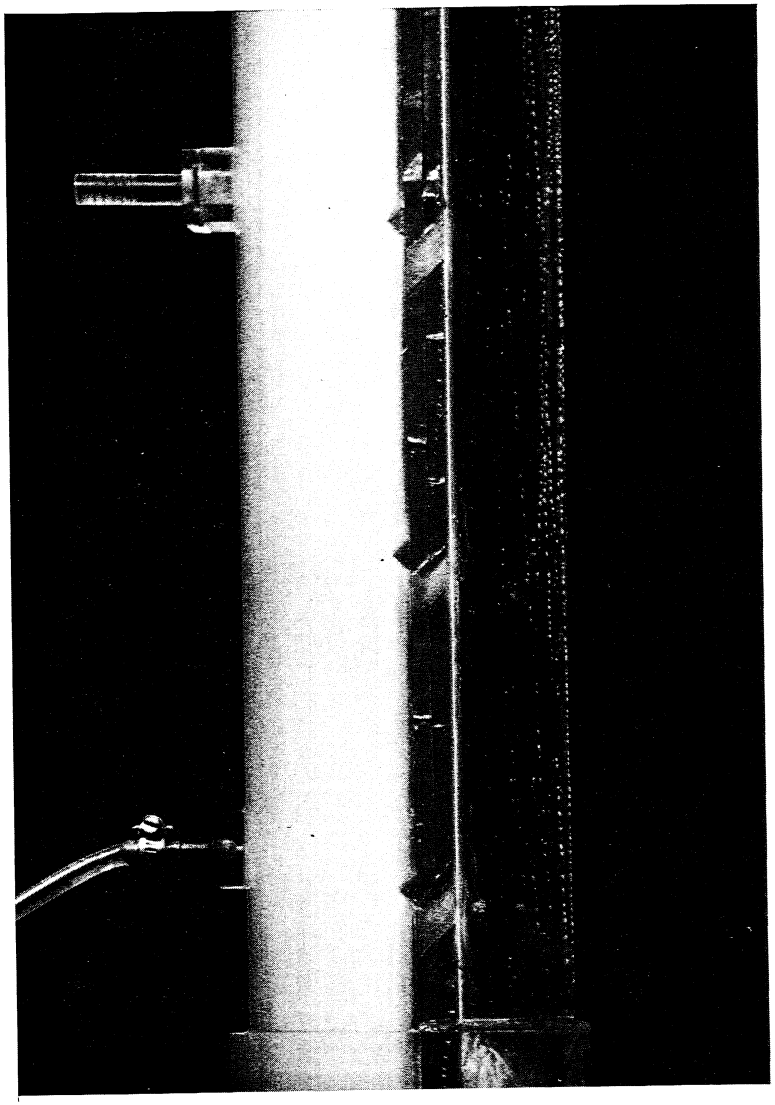

Photo 46

PHOTO 47 (Serial No. 177-151) In this photograph is shown the flow past the smaller modified deflector. Although the flow appears to be rather uniform with a uniform air distribution, it appears that the deflection past the slots is relatively small and apparently ineffective.

PHOTO 48 (Serial No. 177-162) This shows the flow past the small deflectors in the lower region of the drop shaft. Again, the air concentration appears to be well distributed, but the deflection of the streamlines at the deflector is negligibly small.

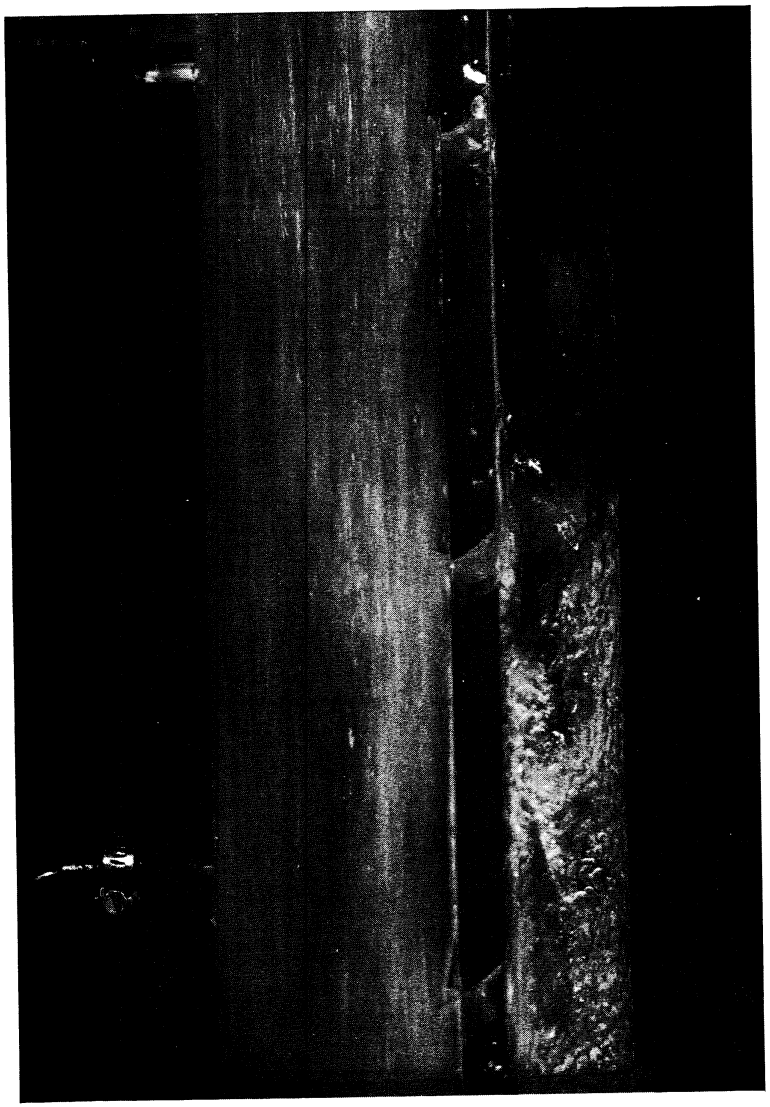

Photo 47

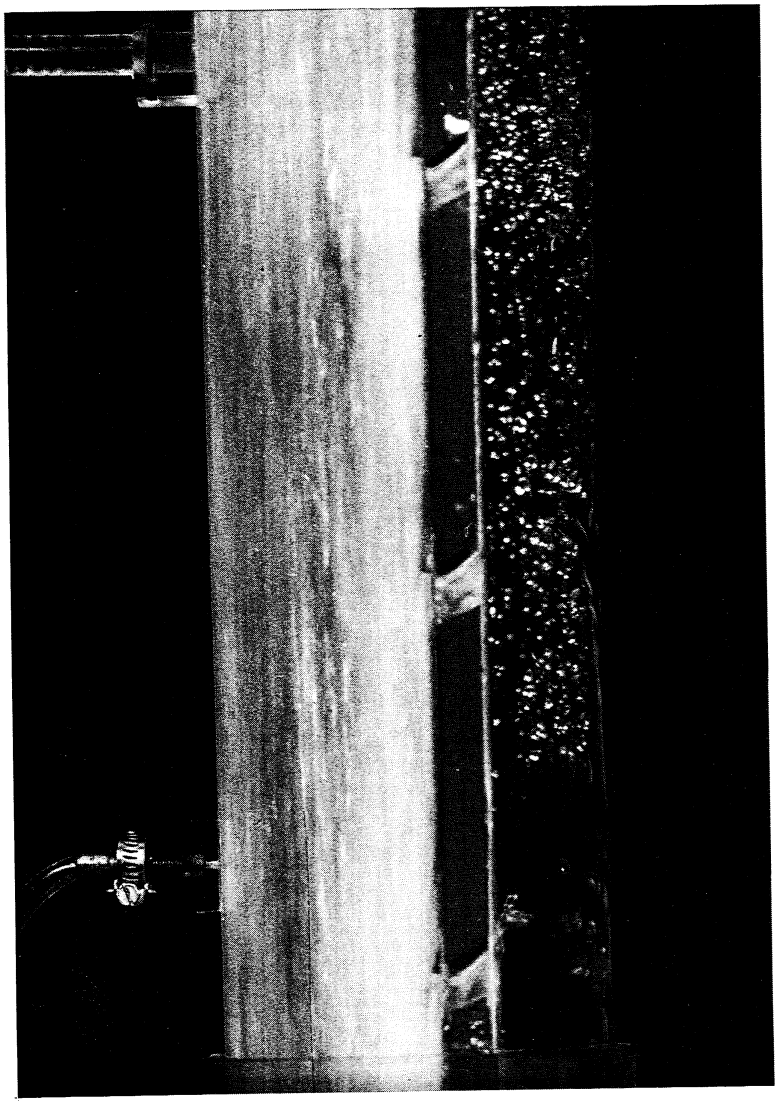

Photo 48

PHOTO 49 (Serial No. 177-232) This is a view of a larger asymmetrical deflector designated E-4. It shows the flow pattern when the discharge is 600 cfs.

PHOTO 50 (Serial No. 177-236) In this photograph the discharge is 600 cfs with a tailwater at elevation 100 ft. The flow past the wedges serving as deflectors is quite smooth and uniform.

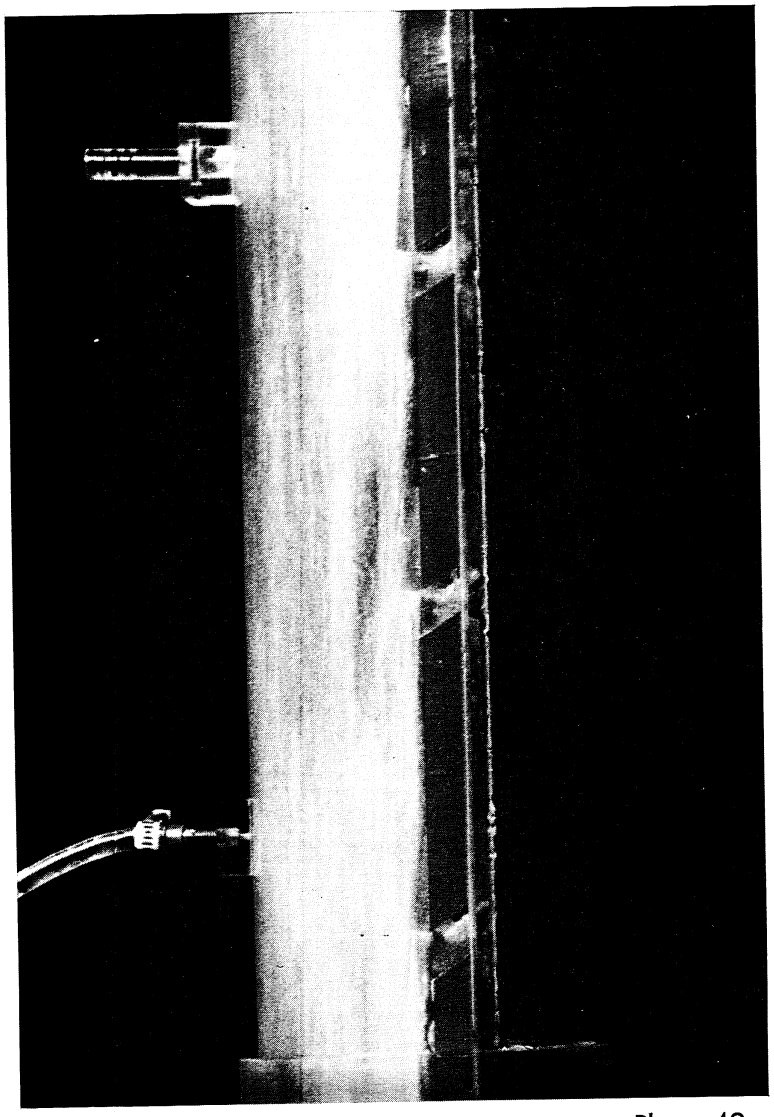

Photo 49

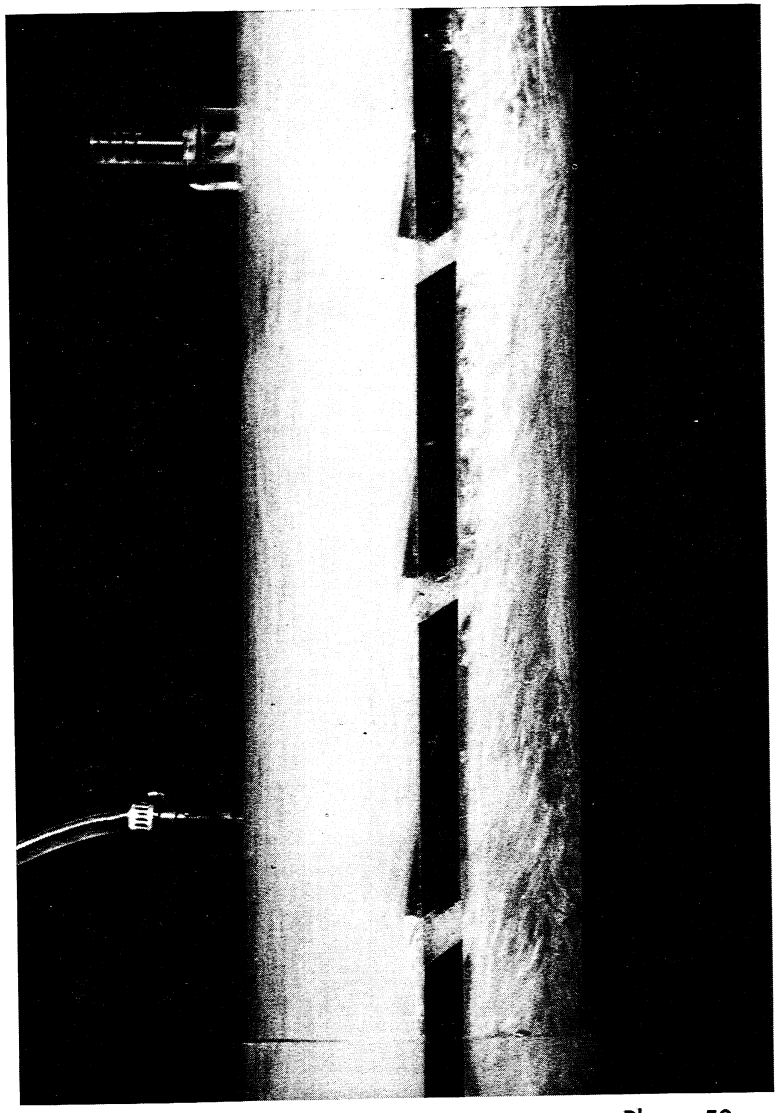

Photo 50

PHOTO 51 (Serial No. 177-269) When the tailwater elevation is raised to 190 ft, which is somewhat below the elevation of the incoming tunnel, the discharge of 600 cfs flows smoothly around the inlet and into the drop shaft proper. As it flows into the drop shaft, air is entrained and mixed with the water. The pressures in the incoming tunnel are atmospheric and the water surface represents the hydraulic gradeline.

PHOTO 52 (Serial No. 177-272) When the tailwater is raised to 225 ft, however, the piezometric pressures in the upstream tunnel are increased, and except for the entrapment of air in this tunnel it would run full, since the piezometric pressures are above the top of the tunnel.

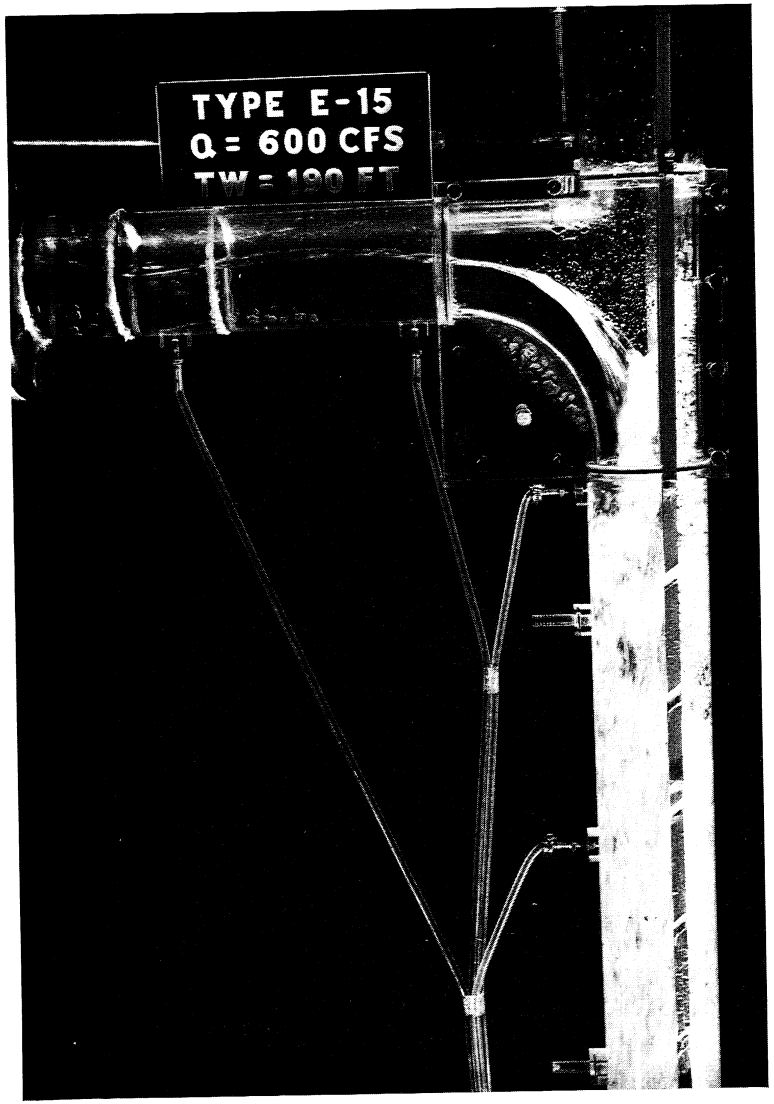

Photo 51

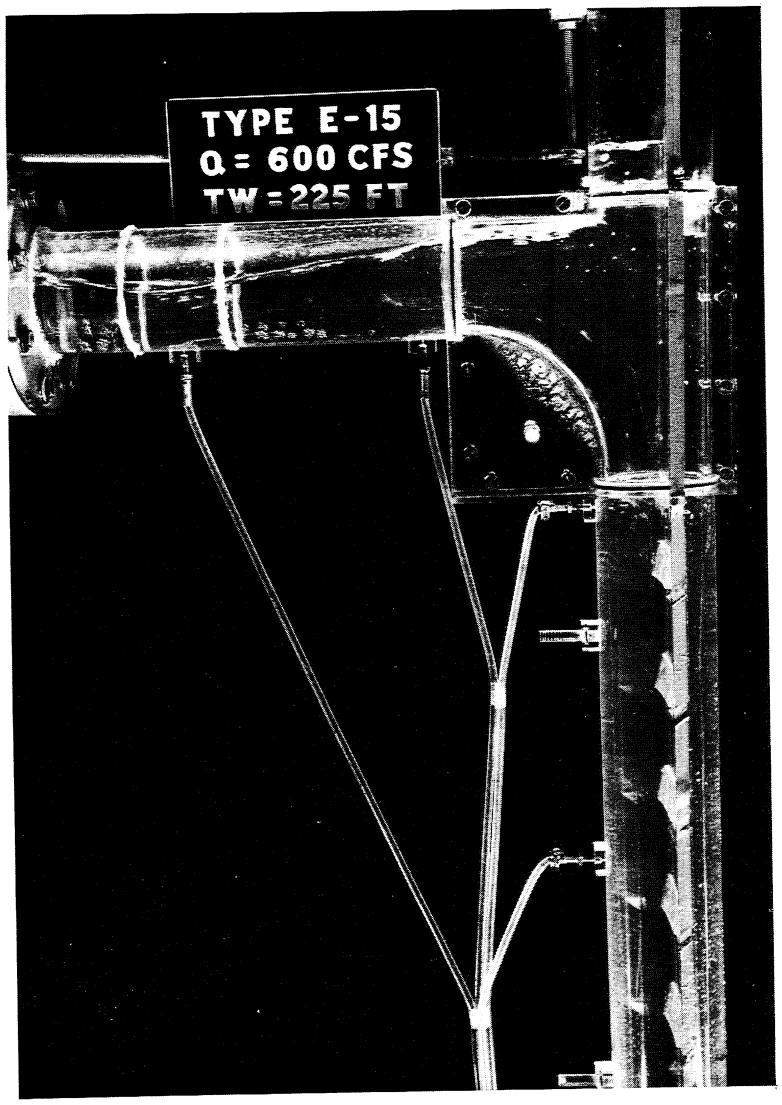

Photo 52

PHOTO 53 (Serial No. 177-474) In the Type F structure the upper and lower inlet conduits are 60 degrees from each other and symmetrical with the perpendicular from the dividing wall. This asymmetric flow at the two inlets generates secondary currents in opposite directions that tend to counteract each other in the region below the lower inlet conduit. They can be seen, however, in the region between the inlet conduits where the entrained air delineates the diagonal currents. It appears that these secondary currents are largely eliminated as the water enters the sump below.

PHOTO 54 (Serial No. 177-477) When the tailwater is raised to elevation 180 ft, the lower inlet and most of the drop structure up to the upper inlet are submerged with a consequent significant reduction in the secondary currents. The photograph shows that for this tailwater elevation the flow pattern is quite straight and parallel to the drop shaft walls.

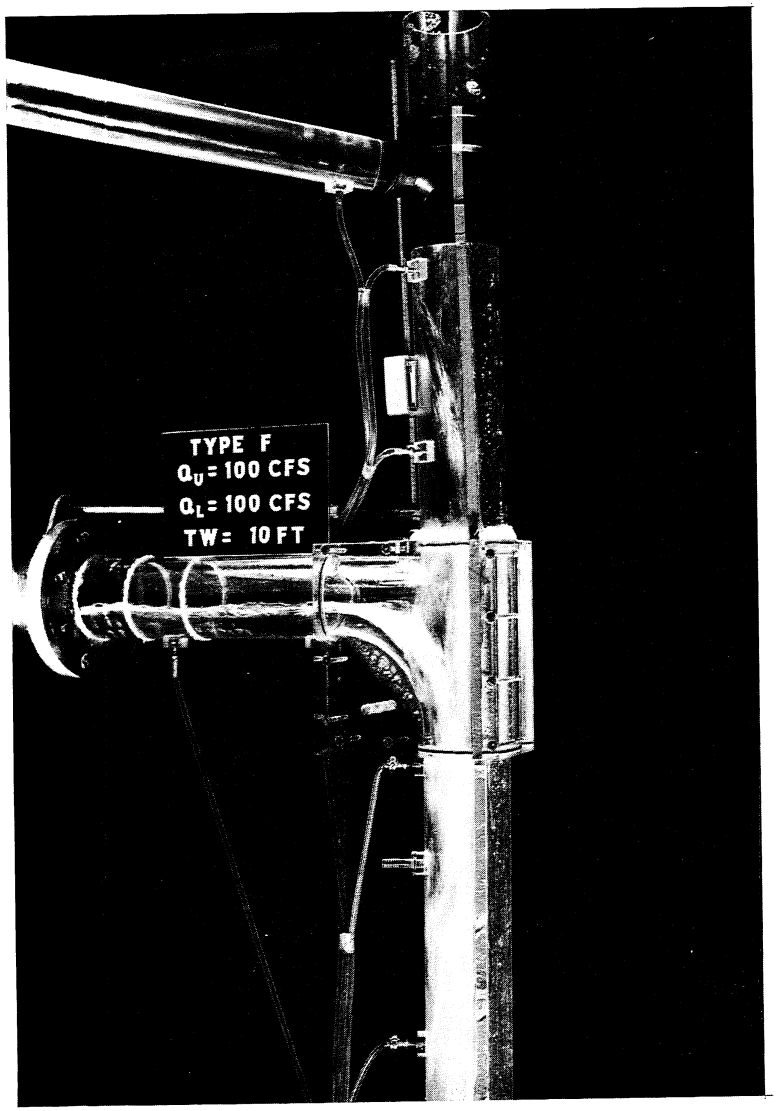

Photo 53

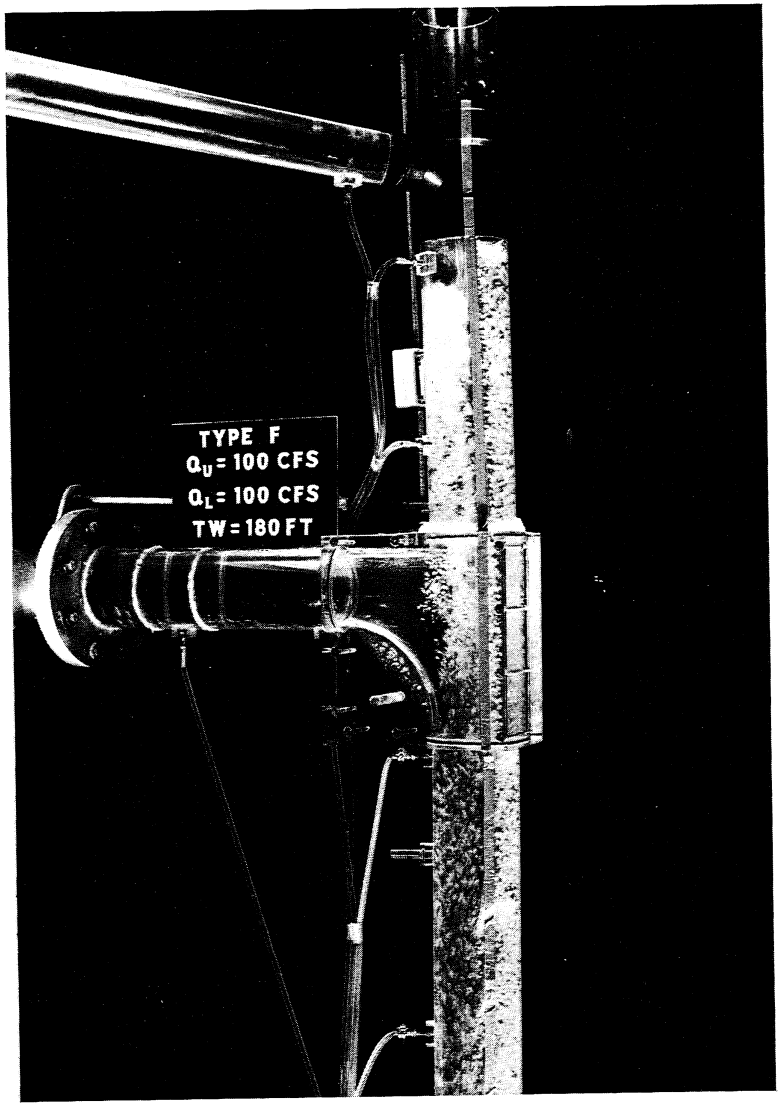

Photo 54

PHOTO 55 (Serial No. 177-493) In the Type F-1 structure the inlet conduits are separated by 90 degrees. This larger separation tends to increase the intensity of the secondary currents which are apparent in the region between the inlet conduits. Even these, however, are effectively dissipated as the flow proceeds down the drop shaft.

PHOTO 56 (Serial No. 177-494) The increased tailwater raised to elevation 180 ft is sufficient to reduce the secondary current, with the result that the flow below the lower inlet is relatively undisturbed.

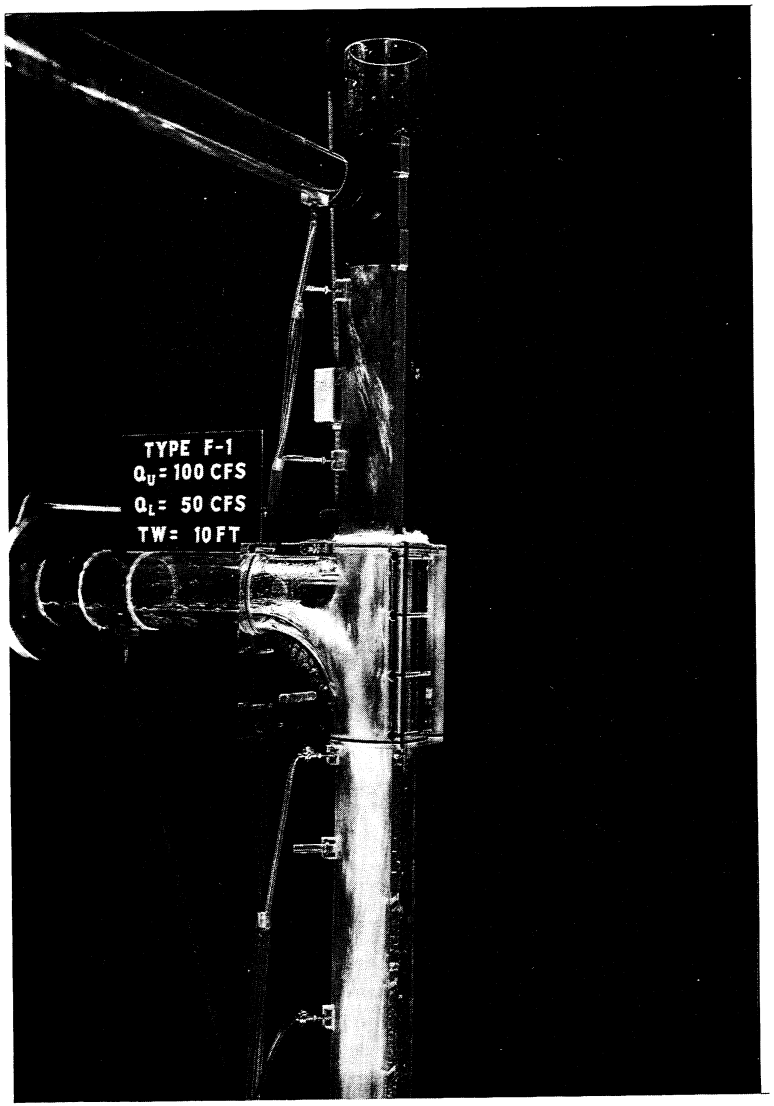

Photo 55

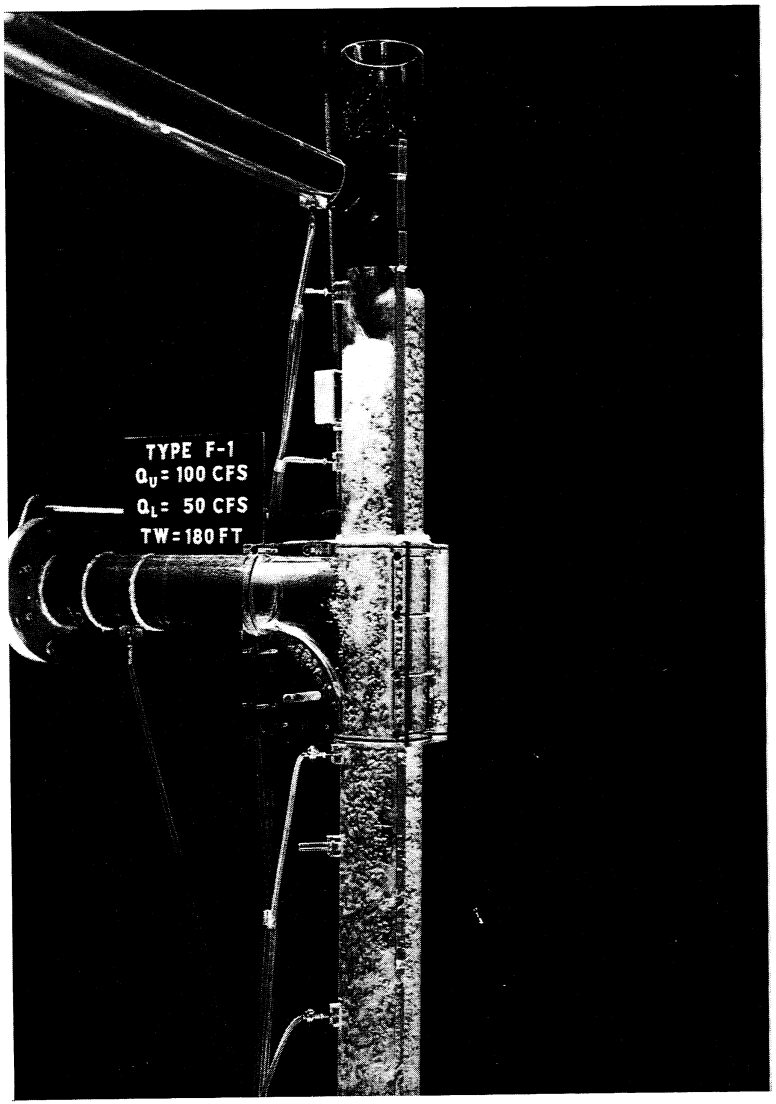

Photo 56

PHOTO 57 (Serial No. 177-511) The effect of the secondary current from the upper inlet is further strengthened when the inlet conduit enters the drop shaft parallel to the dividing wall. The jet strikes the opposite corner and is strongly deflected around the curved wall of the drop shaft proper. These secondary currents between the inlets are clearly shown in the photograph.

PHOTO 58 (Serial No. 177-512) When the tailwater is raised to elevation 180 ft, the secondary currents generated by the upper inlets are absorbed by the tailwater and the symmetrical flow from the lower inlet.

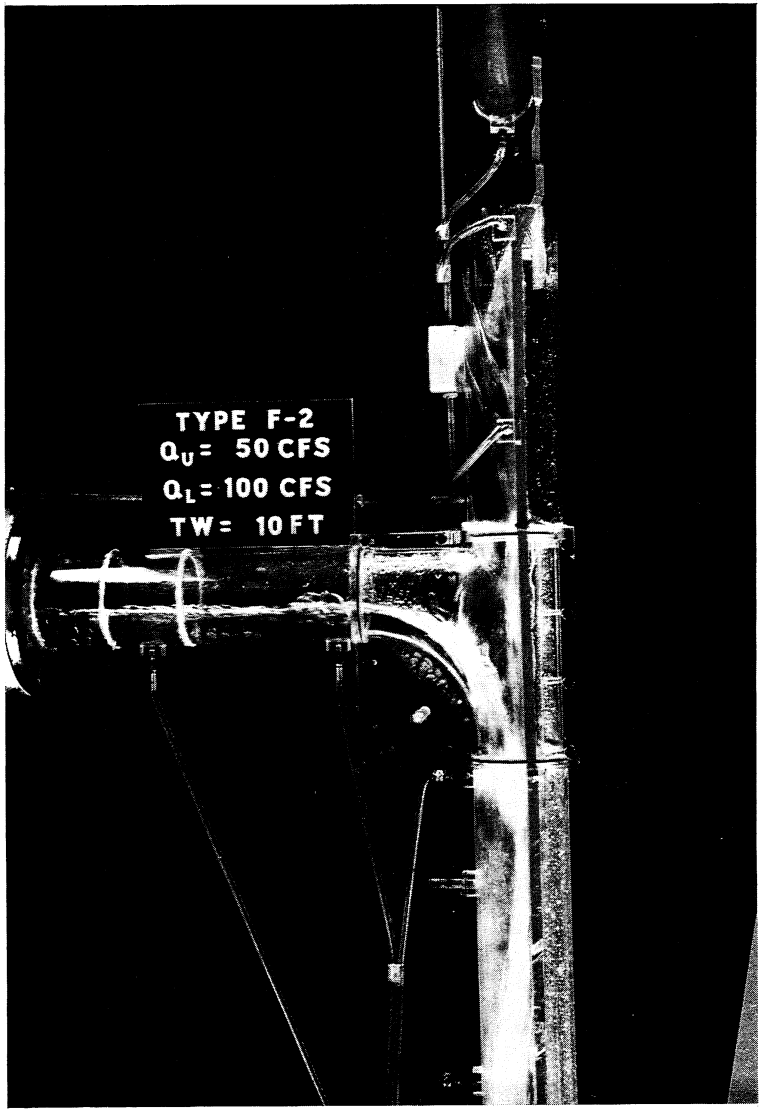

Photo 57

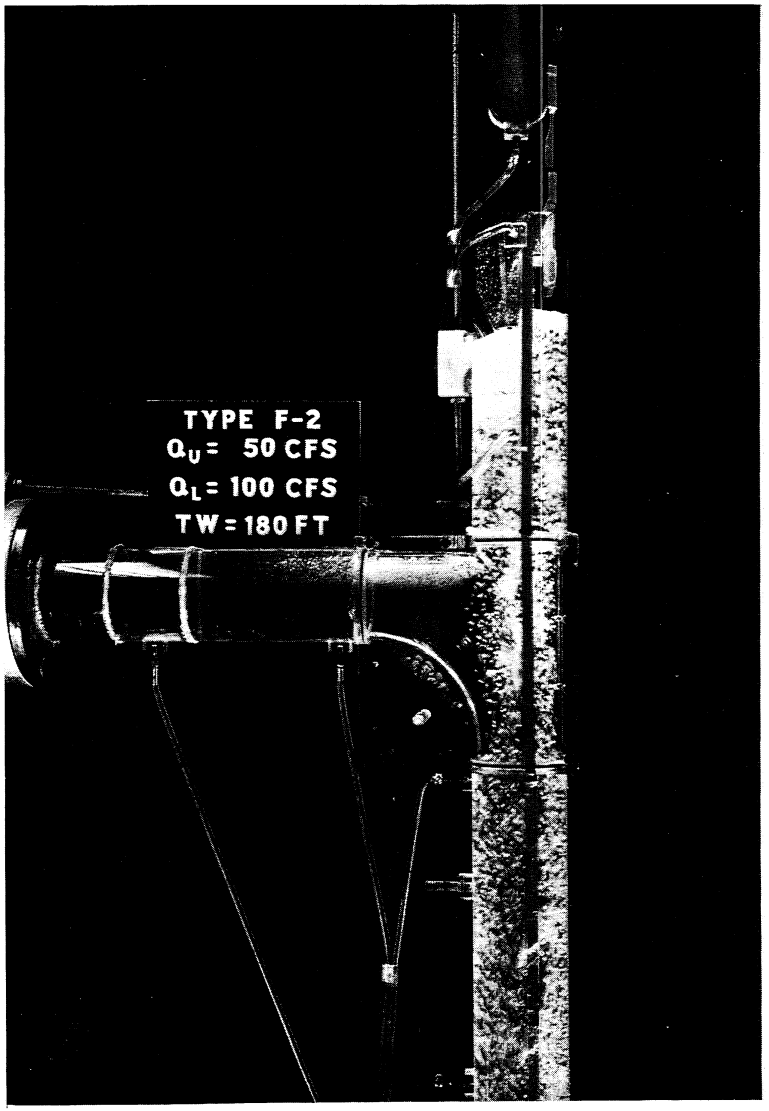

Photo 58

PHOTO 59 (Serial No. 177-424) This photo shows the drop shaft and the attachment of the two-wire capacitance type wave recorder by means of which the water surface fluctuation could be measured. In this experiment the discharge is 600 cfs and the tailwater is 50 ft.

PHOTO 60 (Serial No. 177-425) This is a close-up of the drop shaft shown in Photo 59. The two wires of the wave recorder can be clearly seen.

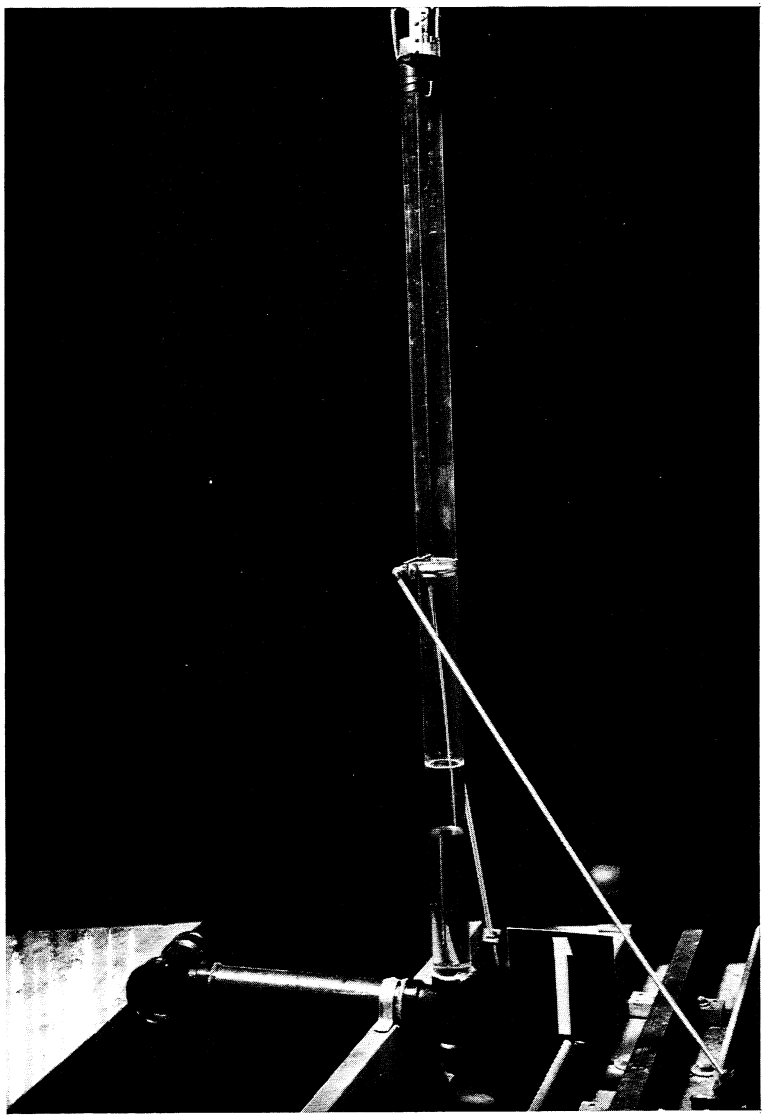

Photo 59

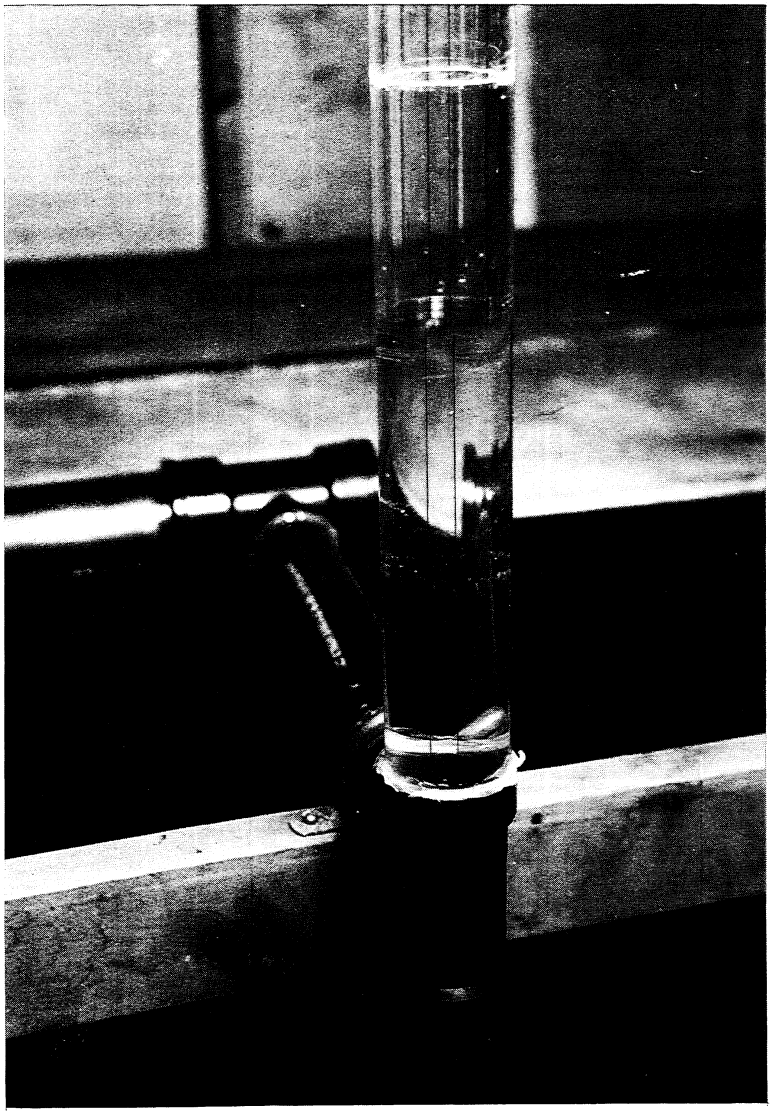

Photo 60

PHOTO 61 (Serial No. 177-428) This shows a discharge of 600 cfs into drop shaft 3 when the tailwater is at elevation 50 ft. The incoming flow causes the water in the system to become highly aerated and turbulent.

PHOTO 62 (Serial No. 177-429) This is a close-up at the lower end of the drop shaft for the conditions shown in Photo 61.

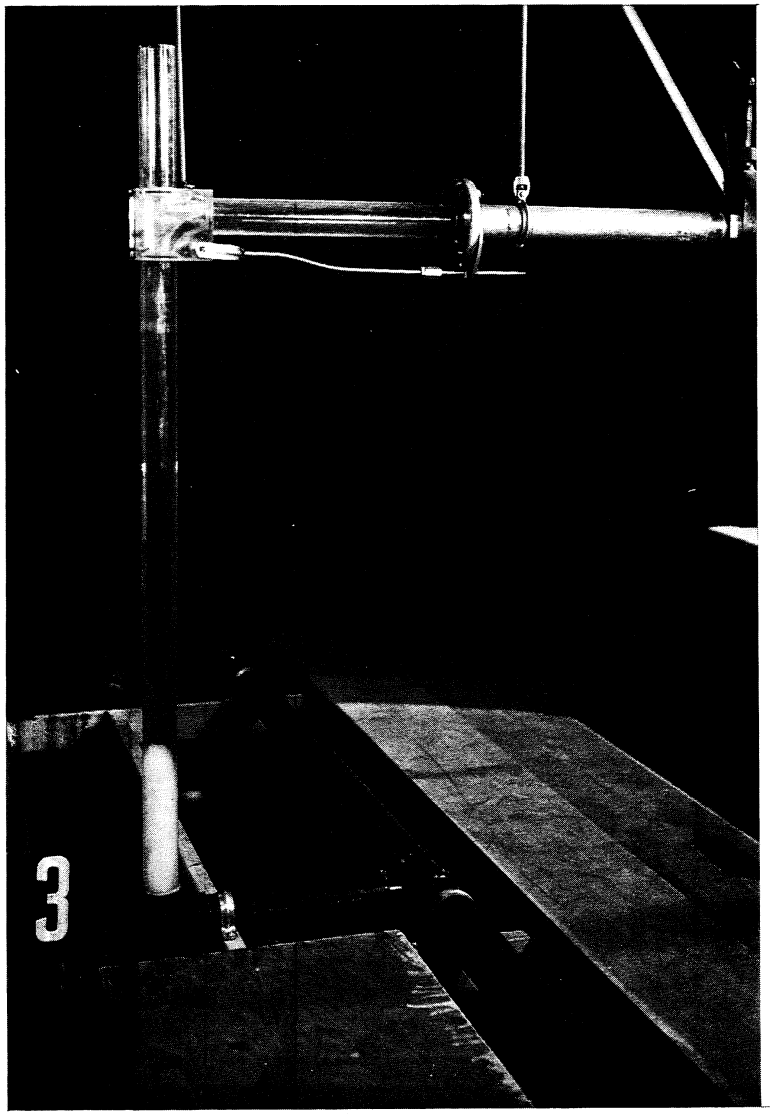

Photo 61

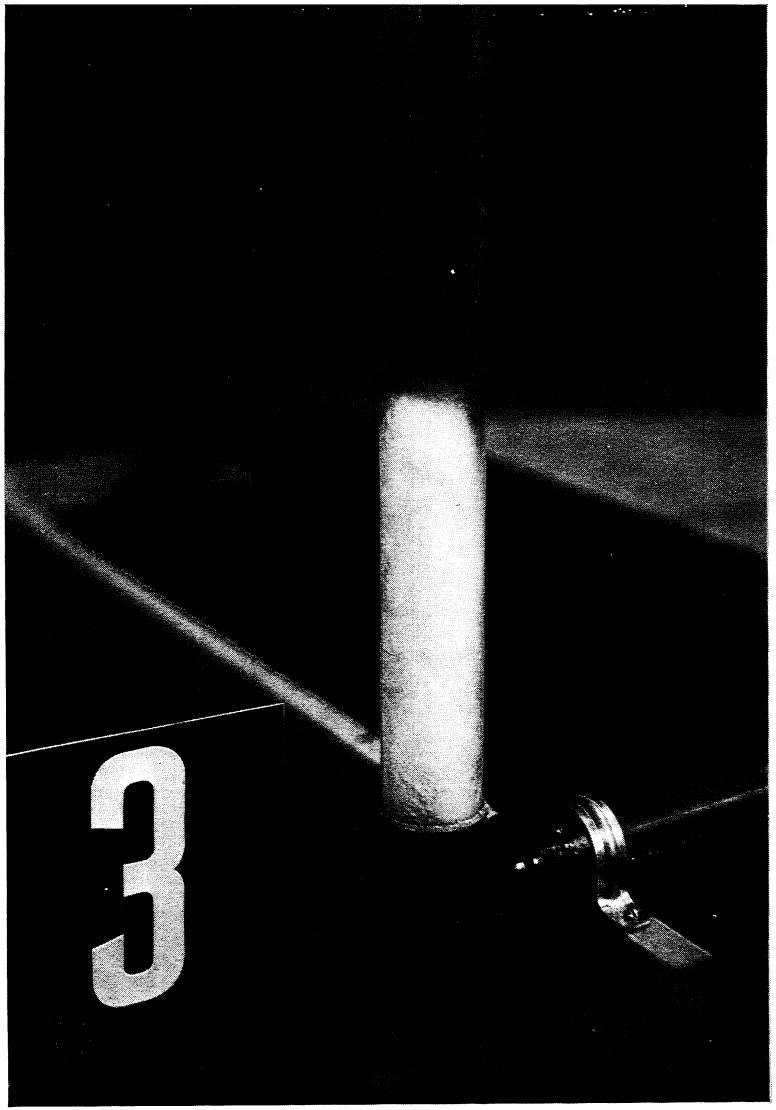

Photo 62

LIST OF CHARTS

CHART 16 (177B474-85) Geometry of the Type E drop shaft designs from Type E-11 through Type E-17.

CHART 17 (177B474-82) Piezometric pressures through the Type E-14 drop shaft for various discharges and tailwater at elevation 10 ft.

CHART 18 (177B474-83) Piezometric pressures in the Type E-14 drop shaft for various discharges and tailwater at elevation 100 ft.

CHART 19 (177B474-84) Piezometric pressures in the Type E-14 drop shaft for various discharges and tailwater at elevation 190 ft.

CHART 20 (177B474-114) Piezometric pressures through Type E-15 drop shaft for various discharges and tailwater at elevation 10 ft.

CHART 21 (177B474-115) Piezometric pressures through Type E-15 drop shaft for various discharges and tailwater at elevation 100 ft.

CHART 22 (177B474-116) Piezometric pressures through Type E-15 drop shaft for various discharges and tailwater at elevation 190 ft.

CHART 23 (177B474-130) Comparison of average air concentration in Types E-14 and E-15 drop shafts for a discharge of 600 cfs and various tailwater elevations.

CHART 24 (177B474-131) Average air concentrations in Type E-15 drop shaft for various discharges and tailwater elevations.

CHART 25 (177B474-78) Piezometric pressures in Type E-14 drop shaft for submerged flow. Tailwater = 225 ft, various discharges.

CHART 26 (177B474-79) Piezometric pressures in Type E-15 drop shaft when submerged. Tailwater = 225 ft, various discharges.

CHART 27 (177B474-81) Piezometric pressures in Type E-17 drop shaft for submerged flow. Tailwater elevation = 225 ft, various discharges.

CHART 28 (177B474-86) Typical pressure fluctuations on the floor of the impact model for various discharges and tailwater at zero elevation.

CHART 29 (177B474-90) Typical pressure fluctuations on the floor of the impact model for various discharges and tailwater maintained at elevation 50 ft.

CHART 30 (177B474-98) Comparison of pressure fluctuations as measured by flush mounted and block mounted pressure transducer in the impact model. Frequency of pressure peaks equal to or greater than given amounts are tabulated.

CHART 31 (177B474-99) Typical pressure fluctuations on the floor of the sump of the Type E-14 drop shaft for various discharges and tailwater at elevation 10 ft.

CHART 32 (177B474-102) Typical pressure fluctuations on the floor of the sump of the Type E-14 drop shaft for various discharges and tailwater maintained at elevation 50 ft.

CHART 33 (177B474-103) Typical pressure fluctuations on the floor of the sump of the Type E-15 drop shaft for various discharges and tailwater at elevation 10 ft.

CHART 34 (177B474-111) Frequency of pressure peaks in the Type E-15 drop shaft for a discharge of 600 cfs and various tailwaters.

CHART 35 (177B474-117) Comparison of impact forces in the Type E-14 and E-15 drop shafts and the impact model. Frequency of pressure peaks above reference elevation with a discharge of 600 cfs and various tailwater elevations.

CHART 36 (177B474-157) Piezometric pressures along the Type F drop shaft for various discharges and tailwater elevations.

CHART 37 (177B474-158) Piezometric pressures along the Type F-1 drop shaft for various discharges and tailwater elevations.

CHART 38 (177B474-159) Piezometric pressures along the Type F-2 drop shaft for various discharges and tailwater elevations.

CHART 39 (177B474-142) Type A surge model. Typical water surface fluctuations in drop shafts. Discharge 600 cfs. Tailwater elevation 10 ft.

CHART 40 (177B474-143) Type A surge model. Typical water surface fluctuations in drop shafts. Discharge 600 cfs. Tailwater 100 ft.

CHART 41 (177B474-144) Type A surge model. Typical water surface fluctuations in drop shafts. Discharge 600 cfs. Tailwater 100 ft. Flow duration approximately one minute.

CHART 42 (177B474-149) Type B surge model. Typical water surface fluctuations in drop shafts. Discharge 600 cfs. Tailwater elevation 10 ft.

CHART 43 (177B474-150) Type B surge model. Typical water surface fluctuations in drop shafts. Discharge 600 cfs. Tailwater elevation 100 ft.

CHART 44 (177B474-151) Type B surge model. Typical water surface fluctuations in drop shafts. Discharge 600 cfs. Tailwater 100 ft. Duration approximately one minute.

CHART 45 (177B474-156) Type A surge model. Summary of water surface fluctuations in drop shafts at model dimensions. Flow conditions varied.

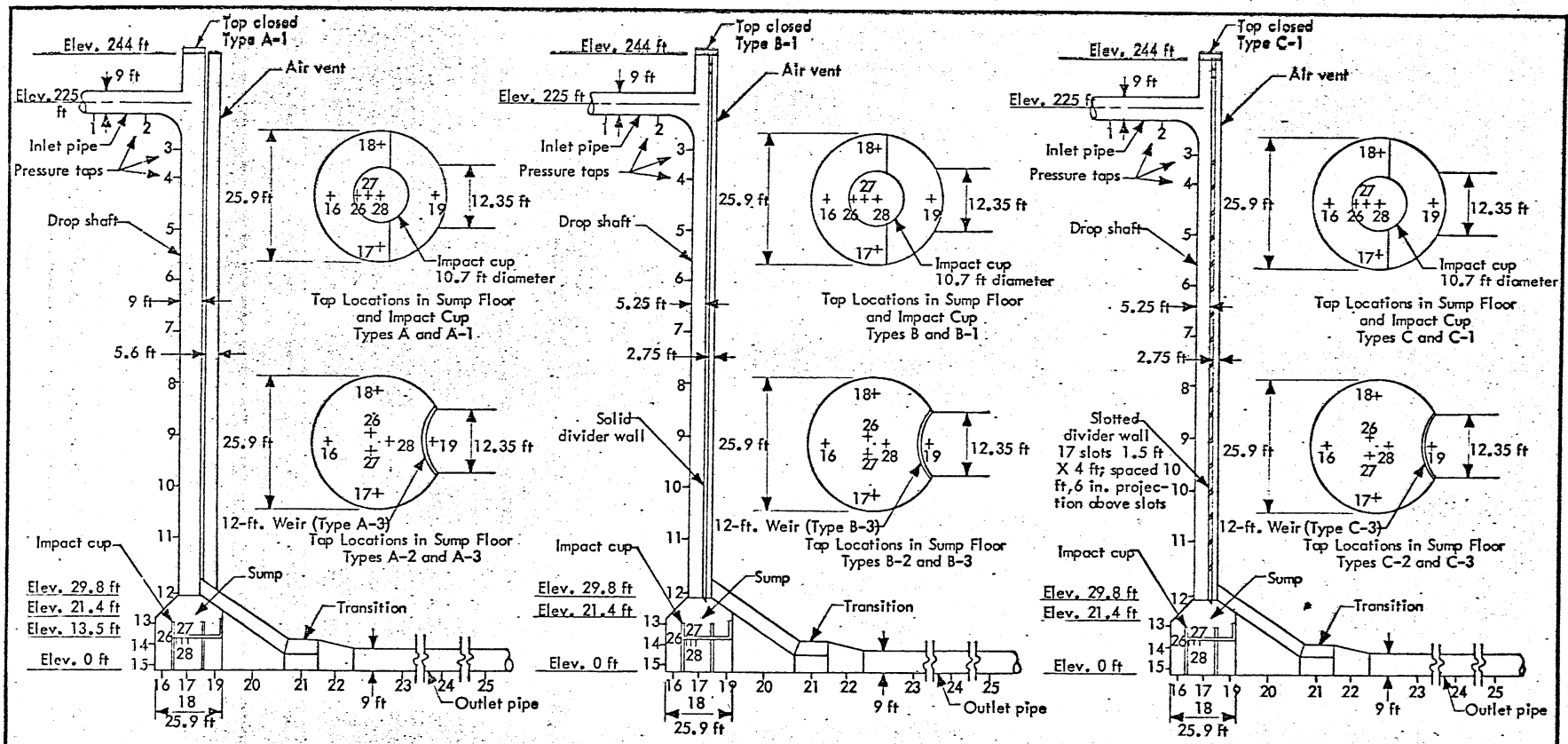

TYPE A Original design as shown
TYPE A-1 Same as Type A with top closed
TYPE A-2 Same as Type A with impact cup removed
TYPE A-3 Same as Type A with impact cup replaced by a 12-ft weir

TYPE B As shown
TYPE B-1 Same as Type B with top closed
TYPE B-2 Same as Type B with impact cup removed
TYPE B-3 Same as Type B with impact cup replaced by a 12-ft weir

TYPE C As shown
TYPE C-1 Same as Type C with top closed
TYPE C-2 Same as Type C with impact cup removed
TYPE C-3 Same as Type C with impact cup replaced by a 12-ft weir
TYPE C-4 Same as Type C-3 with lower 6 slots closed

TYPES A, B, AND C SERIES DROP SHAFTS

Drop Shaft Types Tested
Model Scale 1:27

LAWRENCE AVENUE SEWER SYSTEM
City of Chicago
Harza Engineering Co., Chicago, Ill.
DROP SHAFT STUDIES

SAINT ANTHONY FALLS HYDRAULIC LABORATORY
UNIVERSITY OF MINNESOTA

DRAWN GS	CHECKED	APPROVED
SCALE	DATE 10-18-67	No 177B474 - 37

CHART 1

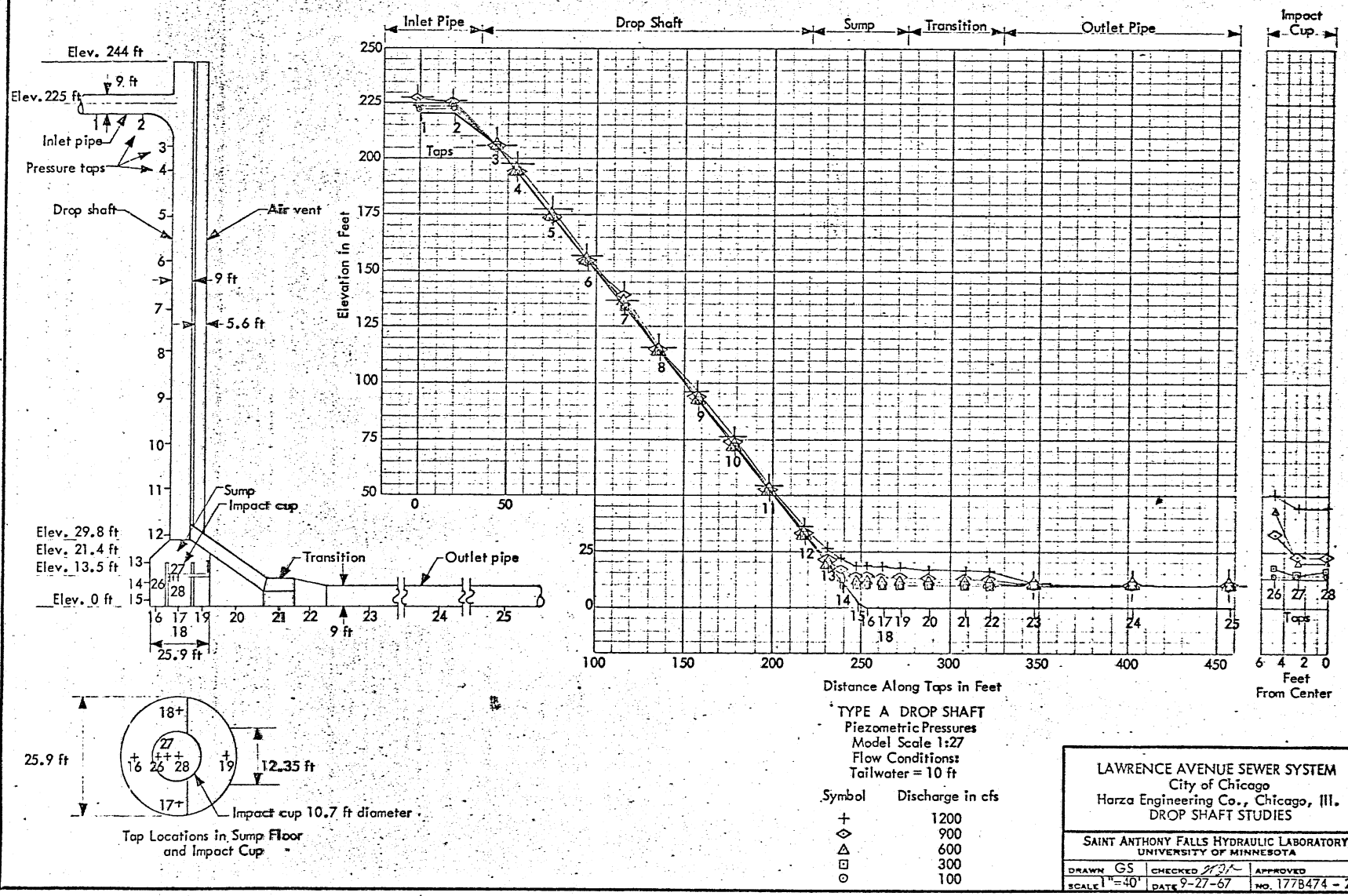

TYPE A DROP SHAFT
Piezometric Pressures
Model Scale 1:27
Flow Conditions:
Tailwater = 10 ft

Symbol	Discharge in cfs
+	1200
◇	900
△	600
⊡	300
⊙	100

LAWRENCE AVENUE SEWER SYSTEM
City of Chicago
Harza Engineering Co., Chicago, Ill.
DROP SHAFT STUDIES

SAINT ANTHONY FALLS HYDRAULIC LABORATORY
UNIVERSITY OF MINNESOTA

DRAWN GS	CHECKED	APPROVED
SCALE 1"=40'	DATE 9-27-67	NO. 177B474 - 2

CHART 2

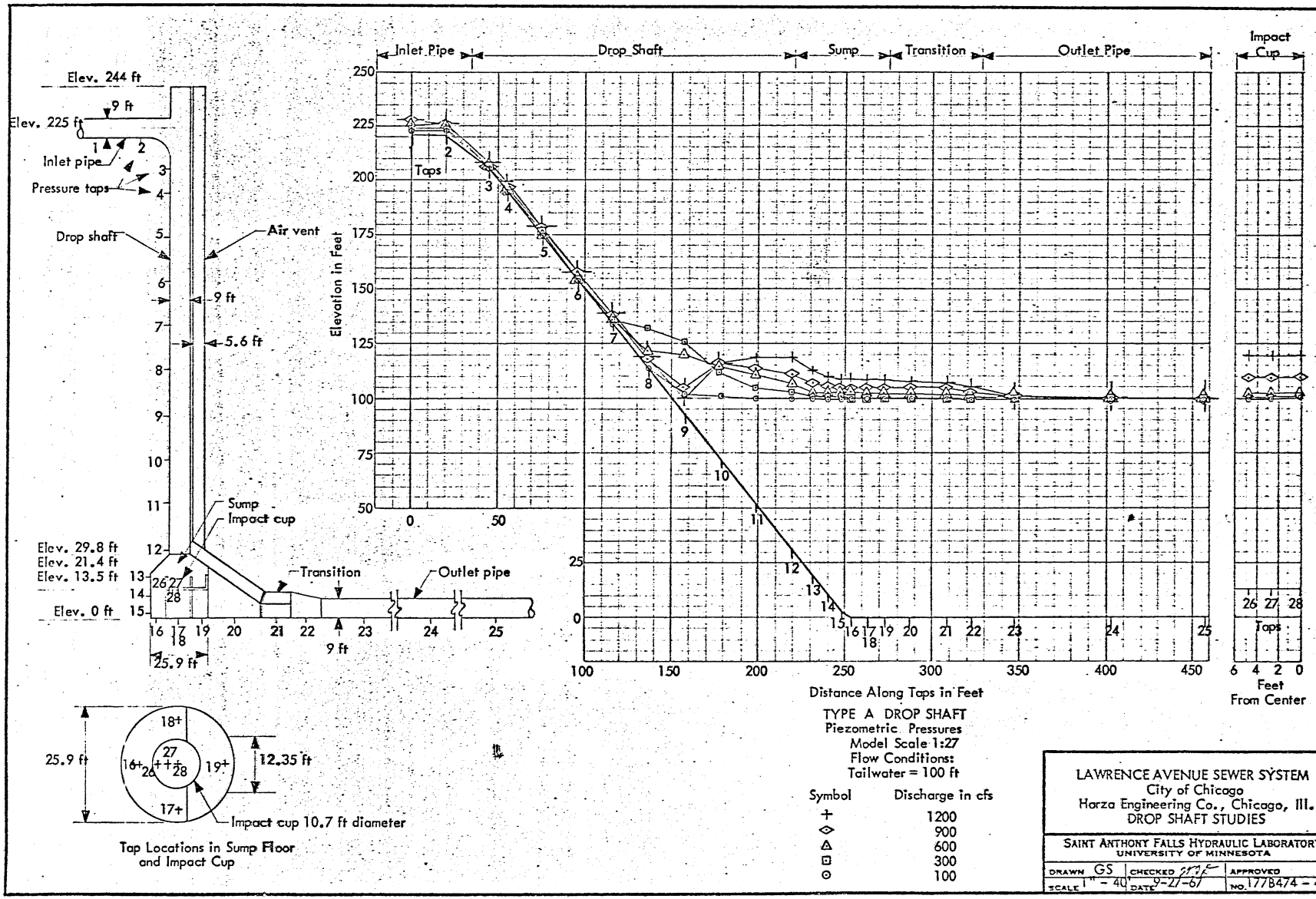

TYPE A DROP SHAFT
Piezometric Pressures
Model Scale 1:27
Flow Conditions:
Tailwater = 100 ft

Symbol	Discharge in cfs
+	1200
◇	900
△	600
□	300
○	100

LAWRENCE AVENUE SEWER SYSTEM
City of Chicago
Harza Engineering Co., Chicago, Ill.
DROP SHAFT STUDIES

SAINT ANTHONY FALLS HYDRAULIC LABORATORY
UNIVERSITY OF MINNESOTA

DRAWN	CHECKED	APPROVED
GS		
SCALE 1" = 40'	DATE 9-27-67	NO. 177B474 - 4

CHART 3

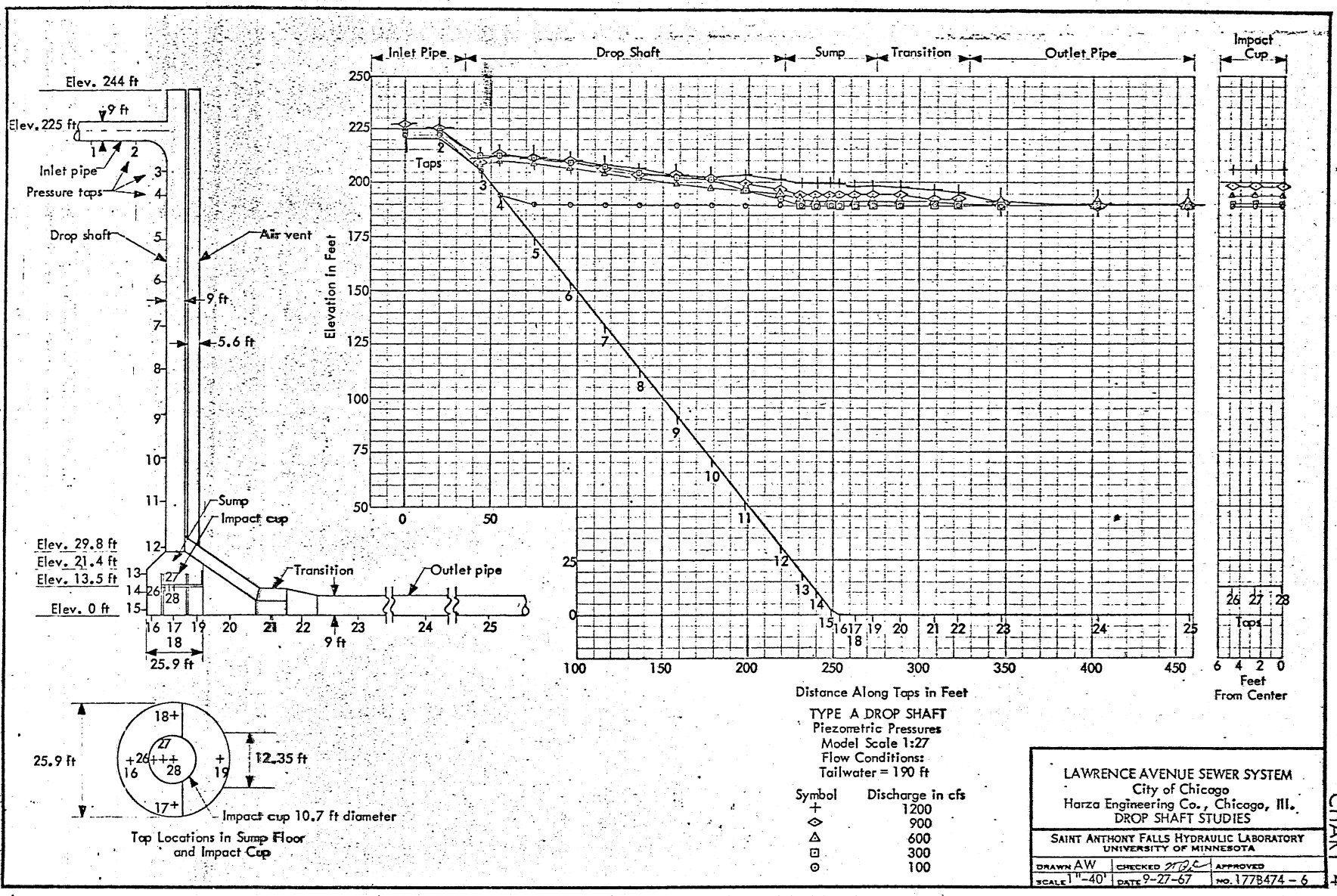

TYPE A DROP SHAFT
Piezometric Pressures
Model Scale 1:27
Flow Conditions:
Tailwater = 190 ft

Symbol	Discharge in cfs
+	1200
◇	900
△	600
⊡	300
⊙	100

LAWRENCE AVENUE SEWER SYSTEM
City of Chicago
Harza Engineering Co., Chicago, Ill.
DROP SHAFT STUDIES

SAINT ANTHONY FALLS HYDRAULIC LABORATORY
UNIVERSITY OF MINNESOTA

DRAWN AW	CHECKED	APPROVED
SCALE 1"=40'	DATE 9-27-67	NO. 177B474 - 6

CHART 4

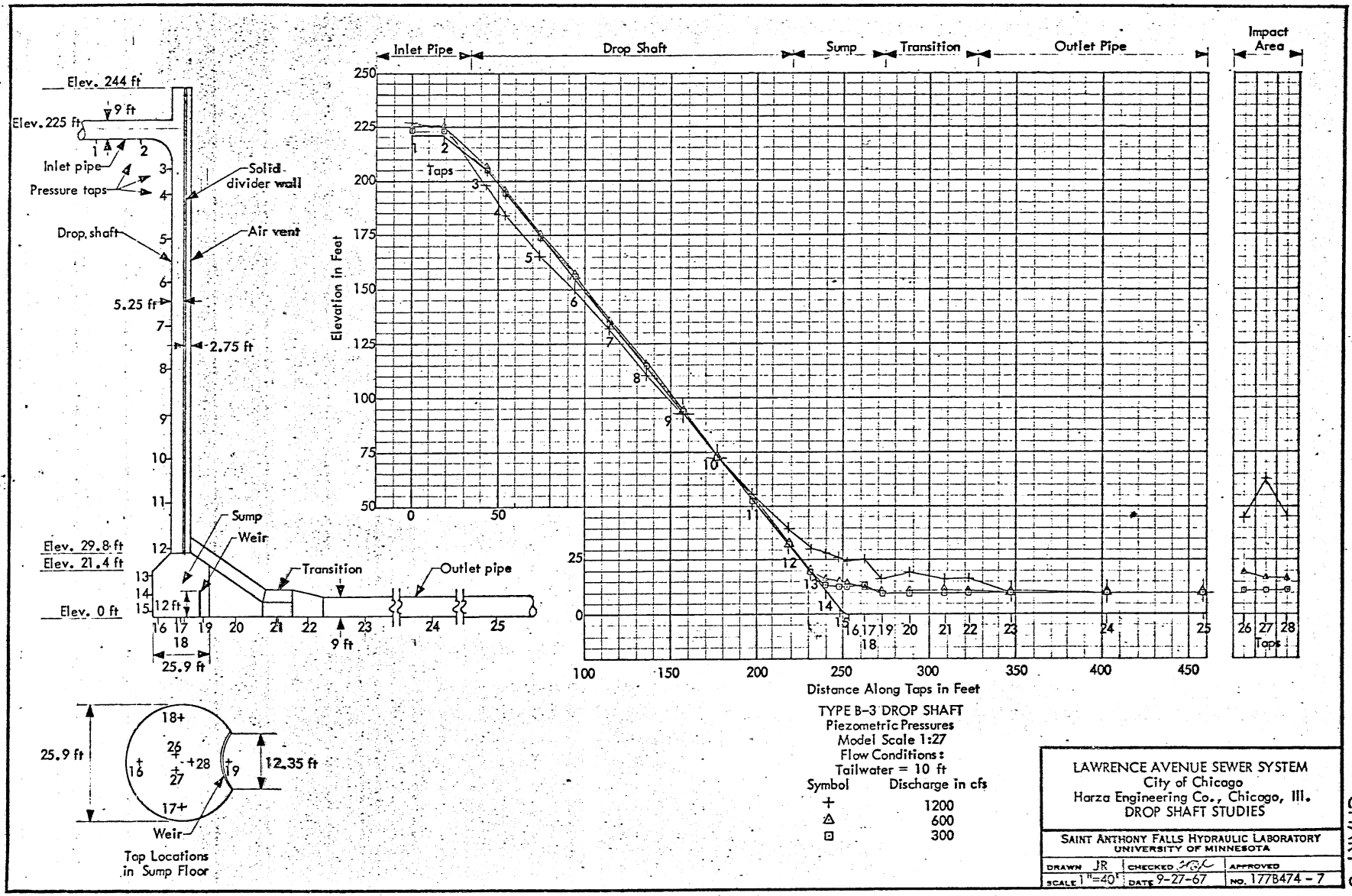

TYPE B-3 DROP SHAFT
Piezometric Pressures
Model Scale 1:27
Flow Conditions:
Tailwater = 10 ft

Symbol	Discharge in cfs
+	1200
△	600
⊡	300

LAWRENCE AVENUE SEWER SYSTEM
City of Chicago
Harza Engineering Co., Chicago, Ill.
DROP SHAFT STUDIES

SAINT ANTHONY FALLS HYDRAULIC LABORATORY
UNIVERSITY OF MINNESOTA

DRAWN	CHECKED	APPROVED
JR		
SCALE 1"=40'	DATE 9-27-67	NO. 177B474 - 7

CHART 5

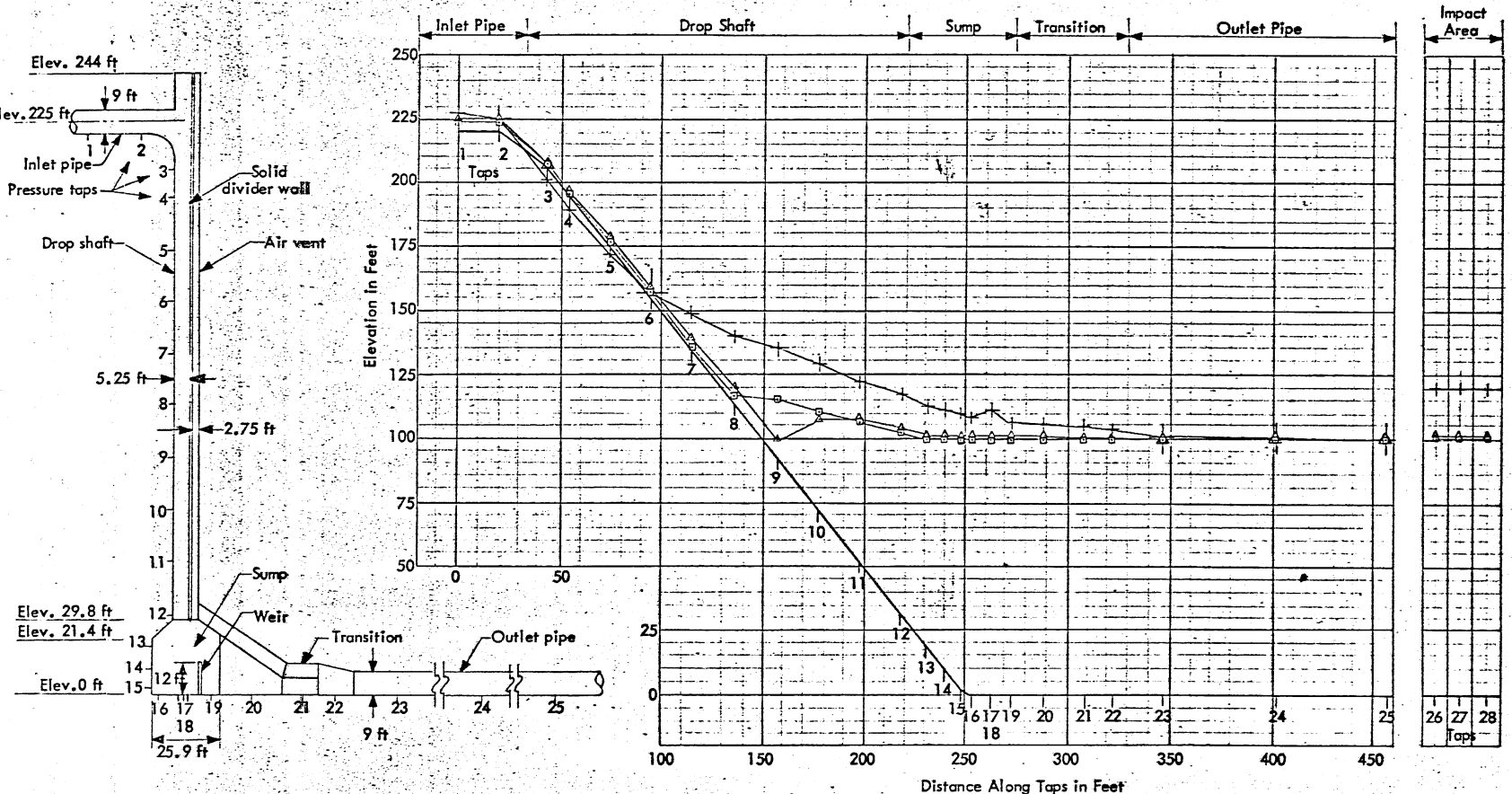

TYPE B-3 DROP SHAFT
Piezometric Pressures
Model Scale 1:27
Flow Conditions:
Tailwater = 100 ft

Symbol	Discharge in cfs
+	1200
△	600
⊡	300

LAWRENCE AVENUE SEWER SYSTEM
City of Chicago
Harza Engineering Co., Chicago, Ill.
DROP SHAFT STUDIES

SAINT ANTHONY FALLS HYDRAULIC LABORATORY
UNIVERSITY OF MINNESOTA

DRAWN	JR	CHECKED		APPROVED	
SCALE	1"=40'	DATE	9-27-67	NO.	177B474 - 8

CHART 6

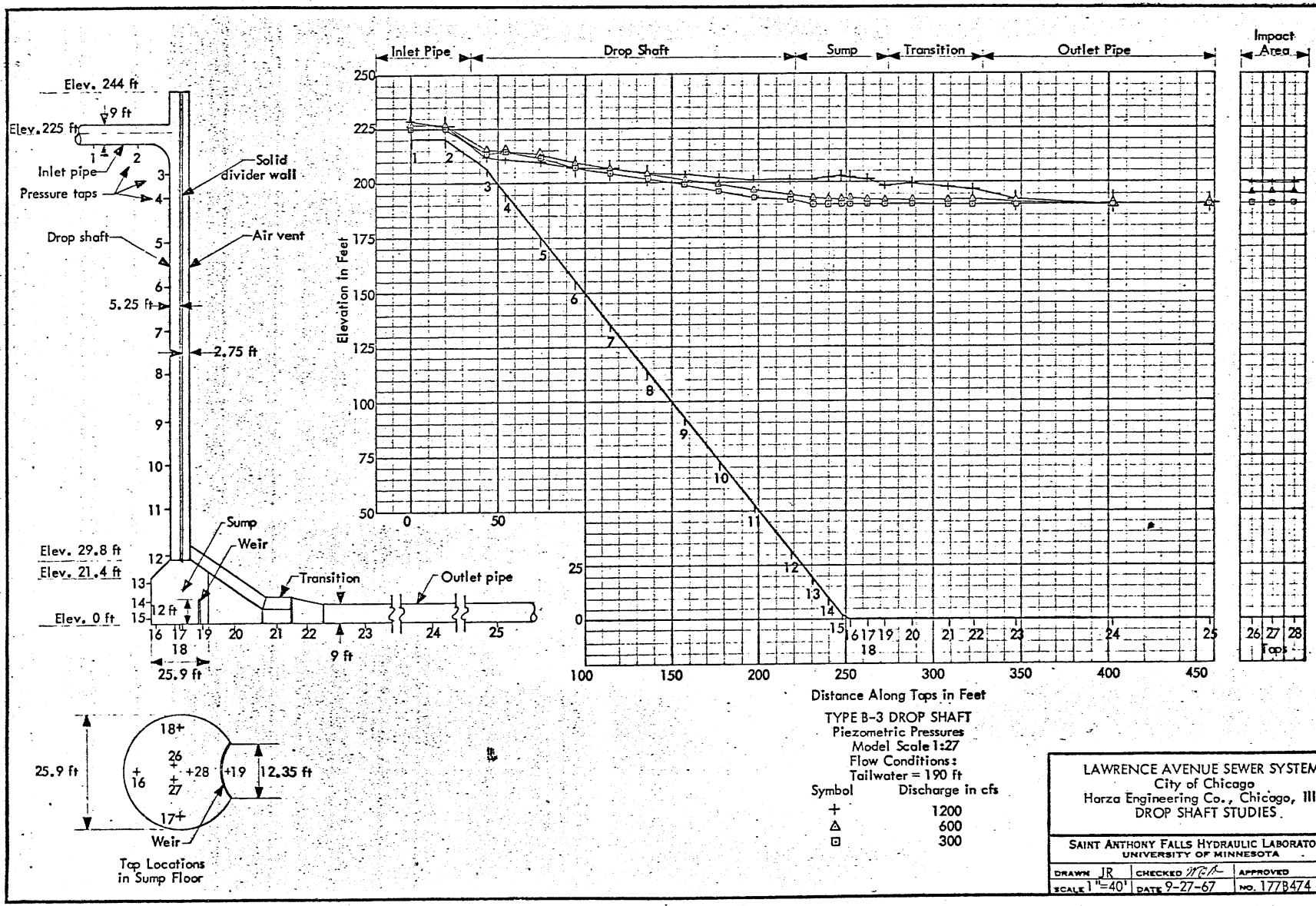

TYPE B-3 DROP SHAFT
Piezometric Pressures
Model Scale 1:27
Flow Conditions:
Tailwater = 190 ft

Symbol	Discharge in cfs
+	1200
△	600
⊡	300

LAWRENCE AVENUE SEWER SYSTEM
City of Chicago
Harza Engineering Co., Chicago, Ill.
DROP SHAFT STUDIES.

SAINT ANTHONY FALLS HYDRAULIC LABORATORY
UNIVERSITY OF MINNESOTA

DRAWN	CHECKED	APPROVED
JR		
SCALE 1"=40'	DATE 9-27-67	NO. 177B474 - 9

CHART 7

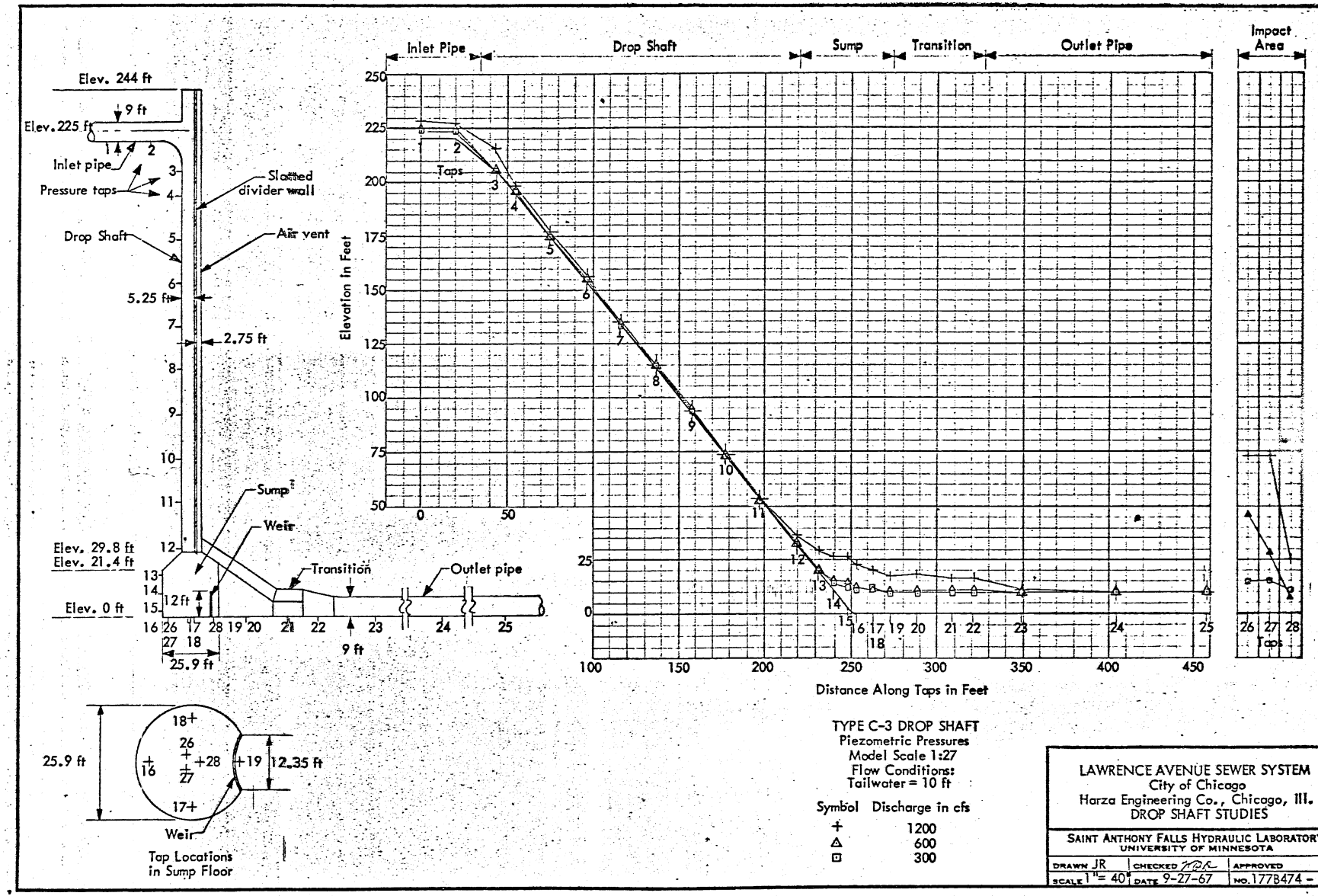

TYPE C-3 DROP SHAFT
Piezometric Pressures
Model Scale 1:27
Flow Conditions:
Tailwater = 10 ft

Symbol	Discharge in cfs
+	1200
△	600
⊡	300

LAWRENCE AVENUE SEWER SYSTEM
City of Chicago
Harza Engineering Co., Chicago, Ill.
DROP SHAFT STUDIES

SAINT ANTHONY FALLS HYDRAULIC LABORATORY
UNIVERSITY OF MINNESOTA

DRAWN JR	CHECKED	APPROVED
SCALE 1" = 40'	DATE 9-27-67	NO. 1778474 - 10

CHART 8

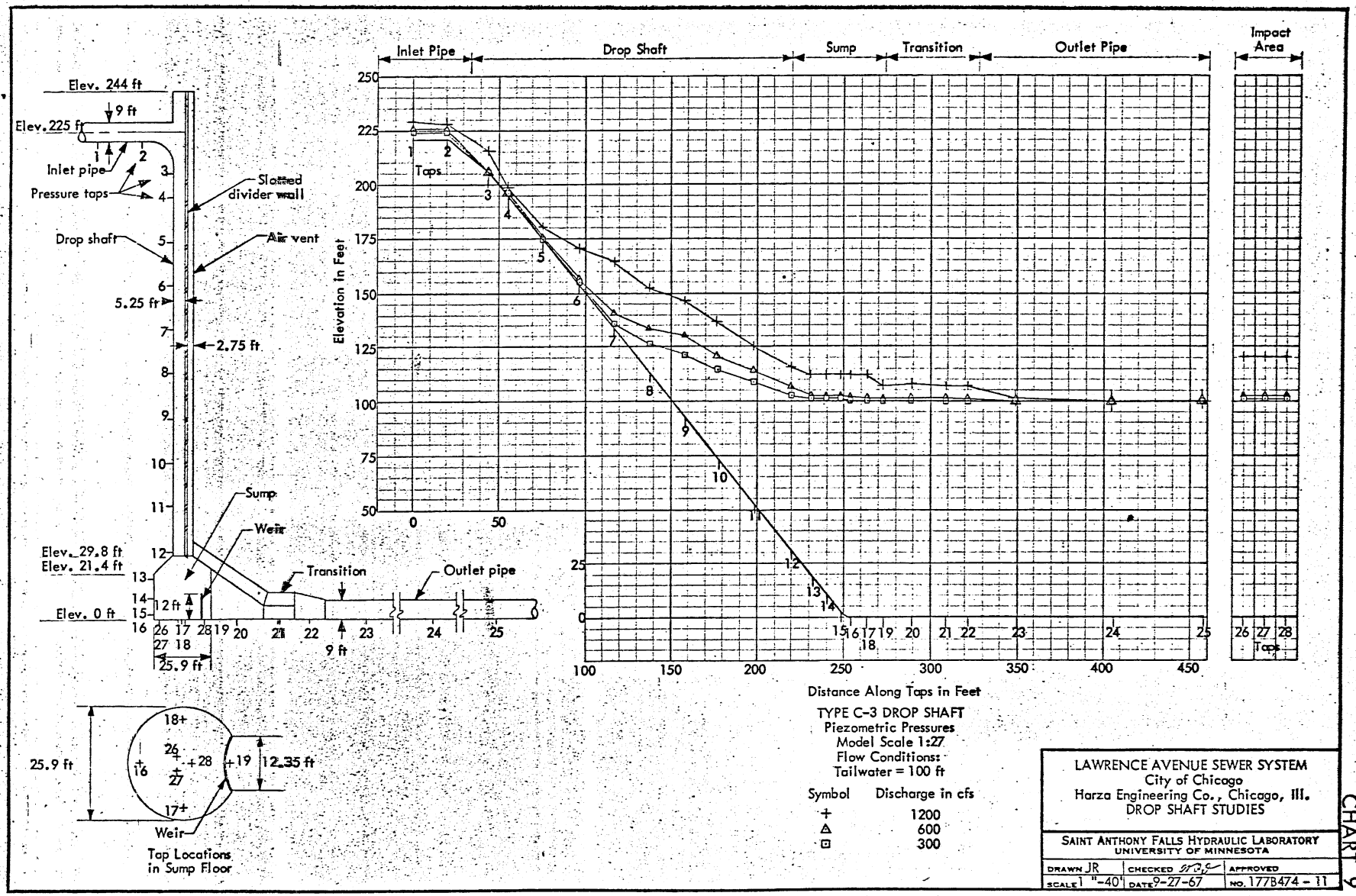

TYPE C-3 DROP SHAFT
Piezometric Pressures
Model Scale 1:27
Flow Conditions:
Tailwater = 100 ft

Symbol	Discharge in cfs
+	1200
△	600
⊡	300

LAWRENCE AVENUE SEWER SYSTEM
City of Chicago
Harza Engineering Co., Chicago, Ill.
DROP SHAFT STUDIES

SAINT ANTHONY FALLS HYDRAULIC LABORATORY
UNIVERSITY OF MINNESOTA

DRAWN JR	CHECKED	APPROVED
SCALE 1"=40'	DATE 9-27-67	NO. 177B474 - 11

CHART 9

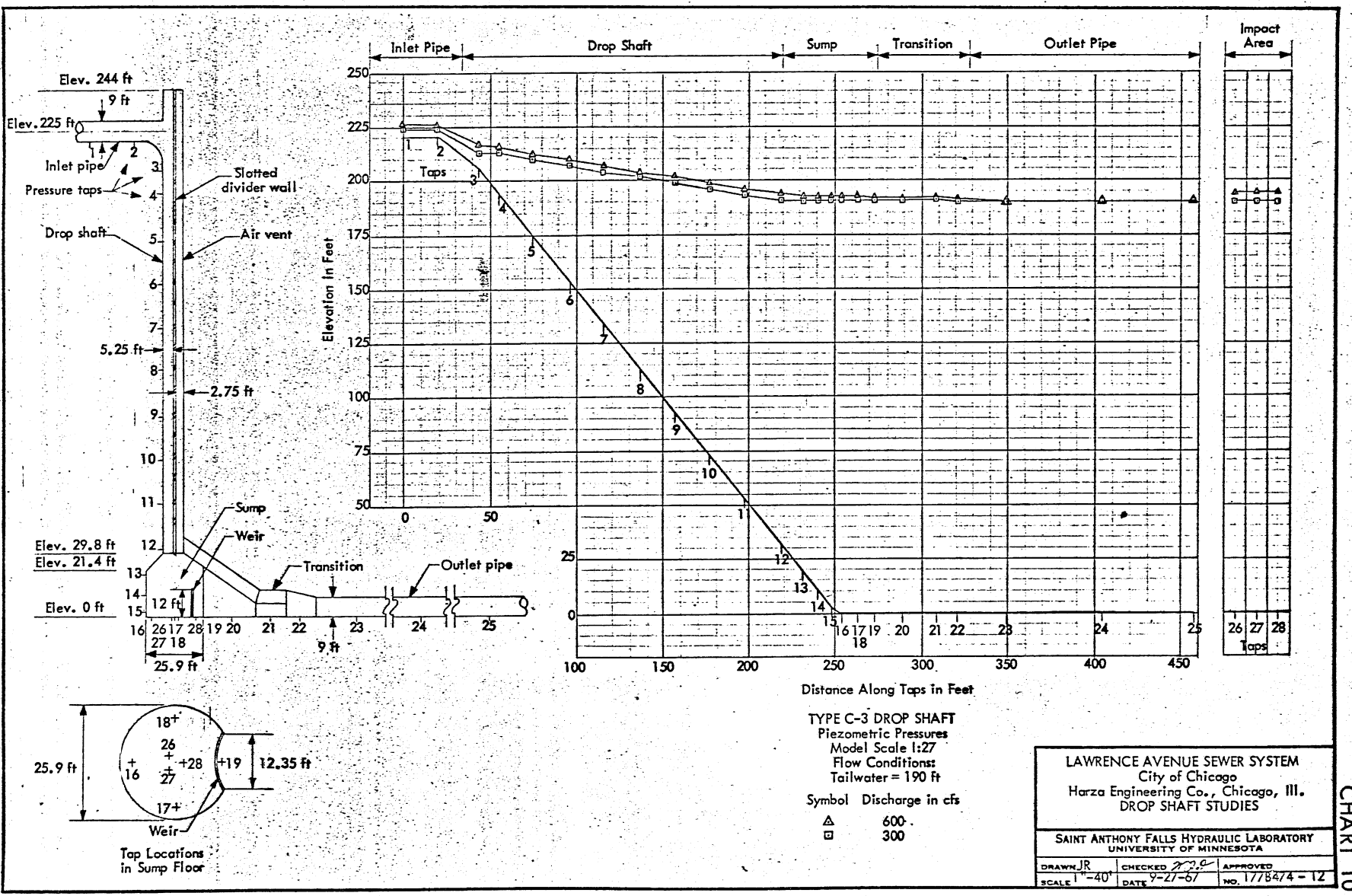

TYPE C-3 DROP SHAFT
Piezometric Pressures
Model Scale 1:27
Flow Conditions:
Tailwater = 190 ft

Symbol	Discharge in cfs
△	600
□	300

LAWRENCE AVENUE SEWER SYSTEM
City of Chicago
Harza Engineering Co., Chicago, Ill.
DROP SHAFT STUDIES

SAINT ANTHONY FALLS HYDRAULIC LABORATORY
UNIVERSITY OF MINNESOTA

DRAWN	CHECKED	APPROVED
JR		
SCALE 1"=40'	DATE 9-27-67	NO. 1778474 - 12

CHART 10

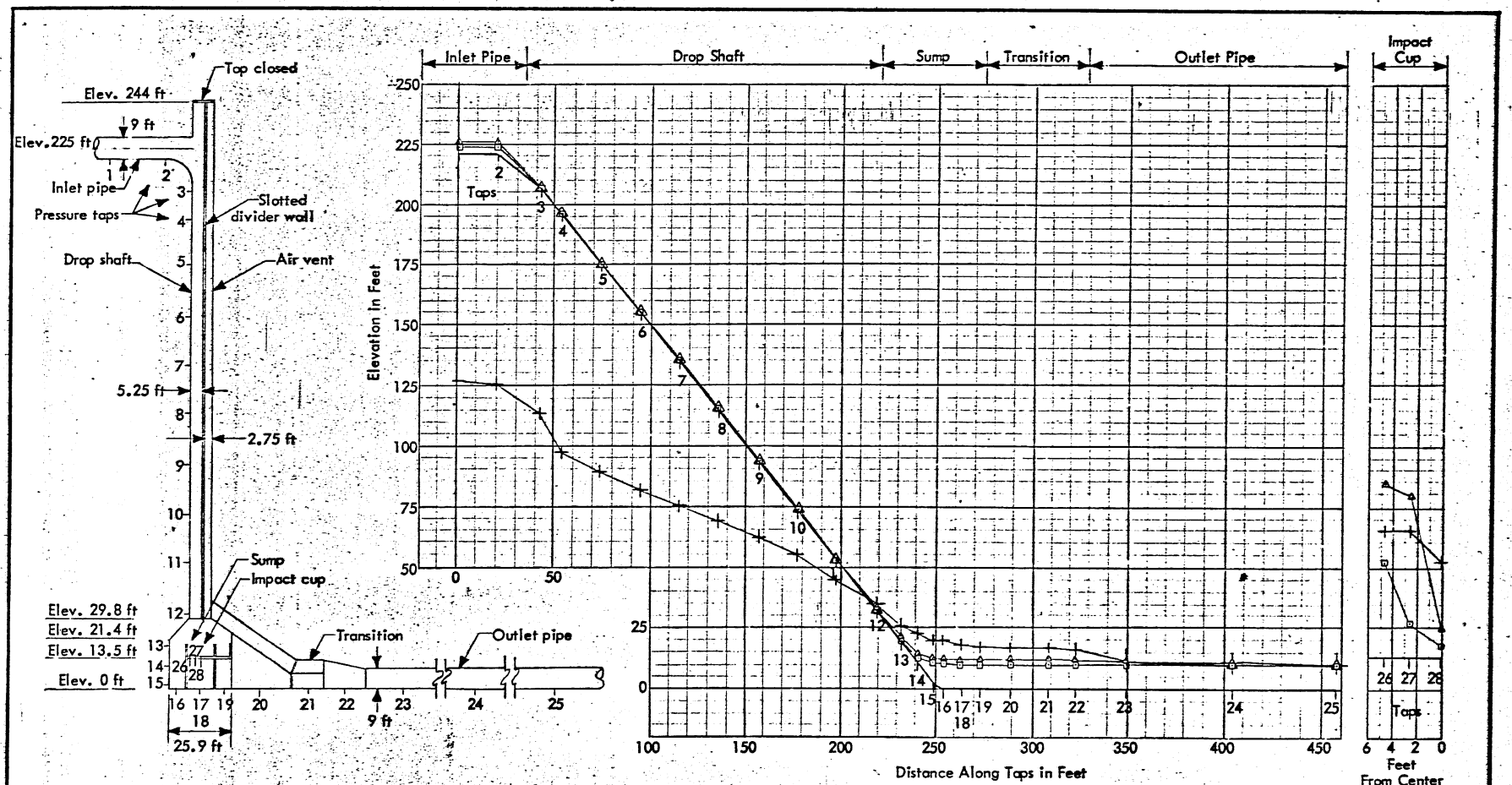

TYPE C-1 DROP SHAFT
Piezometric Pressures
Model Scale 1:27
Flow Conditions:
Tailwater = 10 ft

Symbol	Discharge in cfs
+	1200
△	600
⊡	300

LAWRENCE AVENUE SEWER SYSTEM
City of Chicago
Harza Engineering Co., Chicago, Ill.
DROP SHAFT STUDIES

SAINT ANTHONY FALLS HYDRAULIC LABORATORY
UNIVERSITY OF MINNESOTA

DRAWN	CHECKED	APPROVED
GS		
SCALE 1"=40'	DATE 10-3-67	NO. 1778474 - 25

CHART 11

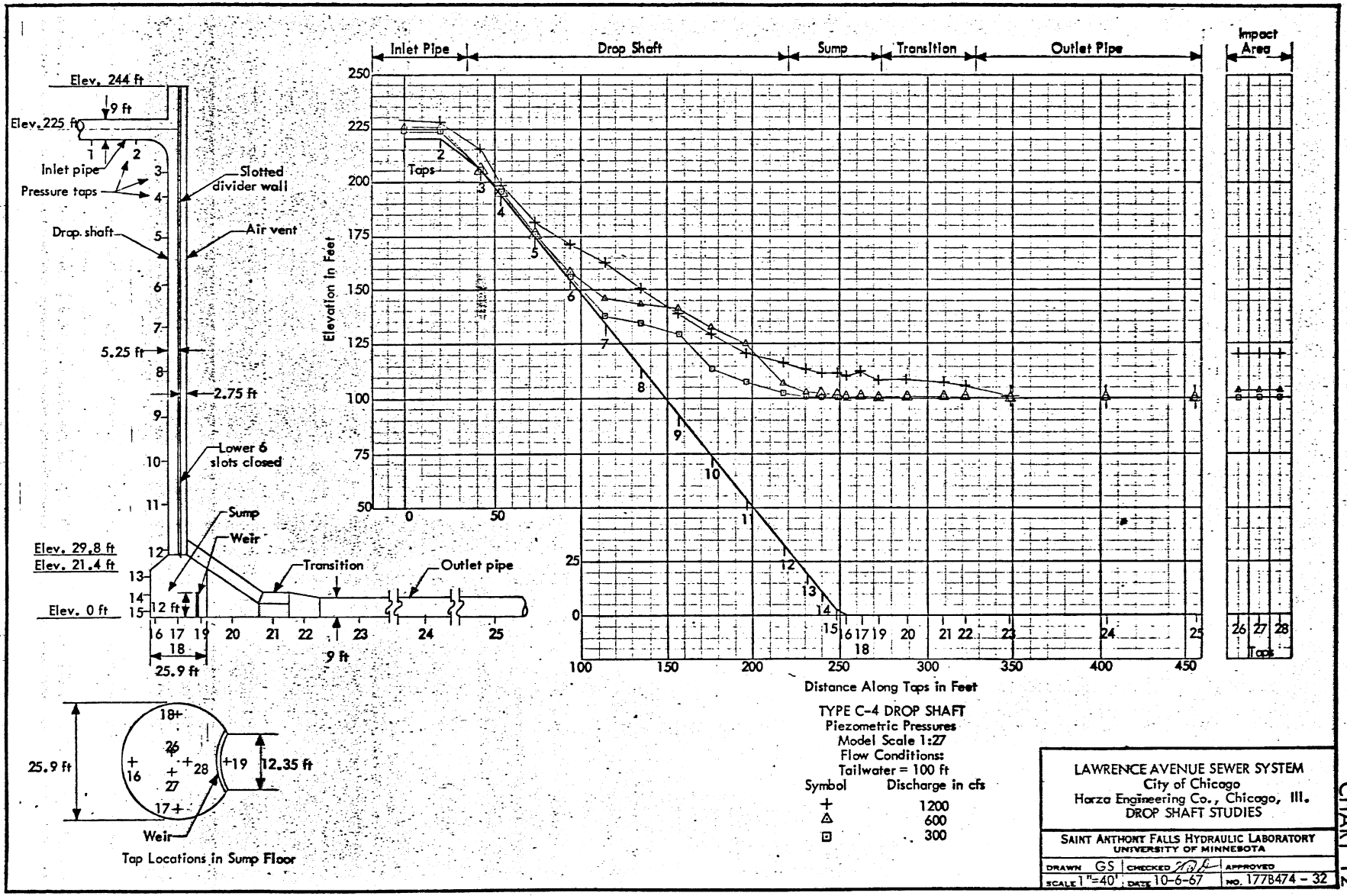

TYPE C-4 DROP SHAFT
Piezometric Pressures
Model Scale 1:27
Flow Conditions:
Tailwater = 100 ft

Symbol	Discharge in cfs
+	1200
△	600
⊡	300

LAWRENCE AVENUE SEWER SYSTEM
City of Chicago
Harza Engineering Co., Chicago, Ill.
DROP SHAFT STUDIES

SAINT ANTHONY FALLS HYDRAULIC LABORATORY
UNIVERSITY OF MINNESOTA

DRAWN GS | CHECKED | APPROVED
SCALE 1"=40' | DATE 10-6-67 | NO. 1778474 - 32

CHART 12

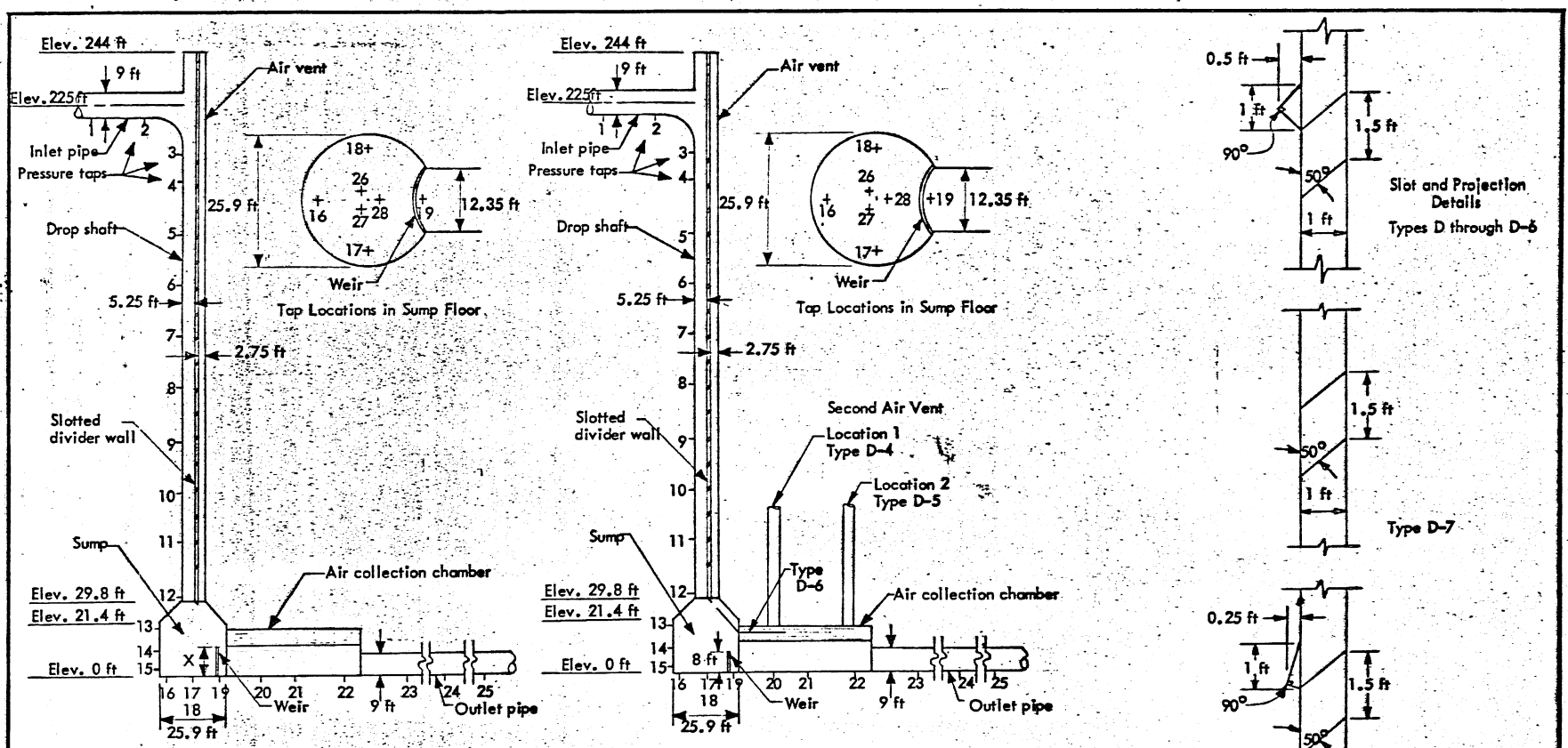

Type D As shown with weir height (X) = 12 ft
Type D-1 As shown with weir height (X) = 8 ft
Type D-2 As shown with weir height (X) = 4 ft
Type D-3 As shown with no weir

D-4 As shown with second air vent at location 1
D-5 As shown with second air vent at location 2
D-6 As shown with a plate in the air collection chamber
D-7 As shown (same as D-1) with no projections over slots
D-8 As shown (same as D-1) with smaller projections over slots

TYPE D SERIES DROP SHAFTS
Drop Shaft Types Tested
Model Scale 1:27

LAWRENCE AVENUE SEWER SYSTEM
City of Chicago
Harza Engineering Co., Chicago, Ill.
DROP SHAFT STUDIES

SAINT ANTHONY FALLS HYDRAULIC LABORATORY
UNIVERSITY OF MINNESOTA

DRAWN GES	CHECKED	APPROVED
SCALE	DATE 11-7-67	NO. 177B474 - 54

CHART 13

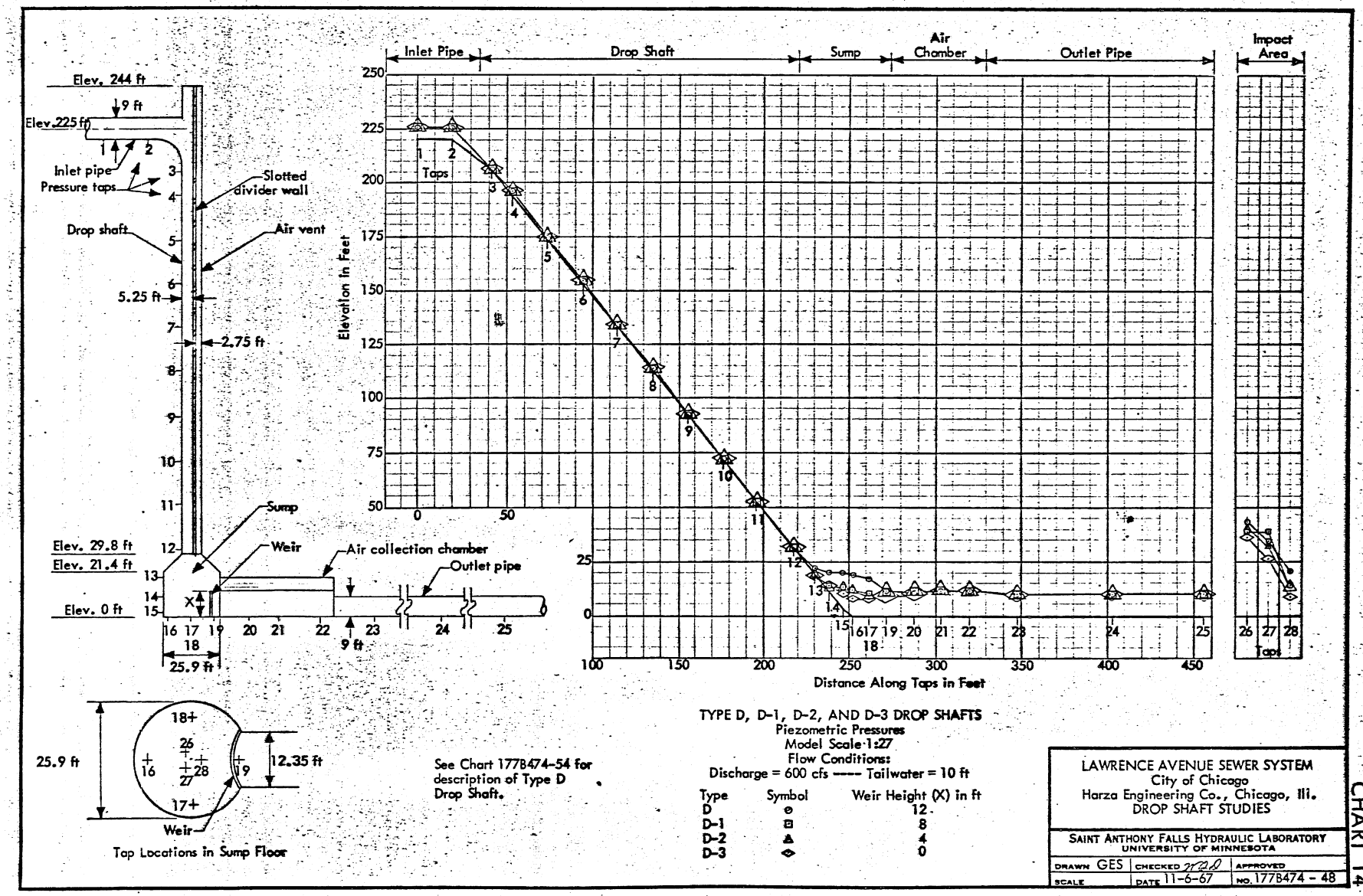
Elev. 244 ft
9 ft
Elev. 225 ft
Inlet pipe
Pressure taps
Slotted divider wall
Drop shaft
Air vent
5.25 ft
2.75 ft
Sump
Elev. 29.8 ft
Elev. 21.4 ft
Weir
Air collection chamber
Outlet pipe
Elev. 0 ft
X
9 ft
25.9 ft
Inlet Pipe
Drop Shaft
Sump
Air Chamber
Outlet Pipe
Impact Area
Elevation in Feet
Taps
Distance Along Taps in Feet
25.9 ft
12.35 ft
Weir
Tap Locations in Sump Floor
See Chart 1778474-54 for description of Type D Drop Shaft.
TYPE D, D-1, D-2, AND D-3 DROP SHAFTS
Piezometric Pressures
Model Scale 1:27
Flow Conditions:
Discharge = 600 cfs ---- Tailwater = 10 ft
Type
Symbol
Weir Height (X) in ft
D
12
D-1
8
D-2
4
D-3
0
LAWRENCE AVENUE SEWER SYSTEM
City of Chicago
Harza Engineering Co., Chicago, Ill.
DROP SHAFT STUDIES
SAINT ANTHONY FALLS HYDRAULIC LABORATORY
UNIVERSITY OF MINNESOTA
DRAWN GES
CHECKED
APPROVED
SCALE
DATE 11-6-67
NO. 1778474 - 48
CHART 14

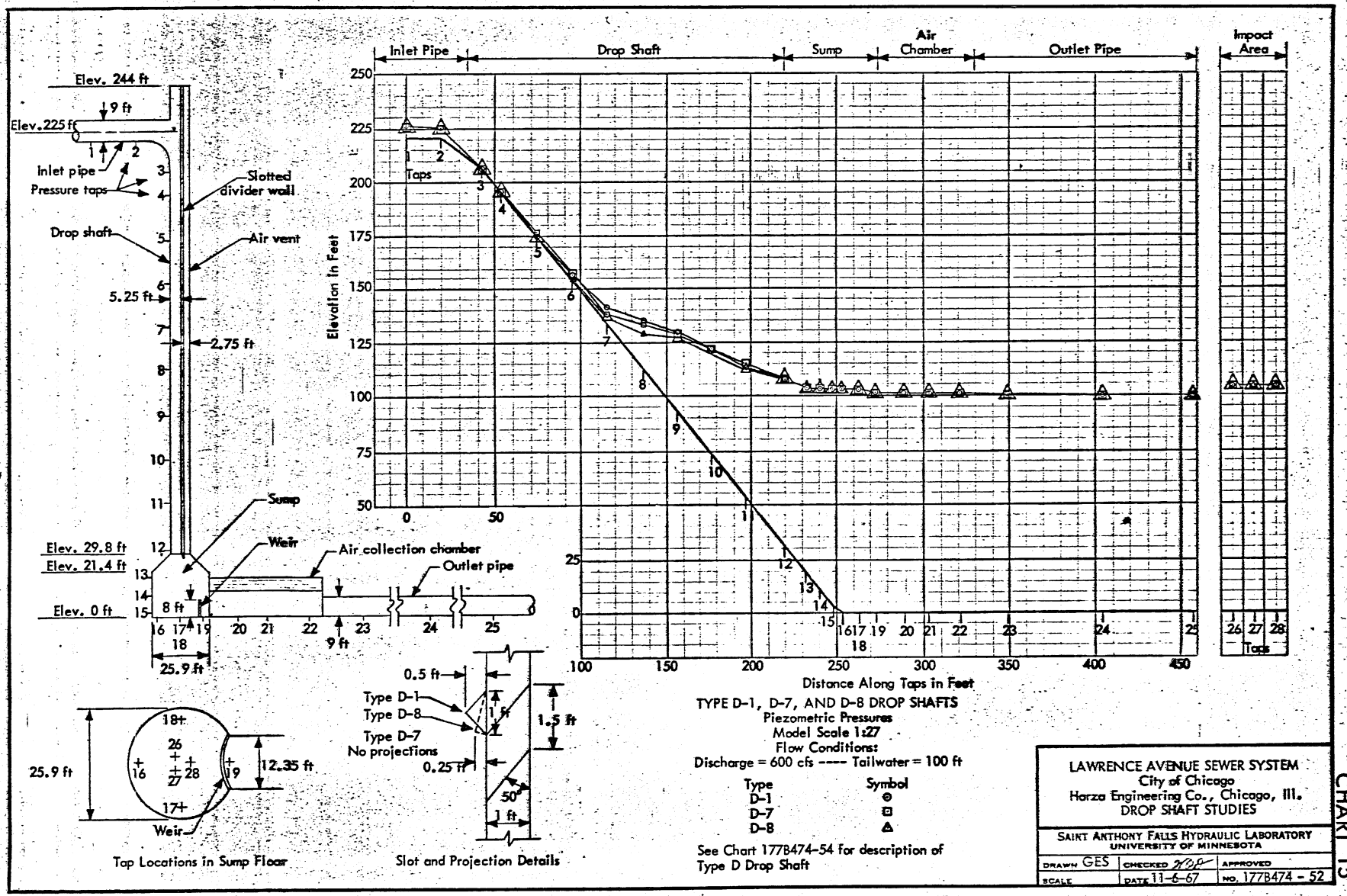

TYPE D-1, D-7, AND D-8 DROP SHAFTS
Piezometric Pressures
Model Scale 1:27
Flow Conditions:
Discharge = 600 cfs ---- Tailwater = 100 ft

Type	Symbol
D-1	⊙
D-7	⊡
D-8	△

See Chart 177B474-54 for description of Type D Drop Shaft

LAWRENCE AVENUE SEWER SYSTEM
City of Chicago
Harza Engineering Co., Chicago, Ill.
DROP SHAFT STUDIES

SAINT ANTHONY FALLS HYDRAULIC LABORATORY
UNIVERSITY OF MINNESOTA

DRAWN GES	CHECKED	APPROVED
SCALE	DATE 11-6-67	NO. 177B474 - 52

CHART 15

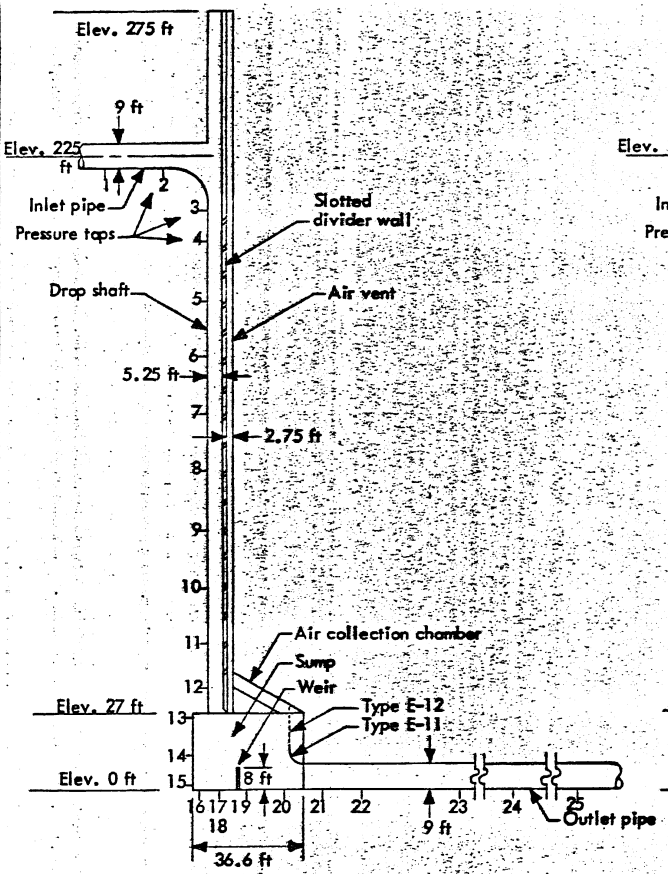

Type E-11 As shown with a 4.5 ft radius projection at the outlet pipe

Type E-12 Same as E-11 with the projection extended to top of sump

Type E-13 Same as E-12 with a 12 ft weir

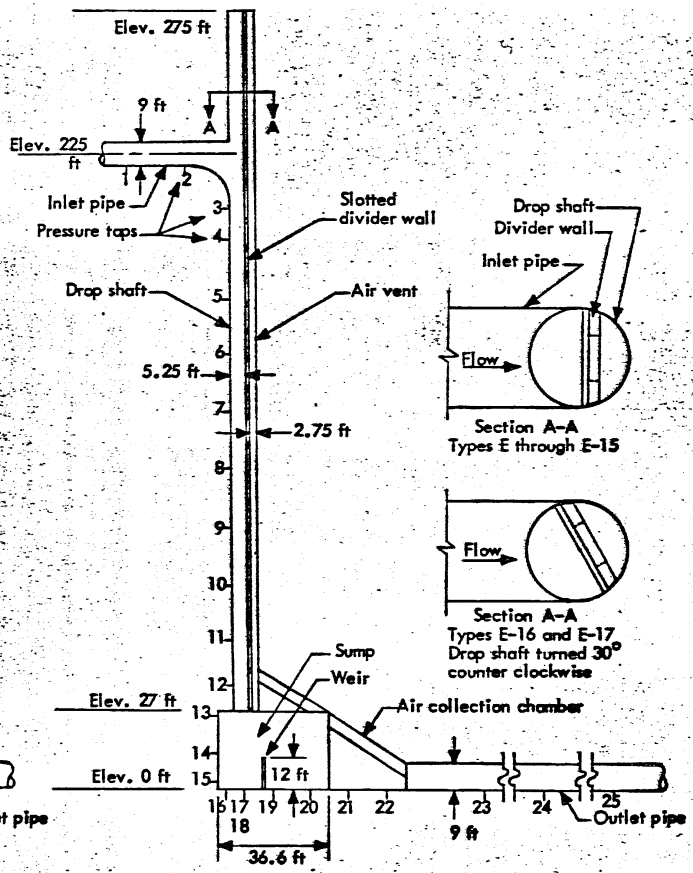

Type E-14 As shown

Type E-15 As shown with no weir

Type E-16 As shown with the drop shaft turned 30° counter clockwise

Type E-17 As shown with the drop shaft turned 30° counter clockwise and no weir

Section A-A
Types E through E-15

Section A-A
Types E-16 and E-17
Drop shaft turned 30° counter clockwise

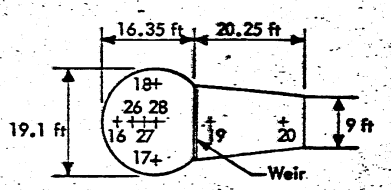

Tap Locations in Sump Floor

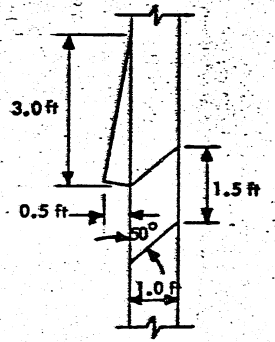

Slot Geometry

TYPE E SERIES DROP SHAFTS
Drop Shaft Types Tested
Model Scale 1:27

LAWRENCE AVENUE SEWER SYSTEM
City of Chicago
Harza Engineering Co., Chicago, Ill.
DROP SHAFT STUDIES

SAINT ANTHONY FALLS HYDRAULIC LABORATORY
UNIVERSITY OF MINNESOTA

DRAWN GS	CHECKED	APPROVED
SCALE	DATE 2-15-68	NO. 177B-474-85

CHART 16

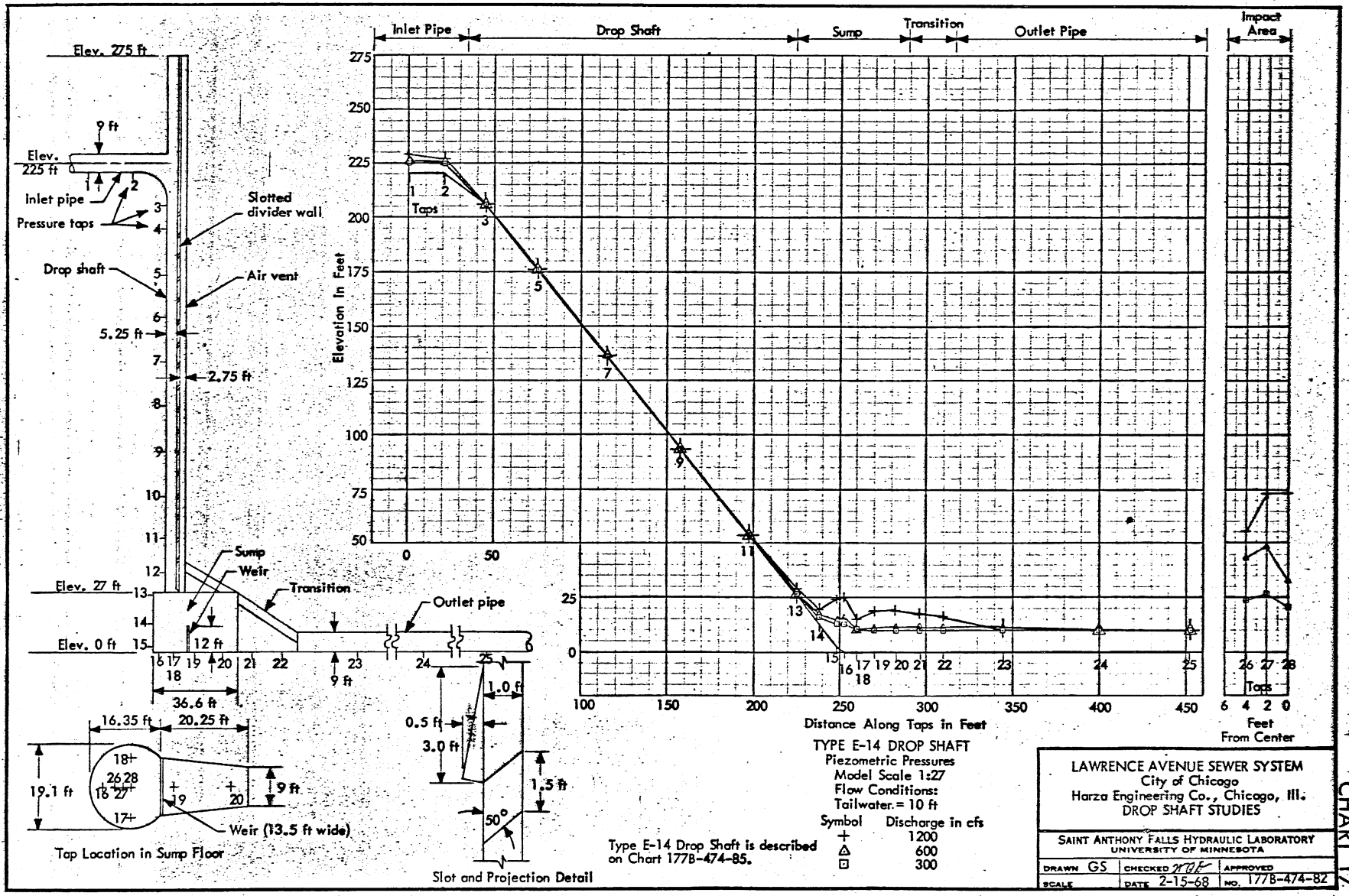

Type E-14 Drop Shaft is described on Chart 177B-474-85.

TYPE E-14 DROP SHAFT
Piezometric Pressures
Model Scale 1:27
Flow Conditions:
Tailwater = 10 ft

Symbol	Discharge in cfs
+	1200
△	600
⊡	300

LAWRENCE AVENUE SEWER SYSTEM
City of Chicago
Harza Engineering Co., Chicago, Ill.
DROP SHAFT STUDIES

SAINT ANTHONY FALLS HYDRAULIC LABORATORY
UNIVERSITY OF MINNESOTA

DRAWN	GS	CHECKED		APPROVED	
SCALE		DATE	2-15-68	NO.	177B-474-82

CHART 17

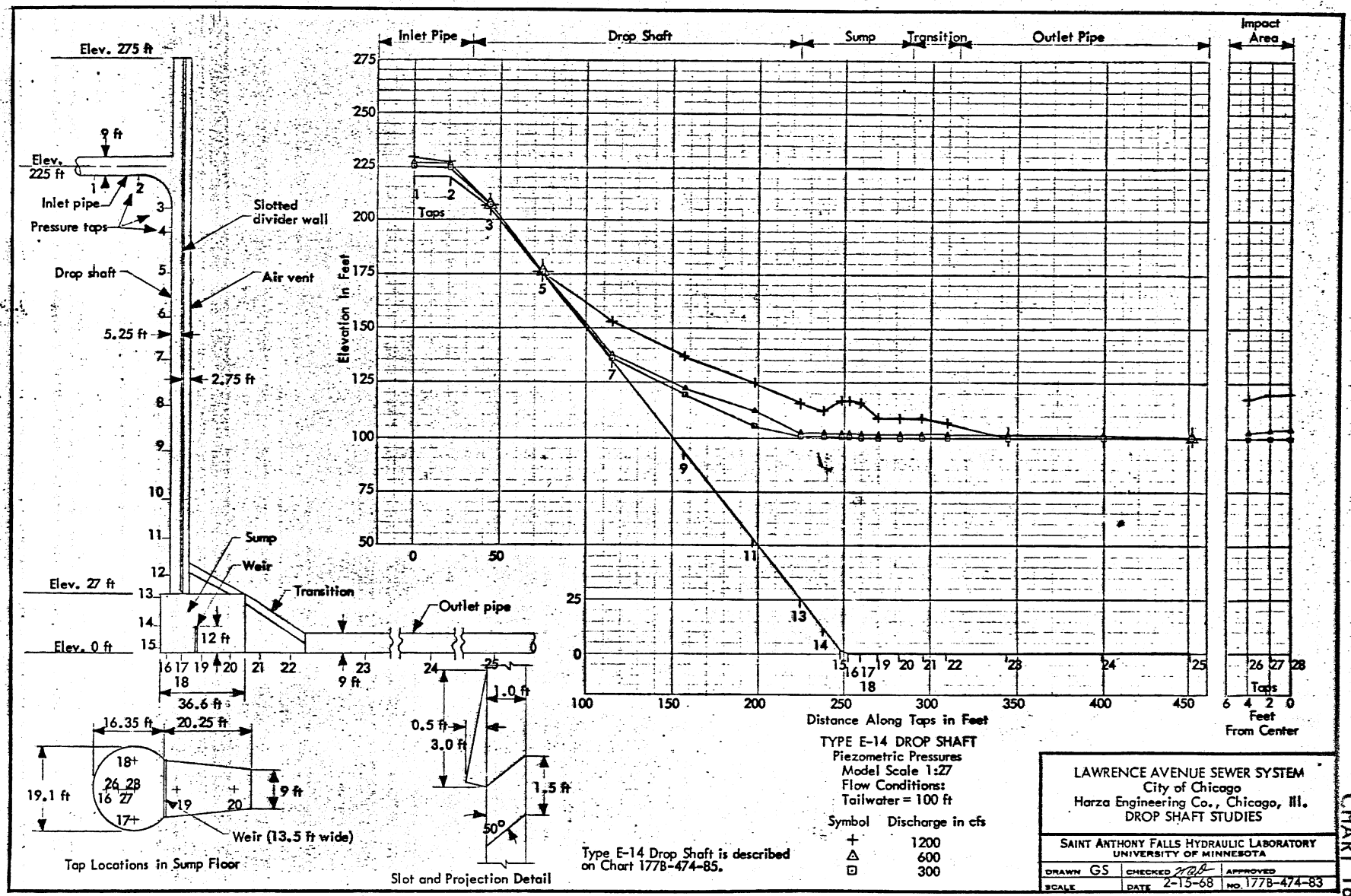
Elev. 275 ft
9 ft
Elev. 225 ft
Inlet pipe
Pressure taps
Slotted divider wall
Drop shaft
Air vent
5.25 ft
2.75 ft
Sump
Weir
Elev. 27 ft
Transition
Outlet pipe
12 ft
Elev. 0 ft
36.6 ft
9 ft
16.35 ft
20.25 ft
19.1 ft
9 ft
Weir (13.5 ft wide)
Tap Locations in Sump Floor
1.0 ft
0.5 ft
3.0 ft
1.5 ft
50°
Slot and Projection Detail
Inlet Pipe
Drop Shaft
Sump
Transition
Outlet Pipe
Impact Area
Elevation in Feet
Taps
Distance Along Taps in Feet
Feet From Center
Type E-14 Drop Shaft is described on Chart 177B-474-85.
TYPE E-14 DROP SHAFT
Piezometric Pressures
Model Scale 1:27
Flow Conditions:
Tailwater = 100 ft
Symbol Discharge in cfs
+ 1200
△ 600
⊡ 300
LAWRENCE AVENUE SEWER SYSTEM
City of Chicago
Harza Engineering Co., Chicago, Ill.
DROP SHAFT STUDIES
SAINT ANTHONY FALLS HYDRAULIC LABORATORY
UNIVERSITY OF MINNESOTA
DRAWN GS
CHECKED
APPROVED
SCALE
DATE 2-15-68
NO. 177B-474-83

CHART 18

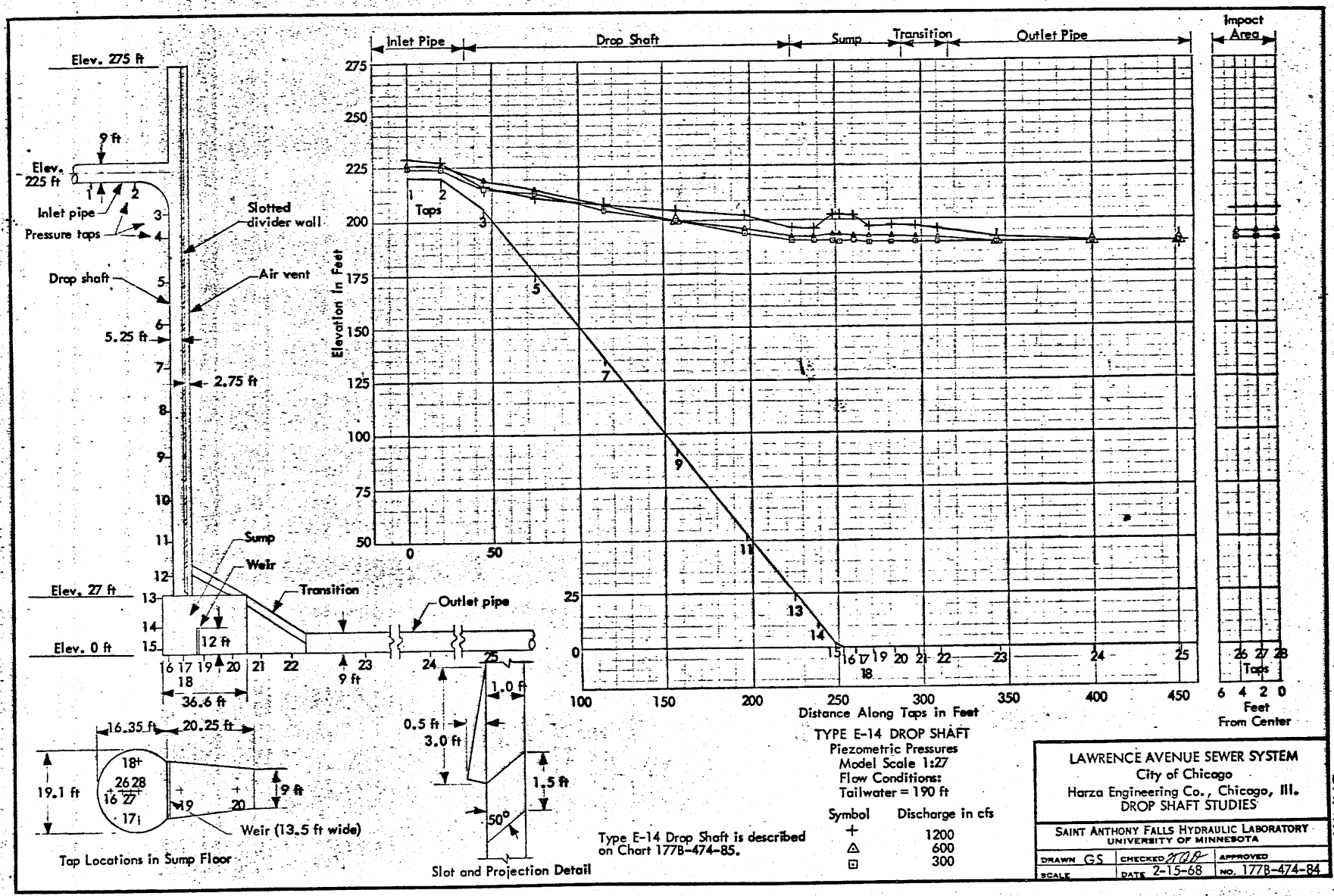
Elev. 275 ft
9 ft
Elev. 225 ft
Inlet pipe
Pressure taps
Slotted divider wall
Air vent
Drop shaft
5.25 ft
2.75 ft
Sump
Weir
Transition
Outlet pipe
Elev. 27 ft
Elev. 0 ft
12 ft
36.6 ft
9 ft
16.35 ft
20.25 ft
19.1 ft
9 ft
Weir (13.5 ft wide)
Tap Locations in Sump Floor
1.0 ft
0.5 ft
3.0 ft
1.5 ft
50°
Slot and Projection Detail
Inlet Pipe
Drop Shaft
Sump
Transition
Outlet Pipe
Impact Area
Elevation in Feet
Taps
Distance Along Taps in Feet
Feet From Center
Type E-14 Drop Shaft is described on Chart 177B-474-85.
TYPE E-14 DROP SHAFT
Piezometric Pressures
Model Scale 1:27
Flow Conditions:
Tailwater = 190 ft
Symbol
Discharge in cfs
+ 1200
△ 600
⊡ 300
LAWRENCE AVENUE SEWER SYSTEM
City of Chicago
Harza Engineering Co., Chicago, Ill.
DROP SHAFT STUDIES
SAINT ANTHONY FALLS HYDRAULIC LABORATORY
UNIVERSITY OF MINNESOTA
DRAWN GS
CHECKED
APPROVED
SCALE
DATE 2-15-68
NO. 177B-474-84
CHART 19

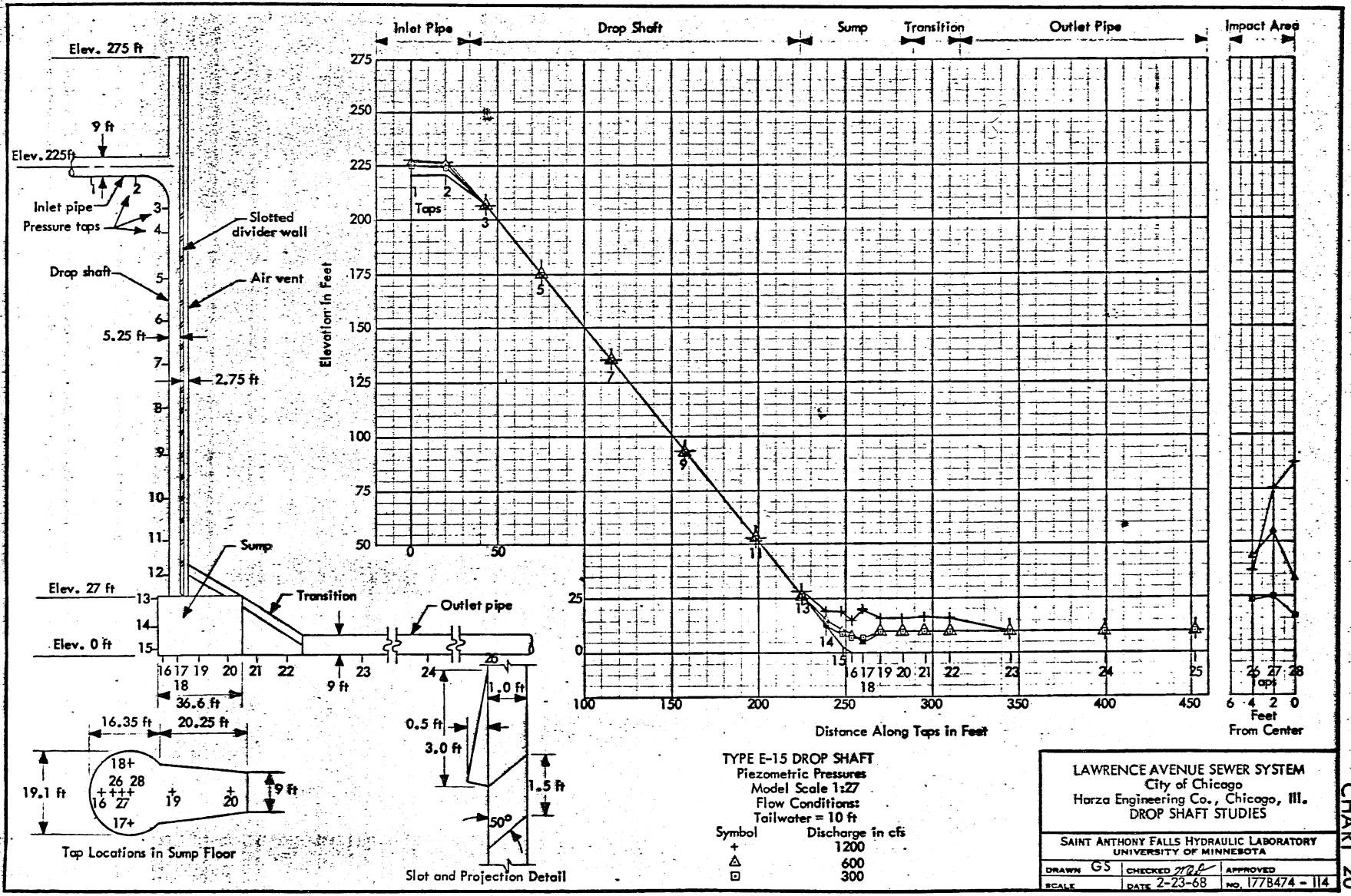
Elev. 275 ft
9 ft
Elev. 225ft
Inlet pipe
Pressure taps
Slotted divider wall
Drop shaft
Air vent
5.25 ft
2.75 ft
Sump
Elev. 27 ft
Transition
Outlet pipe
Elev. 0 ft
36.6 ft
9 ft
16.35 ft
20.25 ft
19.1 ft
9 ft
Tap Locations in Sump Floor
0.5 ft
3.0 ft
1.0 ft
1.5 ft
50°
Slot and Projection Detail
Inlet Pipe
Drop Shaft
Sump
Transition
Outlet Pipe
Impact Area
Elevation in Feet
Taps
Distance Along Taps in Feet
Feet
From Center
TYPE E-15 DROP SHAFT
Piezometric Pressures
Model Scale 1:27
Flow Conditions:
Tailwater = 10 ft
Symbol
Discharge in cfs
+ 1200
△ 600
⊡ 300
LAWRENCE AVENUE SEWER SYSTEM
City of Chicago
Harza Engineering Co., Chicago, Ill.
DROP SHAFT STUDIES
SAINT ANTHONY FALLS HYDRAULIC LABORATORY
UNIVERSITY OF MINNESOTA
DRAWN GS
CHECKED MLC
APPROVED
SCALE
DATE 2-23-68
NO. 1778474 - 114

CHART 20

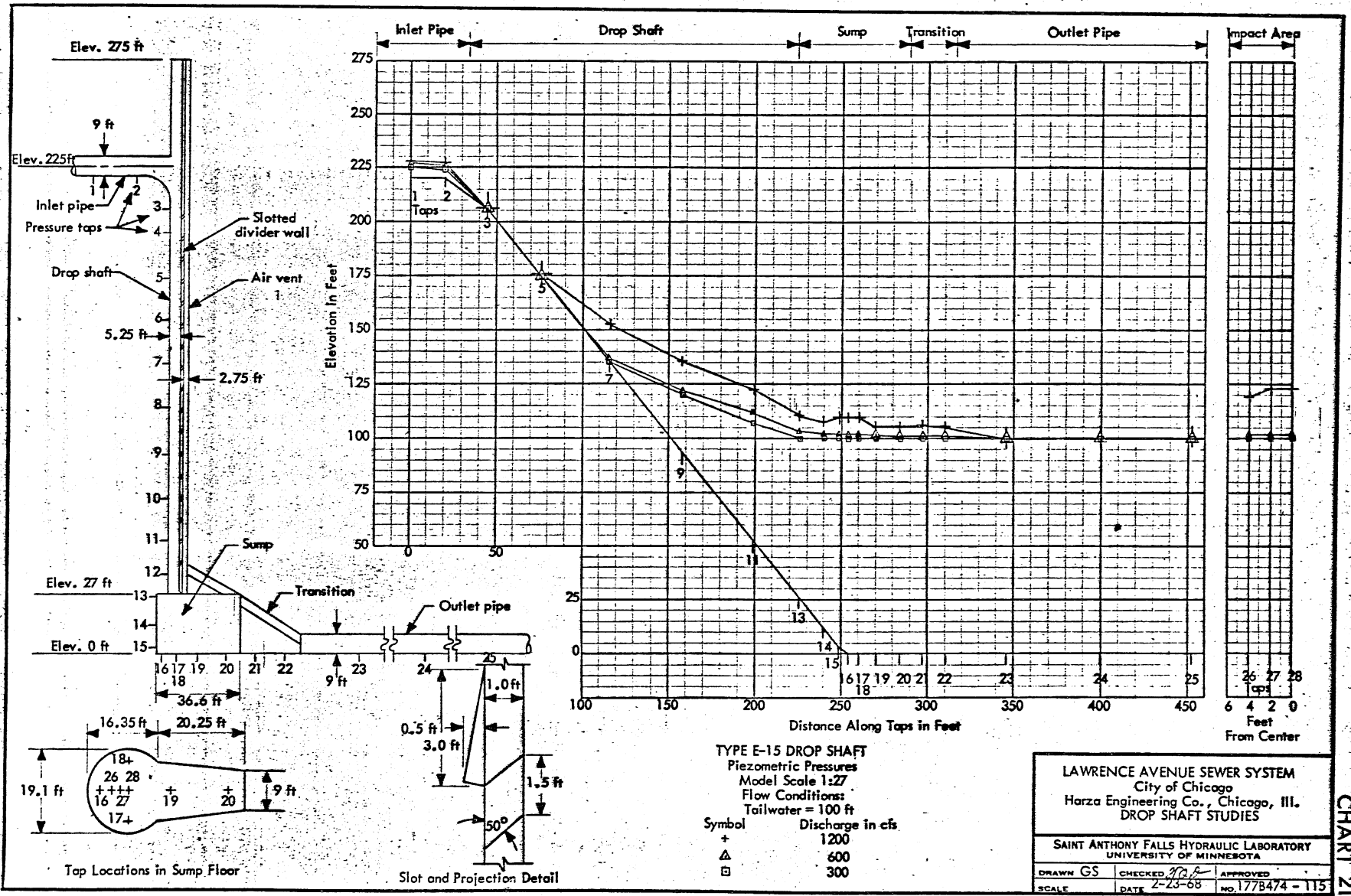

TYPE E-15 DROP SHAFT
Piezometric Pressures
Model Scale 1:27
Flow Conditions:
Tailwater = 100 ft

Symbol	Discharge in cfs
+	1200
△	600
⊡	300

LAWRENCE AVENUE SEWER SYSTEM
City of Chicago
Harza Engineering Co., Chicago, Ill.
DROP SHAFT STUDIES

SAINT ANTHONY FALLS HYDRAULIC LABORATORY
UNIVERSITY OF MINNESOTA

DRAWN GS	CHECKED	APPROVED
SCALE	DATE 2-23-68	NO. 177B474 - 115

CHART 21

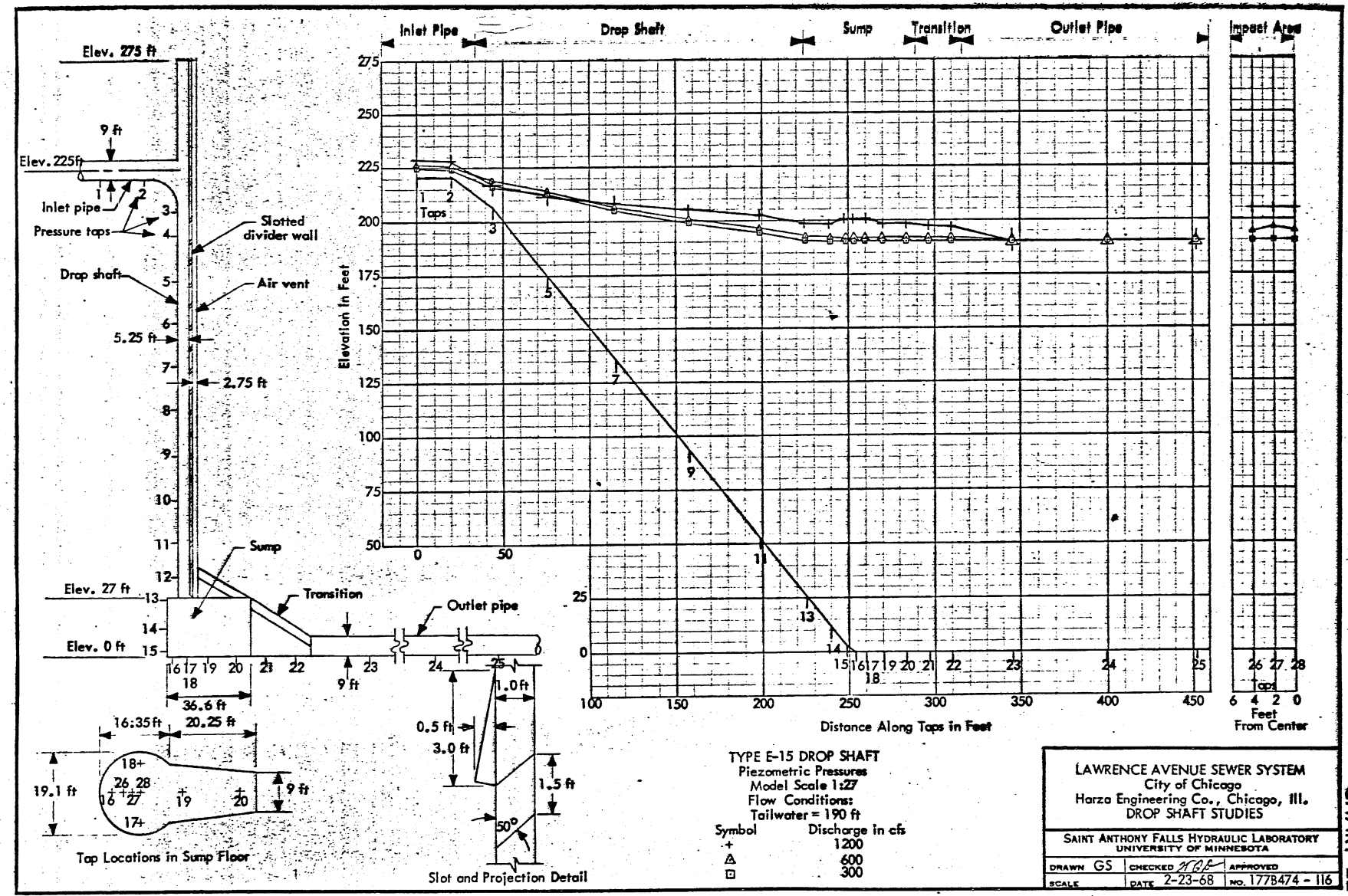
Elev. 275 ft
9 ft
Elev. 225ft
Inlet pipe
Pressure taps
Slotted divider wall
Drop shaft
Air vent
5.25 ft
2.75 ft
Sump
Elev. 27 ft
Elev. 0 ft
Transition
Outlet pipe
9 ft
36.6 ft
16:35ft
20.25 ft
19.1 ft
9 ft
Tap Locations in Sump Floor
0.5 ft
3.0 ft
1.0 ft
1.5 ft
50°
Slot and Projection Detail
Inlet Pipe
Drop Shaft
Sump
Transition
Outlet Pipe
Impact Area
Elevation in Feet
Taps
Distance Along Taps in Feet
Feet From Center
TYPE E-15 DROP SHAFT
Piezometric Pressures
Model Scale 1:27
Flow Conditions:
Tailwater = 190 ft
Symbol Discharge in cfs
+ 1200
△ 600
⊡ 300
LAWRENCE AVENUE SEWER SYSTEM
City of Chicago
Harza Engineering Co., Chicago, Ill.
DROP SHAFT STUDIES
SAINT ANTHONY FALLS HYDRAULIC LABORATORY
UNIVERSITY OF MINNESOTA
DRAWN GS
CHECKED
APPROVED
SCALE
DATE 2-23-68
NO. 177B474 - 116

CHART 22

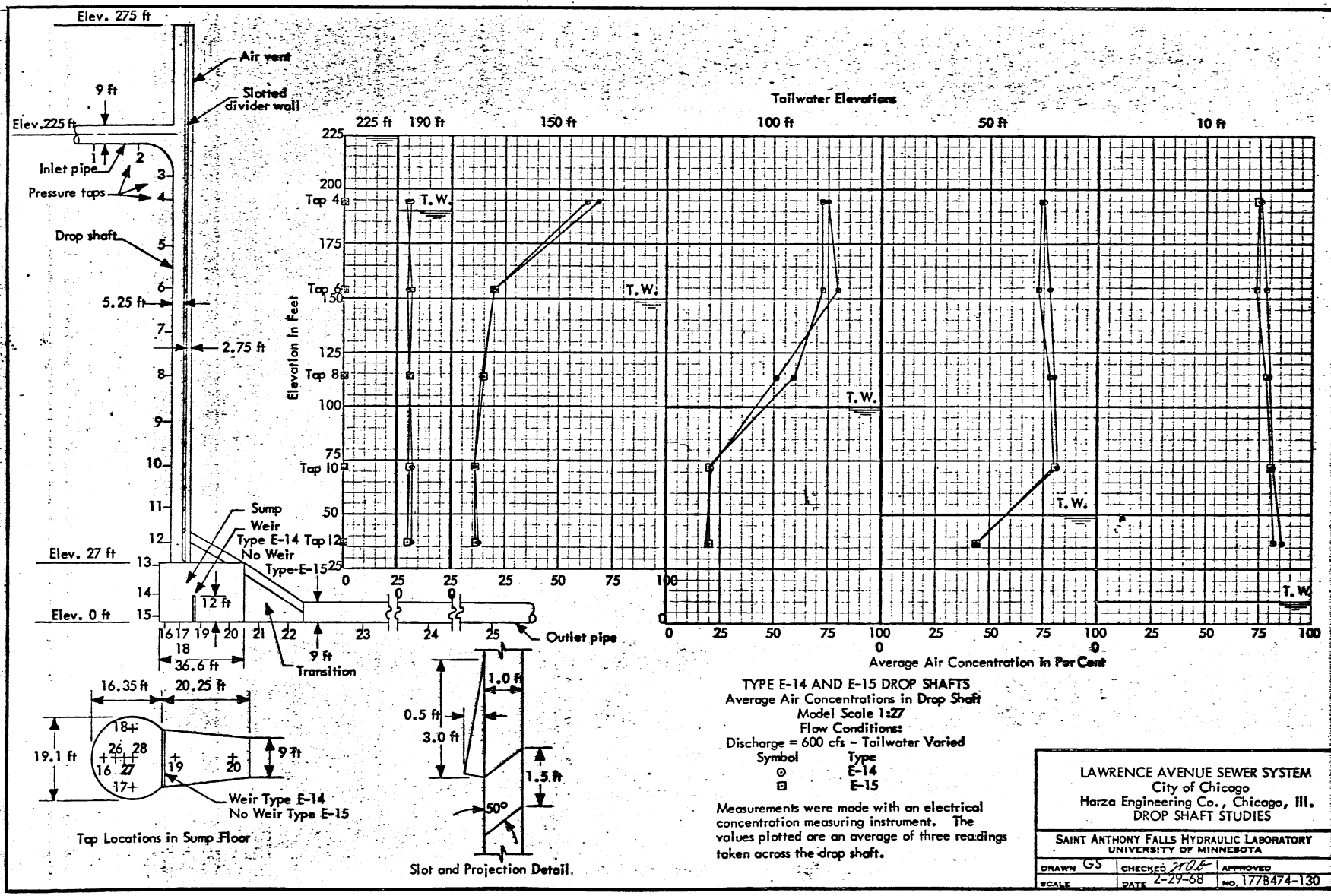

TYPE E-14 AND E-15 DROP SHAFTS
Average Air Concentrations in Drop Shaft
Model Scale 1:27
Flow Conditions:
Discharge = 600 cfs – Tailwater Varied

Symbol	Type
⊙	E-14
⊡	E-15

Measurements were made with an electrical concentration measuring instrument. The values plotted are an average of three readings taken across the drop shaft.

LAWRENCE AVENUE SEWER SYSTEM
City of Chicago
Harza Engineering Co., Chicago, Ill.
DROP SHAFT STUDIES

SAINT ANTHONY FALLS HYDRAULIC LABORATORY
UNIVERSITY OF MINNESOTA

DRAWN	GS	CHECKED	JOE	APPROVED	
SCALE		DATE	2-29-68	NO.	177B474-130

CHART 23

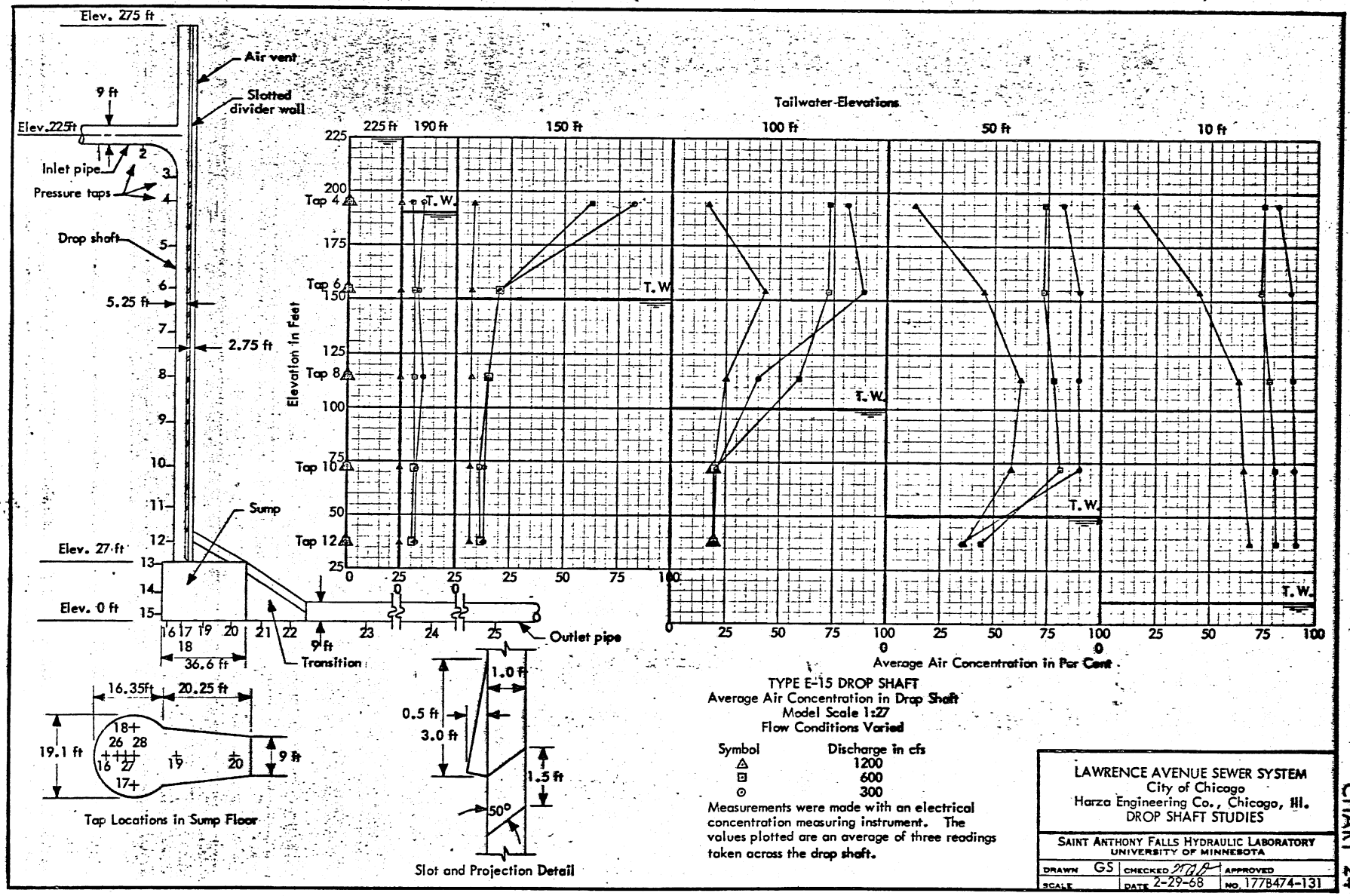

TYPE E-15 DROP SHAFT
Average Air Concentration in Drop Shaft
Model Scale 1:27
Flow Conditions Varied

Symbol	Discharge in cfs
△	1200
⊡	600
⊙	300

Measurements were made with an electrical concentration measuring instrument. The values plotted are an average of three readings taken across the drop shaft.

LAWRENCE AVENUE SEWER SYSTEM
City of Chicago
Harza Engineering Co., Chicago, Ill.
DROP SHAFT STUDIES

SAINT ANTHONY FALLS HYDRAULIC LABORATORY
UNIVERSITY OF MINNESOTA

DRAWN	GS	CHECKED	APPROVED
SCALE		DATE 2-29-68	NO. 177B474-131

CHART 24

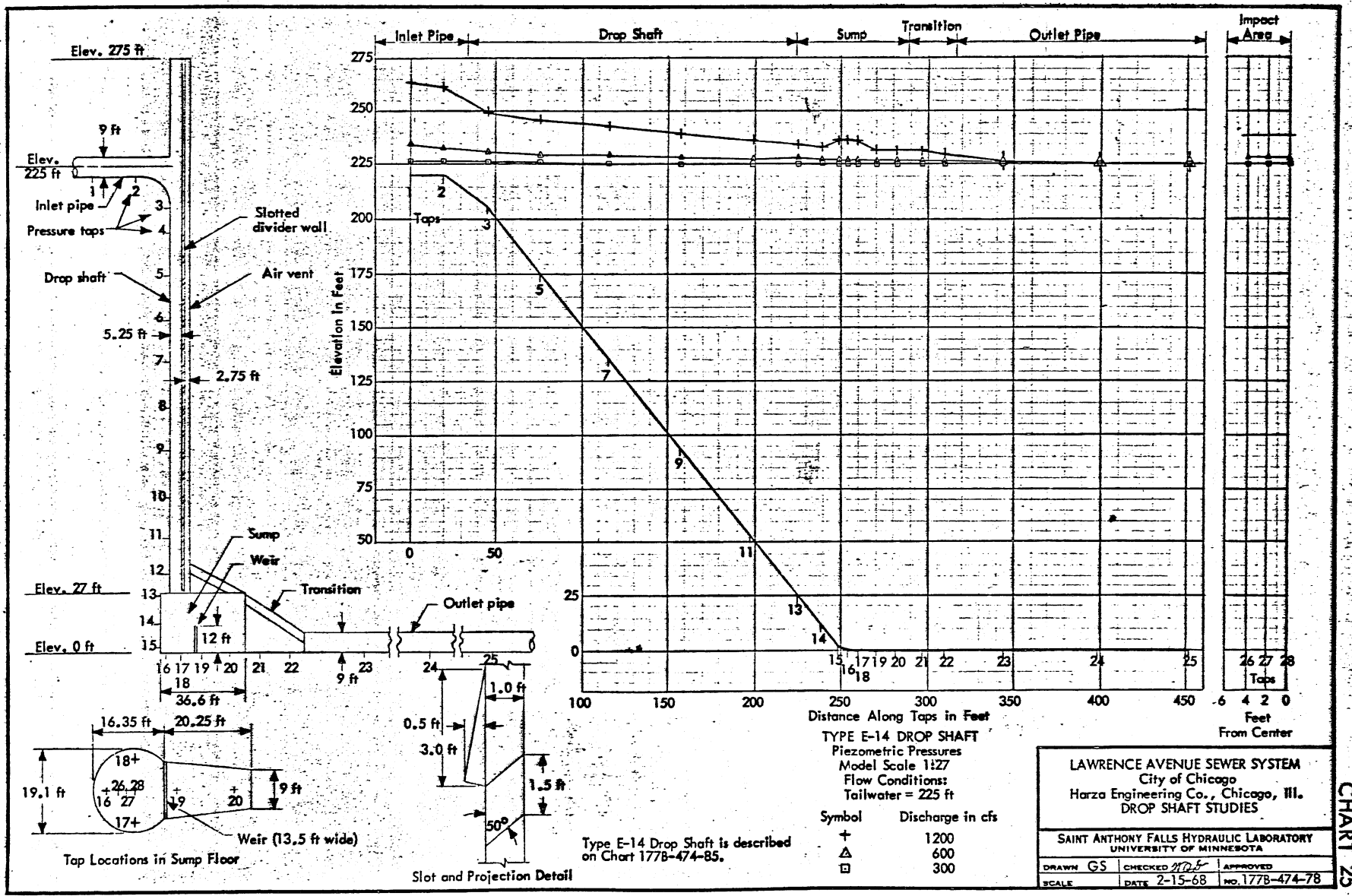

TYPE E-14 DROP SHAFT
Piezometric Pressures
Model Scale 1:27
Flow Conditions:
Tailwater = 225 ft

Symbol	Discharge in cfs
+	1200
△	600
⊡	300

Type E-14 Drop Shaft is described on Chart 1778-474-85.

LAWRENCE AVENUE SEWER SYSTEM
City of Chicago
Harza Engineering Co., Chicago, Ill.
DROP SHAFT STUDIES

SAINT ANTHONY FALLS HYDRAULIC LABORATORY
UNIVERSITY OF MINNESOTA

DRAWN GS	CHECKED MDS	APPROVED
SCALE	DATE 2-15-68	NO. 1778-474-78

CHART 25

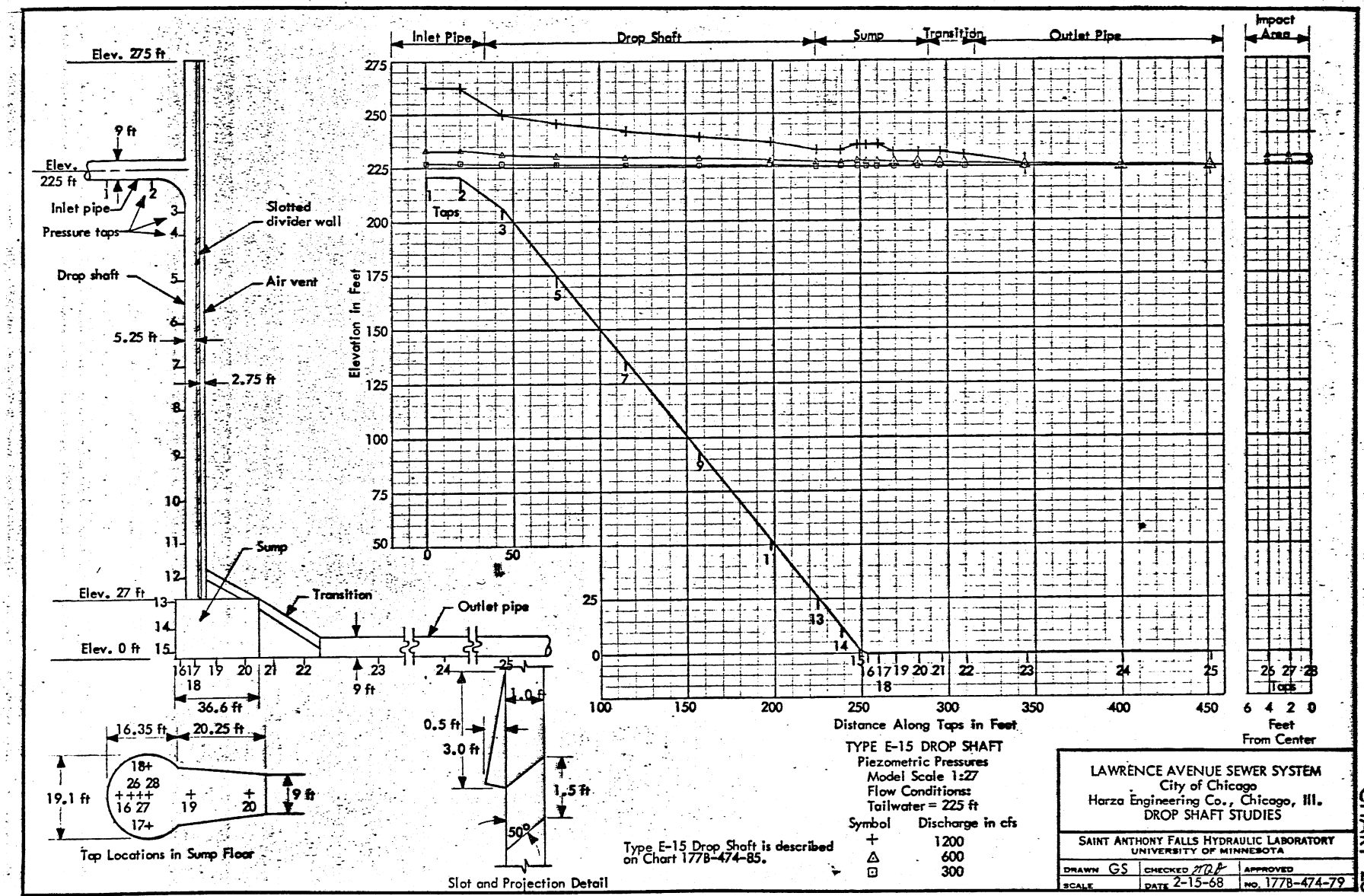
Elev. 275 ft
9 ft
Elev. 225 ft
Inlet pipe
Pressure taps
Slotted divider wall
Drop shaft
Air vent
5.25 ft
2.75 ft
Sump
Elev. 27 ft
Transition
Outlet pipe
Elev. 0 ft
36.6 ft
9 ft
16.35 ft
20.25 ft
19.1 ft
9 ft
Tap Locations in Sump Floor
0.5 ft
3.0 ft
1.0 ft
1.5 ft
50°
Slot and Projection Detail
Inlet Pipe
Drop Shaft
Sump
Transition
Outlet Pipe
Impact Area
Elevation in Feet
Taps
Distance Along Taps in Feet
Feet From Center
Type E-15 Drop Shaft is described on Chart 177B-474-85.
TYPE E-15 DROP SHAFT
Piezometric Pressures
Model Scale 1:27
Flow Conditions:
Tailwater = 225 ft
Symbol Discharge in cfs
+ 1200
△ 600
⊡ 300
LAWRENCE AVENUE SEWER SYSTEM
City of Chicago
Harza Engineering Co., Chicago, Ill.
DROP SHAFT STUDIES
SAINT ANTHONY FALLS HYDRAULIC LABORATORY
UNIVERSITY OF MINNESOTA
DRAWN GS
CHECKED
APPROVED
SCALE
DATE 2-15-68
NO. 177B-474-79

CHART 26

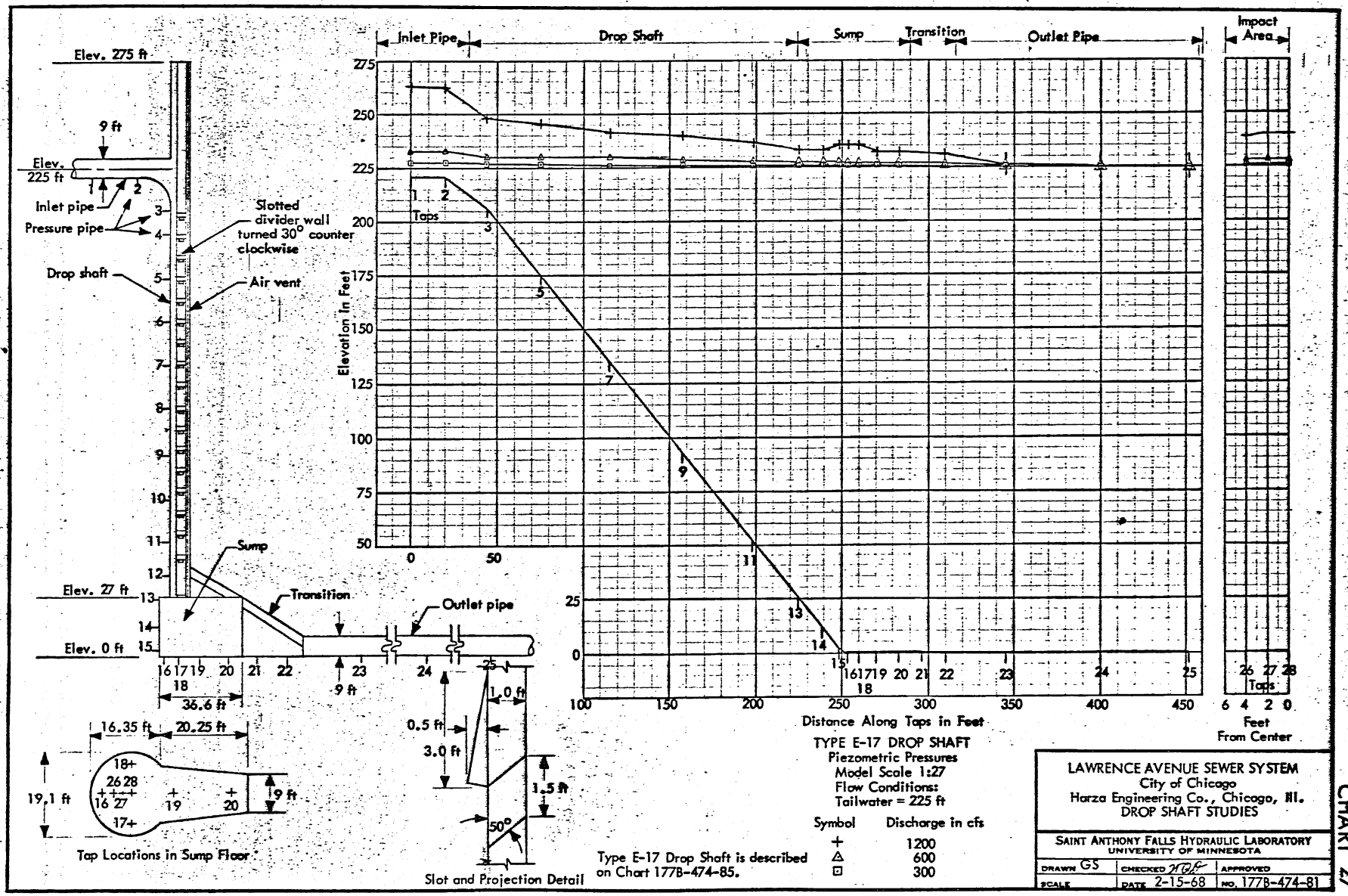

Type E-17 Drop Shaft is described on Chart 177B-474-85.

TYPE E-17 DROP SHAFT
Piezometric Pressures
Model Scale 1:27
Flow Conditions:
Tailwater = 225 ft

Symbol	Discharge in cfs
+	1200
△	600
⊡	300

LAWRENCE AVENUE SEWER SYSTEM
City of Chicago
Harza Engineering Co., Chicago, Ill.
DROP SHAFT STUDIES

SAINT ANTHONY FALLS HYDRAULIC LABORATORY
UNIVERSITY OF MINNESOTA

DRAWN GS	CHECKED HDF	APPROVED
SCALE	DATE 2-15-68	NO. 177B-474-81

CHART 27

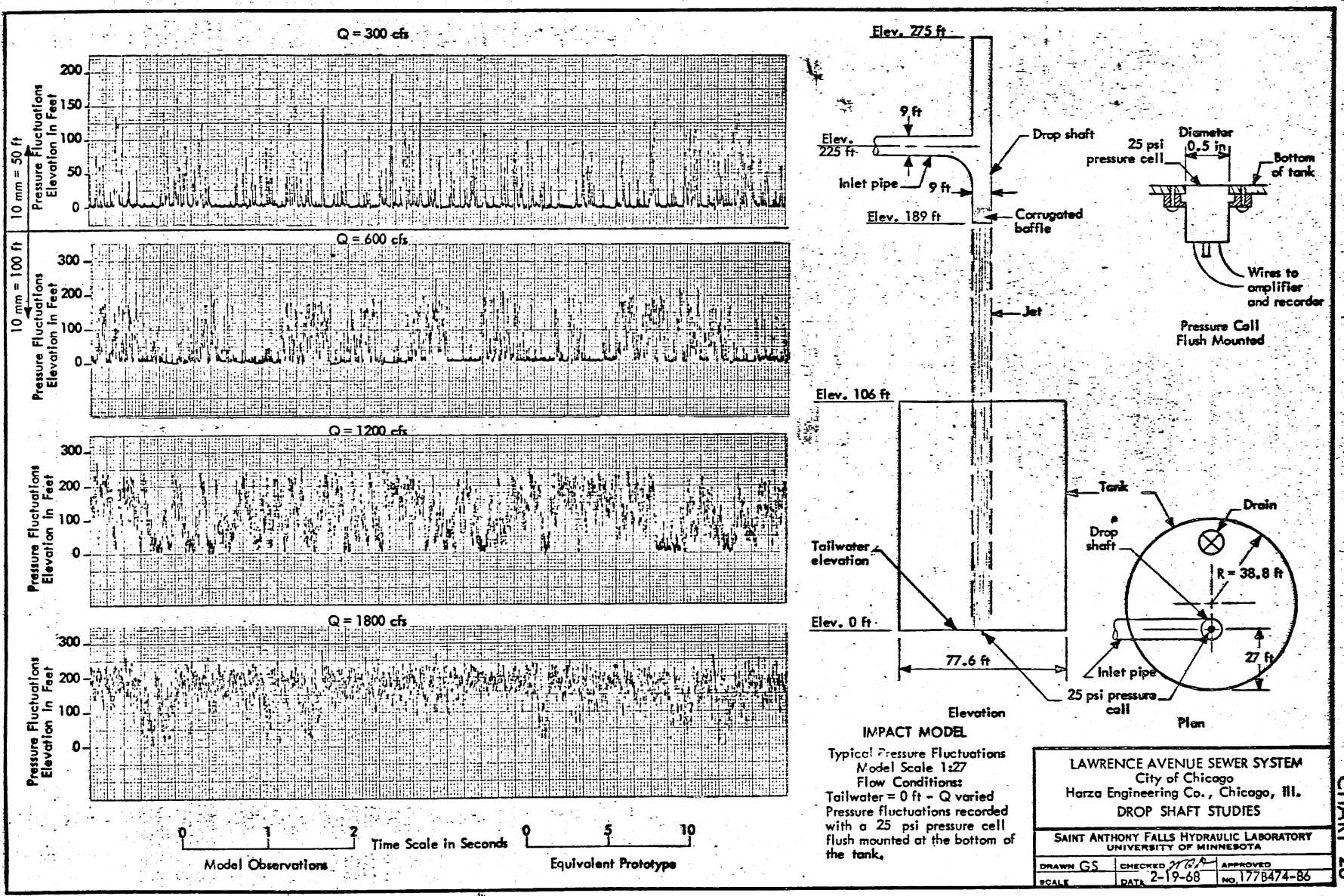

IMPACT MODEL

Typical Pressure Fluctuations
Model Scale 1:27
Flow Conditions:
Tailwater = 0 ft - Q varied
Pressure fluctuations recorded with a 25 psi pressure cell flush mounted at the bottom of the tank.

LAWRENCE AVENUE SEWER SYSTEM
City of Chicago
Harza Engineering Co., Chicago, Ill.
DROP SHAFT STUDIES

SAINT ANTHONY FALLS HYDRAULIC LABORATORY
UNIVERSITY OF MINNESOTA

DRAWN GS	CHECKED	APPROVED
SCALE	DATA 2-19-68	NO. 177B474-86

CHART 28

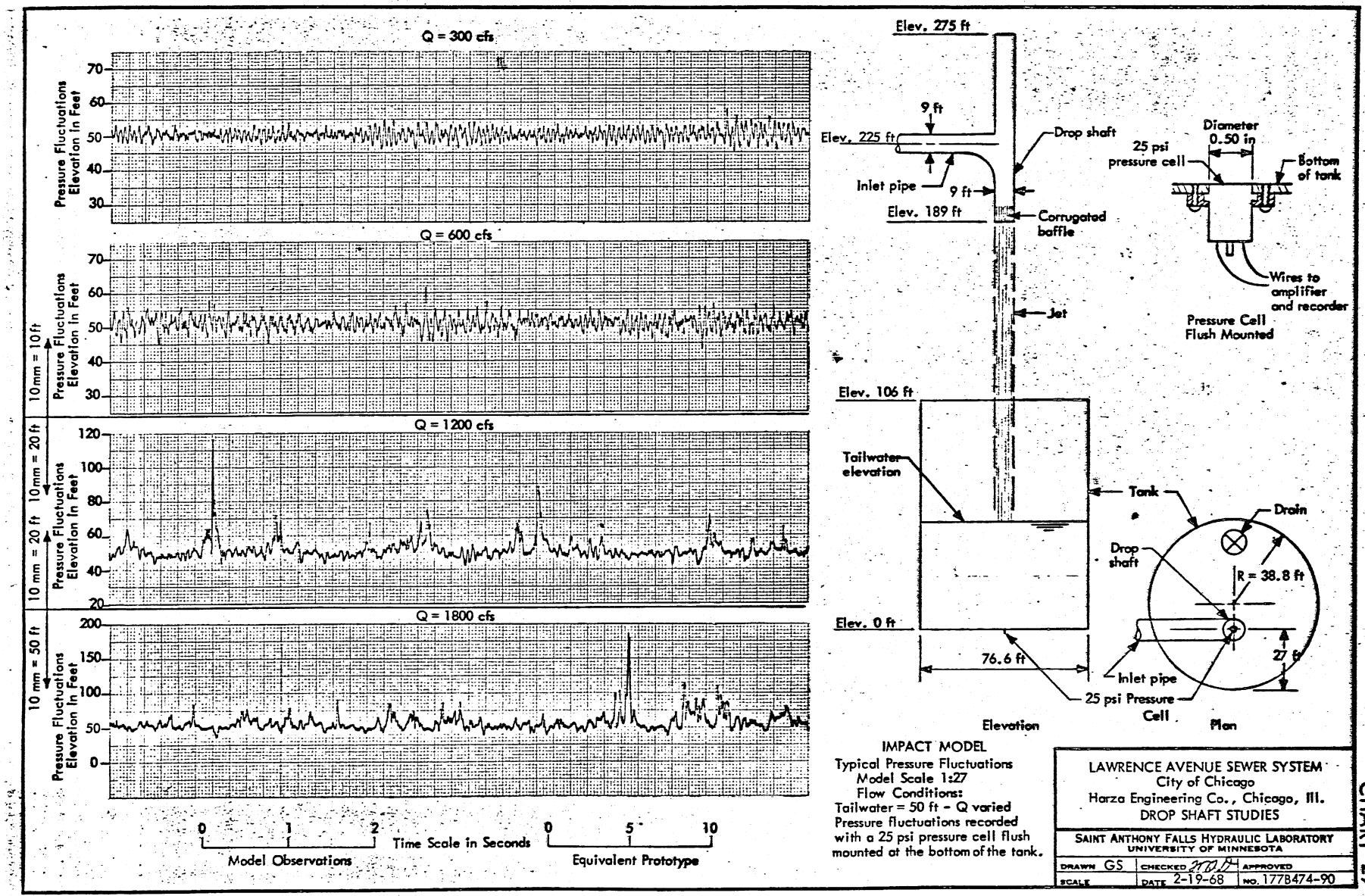

IMPACT MODEL
Typical Pressure Fluctuations
Model Scale 1:27
Flow Conditions:
Tailwater = 50 ft - Q varied
Pressure fluctuations recorded with a 25 psi pressure cell flush mounted at the bottom of the tank.

LAWRENCE AVENUE SEWER SYSTEM
City of Chicago
Harza Engineering Co., Chicago, Ill.
DROP SHAFT STUDIES

SAINT ANTHONY FALLS HYDRAULIC LABORATORY
UNIVERSITY OF MINNESOTA

DRAWN GS	CHECKED	APPROVED
SCALE	DATE 2-19-68	NO. 1778474-90

CHART 29

Maximum Peak Elevations

Q cfs	T.W. Elev. ft.	Flush Mounted Cell in Block P_F-Elev. in ft.	P_B-Elev. in ft.	P_F/P_B
300	0	198	205	0.966
300	10	191	186	1.025
300	15	165	153	1.079
300	25	146	138	1.057
300	50	58	59	0.984
600	0	250	250	1.000
600	10	250	230	1.085
600	15	234	245	0.955
600	25	204	186	1.095
600	50	62	74	0.838
1200	0	280	306	0.915
1200	10	270	271	0.995
1200	15	250	267	0.936
1200	25	235	260	0.904
1200	50	117	120	0.975
1800	0	280	310	0.904
1800	10	270	301	0.896
1800	15	270	285	0.946
1800	25	250	290	0.862
1800	50	185	157	1.179

Number of Peaks Per Minute Above Reference Elevations

Pressure Cell Flush Mounted

Q cfs	T.W. Elev. ft.	Freq. cycles/sec.	Elevation of Peaks in Feet 250	225	200	175	150	125	100	75
300	0	14.8	0	0	0	0.6	4.7	19.6	47.2	119.6
300	10	12.7	0	0	0	0.2	3.8	17.0	35.5	56.0
300	15	11.4	0	0	0	0	0.2	0.4	0.6	1.1
300	25	11.5	0	0	0	0	0	0.4	0.8	1.7
300	50	8.9	0	0	0	0	0	0	0	0
600	0	15.8	0.4	0.9	9.8	53.4	112.2	142.0	199.0	224.2
600	10	14.8	0	0.6	3.8	28.5	60.2	92.0	107.1	129.0
600	15	13.9	0	0.8	5.8	24.9	46.8	73.4	112.8	160.3
600	25	10.8	0	0	0.2	0.9	3.4	6.6	13.6	26.0
600	50	11.7	0	0	0	0	0	0	0	0

Pressure Cell Mounted in Block

300	0	11.2	0	0	0.2	0.9	11.5	55.1	117.5	157.5
300	10	13.3	0	0	0	1.1	5.5	21.5	41.9	59.4
300	15	13.5	0	0	0	0	0.2	0.8	2.6	4.7
300	25	9.6	0	0	0	0	0	0.2	0.6	0.6
300	50	11.5	0	0	0	0	0	0	0	0
600	0	15.4	0.2	3.8	17.2	54.7	97.7	128.8	169.4	210.4
600	10	13.7	0	0.9	10.8	44.7	85.1	107.1	132.6	174.8
600	15	13.1	0	0.9	7.0	24.1	45.6	63.9	87.3	109.4
600	25	12.3	0	0	0	0.8	2.6	7.2	13.6	24.7
600	50	10.6	0	0	0	0	0	0	0	0

P_F/P_B For Various Tailwater Elevations

Symbol	Q-cfs
⊙	300
□	600
△	1200
◇	1800

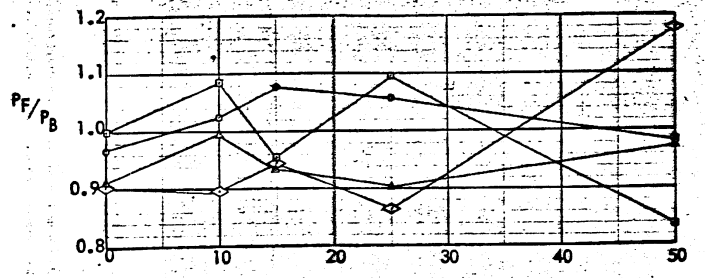

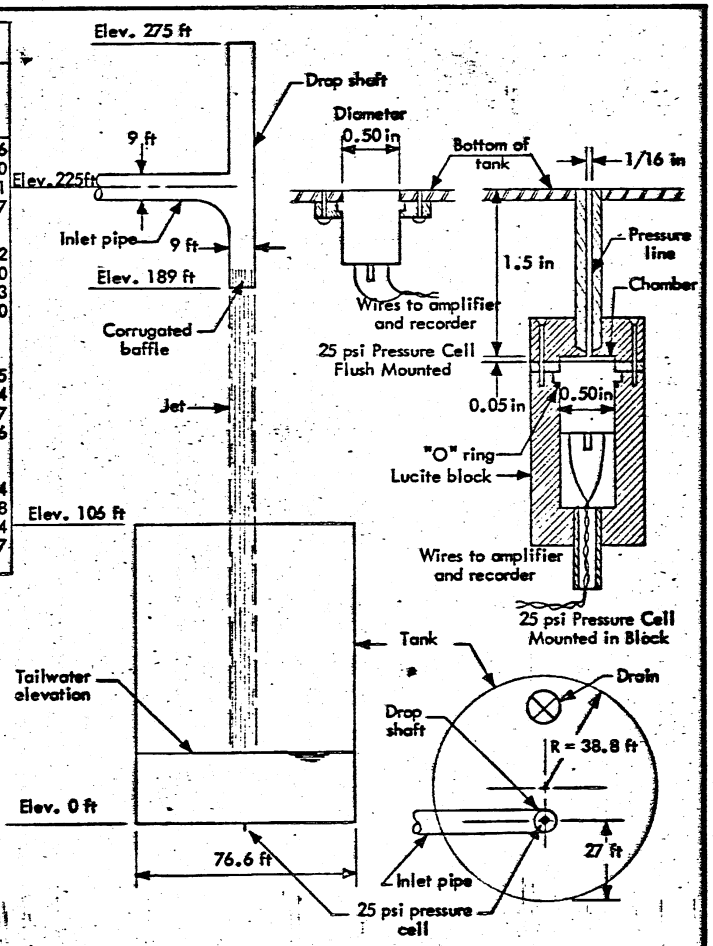

IMPACT MODEL
Maximum Peak Elevations
and Number of Peaks per Minute

Model Scale 1:27
Flow Conditions Varied
A comparison of pressure fluctuations recorded with a 25 psi pressure cell flush mounted and mounted in a block at the bottom of the tank.

LAWRENCE AVENUE SEWER SYSTEM
City of Chicago
Harza Engineering Co., Chicago, Ill.
DROP SHAFT STUDIES

SAINT ANTHONY FALLS HYDRAULIC LABORATORY
UNIVERSITY OF MINNESOTA

DRAWN GS	CHECKED MAP	APPROVED
SCALE	DATE 2-20-68	NO. 177B474 - 98

CHART 30

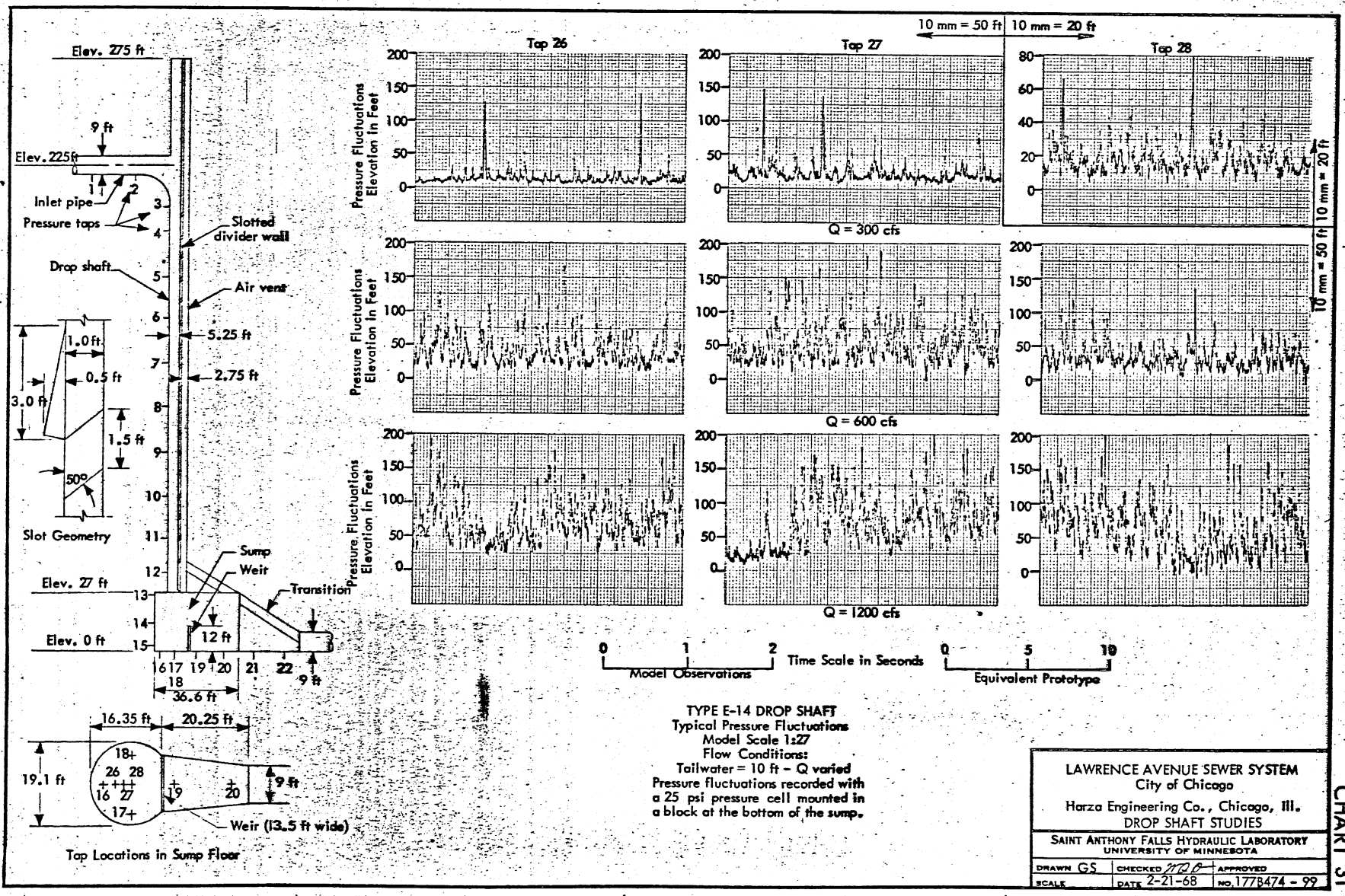

TYPE E-14 DROP SHAFT
Typical Pressure Fluctuations
Model Scale 1:27
Flow Conditions:
Tailwater = 10 ft – Q varied
Pressure fluctuations recorded with a 25 psi pressure cell mounted in a block at the bottom of the sump.

LAWRENCE AVENUE SEWER SYSTEM
City of Chicago
Harza Engineering Co., Chicago, Ill.
DROP SHAFT STUDIES

SAINT ANTHONY FALLS HYDRAULIC LABORATORY
UNIVERSITY OF MINNESOTA

DRAWN GS	CHECKED MDO	APPROVED
SCALE	DATE 2-21-68	NO. 177B474 - 99

CHART 31

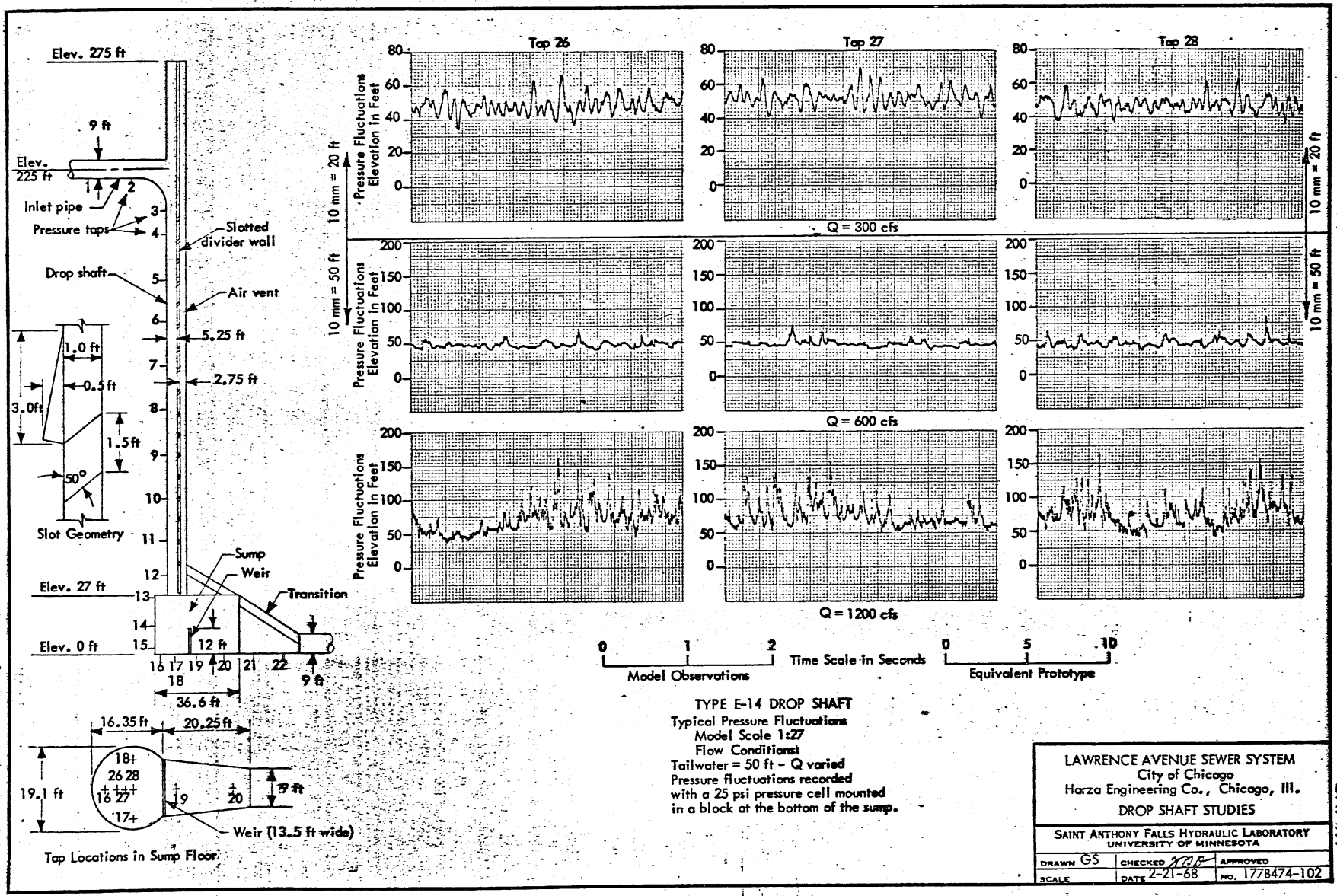

TYPE E-14 DROP SHAFT
Typical Pressure Fluctuations
Model Scale 1:27
Flow Conditions:
Tailwater = 50 ft - Q varied
Pressure fluctuations recorded with a 25 psi pressure cell mounted in a block at the bottom of the sump.

LAWRENCE AVENUE SEWER SYSTEM
City of Chicago
Harza Engineering Co., Chicago, Ill.
DROP SHAFT STUDIES

SAINT ANTHONY FALLS HYDRAULIC LABORATORY
UNIVERSITY OF MINNESOTA

DRAWN GS	CHECKED	APPROVED
SCALE	DATE 2-21-68	NO. 1778474-102

CHART 32

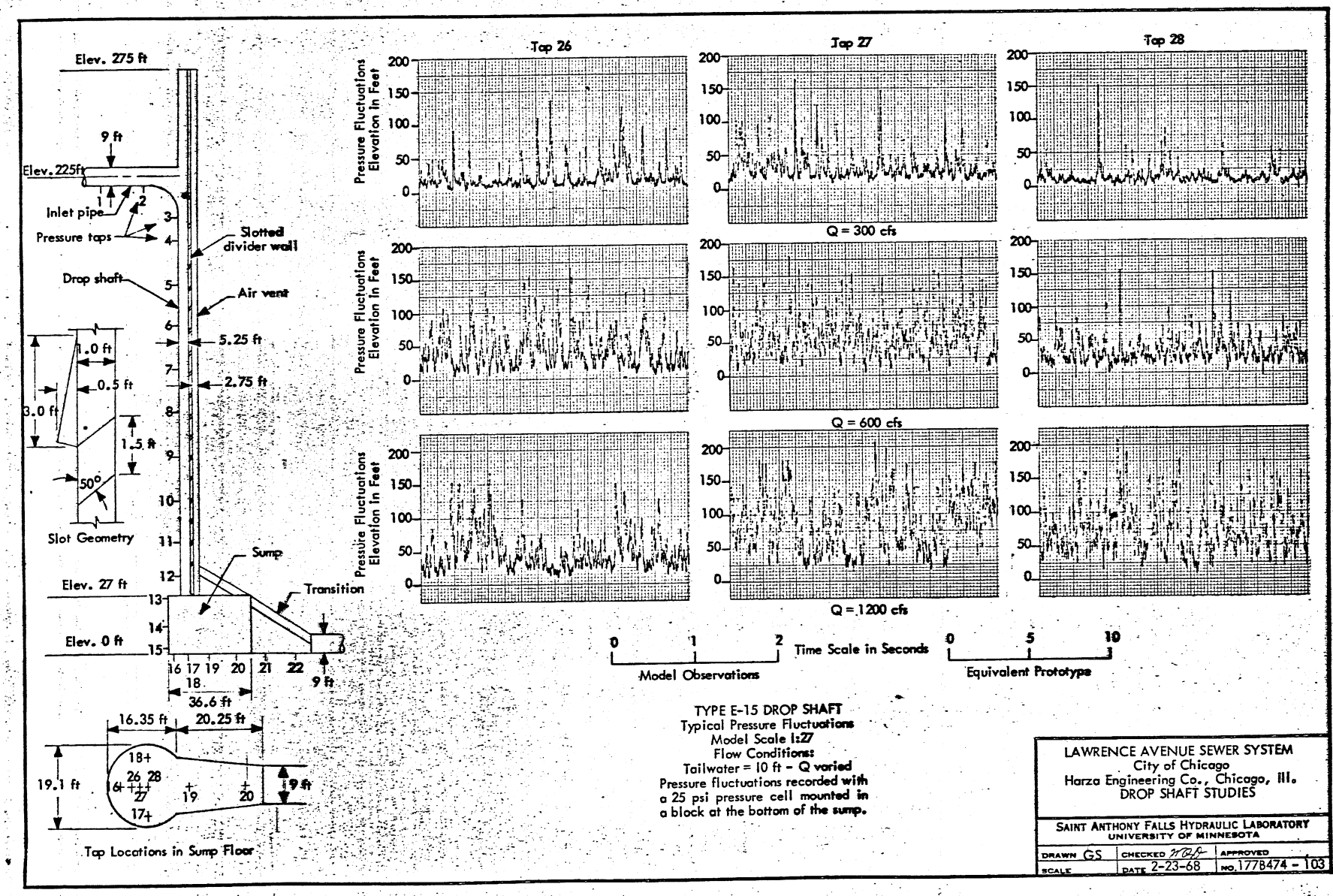

TYPE E-15 DROP SHAFT
Typical Pressure Fluctuations
Model Scale 1:27
Flow Conditions:
Tailwater = 10 ft - Q varied
Pressure fluctuations recorded with a 25 psi pressure cell mounted in a block at the bottom of the sump.

LAWRENCE AVENUE SEWER SYSTEM
City of Chicago
Harza Engineering Co., Chicago, Ill.
DROP SHAFT STUDIES

SAINT ANTHONY FALLS HYDRAULIC LABORATORY
UNIVERSITY OF MINNESOTA

DRAWN GS	CHECKED MAF	APPROVED
SCALE	DATE 2-23-68	NO. 1778474 - 103

CHART 33

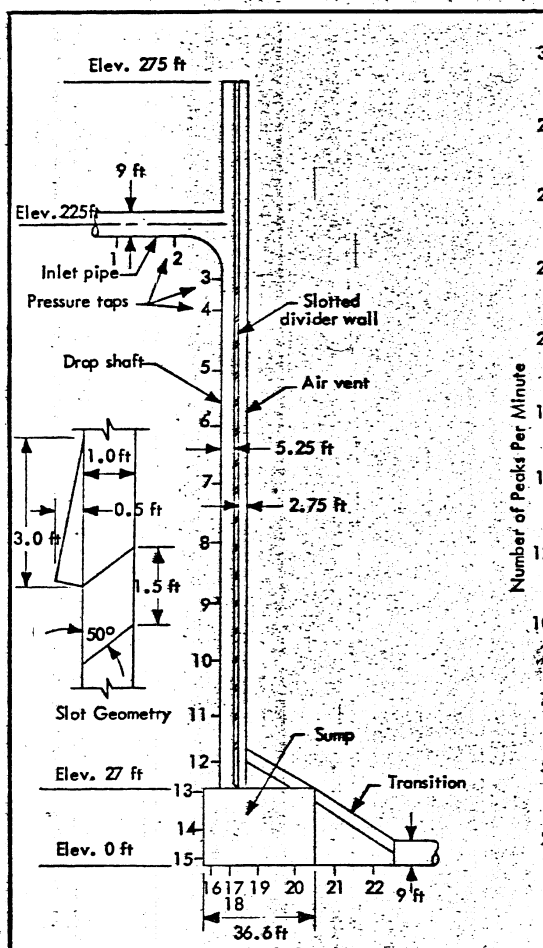

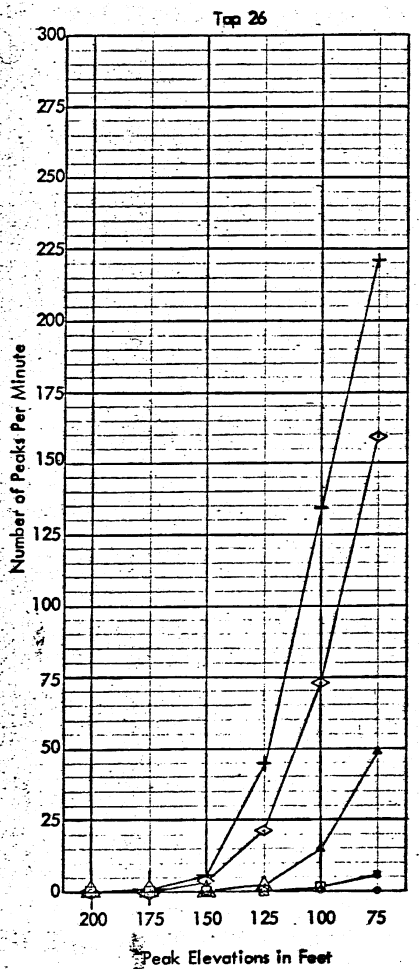

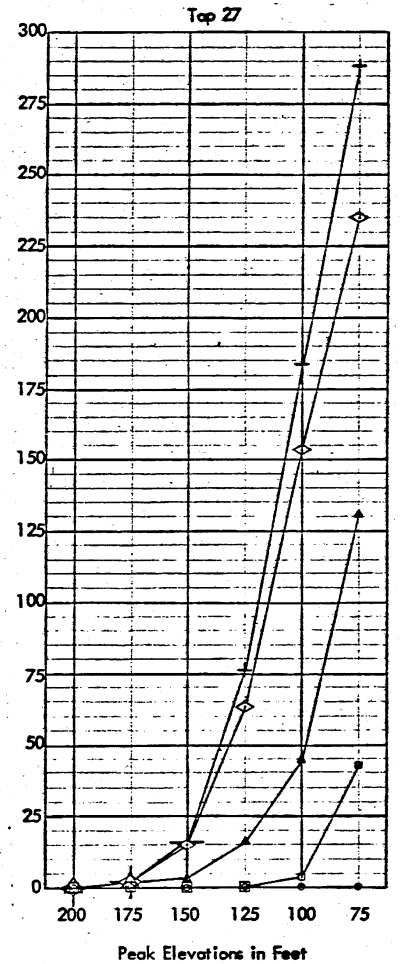

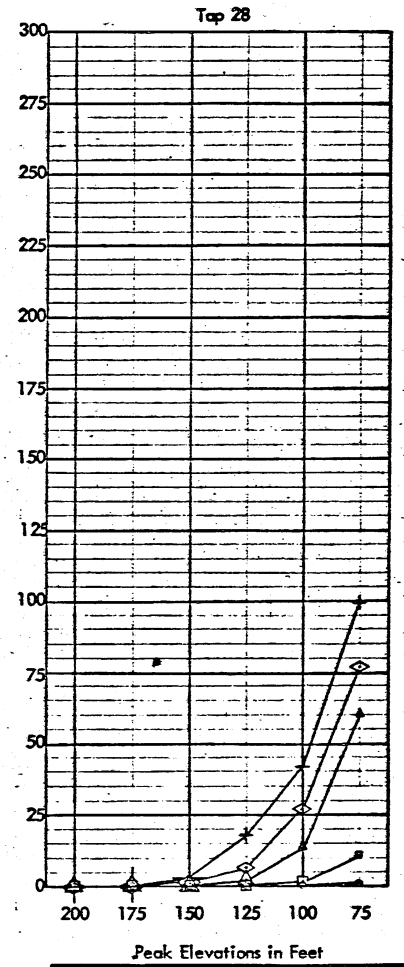

Symbol	Tailwater Elevations in Feet
+	7
◇	10
△	15
⊡	25
⊙	50

TYPE E-15 DROP SHAFT
Number of Peaks Per Minute
Above Reference Elevations
Model Scale 1:27
Flow Conditions:
Q = 600 cfs - Tailwater varied
Pressure fluctuations recorded with a 25 psi pressure cell mounted in a block at the bottom of the sump.

LAWRENCE AVENUE SEWER SYSTEM
City of Chicago
Harza Engineering Co., Chicago, Ill.
DROP SHAFT STUDIES

SAINT ANTHONY FALLS HYDRAULIC LABORATORY
UNIVERSITY OF MINNESOTA

DRAWN	GS	CHECKED		APPROVED	
SCALE		DATE	2-23-68	NO.	1778474 - 111

CHART 34

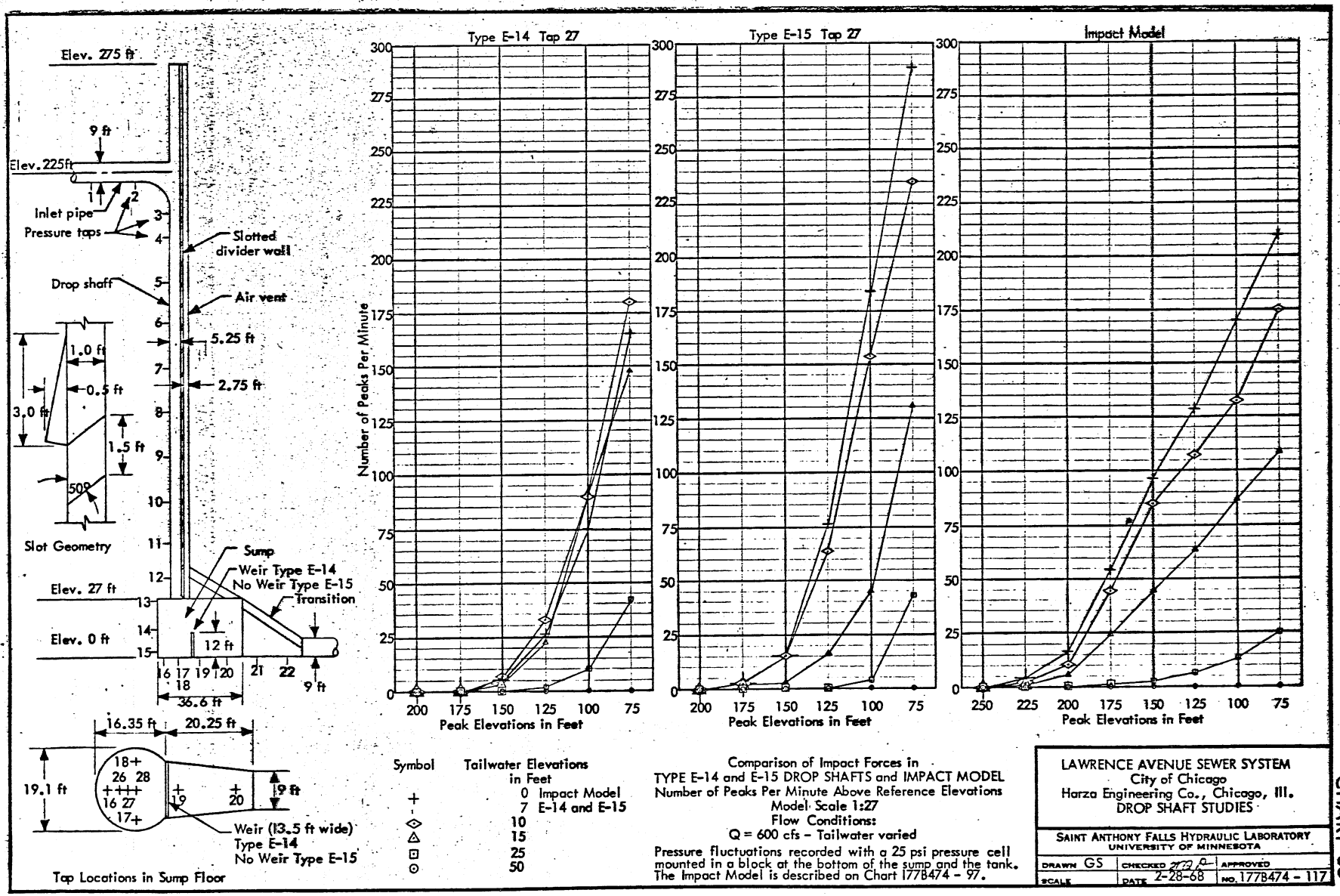

Comparison of Impact Forces in
TYPE E-14 and E-15 DROP SHAFTS and IMPACT MODEL
Number of Peaks Per Minute Above Reference Elevations
Model Scale 1:27
Flow Conditions:
Q = 600 cfs – Tailwater varied

Pressure fluctuations recorded with a 25 psi pressure cell mounted in a block at the bottom of the sump and the tank. The Impact Model is described on Chart 1778474 – 97.

LAWRENCE AVENUE SEWER SYSTEM
City of Chicago
Harza Engineering Co., Chicago, Ill.
DROP SHAFT STUDIES

SAINT ANTHONY FALLS HYDRAULIC LABORATORY
UNIVERSITY OF MINNESOTA

DRAWN	GS	CHECKED		APPROVED	
SCALE		DATE	2-28-68	NO.	1778474 – 117

CHART 35

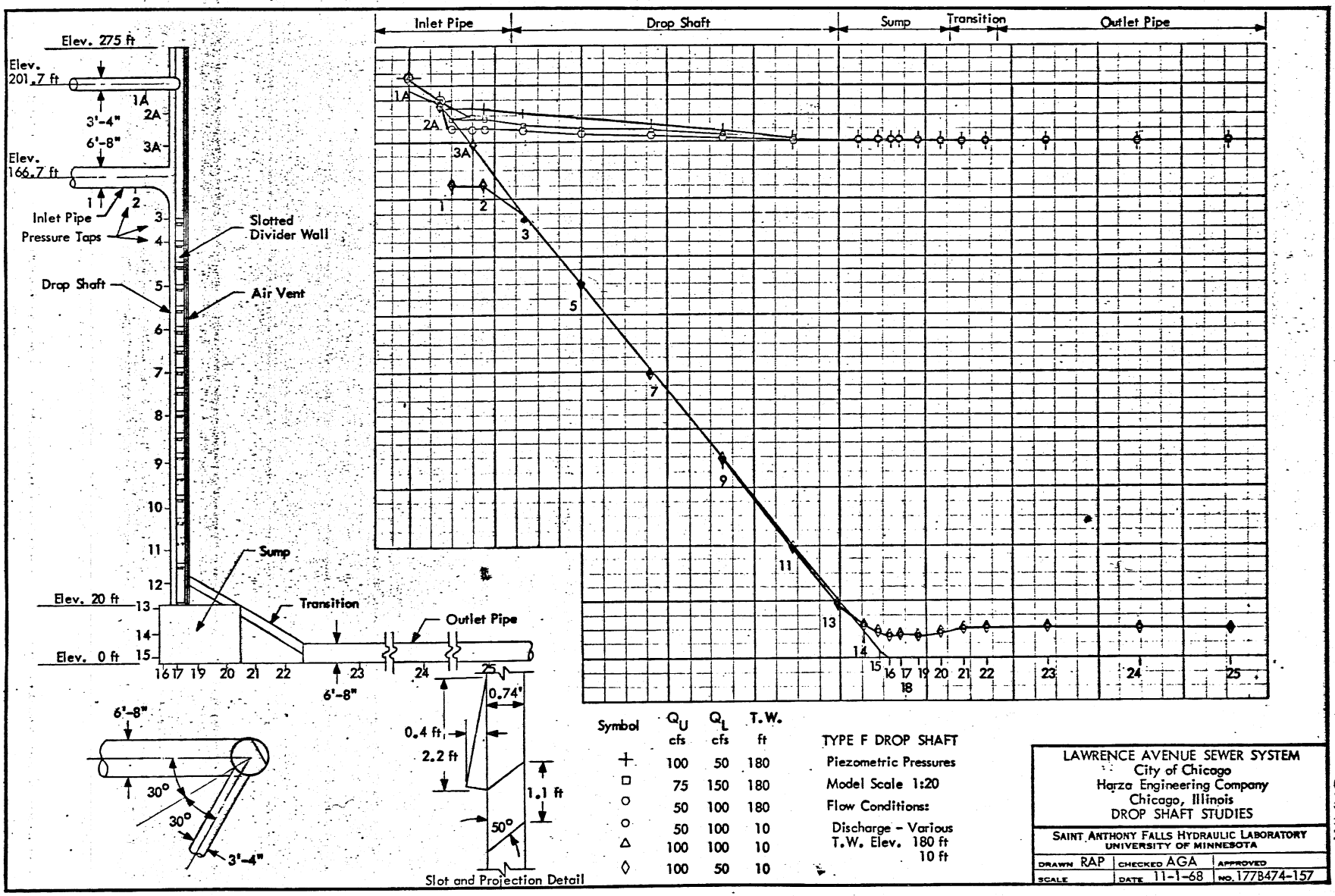
Elev. 275 ft
Elev. 201.7 ft
1A
2A
3A
3'-4"
6'-8"
Elev. 166.7 ft
1
2
3
4
5
6
7
8
9
10
11
12
13
14
15
Inlet Pipe
Pressure Taps
Slotted Divider Wall
Drop Shaft
Air Vent
Sump
Transition
Outlet Pipe
Elev. 20 ft
Elev. 0 ft
16 17 19 20 21 22 23
6'-8"
24
25
Inlet Pipe
Drop Shaft
Sump
Transition
Outlet Pipe
1A
2A
3A
1
2
3
5
7
9
11
13
14
15
16 17 18 19 20 21 22
23
24
25
6'-8"
30°
30°
3'-4"
0.74"
0.4 ft
2.2 ft
1.1 ft
50°
Slot and Projection Detail
Symbol
Q_U cfs
Q_L cfs
T.W. ft
100 50 180
75 150 180
50 100 180
50 100 10
100 100 10
100 50 10
TYPE F DROP SHAFT
Piezometric Pressures
Model Scale 1:20
Flow Conditions:
Discharge - Various
T.W. Elev. 180 ft
10 ft
LAWRENCE AVENUE SEWER SYSTEM
City of Chicago
Harza Engineering Company
Chicago, Illinois
DROP SHAFT STUDIES
SAINT ANTHONY FALLS HYDRAULIC LABORATORY
UNIVERSITY OF MINNESOTA
DRAWN RAP
CHECKED AGA
APPROVED
SCALE
DATE 11-1-68
NO. 1778474-157
CHART 36

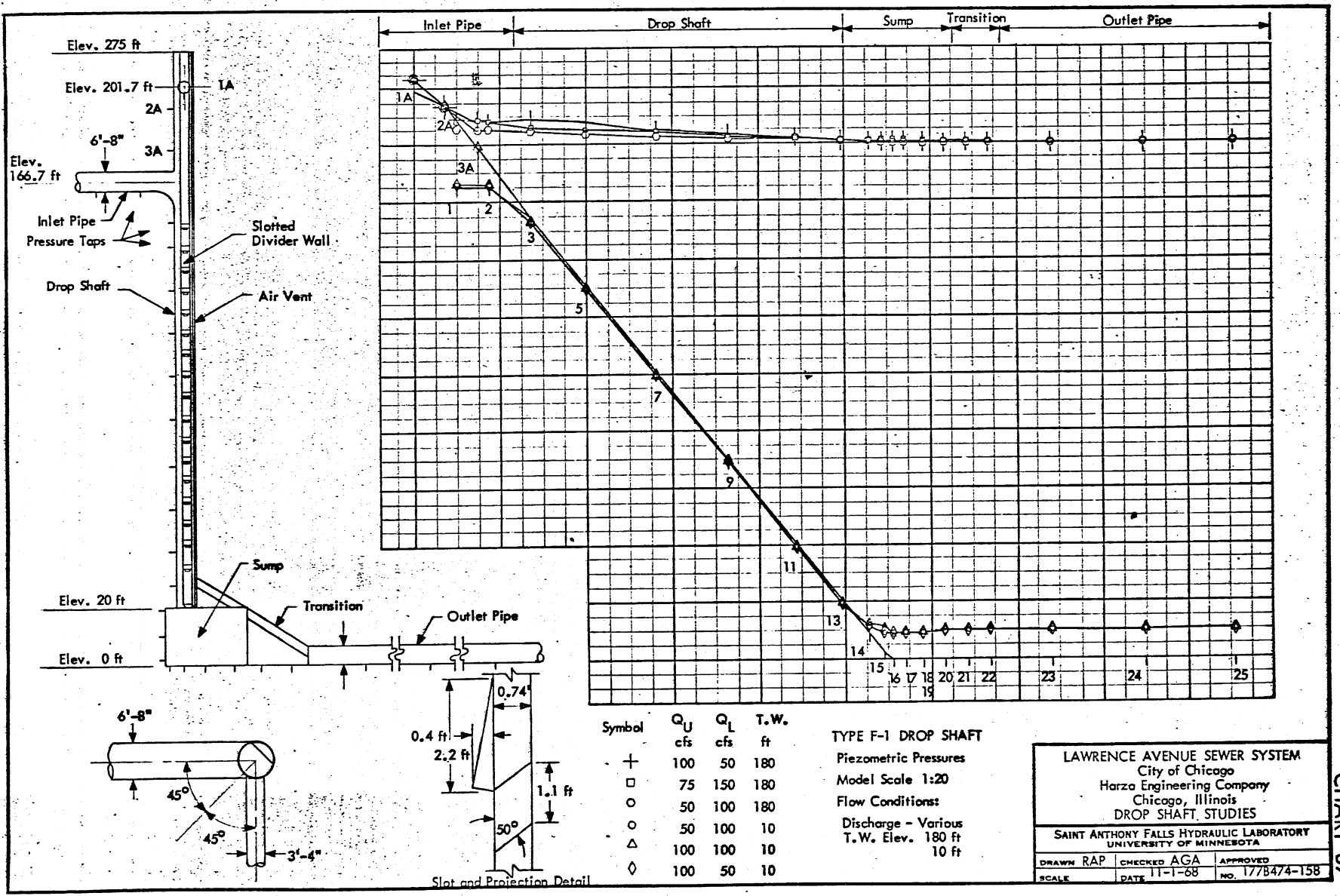

Symbol	Q_U cfs	Q_L cfs	T.W. ft
+	100	50	180
□	75	150	180
○	50	100	180
○	50	100	10
△	100	100	10
◇	100	50	10

TYPE F-1 DROP SHAFT

Piezometric Pressures

Model Scale 1:20

Flow Conditions:

Discharge - Various

T.W. Elev. 180 ft
10 ft

LAWRENCE AVENUE SEWER SYSTEM
City of Chicago
Harza Engineering Company
Chicago, Illinois
DROP SHAFT STUDIES

SAINT ANTHONY FALLS HYDRAULIC LABORATORY
UNIVERSITY OF MINNESOTA

DRAWN	CHECKED	APPROVED
RAP	AGA	
SCALE	DATE 11-1-68	NO. 177B474-158

CHART 37

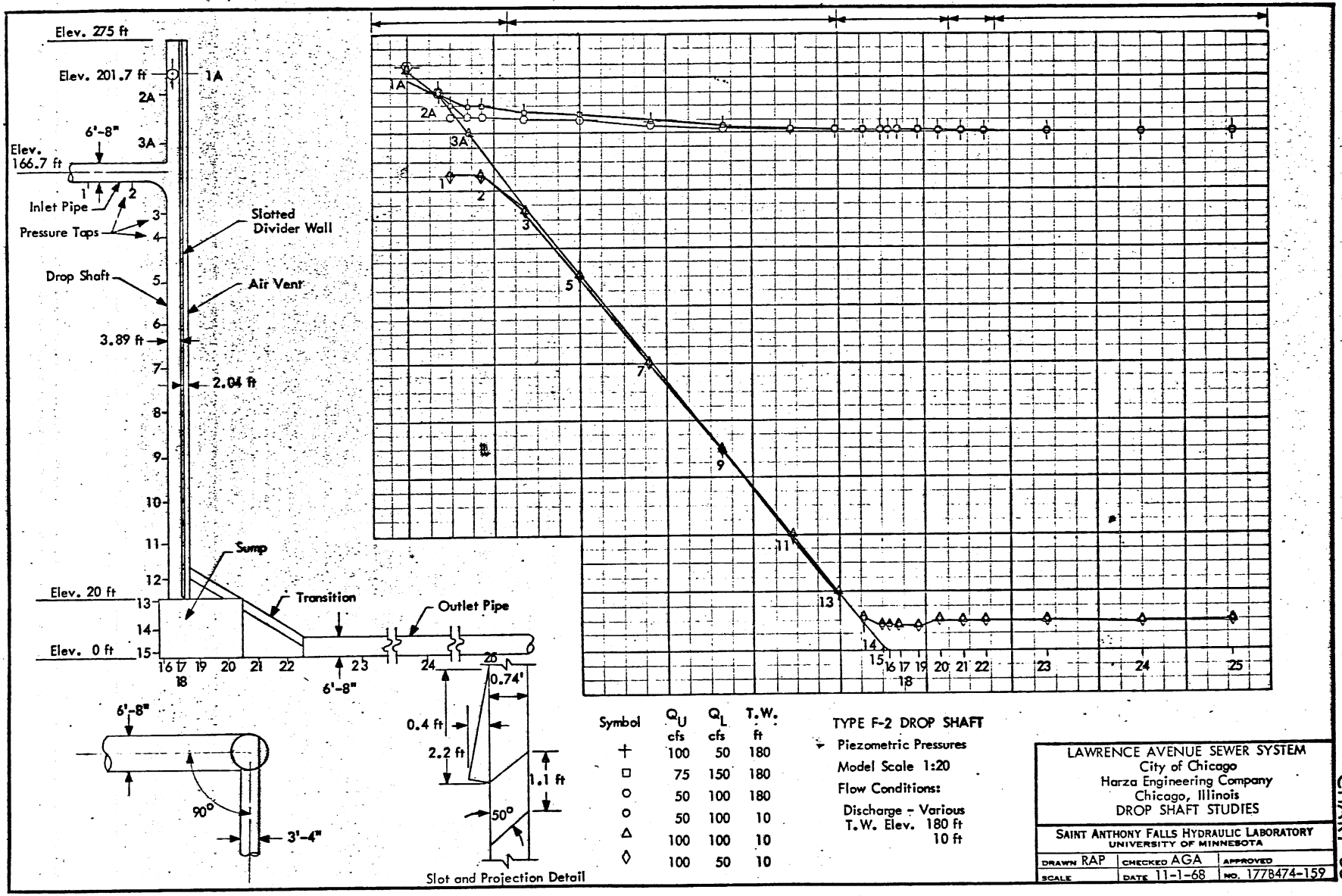
Elev. 275 ft
Elev. 201.7 ft
1A
2A
6'-8"
3A
Elev. 166.7 ft
Inlet Pipe
Pressure Taps
Slotted Divider Wall
Drop Shaft
Air Vent
3.89 ft
2.04 ft
Sump
Elev. 20 ft
Transition
Outlet Pipe
Elev. 0 ft
6'-8"
0.74'
0.4 ft
2.2 ft
1.1 ft
90°
50°
3'-4"
Slot and Projection Detail
Symbol
Q_U cfs
Q_L cfs
T.W. ft
100 50 180
75 150 180
50 100 180
50 100 10
100 100 10
100 50 10
TYPE F-2 DROP SHAFT
Piezometric Pressures
Model Scale 1:20
Flow Conditions:
Discharge - Various
T.W. Elev. 180 ft
10 ft
LAWRENCE AVENUE SEWER SYSTEM
City of Chicago
Harza Engineering Company
Chicago, Illinois
DROP SHAFT STUDIES
SAINT ANTHONY FALLS HYDRAULIC LABORATORY
UNIVERSITY OF MINNESOTA
DRAWN RAP
CHECKED AGA
APPROVED
SCALE
DATE 11-1-68
NO. 1778474-159
CHART 38

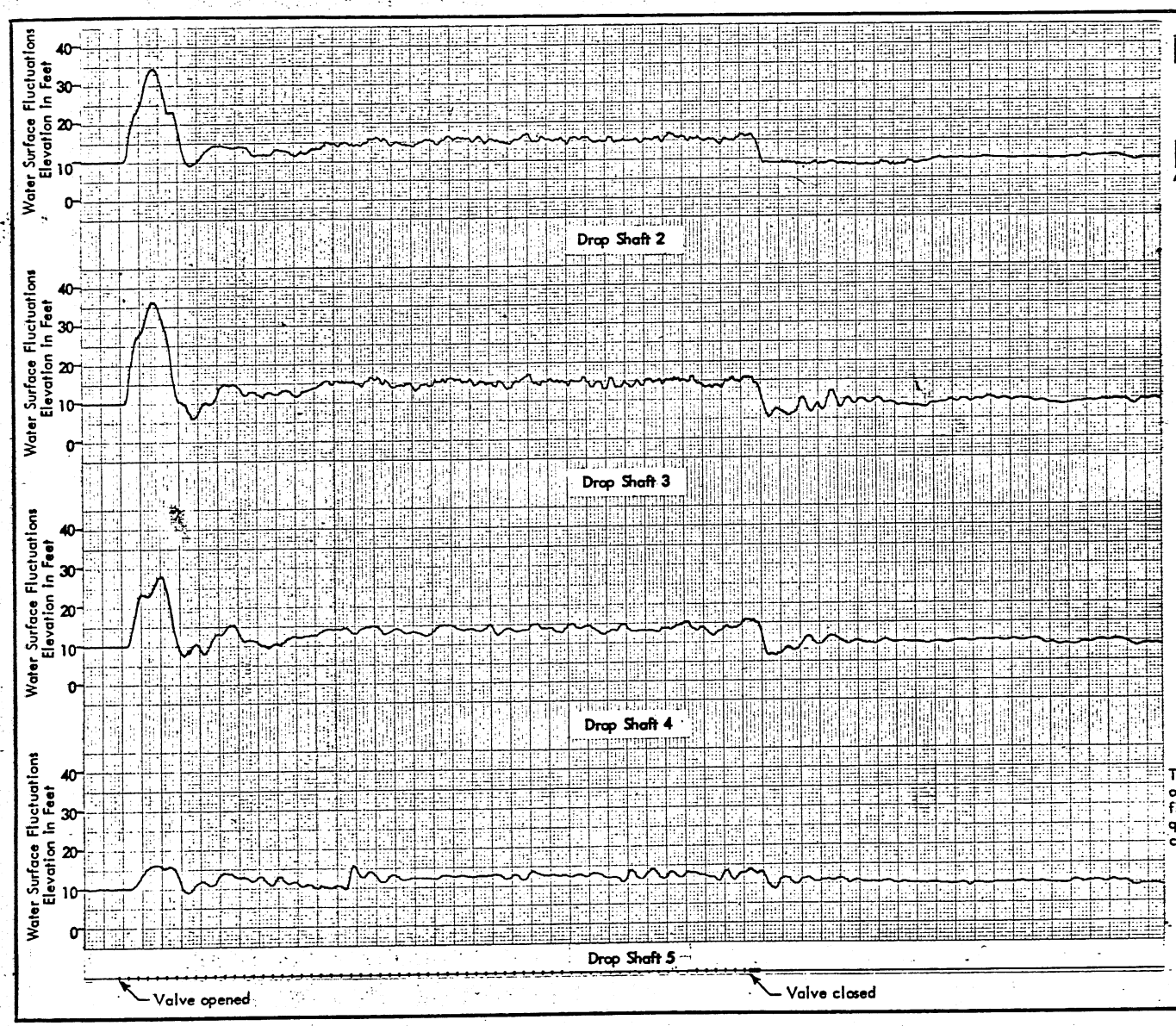

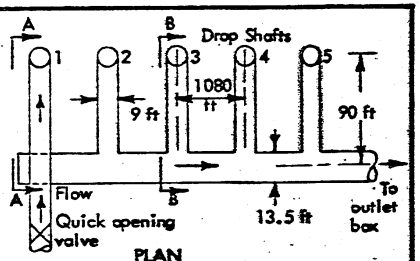

PLAN
Not to scale

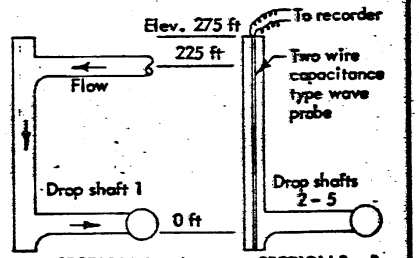

SECTION A – A

SECTION B – B

Time Scale in Seconds
0 10 20

Model Observations
0 50 100

Equivalent Prototype

TYPE A SURGE MODEL
Typical Water Surface Fluctuations in Drop Shafts
Model Scale 1:54
Flow Conditions:
Discharge = 600 cfs – Tailwater = 10 ft

The tailwater level in the system was set by means of an adjustable weir in the outlet box with no flow in the drop shaft. The valve was then opened quickly introducing the flow and the surging recorded in the various drop shafts.

LAWRENCE AVENUE SEWER SYSTEM
City of Chicago
Harza Engineering Co., Chicago, Ill.
SURGE MODEL STUDIES

SAINT ANTHONY FALLS HYDRAULIC LABORATORY
UNIVERSITY OF MINNESOTA

DRAWN WQD	CHECKED	APPROVED
SCALE	DATE 4-23-68	NO. 1778474 - 142

CHART 39

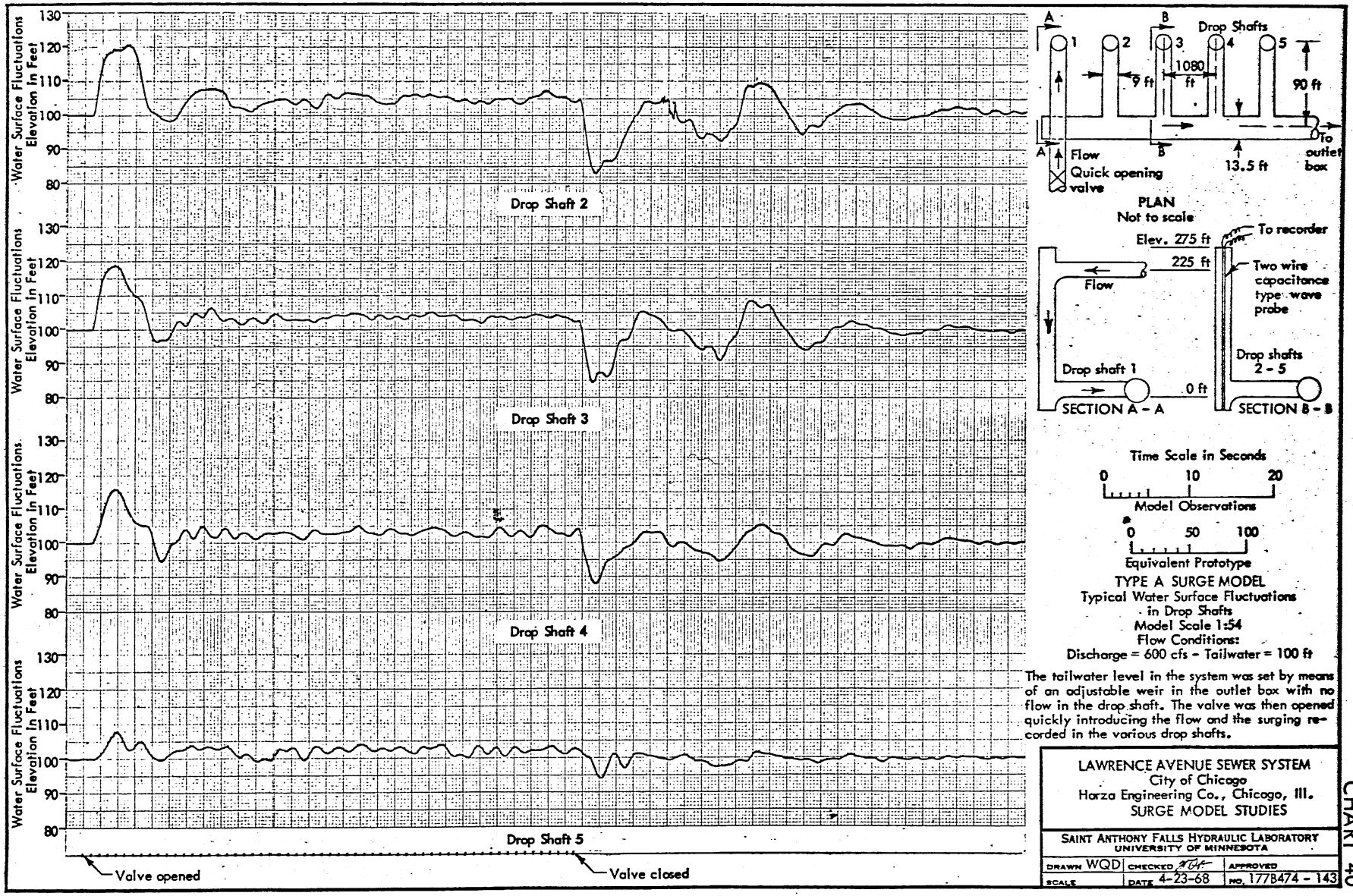

TYPE A SURGE MODEL
Typical Water Surface Fluctuations in Drop Shafts
Model Scale 1:54
Flow Conditions:
Discharge = 600 cfs - Tailwater = 100 ft

The tailwater level in the system was set by means of an adjustable weir in the outlet box with no flow in the drop shaft. The valve was then opened quickly introducing the flow and the surging recorded in the various drop shafts.

LAWRENCE AVENUE SEWER SYSTEM
City of Chicago
Harza Engineering Co., Chicago, Ill.
SURGE MODEL STUDIES

SAINT ANTHONY FALLS HYDRAULIC LABORATORY
UNIVERSITY OF MINNESOTA

DRAWN WQD	CHECKED	APPROVED
SCALE	DATE 4-23-68	NO. 1778474 - 143

CHART 40

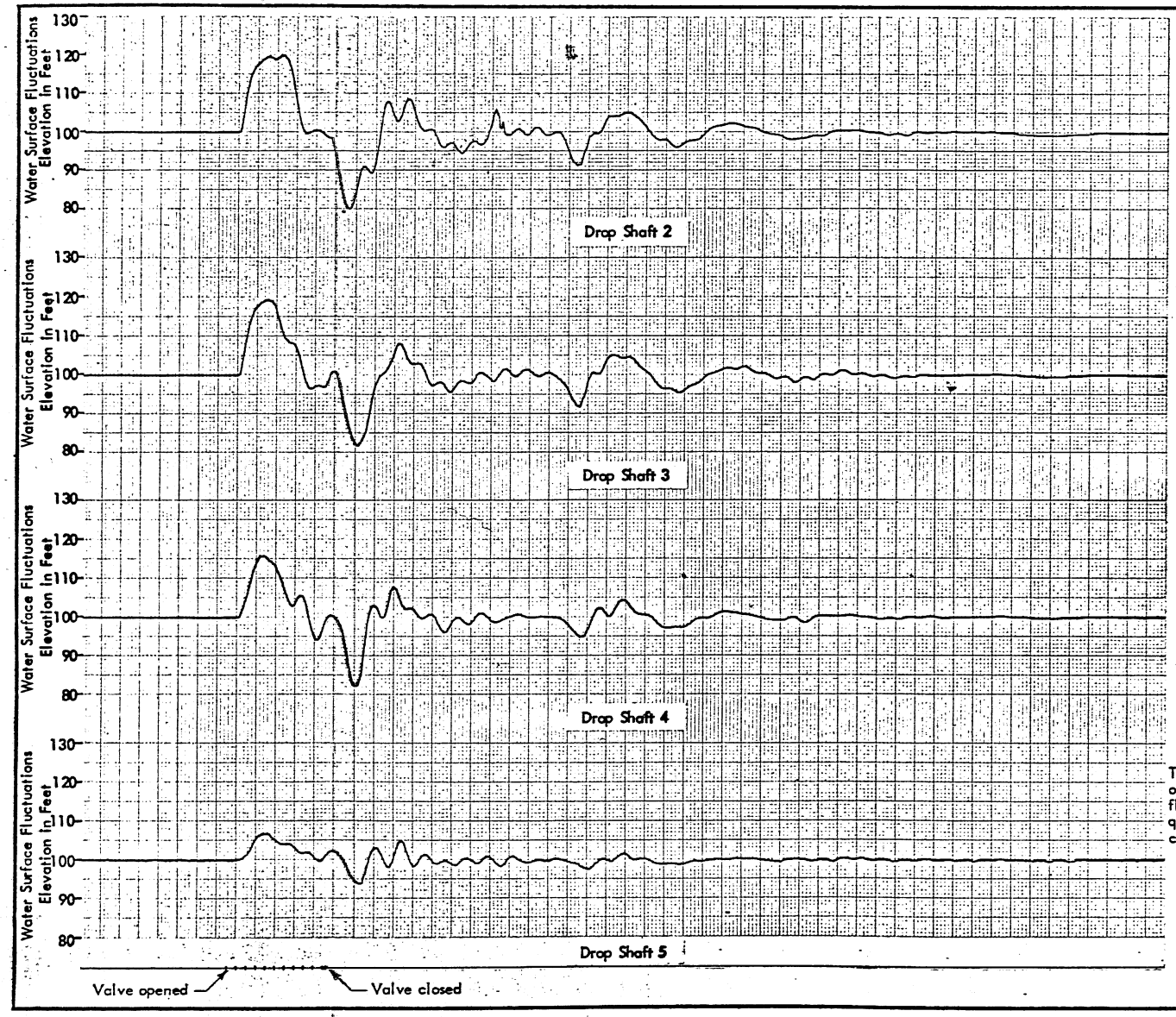

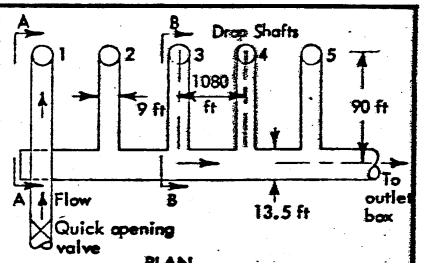

PLAN
Not to scale

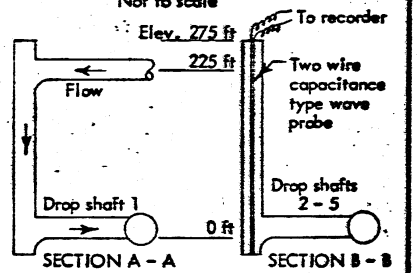

SECTION A - A SECTION B - B

Time Scale in Seconds
0 10 20
Model Observations
0 50 100
Equivalent Prototype

TYPE A SURGE MODEL
Typical Water Surface Fluctuations in Drop Shafts
Model Scale 1:54
Flow Conditions:
Discharge = 600 cfs - Tailwater = 100 ft

The tailwater level in the system was set by means of an adjustable weir in the outlet box with no flow in the drop shaft. The valve was then opened quickly introducing the flow and the surging recorded in the various drop shafts.

LAWRENCE AVENUE SEWER SYSTEM
City of Chicago
Harza Engineering Co., Chicago, Ill.
SURGE MODEL STUDIES

SAINT ANTHONY FALLS HYDRAULIC LABORATORY
UNIVERSITY OF MINNESOTA

DRAWN WQD	CHECKED	APPROVED
SCALE	DATE 4-23-68	NO. 177B474 - 144

CHART 41

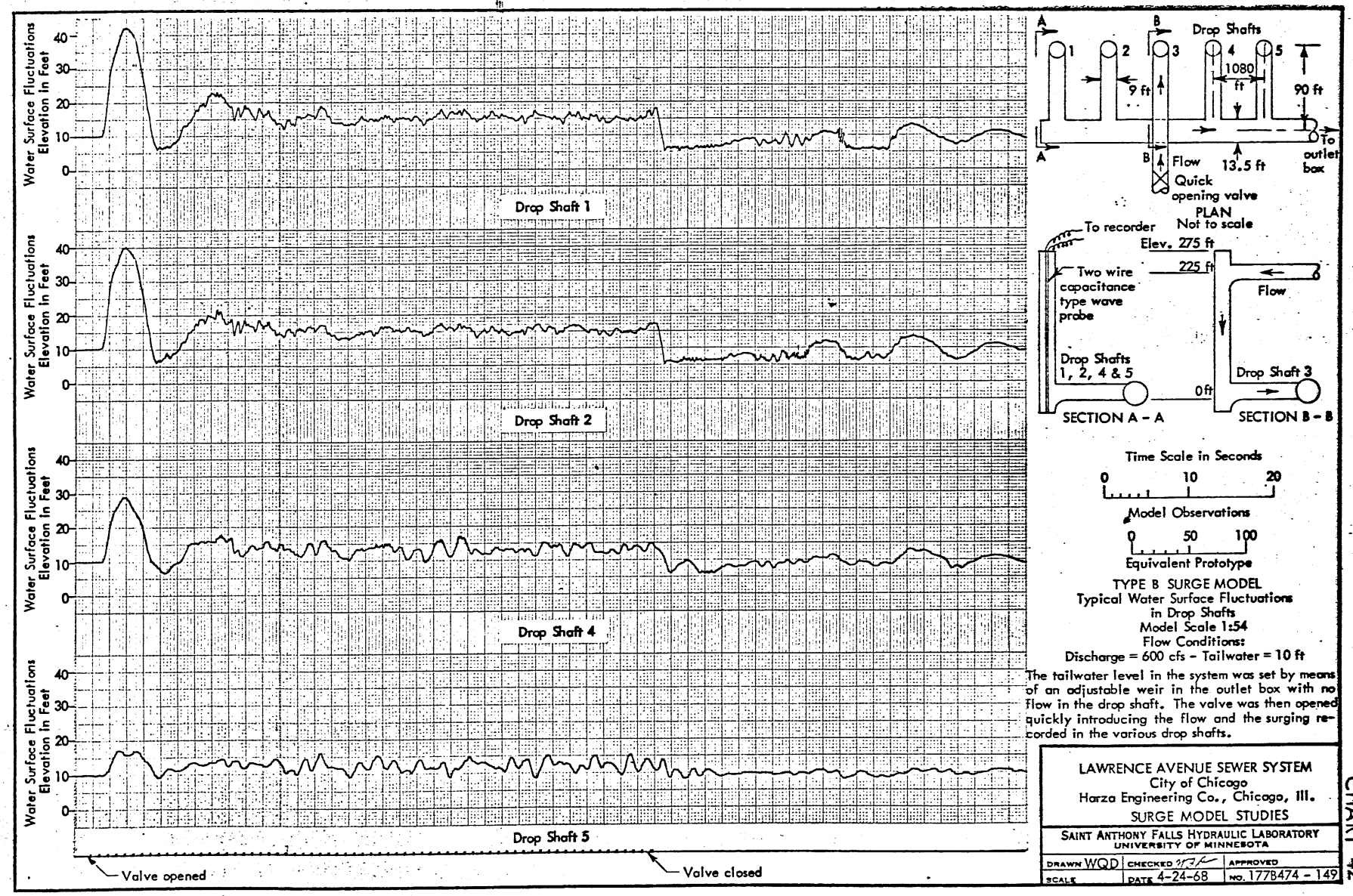

TYPE B SURGE MODEL
Typical Water Surface Fluctuations
in Drop Shafts
Model Scale 1:54
Flow Conditions:
Discharge = 600 cfs - Tailwater = 10 ft

The tailwater level in the system was set by means of an adjustable weir in the outlet box with no flow in the drop shaft. The valve was then opened quickly introducing the flow and the surging recorded in the various drop shafts.

LAWRENCE AVENUE SEWER SYSTEM
City of Chicago
Harza Engineering Co., Chicago, Ill.
SURGE MODEL STUDIES

SAINT ANTHONY FALLS HYDRAULIC LABORATORY
UNIVERSITY OF MINNESOTA

DRAWN WQD	CHECKED	APPROVED
SCALE	DATE 4-24-68	NO. 1778474 - 149

CHART 42

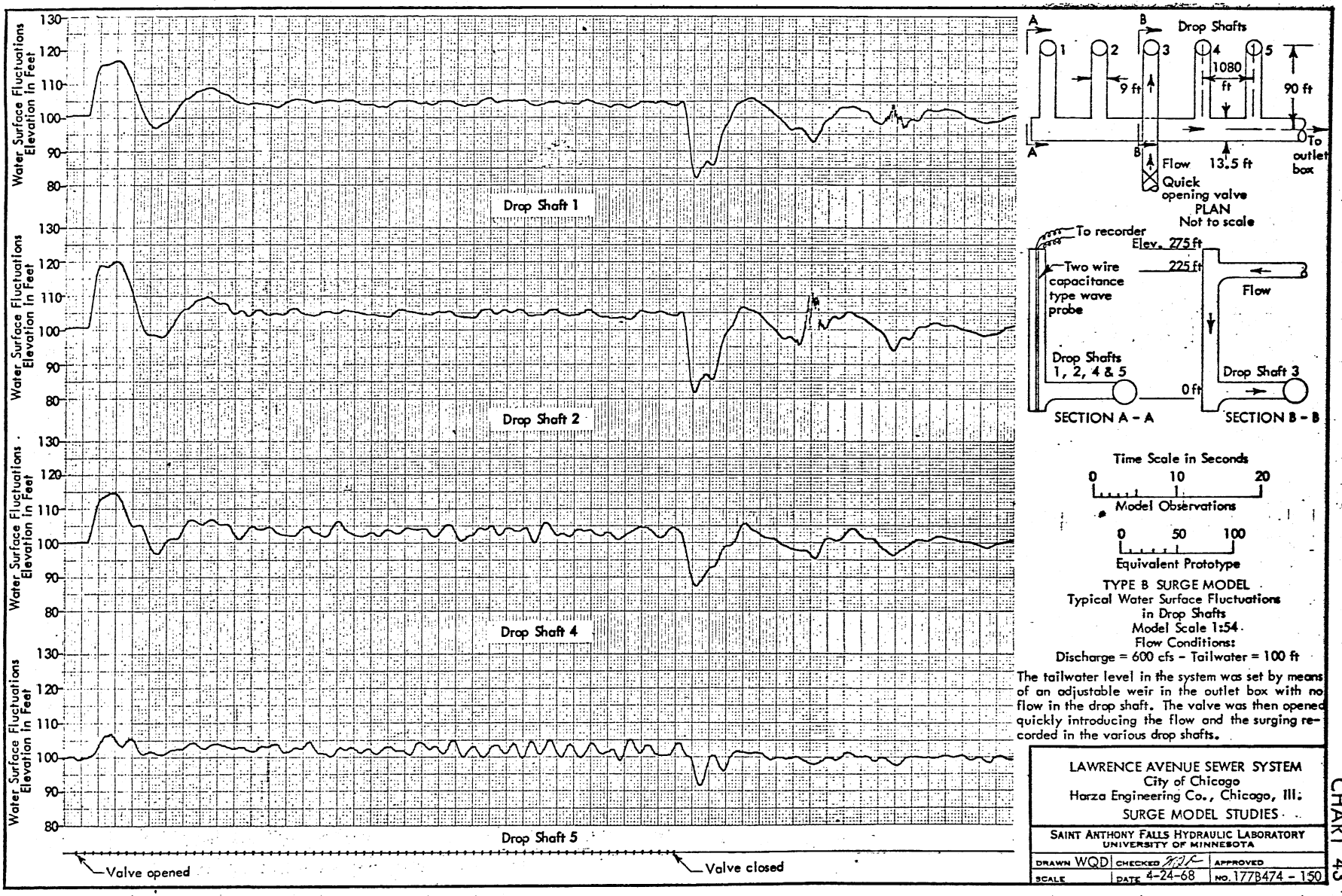

TYPE B SURGE MODEL
Typical Water Surface Fluctuations
in Drop Shafts
Model Scale 1:54
Flow Conditions:
Discharge = 600 cfs - Tailwater = 100 ft

The tailwater level in the system was set by means of an adjustable weir in the outlet box with no flow in the drop shaft. The valve was then opened quickly introducing the flow and the surging recorded in the various drop shafts.

LAWRENCE AVENUE SEWER SYSTEM
City of Chicago
Harza Engineering Co., Chicago, Ill.
SURGE MODEL STUDIES

SAINT ANTHONY FALLS HYDRAULIC LABORATORY
UNIVERSITY OF MINNESOTA

DRAWN WQD	CHECKED	APPROVED
SCALE	DATE 4-24-68	NO. 177B474 - 150

CHART 43

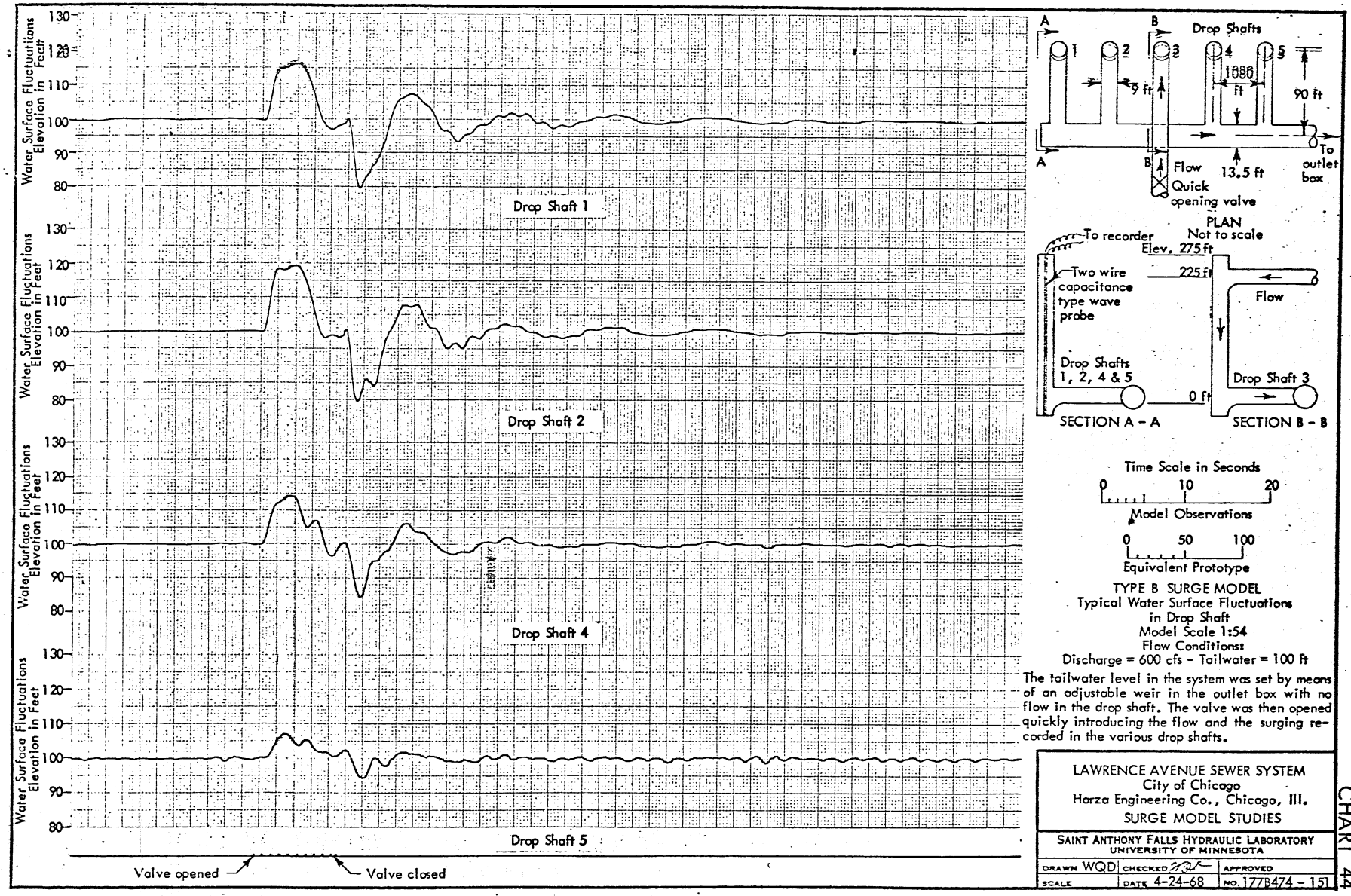

TYPE B SURGE MODEL
Typical Water Surface Fluctuations in Drop Shaft
Model Scale 1:54
Flow Conditions:
Discharge = 600 cfs - Tailwater = 100 ft

The tailwater level in the system was set by means of an adjustable weir in the outlet box with no flow in the drop shaft. The valve was then opened quickly introducing the flow and the surging recorded in the various drop shafts.

LAWRENCE AVENUE SEWER SYSTEM
City of Chicago
Harza Engineering Co., Chicago, Ill.
SURGE MODEL STUDIES

SAINT ANTHONY FALLS HYDRAULIC LABORATORY
UNIVERSITY OF MINNESOTA

DRAWN WQD	CHECKED	APPROVED
SCALE	DATE 4-24-68	NO. 177B474 - 151

CHART 44

Summary of Water Surface Fluctuations in Drop Shafts									Piezometric Elevations		
Q cfs	T.W. ft	Drop Shaft Number	Max. Elev. ft	Time to Max-sec	Min. Elev. ft	Time to Min-sec	Average time to Stabilize sec	Average Elev. after Stabilized ft	Piezometric Elev. - ft	*Slope S	**Friction Factor-f
0.014	0.185	2	0.337	4.5	0.152	9.2	24	0.213	0.220		
		3	0.394	4.6	0.107	8.6	26	0.213	0.215		
		4	0.324	5.4	0.107	9.2	22	0.213	0.215		
		5	0.248	6.0	0.157	9.4	35	0.204	0.210	0.000167	0.0329
0.014	1.852	2	2.039	5.0	1.815	9.7	45	1.888	1.885		
		3	2.010	5.0	1.790	9.0	45	1.886	1.880		
		4	1.970	4.0	1.790	9.3	40	1.886	1.880		
		5	1.906	4.0	1.820	10.0	35	1.872	1.875	0.000167	0.0329
0.028	0.185	2	0.640	3.8	0.148	7.7	22	0.287	0.270		
		3	0.672	3.8	0.111	8.0	22	0.278	0.255		
		4	0.519	4.5	0.141	6.8	22	0.259	0.240		
		5	0.300	3.8	0.167	7.2	28	0.241	0.230	0.000667	0.0329
0.028	1.852	2	2.235	5.2	1.818	10.2	28	1.948	1.930		
		3	2.200	3.8	1.785	8.5	28	1.925	1.915		
		4	2.150	4.0	1.750	9.4	20	1.935	1.900		
		5	2.000	4.0	1.842	9.0	15	1.900	1.890	0.000667	0.0329
0.056	0.185	2	1.945	4.8	0.130	8.2	12	0.426	0.390		
		3	1.241	5.0	0.093	7.2	12	0.407	0.350		
		4	0.907	5.2	0.056	10.0	14	0.333	0.310		
		5	0.426	5.6	0.185	7.2	16	0.259	0.260	0.00217	0.0267
0.056	1.852	2	3.260	3.5	1.574	8.4	22	2.085	2.060		
		3	2.855	3.2	1.668	9.0	22	2.035	2.015		
		4	2.630	4.0	1.408	11.2	22	1.980	1.970		
		5	2.185	4.0	1.815	12.0	22	1.906	1.930	0.00217	0.0267

*S - Slope between drop shafts 2 and 5 computed from piezometric elevations

**Friction Factor f - Computed from:

$$f = \frac{h_f \times D \times 2g}{L \times V^2}$$

h_f = decrease in piezometric head in feet

D = diameter of pipe in feet

g = 32.2 ft/sec^2

L = length of pipe in feet

V = velocity of flow in pipe in feet per second

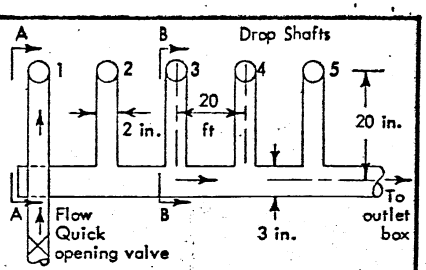

PLAN
Not to Scale

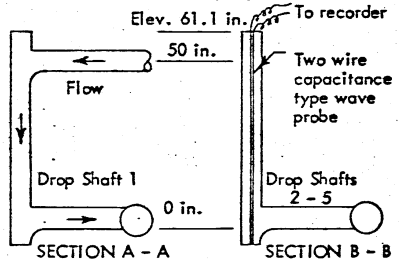

TYPE A SURGE MODEL
Summary of Water Surface Fluctuations in Drop Shafts
Model Scale 1:54
Model Dimensions are Given
Flow Conditions Varied

The tailwater level in the system was set by means of an adjustable weir in the outlet box with no flow in the drop shaft. The valve was opened quickly introducing the flow and the surging recorded in the various drop shafts. Piezometric elevations were recorded from pressure taps in each drop shaft and used in computing slope and friction factor.

LAWRENCE AVENUE SEWER SYSTEM
City of Chicago
Harza Engineering Co., Chicago, Ill.
SURGE MODEL STUDIES

SAINT ANTHONY FALLS HYDRAULIC LABORATORY
UNIVERSITY OF MINNESOTA

DRAWN WQD	CHECKED	APPROVED
SCALE	DATE 5-16-68	NO. 177B474-156

CHART 45

Project Report No. 100

MODEL STUDIES - LAWRENCE AVENUE SEWER SYSTEM
CITY OF CHICAGO
Supplement 1 - Effect of Air and Detergents on Flow Pattern

by
Alvin G. Anderson
and
Warren Q. Dahlin

Prepared for
HARZA ENGINEERING COMPANY
Chicago, Illinois

January 1969

CONTENTS

were taken of the flow for several air ejection rates in order to observe the nature of the flow pattern within the structure or the outlet tunnel when large air discharge rates occurred.

The experiments dealing with the detergents were carried out to see what effect large quantities of detergent would have upon the operation of the drop shaft. For this purpose a tank was connected to the inflow tunnel. From the tank a concentrated mixture of detergent and water could be fed into the inlet tunnel at a reasonably high rate. As the apparatus was functioning with the detergent in the inflow, air concentration measurements were made in the drop shaft in order to see what changes might have occurred in the entrainment characteristics as a result of the detergent. Photographs of this phase were also taken for comparison and for observation of the effect of the detergents on the flow pattern.

The experiments described here were carried out in conjunction with other studies on the design of the sump and air collector. The model drop shaft that was actually used when these tests were performed has been designated as Type E-22. The particular geometry of the sump was the outgrowth of the very early experiments in which the impact cup was used (Project Report No. 100, page 5 and Chart 1). In this arrangement the impact cup elevation was approximately halfway between the floor and the bottom end of the drop shaft. It appeared that since the bottom of the sump served the same purpose as the impact cup, complete excavation should not be necessary. The experiments dealing with the Type E-22 drop shaft showed that it operated as effectively as Type E-14 or Type E-15, which had been established as the final design. It had the disadvantage, however, that the steep slope in the air collector inhibited the entrance and exit of cleaning machinery and the removal of debris collected from the main tunnel which was ordinarily removed through the drop shaft. Because of these disadvantages the Type E-22 drop shaft was not studied in detail. The use of the Type E-22 drop shaft, however, was not detrimental to the experiments dealing with large air discharges from the main tunnel or with the detergents. Since both of these studies were concerned primarily with the flow near the inlet and in the drop shaft, it was not felt that this model would influence the results.

II. EFFECT OF AIR INJECTION INTO THE AIR CHAMBER

The results of the experiments in which the air concentration was measured for different rates of air injection and for the design water discharge of 600 cfs are shown in Chart 1. A single value of 10 ft for the tailwater elevation was used, since it was expected that a possible backflow of air from the main channel would occur only for the low tailwater. The results given in Chart 1 show that the air concentration down the drop shaft is the same for all rates of air flow and furthermore is constant at about 85 per cent at all levels in the drop shaft. These results are in very good agreement with those obtained previously with no air injection (Charts 23 and 24 of Project Report 100). The results given in Chart 1 also include the air concentration when the air injection rate is zero and show essentially no change from those air concentrations measured for other rates of air injection. The appearance of the flow in the air chamber and the downstream tunnel for various rates of air injection is shown in Photo 1 through Photo 4. It is immediately apparent that the appearance of the flow including the entrained air is practically the same for all rates of air injection. As the air injection rate increases, its velocity through the injection pipe also increases, and the jet therefrom disturbs the water surface to a greater or lesser extent in the air chamber. At a tailwater elevation of 10 ft some air escapes through the downstream tunnel for each injection rate, and the photos indicate that the air cushion at the top of the outlet tunnel is essentially the same for each air discharge.

It appears from these photos and the results in Chart 1 that the release of air from the main tunnel at the low tailwater elevation has essentially no effect upon the air concentration and hence the flow pattern in the drop shaft. Apparently the high velocity of flow through the air vent does not create pressure differences sufficiently large for air to be insufflated into the downcoming flow. It would appear therefore that the effect of the air cushion at the top of the main tunnel and the release of air through the various drop shafts will not interfere with the flow that might exist in the drop shaft at that time.

III. EFFECT OF DETERGENTS ON THE FLOW PATTERN IN THE DROP SHAFT

In the event that detergents are introduced into the incoming flow to the drop shafts it was felt that the foaming action of these detergents might influence the flow pattern in the structure. Several experiments were made to qualitatively examine this feature by providing for the introduction of a detergent into the inflow tunnel of the drop shaft. The data are shown in Charts 2 and 3 for a discharge of 600 cfs and various tailwater elevations. Chart 2 shows the actual air concentration measurements at three points at each tap for these discharges and tailwaters both with and without detergents added. Chart 3 is a graphical comparison of the average air concentrations at different levels within the drop shaft. For a tailwater elevation of 150 ft there is a considerable difference in the air concentrations in the region above the tailwater elevation, but for elevations below the tailwater level the air concentrations in the flow portion of the drop shaft are very constant and uniform regardless of the presence of the detergent. When the tailwater is at elevation 100 ft the air concentrations are nearly the same at the upper levels of the drop shaft and down at the sump level with a considerable difference again existing just above the tailwater level. When the tailwater is dropped to 50 ft, the air concentration is essentially the same at all elevations in the drop shaft with or without the detergent. The reason for this variation in air concentration is not apparent, but photographs of these flows with and without detergents present show a significant difference in their appearance. Photos 5 and 6 show the character of the flow in the air chamber when the detergent is added to the flow. In both cases the discharge is 600 cfs, but in Photo 5 the tailwater elevation is 10 ft and in Photo 6 the tailwater elevation is 50 ft. The appearance of the flow is similar in both cases, and even though the tailwater is at elevation 50 ft, a considerable quantity of detergent has entered the downstream outlet tunnel, just as occurs when the tailwater is lowered to elevation 10 ft. In Photo 7 the detergent has been removed so that only the air which is insufflated by the incoming flow has been carried to the chamber, from which it is easily removed up the air vent. Photo 8, on the other hand, shows the same flow when detergent has been added. The thick foam has filled the air chamber and has begun to flow out of the downstream outlet tunnel. It appears that when the detergent gets into the outlet tunnel it becomes relatively stationary and forms

an interface with the clear water flowing under the detergent. The air chamber is effective in separating much of the detergent, so that the water flowing under the foam appears to be relatively clear.

Photos 9 through 12 show the nature of the flow at the drop shaft inlet and the exit of the air vent when a detergent has been added to the incoming discharge. The concentration of the detergent was arbitrary and was used only to delineate the nature of the flow when a foaming agent is present. In Photos 9 and 10, for a discharge of 600 cfs, the tailwater has been established at 100 ft and 150 ft, respectively. When the tailwater is at elevation 100 ft, the level of detergent in the air vent is considerably greater and stationary at approximately elevation 190 ft. For the same conditions when the tailwater has been raised to 150 ft, the detergent rises in the air vent to overflow the dividing wall and re-enter the downflow portion of the shaft. The divider wall is initially overtopped by detergent when the tailwater elevation is approximately 140 ft. For these tests the inlet flow was milky in appearance, a condition which was probably due to accidental agitation of the tank containing the detergent. A comparison between Photos 9 and 10 shows that the detergent flowing over the dividing wall in Photo 10 has a damping effect on the flow in the upper regions of the downflowing section. Furthermore, in Photo 10 some detergent has collected above the dividing wall and appears to be unaffected by the flow going over the dividing wall. In Photos 11 and 12, with an even higher tailwater, the detergent rising in the air vent flows relatively smoothly over the dividing wall and mixes with the incoming flow. In Photo 11 the tailwater has been raised to elevation 190 ft, but the detergent overflow is smooth and steady. In Photo 12 the tailwater has been increased to 225 ft. For this flow the entrainment of air at the inlet is negligible, and both the downflow section and the air vent are relatively free of air and, in this case, detergent foam. When the inflow pipe is submerged, the mixing process both here and in the sump is drastically curtailed, so that relatively little air is entrained and the degree of agitation causing foaming of the detergent is greatly reduced. Observations in the course of the experiment showed that if the tailwater is raised rapidly, the detergent surges over the top of the dividing wall and tends to rise in the drop shaft above the inlet. This is shown to a certain extent in Photo 10, where the detergent deposited above the inlet is bypassed by the additional flow rising in the air vent.

IV. SUMMARY

The experiments described in this supplement show that in general any air that may escape from the main tunnel through the drop structure will have practically no influence on the flow pattern or on the concentration of air insufflated through the air slots in the dividing wall. On the other hand, if detergents are added in sufficient quantities to the incoming flow, the foaming action generated in the drop shaft fills the air chamber and the air vent to an elevation somewhat higher than that of the tailwater, and in some cases may be carried into the main tunnels. As the tailwater elevation is increased, the detergent rises in the air vent until with the tailwater at approximately elevation 140 ft the foam flows over the dividing wall and mixes with the incoming flow to be returned to the drop shaft. If the tailwater elevation is not raised too rapidly the detergent flows over the dividing wall with little dusturbance; but if the tailwater elevation is raised rapidly the surge of the detergent up the air vent overtops the dividing wall, and portions of it can become lodged in the drop shaft above the dividing wall and be relatively unaffected by the continuing flow.

Experiments indicated that the Type E-22 drop shaft was essentially as effective as the Type E-14 or E-15 drop shaft. Although the size of the sump was reduced by this device, the disadvantages incurred in the manipulation of maintenance equipment and the removal of debris from the tunnel caused this alternative to be rejected in favor of the Type E-15 drop shaft, which was recommended.

LIST OF PHOTOS

PHOTO 1 (Serial No. 177-399) This photograph shows the appearance of the flow in the air chamber and the outlet tunnel when air is injected into the air chamber. When the air discharge is zero, the flow is similar to that previously observed in the experiment with drop shaft development.

PHOTO 2 (Serial No. 177-400) When the air discharge is 600 cfs no observable influence is seen except for disturbances in the air chamber created by the air jet. At a tailwater elevation of 10 ft, a small amount of air passes through the outlet tunnel.

PHOTO 3 (Serial No. 177-401) This photograph shows the appearance of the flow in the air chamber when the air discharge is 1500 cfs.

PHOTO 4 (Serial No. 177-402) A large air discharge of 2200 cfs does not appreciably change the flow pattern in the air chamber and the outlet tunnel. The high velocity in the air jet creates a greater disturbance within the air chamber. The relative increase of this disturbance is apparent in the series of photographs.

PHOTO 5 (Serial No. 177-403) When a detergent is added to the incoming flow, the air chamber is filled with foam, and when the tailwater elevation is 10 ft the foam penetrates the outlet tunnel and forces the relatively clear water to flow under the stationary foam.

PHOTO 6 (Serial No. 177-406) This photo shows that when the tailwater elevation is increased to 50 ft the detergent foam collected in the air chamber is still forced into the outlet tunnel so that it is approximately half filled with foam. The water is forced to flow in the region below the detergent foam.

PHOTO 7 (Serial No. 177-408) For comparison, this photograph shows the flow pattern without detergent for the same discharge and tailwater elevation as in Photo 6.

PHOTO 8 (Serial No. 177-409) For comparison with Photo 7 and for the same flow conditions, detergent has been added to the flow, and as is apparent, fills the air chamber and a portion of the downstream tunnel.

PHOTO 9 (Serial No. 177-522) The foaming detergent in the inflow rises in the air vent to a stable elevation considerably in excess of the tailwater elevation. For this experiment the discharge was 600 cfs and the tailwater was at elevation 100 ft. There is relatively little mixing or insufflation of detergent through the dividing wall at this elevation.

PHOTO 10 (Serial No. 177-523) When the tailwater elevation is increased to 150 ft the detergent foam rises sufficiently in the air vent to overtop the dividing wall and mingle with the incoming flow. This forms a uniform mixture flowing down the drop shaft. Some of the detergent has been deposited in the shaft above the divider wall and over the flowing detergent foam.

PHOTO 11 (Serial No. 177-524) This photo shows the relatively smooth flow over the divider wall when the tailwater is sufficiently high. The discharge was 600 cfs and the tailwater was raised to elevation 190 ft. With this tailwater the mixing is less intense and the detergent foam is not as concentrated.

PHOTO 12 (Serial No. 177-525) When the tailwater has been raised to elevation 225 ft the inlet is completely submerged and the mixing of air and detergent has been reduced to a minimum. Very little air has been insufflated, and the effect of the detergent appears to be minimal.

PHOTO 1 (Serial No. 177-399) This photograph shows the appearance of the flow in the air chamber and the outlet tunnel when air is injected into the air chamber. When the air discharge is zero, the flow is similar to that previously observed in the experiment with drop shaft development.

PHOTO 2 (Serial No. 177-400) When the air discharge is 600 cfs no observable influence is seen except for disturbances in the air chamber created by the air jet. At a tailwater elevation of 10 ft, a small amount of air passes through the outlet tunnel.

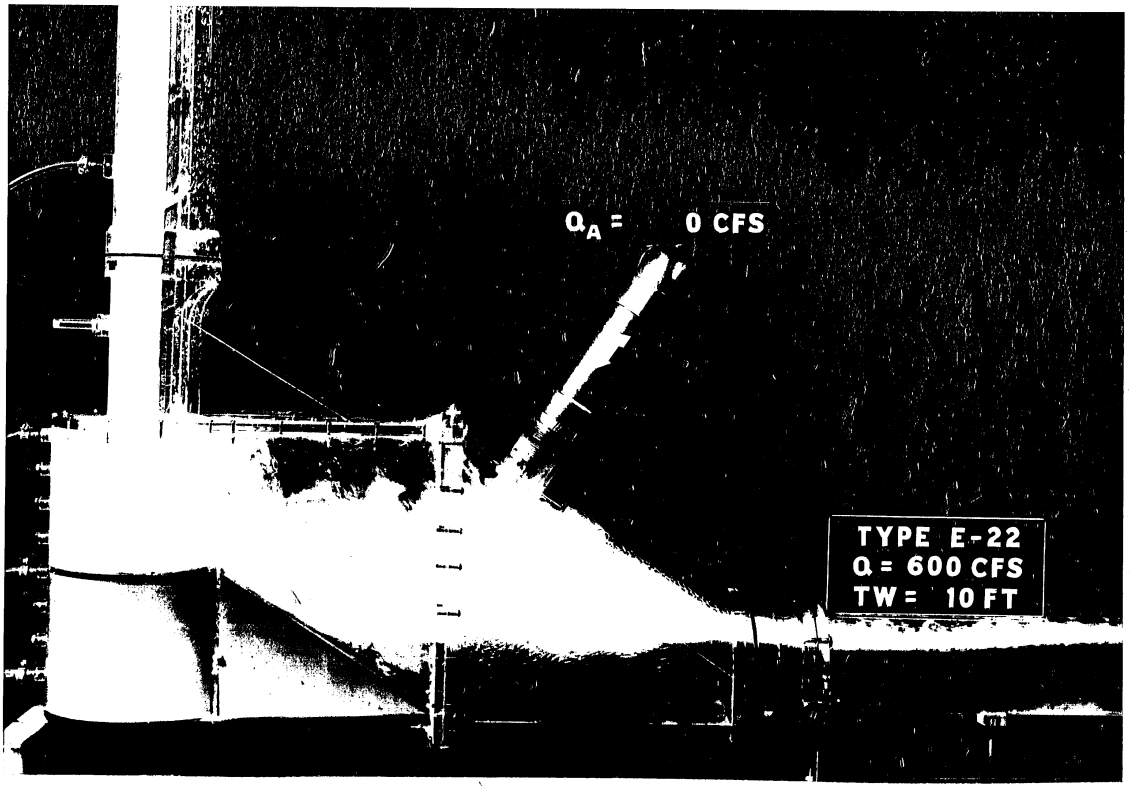

Photo 1

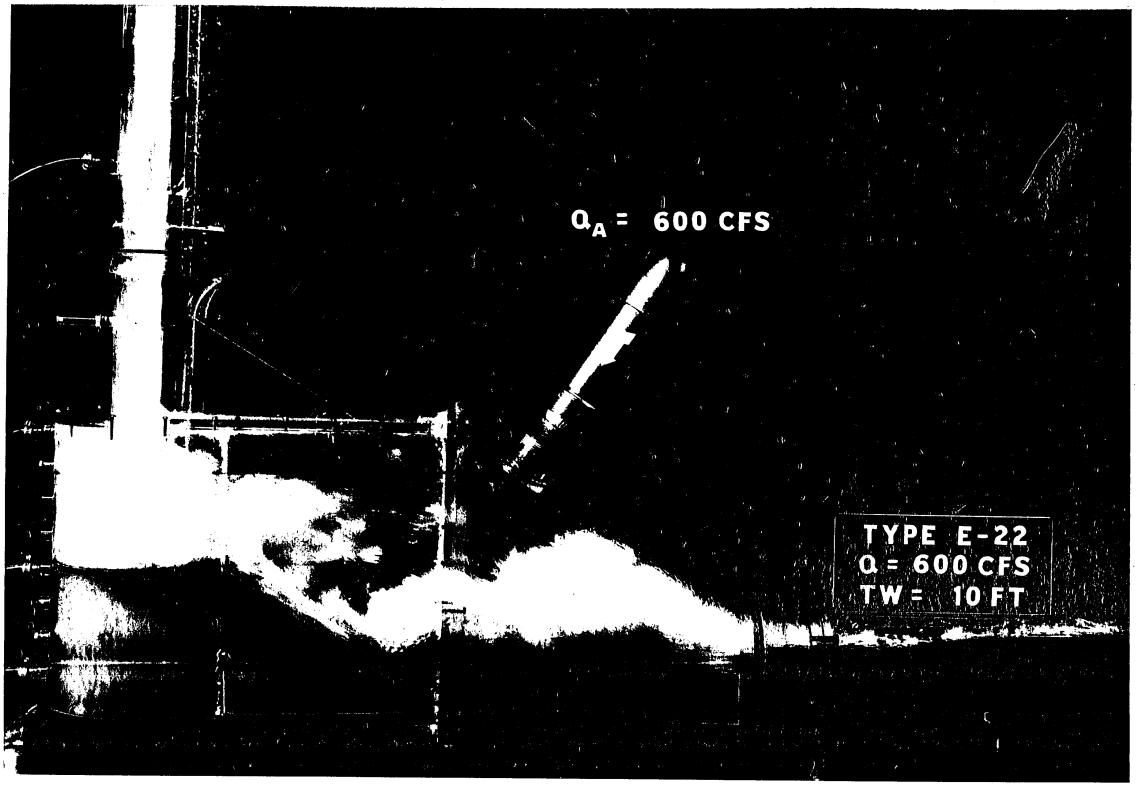

Photo 2

PHOTO 3 (Serial No. 177-401) This photograph shows the appearance of the flow in the air chamber when the air discharge is 1500 cfs.

PHOTO 4 (Serial No. 177-402) A large air discharge of 2200 cfs does not appreciably change the flow pattern in the air chamber and the outlet tunnel. The high velocity in the air jet creates a greater disturbance within the air chamber. The relative increase of this disturbance is apparent in the series of photographs.

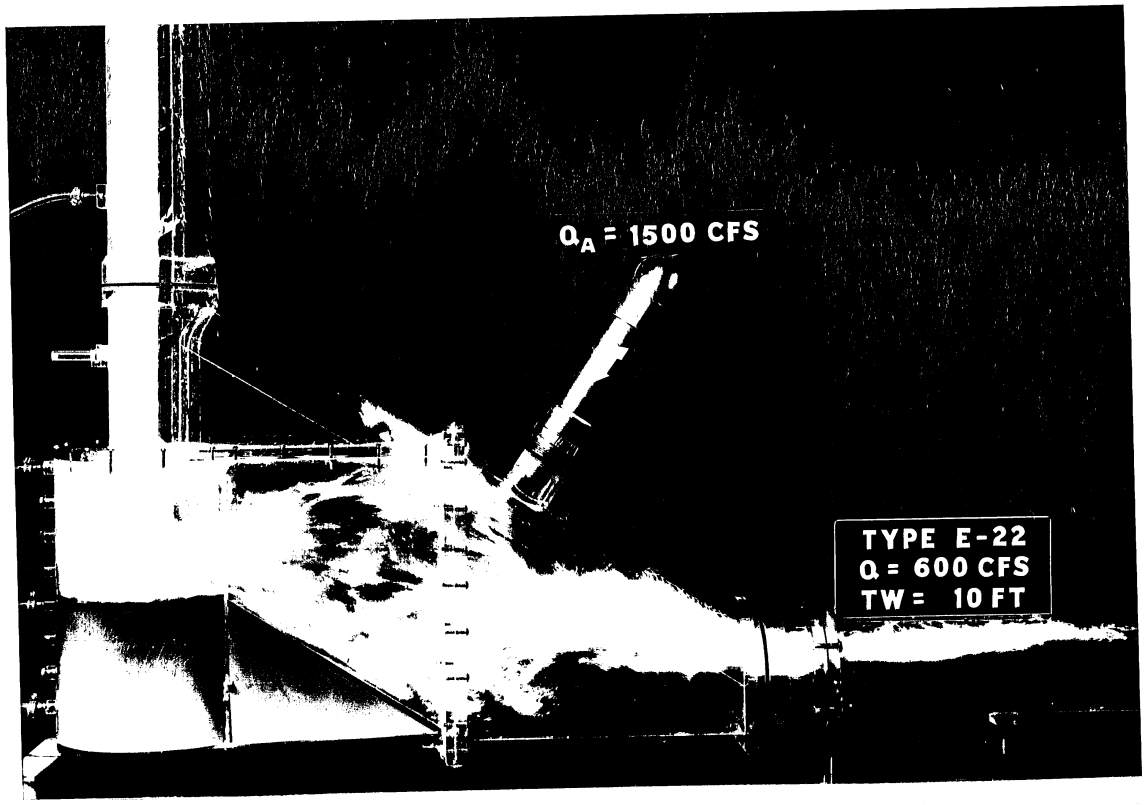

Photo 3

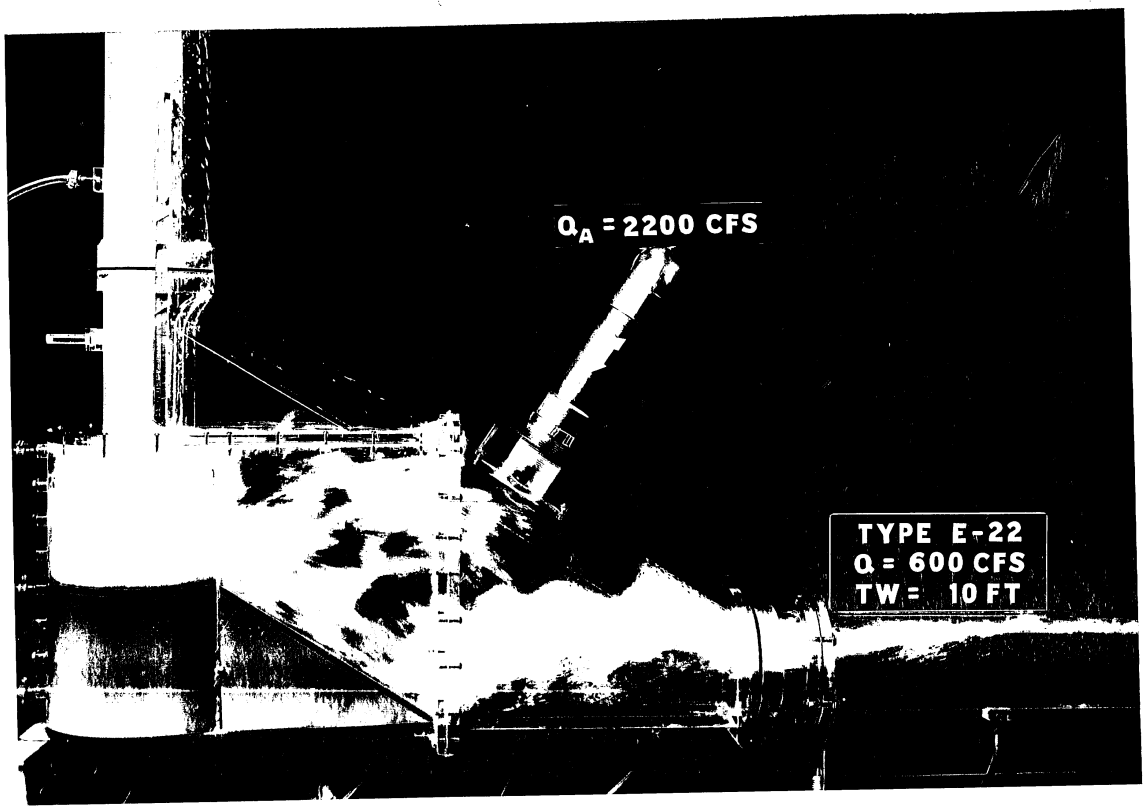

Photo 4

PHOTO 5 (Serial No. 177-403) When a detergent is added to the incoming flow, the air chamber is filled with foam, and when the tailwater elevation is 10 ft the foam penetrates the outlet tunnel and forces the relatively clear water to flow under the stationary foam.

PHOTO 6 (Serial No. 177-406) This photo shows that when the tailwater elevation is increased to 50 ft the detergent foam collected in the air chamber is still forced into the outlet tunnel so that it is approximately half filled with foam. The water is forced to flow in the region below the detergent foam.

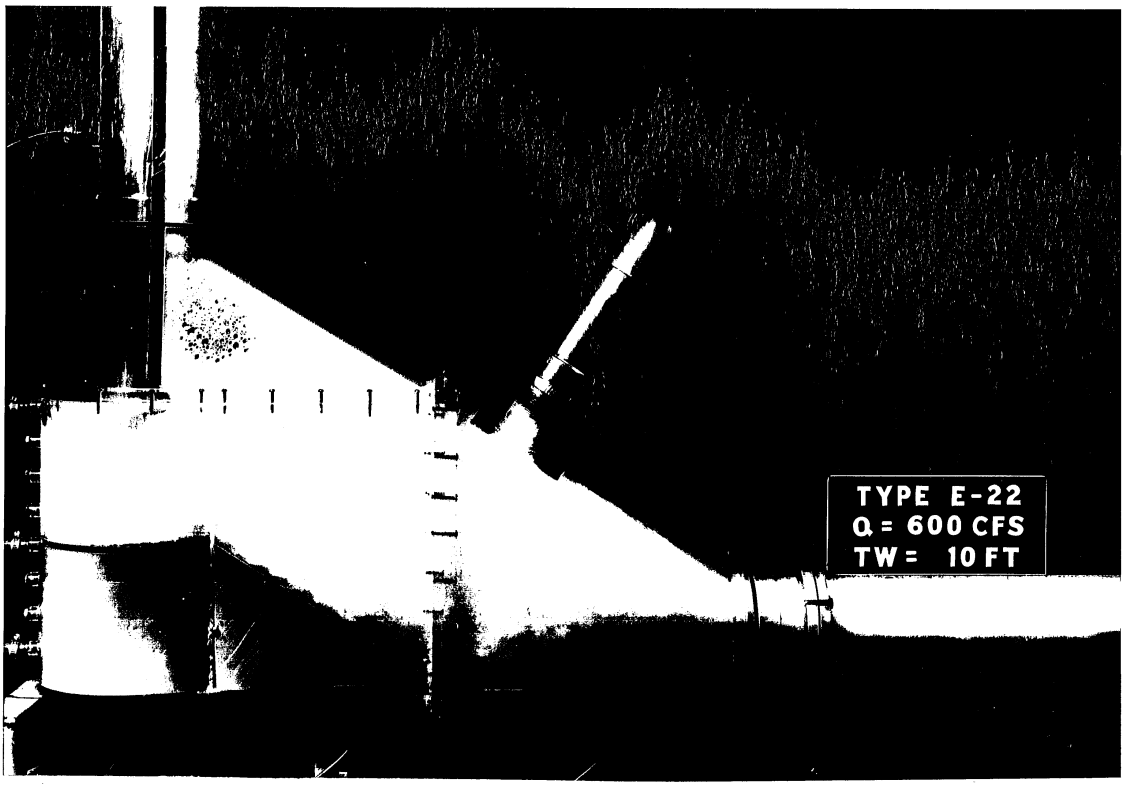

Photo 5

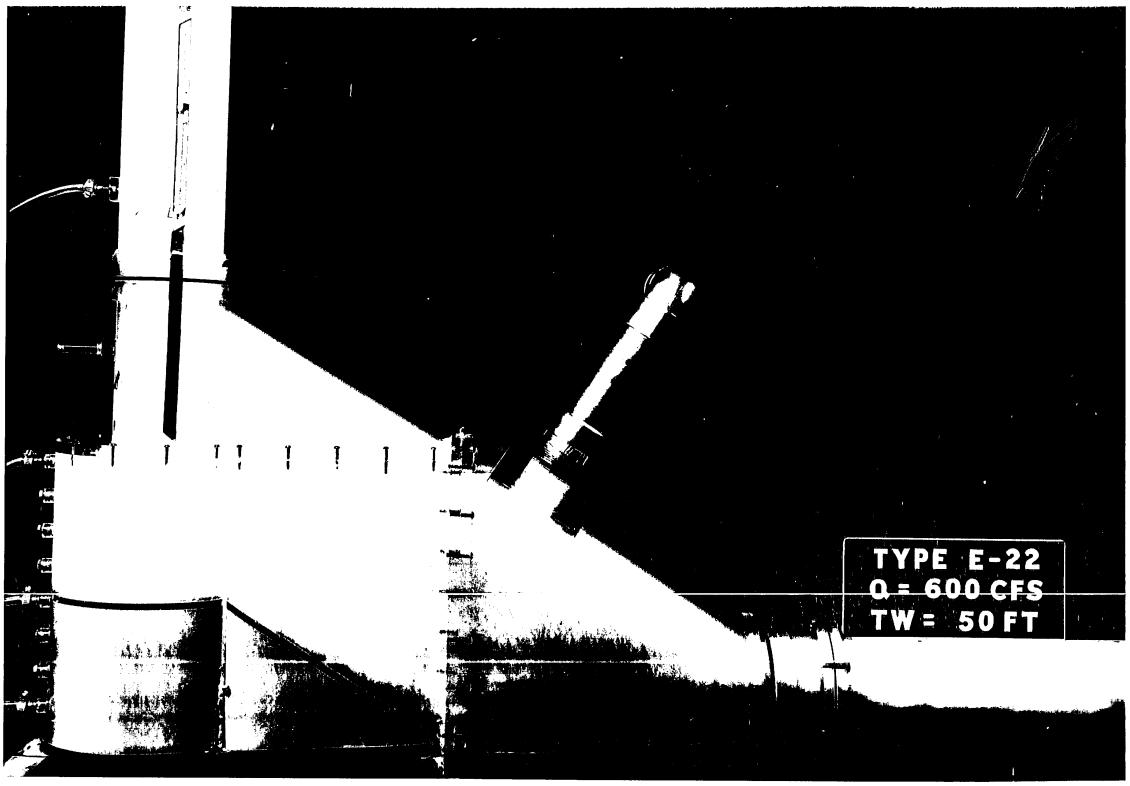

Photo 6

PHOTO 7 (Serial No. 177-408) For comparison, this photograph shows the flow pattern without detergent for the same discharge and tailwater elevation as in Photo 6.

PHOTO 8 (Serial No. 177-409) For comparison with Photo 7 and for the same flow conditions, detergent has been added to the flow, and as is apparent, fills the air chamber and a portion of the downstream tunnel.

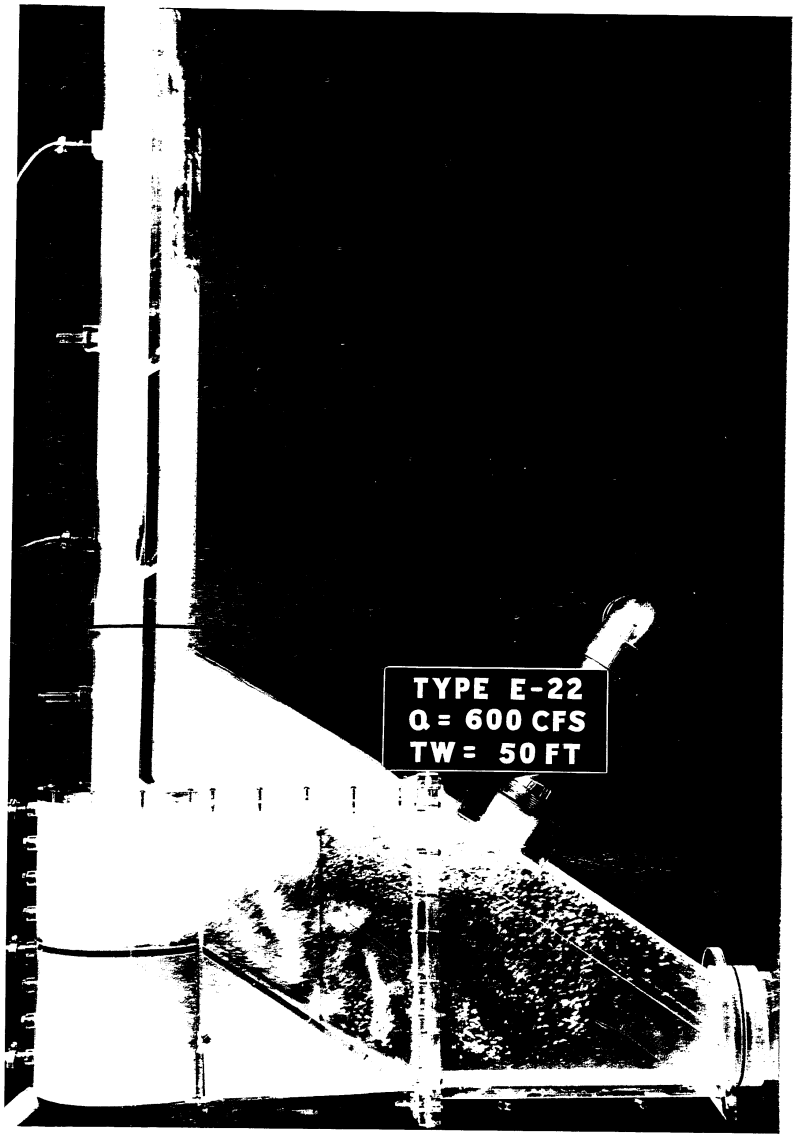

Photo 7

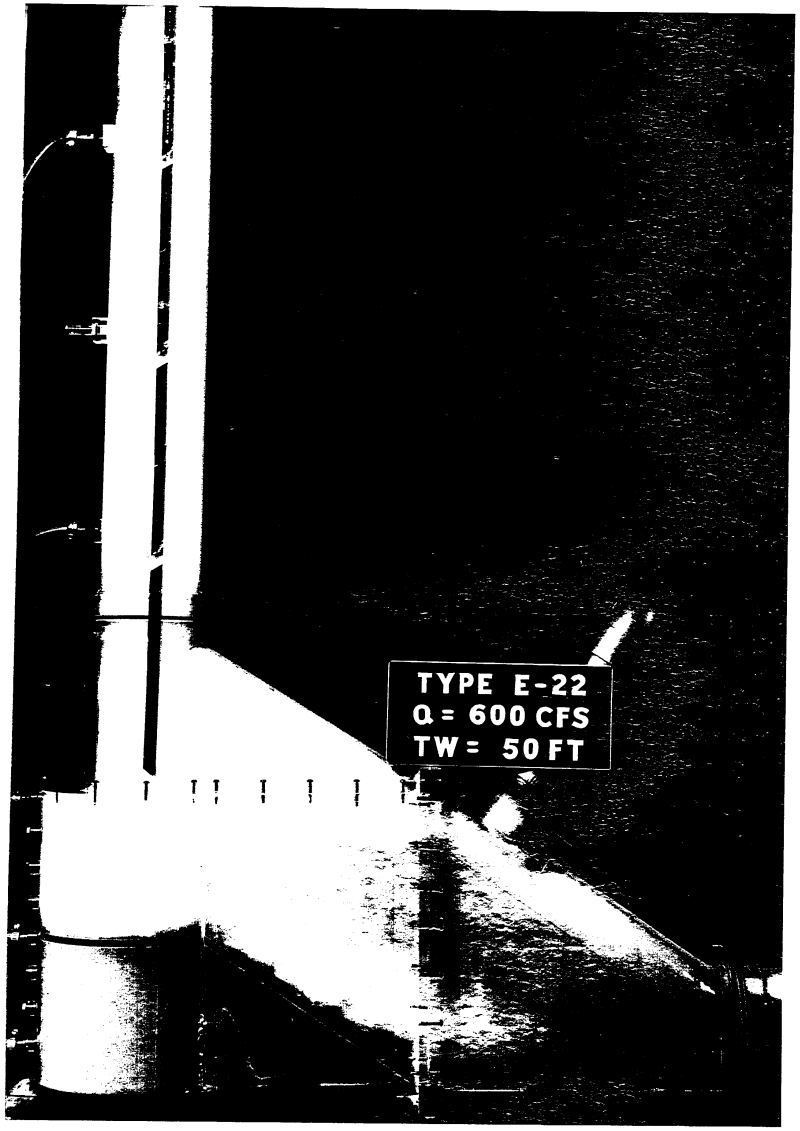

Photo 8

PHOTO 9 (Serial No. 177-522) The foaming detergent in the inflow rises in the air vent to a stable elevation considerably in excess of the tailwater elevation. For this experiment the discharge was 600 cfs and the tailwater was at elevation 100 ft. There is relatively little mixing or insufflation of detergent through the dividing wall at this elevation.

PHOTO 10 (Serial No. 177-523) When the tailwater elevation is increased to 150 ft the detergent foam rises sufficiently in the air vent to overtop the dividing wall and mingle with the incoming flow. This forms a uniform mixture flowing down the drop shaft. Some of the detergent has been deposited in the shaft above the divider wall and over the flowing detergent foam.

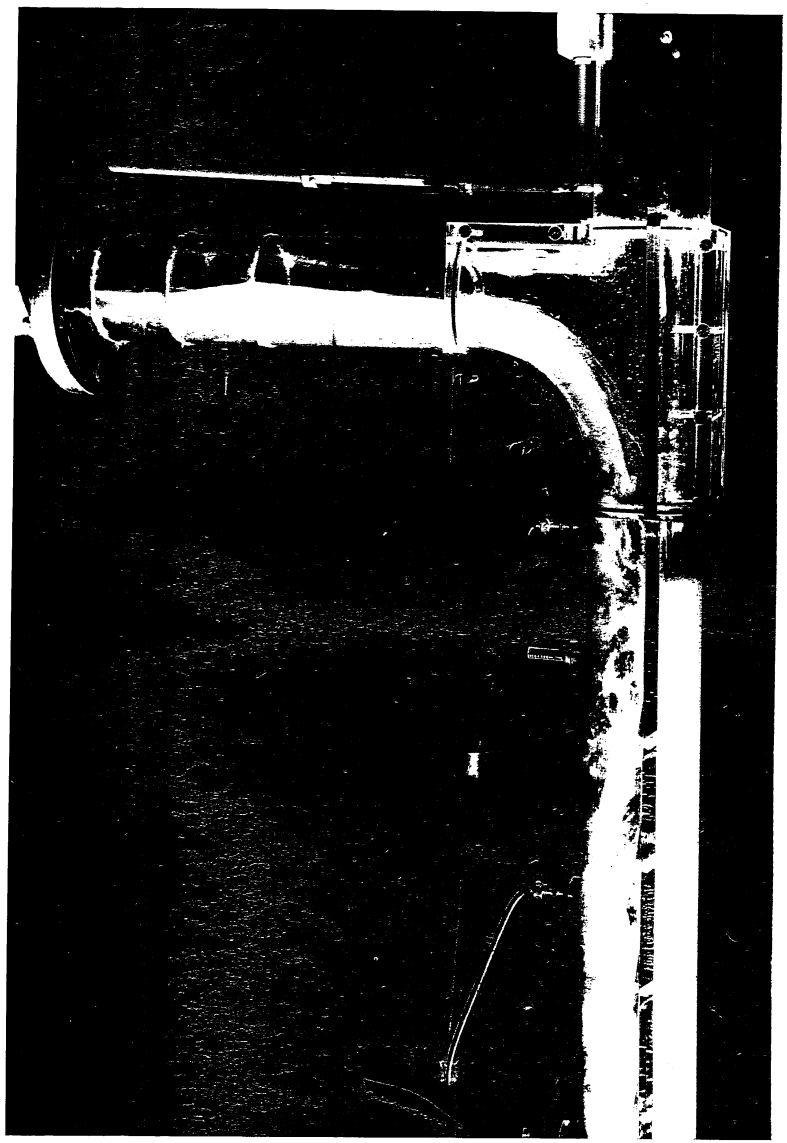

Photo 9

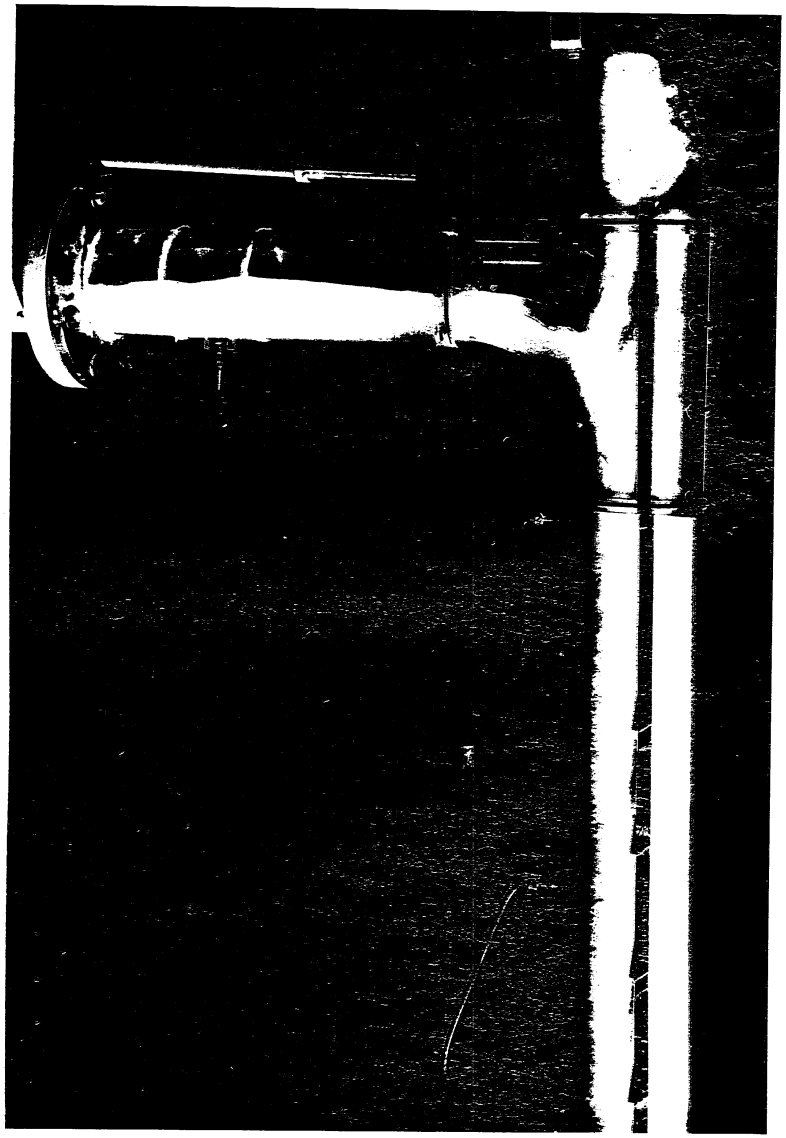

Photo 10

PHOTO 11 (Serial No. 177-524) This photo shows the relatively smooth flow over the divider wall when the tailwater is sufficiently high. The discharge was 600 cfs and the tailwater was raised to elevation 190 ft. With this tailwater the mixing is less intense and the detergent foam is not as concentrated.

PHOTO 12 (Serial No. 177-525) When the tailwater has been raised to elevation 225 ft the inlet is completely submerged and the mixing of air and detergent has been reduced to a minimum. Very little air has been insufflated, and the effect of the detergent appears to be minimal.

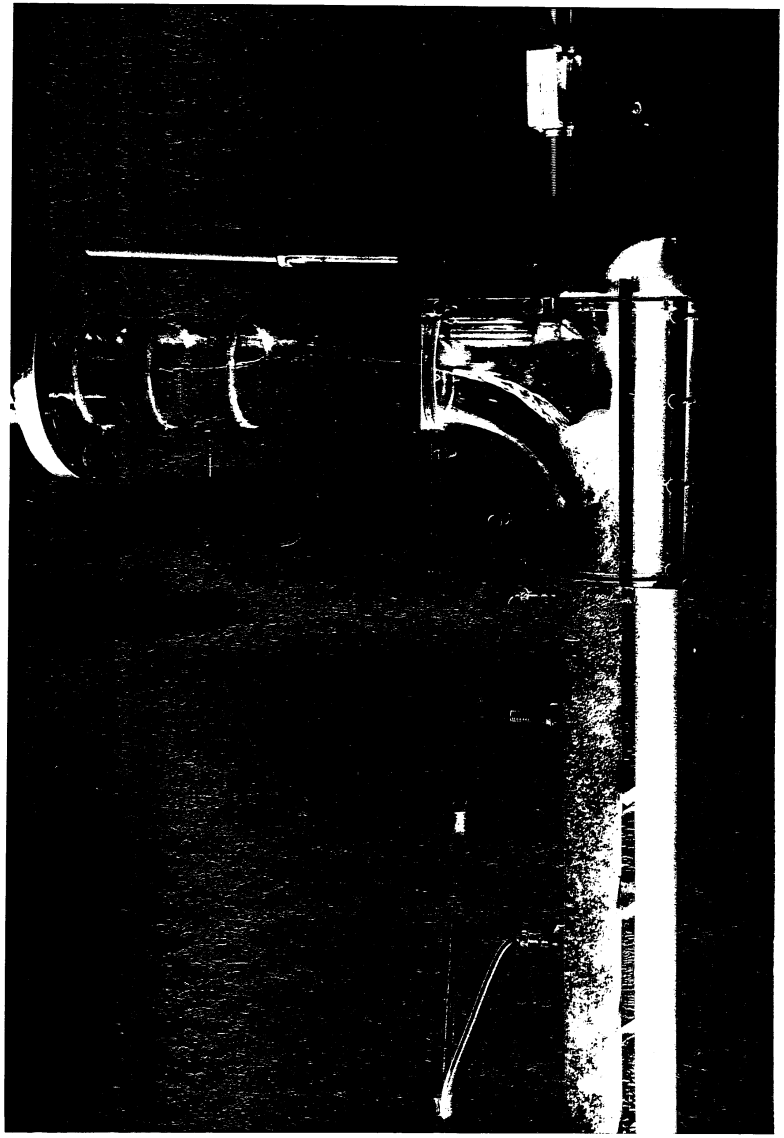

Photo 11

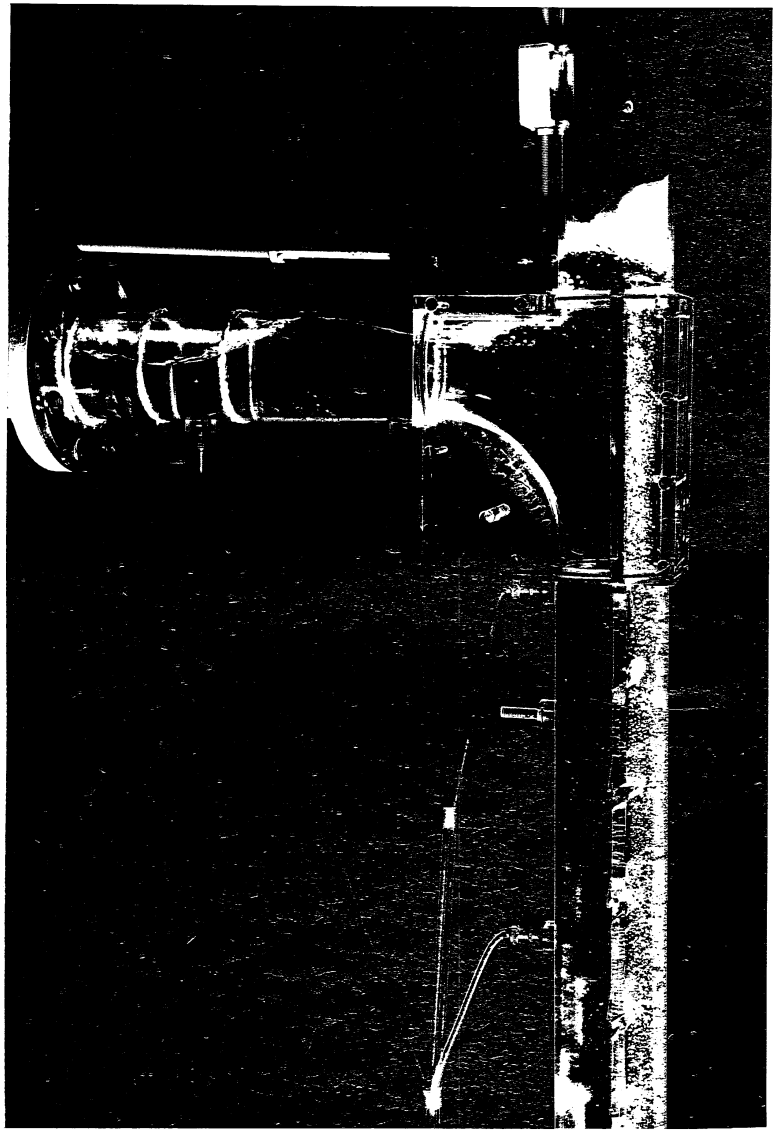

Photo 12

LIST OF CHARTS

CHART 1 (177B474-136) Air concentrations in drop shaft with air injected. Model scale 1:27, discharge 600 cfs, tailwater 10 ft.

CHART 2 (177B474-137) Air concentrations in the drop shaft with and without detergent. Model scale 1:27, discharge 600 cfs, varied tailwater.

CHART 3 (177B474-138) Average air concentrations in the drop shaft with and without detergent. Model scale 1:27, discharge 600 cfs, tailwater elevation varied.

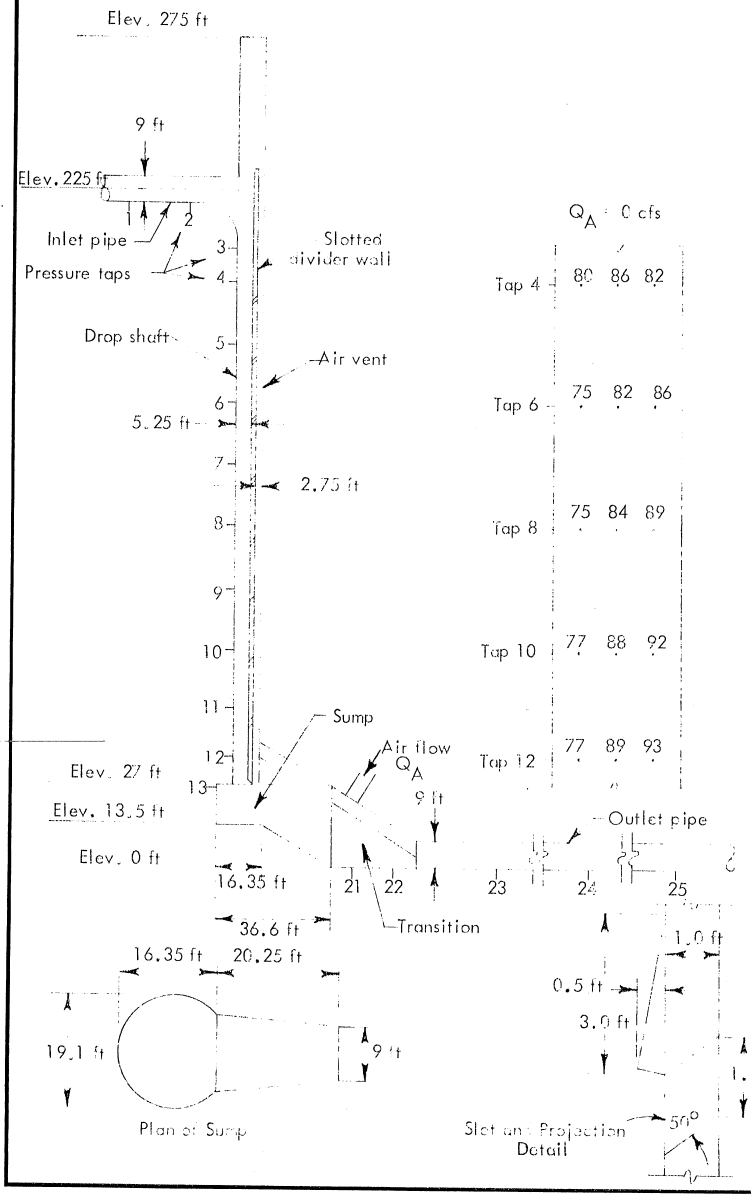

Air Flow

	Q_A = 0 cfs	Q_A = 600 cfs	Q_A = 1500 cfs	Q_A = 2200 cfs
Tap 4	80 86 82	80 87 85	80 87 82	78 86 82
Tap 6	75 82 86	75 82 86	75 83 87	73 83 87
Tap 8	75 84 89	76 87 90	75 87 91	75 86 92
Tap 10	77 88 92	77 88 92	78 88 93	76 88 93
Tap 12	77 89 93	77 89 93	80 90 93	80 90 93

Air Concentrations in Per Cent

TYPE E-22 DROP SHAFT
Air Concentrations in Drop Shaft
With Air Injected
Model Scale 1:27
Flow Conditions:
Discharge = 600 cfs - Tailwater = 10 ft

Air was injected in the transition as shown and air concentration measurements made in the drop shaft with an electrical concentration measuring instrument.

Type E-22 Drop Shaft is described on Chart 1776474 - 119.

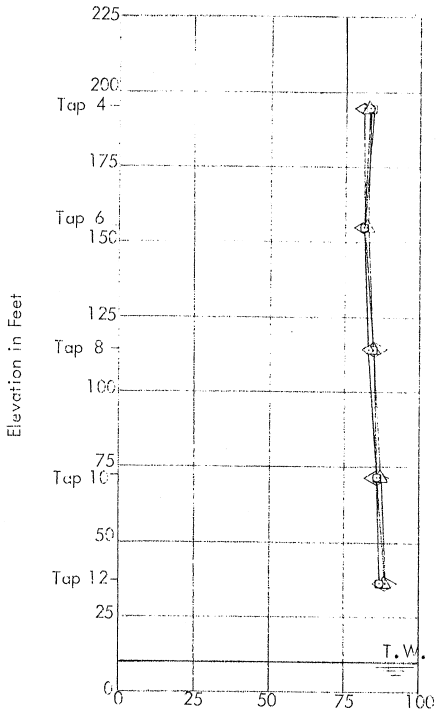

Average Air Concentrations in Per Cent
Q_A = 0 cfs
= 600 cfs
= 1500 cfs
= 2200 cfs

LAWRENCE AVENUE SEWER SYSTEM
City of Chicago
Harza Engineering Co., Chicago, Ill.
DROP SHAFT STUDIES

SAINT ANTHONY FALLS HYDRAULIC LABORATORY
UNIVERSITY OF MINNESOTA

DRAWN WQD	CHECKED	APPROVED
SCALE	DATE 4-18-68	NO. 1778474-136

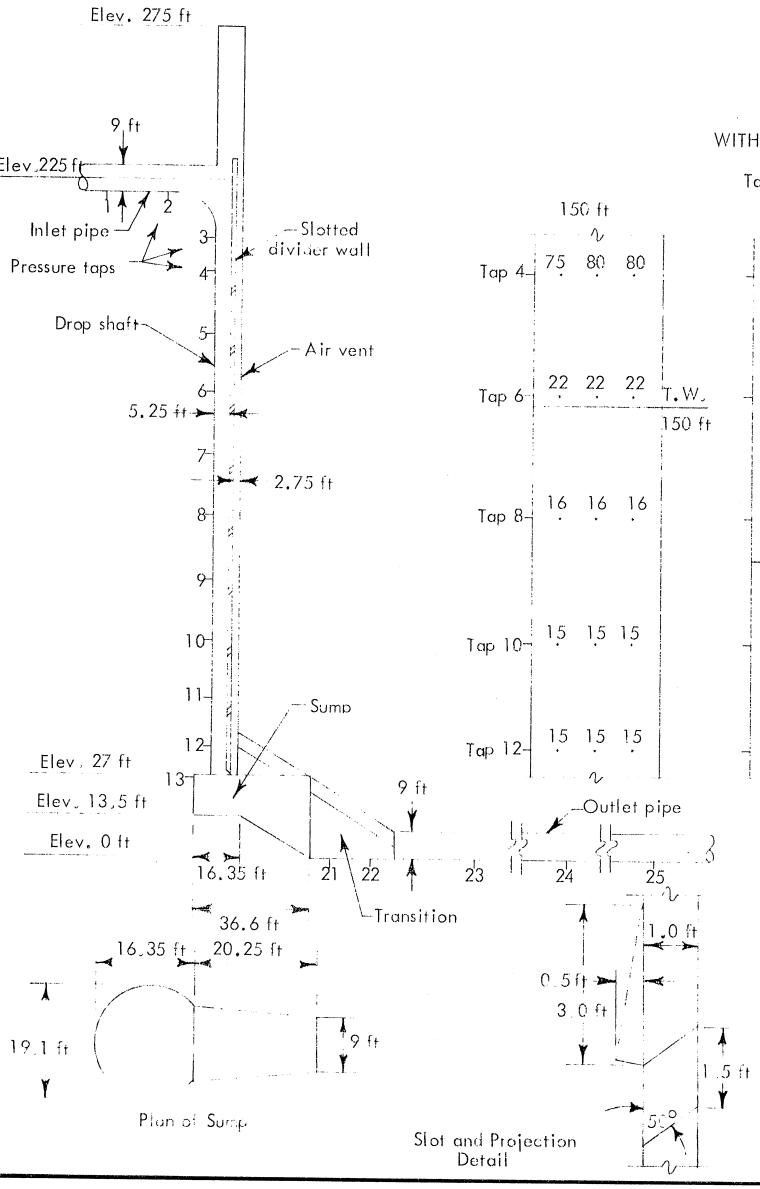

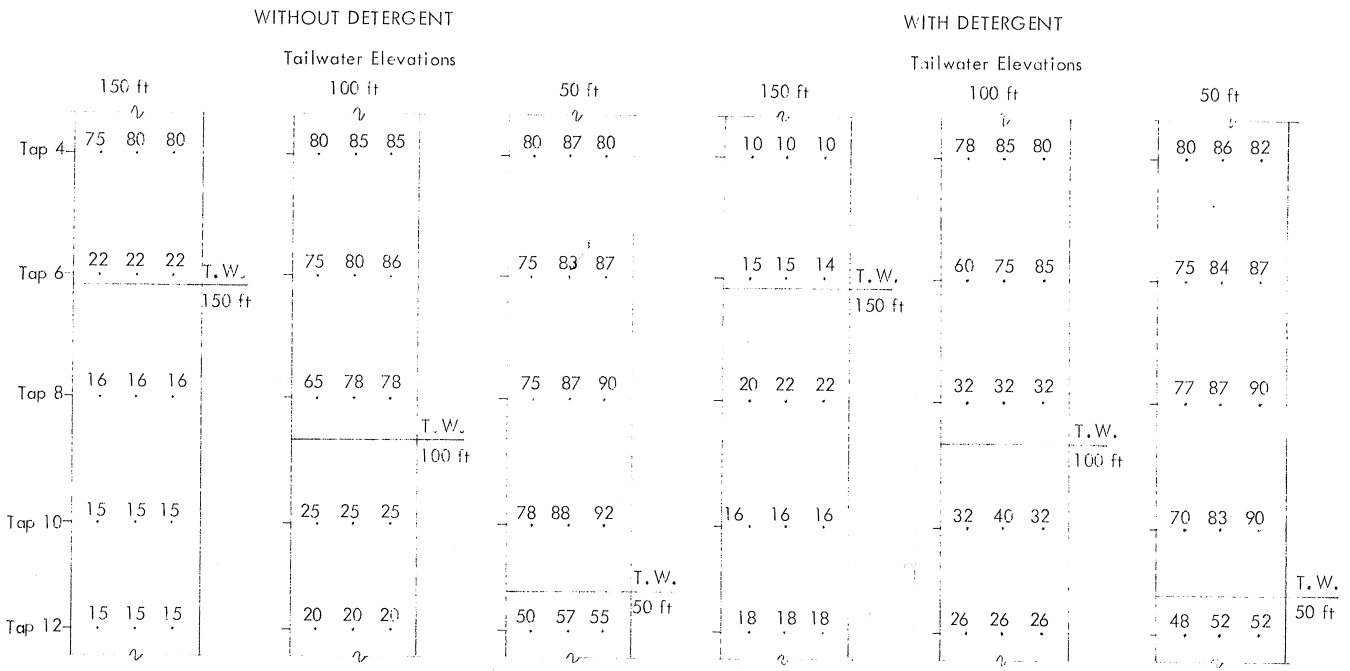

Air Concentrations in Per Cent

TYPE E-22 DROP SHAFT
Air Concentrations in Drop Shaft
With and Without Detergent
Model Scale 1:27
Flow Conditions:
Discharge = 600 cfs - Tailwater Varied

Concentrated detergent was injected in the water supply line upstream of the model at about a 0.006 per cent rate of the flow. Air concentration measurements were made in the drop shaft with an electrical concentration measuring instrument.

Type E-22 Drop Shaft is described on Chart 177B474 - 113.

LAWRENCE AVENUE SEWER SYSTEM
City of Chicago
Harza Engineering Co., Chicago, Ill.
DROP SHAFT STUDIES

SAINT ANTHONY FALLS HYDRAULIC LABORATORY
UNIVERSITY OF MINNESOTA

DRAWN WQD	CHECKED	APPROVED
SCALE	DATE 4-18-68	NO. 177B474-137

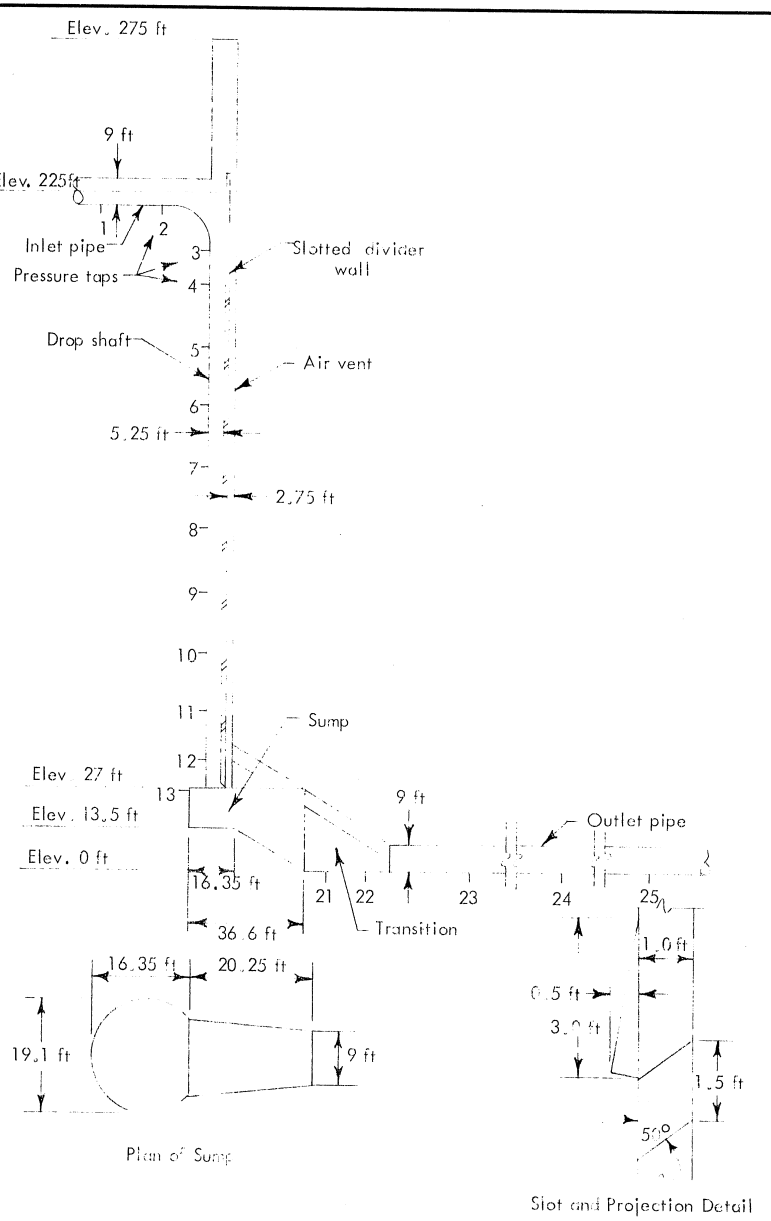

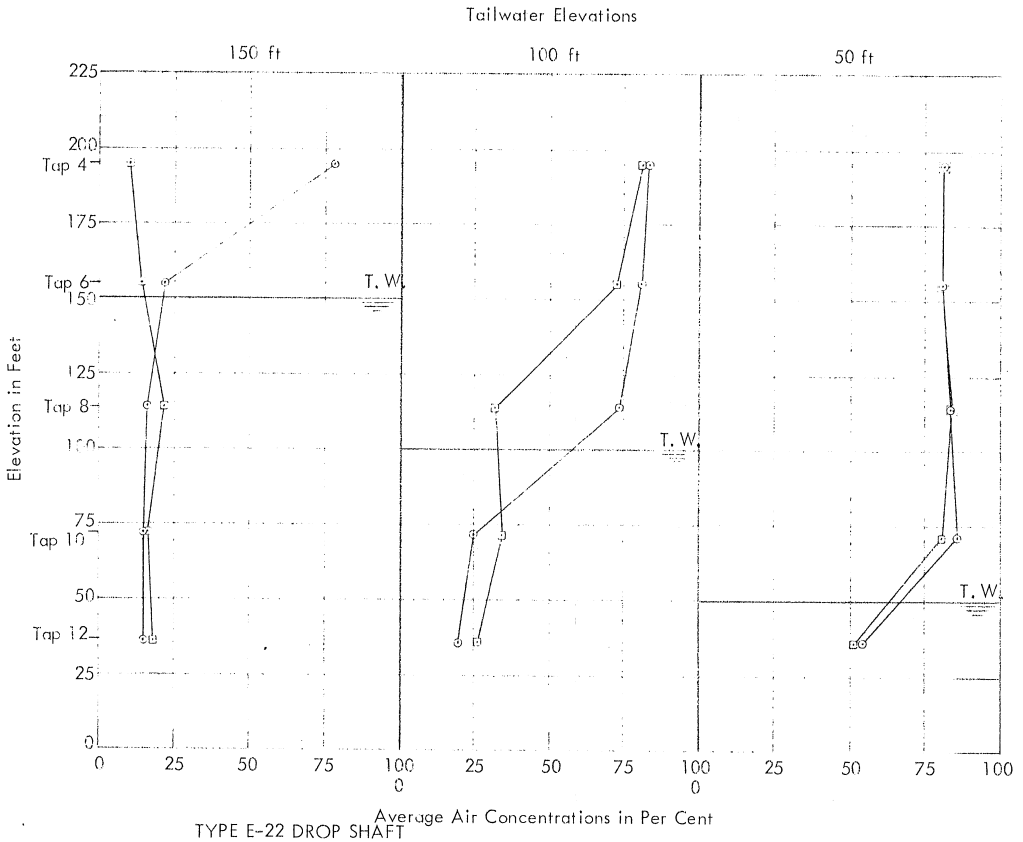

TYPE E-22 DROP SHAFT
Average Air Concentrations in Drop Shaft
With and Without Detergent
Model Scale 1:27
Flow Conditions: Discharge = 600 cfs - Tailwater Varied
○ Without detergent
△ With detergent

Concentrated detergent was injected in the water supply line upstream of the model at about a 0.006 per cent rate of the flow. Air concentration measurements were made in the drop shaft with an electrical concentration measuring instrument. The values plotted are an average of three readings taken across the drop shaft.

Type E-22 Drop Shaft is described on Chart 177B474 - 119.

LAWRENCE AVENUE SEWER SYSTEM
City of Chicago
Har. a Engineering Co., Chicago, Ill.
DROP SHAFT STUDIES

SAINT ANTHONY FALLS HYDRAULIC LABORATORY
UNIVERSITY OF MINNESOTA

DRAWN WQD	CHECKED	APPROVED
SCALE	DATE 4-18-68	NO 177B474 - 138